Power system real-time thermal rating estimation

Andrea Michiorri

A Thesis presented for the degree of
Doctor of Philosophy

Energy Group
School of Engineering and Computing Science
Durham University
UK

May 2010

Power system real-time thermal rating estimation

Andrea Michiorri

Submitted for the degree of Doctor of Philosophy

April 2010

Abstract

This Thesis describes the development and testing of a real-time rating estimation algorithm developed at Durham University within the framework of the partially Government-funded research and development project “Active network management based on component thermal properties”, involving Durham University, ScottishPower EnergyNetworks, AREVA-T&D, PB Power and Imass. The concept of real time ratings is based on the observation that power system component current carrying capacity is strongly influenced by variable environmental parameters such as air temperature or wind speed. On the contrary, the current operating practice consists of using static component ratings based on conservative assumptions. Therefore, the adoption of real-time ratings would allow latent network capacity to be unlocked with positive outcomes in a number of aspects of distribution network operation. This research is mainly focused on facilitating renewable energy connection to the distribution level, since thermal overloads are the main cause of constraints for connections at the medium and high voltage levels. Additionally its application is expected to facilitate network operation in case of thermal problems created by load growth, delaying and optimizing network reinforcements. The work aims at providing a solution to part of the problems inherent in the development of a real-time rating system, such as reducing measurements points, data uncertainty and communication failure. An extensive validation allowed a quantification of the performance of the algorithm developed, building the necessary confidence for a practical application of the system developed.

...
de' remi facemmo ali al folle volo
…

Dante: Inferno, XXVI

Declaration

I hereby declare that this thesis is a record of work undertaken by myself, that it has not been the subject of any previous application for a degree, and that all sources of information have been duly acknowledged.

Acknowledgements

I would like to thank my supervisor, Prof. Phil Taylor, for his continuous support and guidance during my time at Durham. I would also like to thank the Department for Innovation, Universities and Skills for funding, and the staff from AREVA T&D, Imass, PB Power, ScottishPower EnergyNetworks and the MetOffice for their valuable input to this work.

I would like also to thank my family: my father, my mother, my grandmother and my sister for their support in these three years, and to send a special thanks to my friends Elahe, Pavlos, Pierpaolo and Greg for the good and bad moments that they have shared with me. Impossible not to mention also Elena, Gianpiera, Mates, Lenka, Maria, Daniele, Dimitris, Massimiliano, Asia, Magda, Giovanni, Sam, Padraigh, Elisa, Mita, Fateme, Etienne Lecouffe, Andrew Strathclyde, Gusdorf, and all the others who made memorable my stay in Durham.

Contents

Figures ..... **x**

Nomenclature ..... **xv**

Chapter 1 Introduction **1**

1.1 Current state of the electrical power industry 1

1.2 Current research trends 3

1.3 Active network management based on component thermal properties 5

1.4 Dynamic line ratings 8

1.4.1 Statement of the problem 8

1.4.2 Possible solutions 9

1.5 Research Objectives 13

1.6 Thesis overview 14

1.7 Author's publications 16

Chapter 2 Literature review **19**

2.1 Related work 19

2.2 Component modelling 21

2.2.1 Overhead lines 21

2.2.2 Electric cables 23

2.2.3 Power transformers 26

2.3 Environmental condition modelling 28

2.3.1 Wind speed and direction 29

2.3.2 Air temperature and solar radiation 30

2.3.3 Soil temperature and thermal resistivity 31

2.4 Power System State estimation 31

2.5 Conclusion 34

Chapter 3 Algorithm development: Modelling **37**

3.1 Component modelling 37

3.1.1 Overhead lines 37

3.1.2 Electric cables 46

3.1.3 Power transformers 50

3.1.4 Sensitivity analysis 56

3.2 Environmental condition modelling 58

3.2.1 Interpolation 58

3.2.2 Wind speed correction 59

3.2.3 Soil temperature and thermal resistance modelling 61

3.3 Conclusion 62

Chapter 4 Algorithm development: Estimation technique **66**

4.1 Review of possible techniques 66
4.1.1 Data and models structure 66
4.1.2 State estimation techniques 67
4.2 Monte Carlo simulation 71
4.2.1 Structure 71
4.2.2 Variate generation 75
4.2.3 Probability density function 78
4.2.4 Random number generation 85
4.3 Conclusion 86

Chapter 5 Software design and development 88
5.1 Introduction 88
5.2 Classes 91
5.3 Databases 95
5.4 Structure of the algorithm 97
5.5 Conclusion 102

Chapter 6 Validation 105
6.1 Validation strategy 105
6.1.1 What to measure 105
6.1.2 Datasets for validation 108
6.1.3 How to measure it 110
6.2 Model validation 112
6.2.1 Overhead line conductor rating model validation 112
6.2.2 Environmental conditions models validation 117
6.3 State estimation validation 134
6.4 Discussion 140
6.5 Conclusion 141

Chapter 7 Real-time rating impact quantification 143
7.1 Datasets 143
7.2 Results 149
7.2.1 Rating comparison of different component types 150
7.2.2 Rating comparison of overhead line types 152
7.2.3 Power transfer accommodation assessment 154
7.2.4 Impact of different control strategies 157
7.3 Conclusion 161

Chapter 8 Discussion 162
8.1 Real-time rating system 163
8.1.1 Modelling 163
8.1.2 Thermal state estimation 166
8.1.3 Software design and development 167
8.1.4 Validation and impact quantification 169
8.2 Real-time rating system for distributed generation control 174
8.3 Real-time rating system site trial 177

Chapter 9 Conclusion and Further Work 182
9.1 Conclusion 182

9.2 Further work 186
9.2.1 Modelling 186
9.2.2 Estimation technique 188
9.2.3 Software design and development 188
9.2.4 Validation and impact quantification 189
9.2.5 Off-line planning tool 190
9.2.6 Rating forecast 191

References 194

Appendix ..... A 1
Algorithm details ..... A 2
Classes ..... A 2
Databases ..... A 39
Data Flow ..... A 43
Publications ..... A 49

Figures

Figure 1: Circuit thermal rating algorithm, flow chart 12
Figure 2: Maximum conductor sag under different wind speeds 39
Figure 3: Transformers: coolant circuit 51
Figure 4: Soil surface roughness effect on wind speed vertical profile, example 60
Figure 5: Monte Carlo method example 72
Figure 6: Example of overhead line rating estimation 74
Figure 7: Acceptance rejection method 77
Figure 8: Beta distribution for different shape parameters values 80
Figure 9: Kumaraswamy distribution for different shape parameters values 81
Figure 10: Triangular distribution for different shape parameter values 82
Figure 11: Truncated normal distribution for different shape parameters values 83
Figure 12: Real-time thermal rating algorithm in the control architecture 89
Figure 13: Class diagram, example 93
Figure 14: Whole system class static diagram 94
Figure 15: Circuit thermal rating algorithm, flow chart 98
Figure 16: Monte Carlo method algorithm, flow chart 99
Figure 17: Circuit real-time rating estimation functions and data flow 101
Figure 18: Accuracy and precision 106
Figure 19: Monitored network area 109
Figure 20: Conductor temperature, comparison between calculated and measured values in MS 2 for the period 07-13/12/2008 113
Figure 21: Conductor temperature, comparison between calculated and measured values in MS 1, MS 3, MS 4 and MS 5 (clockwise) for the period 07-13/12/2008 114
Figure 22: Conductor temperature, error PDF and CDF 116
Figure 23: Wind speed, comparison between calculated and measured values for MS2 in the period 07-13/12/2008 118
Figure 24: Wind speed, comparison between calculated and measured values for MS 1, MS 3, MS 4 and MS 5 (clockwise) in the period 07-13/12/2008 120

Figure 25: Wind speed, error PDF and CDF 121
Figure 26: Wind direction, comparison between calculated and measured values 123
Figure 27: Wind direction, comparison between calculated and measured values for MS 1, MS 3, MS 4 and MS 5 (clockwise)in the period 07-13/12/2008 124
Figure 28: Wind direction, error probability density function and CDF 125
Figure 29: Air temperature, comparison between calculated and measured values 127
Figure 30: Air temperature, comparison between calculated and measured values for MS 1, MS 3, MS 4 and MS 5 (clockwise)in the period 07-13/12/2008 128
Figure 31: Air temperature, error PDF and CDF 129
Figure 32: Solar radiation, comparison between calculated and measured values 131
Figure 33: Solar radiation, comparison between calculated and measured values for MS 1, MS 3, MS 4 and MS 5 (clockwise) in the period 07-13/12/2008 132
Figure 34: Solar radiation, error PDF and CDF 133
Figure 35: Conductor temperature estimation, comparison between estimated and measured values 135
Figure 36: Conductor temperature estimation and error in MS2 for the day 09/12/2008 136
Figure 37: Conductor temperature, comparison between estimated and measured values for MS 1, MS 3, MS 4 and MS 5 (clockwise) in the period 07-13/12/2008 137
Figure 38: Conductor temperature estimation, error PDF and CDF 139
Figure 39: Performance degradation in consequences of measurement or communication failures .. 139
Figure 40: Wind speed probability distribution 144
Figure 41: Air temperature probability distribution 145
Figure 42: Soil temperature probability distribution 145
Figure 43: Site trial 146
Figure 44: UKGDS A 147
Figure 45: UKGDS B 147
Figure 46: UKGDS C 147
Figure 47: Rating cumulative probability for SITE network components exposed to the Valley climatic scenario 151
Figure 48: Magnified rating cumulative probability for SITE network components exposed to the Valley climatic scenario 152
Figure 49: Influence of different UK climates on overhead lines power transfer headroom 153
Figure 50: Cumulative probability comparison for a Lynx conductor in the Valley scenario 156
Figure 51: Control algorithm flowchart 176
Figure 52: Schematic representation of the real-time rating system developed 178
Figure 53: Meteorological station in a distribution substation and particular. a) pressure sensor, b) solar radiation sensor, c) wind speed and direction sensor 180

Figure 54: Substation relay user interface 181
Figure 55: Substation relay: a) input from meteorological station (Figure 1). b) modem for communication to the outside world 181
Figure 56: 132kV overhead line in the site trial area 181
Figure 57: Rating forecast at different time horizons 193

Figure A - 1: Component_Class static diagram ..... A 3
Figure A - 2: Environment class static structure ..... A 19
Figure A - 3: PDF class static structure ..... A 32
Figure A - 4: Auxiliary_Procedures class static structure ..... A 35
Figure A - 5: Database_Components tables and relations diagram ..... A 40
Figure A - 6: Database "Environment" tables and relations diagram ..... A 41
Figure A - 7: Database "Geo_DB" table "Coordinates" diagram ..... A 42
Figure A - 8: Database "Errors", table "Errors" diagram ..... A 43
Figure A - 9: Database "Output", table "Ratings_PDF" diagram ..... A 43
Figure A - 10: Circuit real-time rating estimation functions and data flow ..... A 47

Tables

Table 1: Technologies comparison against main performance parameters..... 12
Table 2: Environmental condition sensitivity analysis (parameter variation versus rating variation) .. 57
Table 3: Frequency percentages of measured environmental conditions at the five meteorological stations and measured current flowing in the conductor in the same locations for the period 07/12/2008-18/02/2009. 110
Table 4: Conductor temperature, error average and standard deviation 115
Table 5: Correlation between conductor temperature calculation and environmental condition values. Absolute values greater than 0.1 are highlighted..... 117
Table 6: Wind speed, error average and standard deviation 121
Table 7: Correlation between wind speed calculation error and wind speed measurement in the other locations..... 122
Table 8: Wind direction, error average and standard deviation 125
Table 9: Correlation between wind direction calculation error and wind direction measurement in the other locations 126
Table 10: Air temperature, error average and standard deviation..... 129
Table 11: Correlation between air temperature calculation error and air temperature measurements in the other locations..... 130
Table 12: Solar radiation, error average and standard deviation..... 133
Table 13: Correlation between solar radiation calculation error and solar radiation measurement in the other locations 134
Table 14: Conductor temperature estimation, average computational-time, error average and standard deviation, estimation average standard deviation..... 138
Table 15: Network components 148
Table 16: Simulation results, component ratings and theoretical headroom..... 149
Table 17: Simulation results for SITE network components exposed to the Valley climatic scenario150
Table 18: Quantification methodology results..... 159

Table A - 1: Component.Network class.....A 4
Table A - 2: Component.Circuit class.....A 5
Table A - 3: Component.Element class.....A 6
Table A - 4: Component.General_Parameters .....A 8
Table A - 5: Component.OHL class.....A 11
Table A - 6: Component.UGC class.....A 14

Table A - 7: Component.PTR class....A 17
Table A - 8: Environment class....A 20
Table A - 9: Environment.Environment_for_Rating class....A 22
Table A - 10: Environment.Environment_for_Observation....A 23
Table A - 11: Environment.Place cass....A 24
Table A - 12: Monte_Carlo_Method class....A 28
Table A - 13: Thermal State Estimation class....A 31
Table A - 14: PDF.Beta class....A 34
Table A - 15: Auxiliary_Procedures.Configuration class....A 37
Table A - 16: Auxiliary_Procedures.Manage_DB class....A 38
Table A - 17: Web service class....A 39

Nomenclature

a	Beta PDF minimum value	
A_a	Aluminium cross sectional area	[m^2]
A_c	Conductor's cross sectional area	[m^2]
A_i	Wind direction correction relationship coefficient	
A_s	Steel cross sectional area	[m^2]
b	Beta PDF maximum value	
B_i	Wind direction correction relationship coefficient	
CDF_j	Cumulative density function j	
C_{drag}	Drag coefficient	
C_{ins}	Insulation loss factor	
$C_j^{D/A}$	Direct/alternated current relationship coefficient	
C_l	Electric cable losses coefficient	
C_{rp}	Proximity effect factor	
C_{rs}	Skin effect factor	
C_{Tij}	IEC time dependant functions coefficients	
C_{To}	Transformer oil exponent	
C_{Tr}	Winding resistance correction factor	
C_{Tr-0}	Rated winding resistance correction factor	
C_{Tw}	Transformer winding exponent	

Cap	Capacitance	[F]
Cth	Generic thermal capacitance	[J·kg^{-1}·K^{-1}]
Cth_a	Air thermal capacity	[J·kg^{-1}·K^{-1}]
Cth_s	Soil thermal capacity	[J·kg^{-1}·K^{-1}]
DB	database	
D_c	Conductor diameter	[m]
D_{core}	Conductor core diameter	[m]
D_e	External diameter	[m]
D_i	Internal diameter	[m]
E_a	Aluminium Young modulus	[Pa]
E_c	Conductor's Young modulus	[Pa]
E_s	Steel Young modulus	[Pa]
f	Frequency	[Hz]
F_{pg}	Conductor weight	[N]
F_{pice}	Ice weight	[N]
F_p	Longitudinal force	[N]
F_t	Tangential force	[N]
g	Gravitational constant	[m·s^{-2}]
Gr	Grashof number	
h	Thermal transfer coefficient	[W·m^{-1}·K^{-1}]
I	Current	[A]
I_{AC}	Alternated current	[A]
I_{DC}	Direct current	[A]
I_o	Rated current	[A]

k_{Ri}	Coefficients of the pseudorandom linear congruencies generator	
$k_{s-\theta}$	Soil unsaturated hydraulic conductivity	[m·s^{-1}]
K_{loss}	Loss coefficient	
K_{loss0}	Rated loss coefficient	
$Krain_2$	normalized net rainfall coefficient	[day^{-1}·mm^{-1}]
$Krain_1$	Normalized soil water loss	[day-1]
$Kshear_i$	Wind shear coefficient at the location *i*	
lr	Rainfall	[mm]
L	Length	[m]
L_{axes}	Distance between cables' axes	[m]
L_{burial}	Cable burial depth	[m]
L_{ik}	Distance between the points *i* and *k*	[m]
L_{sag}	Overhead line conductor sag	[m]
L_{span}	Span length	[m]
$Load$	Transformer dimensionless load	
$Load_0$	Transformer dimensionless rated load	
MS	meteorological station	
N_i	Monte Carlo simulation number of samples	
N	Sum of sand and clay percentage	
Nu	Nusselt number	
Nu_{90}	Wind direction coefficient	
OHL	Overhead line	
p	Beta PDF first shape coefficient	
Pr	Prandtl number	
P_n	Probability at the nth step	

PD	probability density	
PDF_j	Probability density function *j*	
PTR	Power transformer	
q	Beta PDF second shape coefficient	
q_l	Heat generated per unit length by Joule effect	[W·m^{-1}]
q_{tot}	Total heat exchanged per unit length	[W·m^{-1}]
q_c	heat exchanged per unit length by convection	[W·m^{-1}]
q_d	dielectric loss per length unit	[W·m^{-1}]
q_r	heat exchanged per unit length by irradiation	[W·m^{-1}]
q_s	Heat gained per unit length by solar radiation	[W·m^{-1}]
$\dot{Q}_{cu}$	Winding losses	[W]
$\dot{Q}_{cu+fe}$	Winding and core losses	[W]
$\dot{Q}_{fe}$	Core losses	[W]
r	Electric resistance per unit length	[W·m^{-1}]
RTR	Real-time rating	
Re	Reynolds number	
Rth	Generic thermal resistance	[m·K·W^{1}]
Rth_{HE}	Heat exchanger thermal resistance	[m·K·W^{1}]
Rth_i	I-th layer thermal resistance per unit length	[m·K·W^{1}]
Rth_w	winding therml resisitance	[m·K·W^{1}]
S_{rdiff}	diffuse solar radiation	[W·m^{-2}]
S_{rdir}	direct solar radiation	[W·m^{-2}]
t	time	[s]
T	temperature	[K]

TSE	Thermal state estimation	
T_a	air temperature	[K]
T_{ccore}	conductor core temperature	[K]
T_{csurf}	conductor surface temperature	[K]
T_c	conductor temperature	[K]
T_f	final temperature	[K]
T_{HS}	hot spot temperature	[K]
T_i	initial temperature	[K]
UGC	Underground cable	
UKGDS	United Kingdom generic distribution systems	
V	Voltage level	[V]
Wd	wind direction	[deg]
Ws	wind speed	[m s-1]
Ws_a	wind speed at the anemometer	[$m \cdot s^{-1}$]
x_{inf}	interval inferior boundary	
x_m	distribution average	
x_{sup}	interval superior boundary	
z_a	height of the anemometer	[m]
Z_k	generic environmental condition at the point *k*	
z_{ref}	reference height	[m]

α_{abs}	Conductor's absorption coefficient
α_{cap}	Insuation electrical relative permittivity
α_{em}	Conductor's absorption coefficient

α_r	Electrical resistance rise on temperature ratio	
β_a	Aluminium thermal expansion coefficient	[K^{-1}]
β_{air}	Air thermal expansion coefficient	[K^{-1}]
β_c	Conductor's thermal expansion coefficient	[K^{-1}]
β_s	Steel thermal expansion coefficient	[K^{-1}]
δth_s	Soil thermal diffusivity	[$m^2 \cdot s^{-1}$]
ΔT_{a-O0}	Rated air-oil temperature gradient	[K]
ΔT_{a-Of}	Final air-oil temperature gradient	[K]
ΔT_{a-Oi}	Initial air-oil temperature gradient	[K]
ΔT_{a-O}	Air-oil temperature gradient	[K]
ΔT_{iR}	Generic transformer temp. gradient in standard conditions	[K]
ΔT_{O-HSR}	Rated oil-hot spot temperature gradient	[K]
ΔT_{O-HSf}	Final oil-hot spot temperature gradient	[K]
ΔT_{O-HSi}	Initial oil-hot spot temperature gradient	[K]
ΔT_{O-HS}	Oil-hot spot temperature gradient	[K]
ε_i	Source of uncertainty	
$\bar{\mu}$	Dimensionless distribution average	
$\xi_{\rho th_s}$	Soil thermal resistivity correction coefficient	[$W \cdot m^{-1} \cdot K^{-1}$]
ξ_T	Soil temperature correction coefficient	[K^{-1}]
ξ_i	Affine form coefficients	
ρ_a	Air density	[$kg \cdot m^{-3}$]
ρ_s	Soil density	[$kg \cdot m^{-3}$]
ρth_a	Air thermal resistivity	[$m \cdot K \cdot W^{1}$]
ρth_c	Conductor thermal resistivity	[$m \cdot K \cdot W^{1}$]

ρth_j	j[th] layer thermal resistivity	[m·K·W^{1}]
ρth_{s0}	Standard soil thermal resistivity	[m·K·W^{1}]
ρth_s	Soil thermal resistivity	[m·K·W^{1}]
$\bar{\sigma}$	Dimensionless distribution standard deviation	
σ_m	Distribution standard deviation	
σ_{sb}	Stefen-Boltzman constant	[W·m^{-2}·K^{-4}]
τ	Time constant	[s^{-1}]
τ_o	Transformer oil time constant	[s^{-1}]
τ_w	Transformer winding time constant	[s^{-1}]
ϵ_N	Expected error in the Monte Carlo simulation	
θ	Soil water content	
μ	Air dynamic viscosity	[Pa·s]

Chapter 1 Introduction

1.1 Current state of the electrical power industry

Currently the electricity industry is facing a series of transformations caused by technological, economical and political changes. Some of these changes represent an opportunity for distribution network operators for improving service quality and returns, whilst others represent challenges that tend to modify previous operational methods. The development of technologies in other areas such as telecommunications and computer science represents an opportunity for distribution network operators. This makes lower cost effective communication and computational power available, which can be used for broadening the monitoring of the state of the power network and extending the application of automated control, thanks also to improvements in the fields of artificial intelligence. Improvements were also made inside the electric industry, in areas such as power generation from small-scale generators (mainly combined heat and power generators in industrial plants) and power generation from renewable resources.

This allows energy to be converted in power plants requiring reduced initial investments, but also to be connected to the medium voltage electric network, often closer to the final customer but sometimes in very remote areas of the network. This can often become a problem since the distribution network was conceived for transferring electricity transmitted at high voltages to the final customers at low voltages, and often it lacks a complete monitoring of its state. The application of new technologies to the electric distribution

network in order to make it more responsive to changes and to integrate the action of all its users is usually identified with the concept of Smart Grid, described in detail in Section 1.2.

From an economic point of view, developed countries saw a reduced increase in energy consumption, and the energy intensity of their economies continued to shrink since the ‘70s. Improved quality of supply, along with the efficiency improvement of the whole system is a method for electricity companies to increase their revenues without counting only on increased demand. Another economic problem faced by the electric industry in many developed countries, is the ageing of the infrastructure: with an electric network built mainly in the ‘60s, many components are at the end or in the second half of their expected life cycle. This situation represents both a challenge and an opportunity, since older components can be replaced by more advanced ones, but it also makes techniques for extending component lifetime and delaying replacements and network reinforcements interesting.

From a political point of view, the electric industry in developed countries is pushed to reduce its production of greenhouse gases, mainly CO_2. This is achievable with electricity consumption reduction and with the reduction of the fraction of electricity produced using fossil fuels. Public incentives for electricity produced with renewable resources are at the origin of the recent steady growth of electric power generated by renewable resources, mainly wind, waste, biomass and solar. Incentives in some countries have also the intention of creating a competitive industry with positive effects on the employment and reduction of fossil fuel imports. Politics influence the electric industry also through direct regulation. Currently in the UK, the previously nationalised electricity industry was privatised and assumed a complex structure, with several companies acting as generators, distributors or suppliers, each one with its own regulations. Another political aspect influencing this research is represented by the increasing difficulties in obtaining building permission for new infrastructure. This makes it preferable to increase the utilisation of existing assets or

alternatively, to refurbish existing facilities or building new ones in sites already used for the same scope.

In summary the current drivers for the electric industry that are expected to continue to shape its aspect in the future are: increased connection of distributed generation, increased connection of renewable energy characterised by a relatively uncontrollable output, ageing of the infrastructure and availability of new technologies for active network management. The work described in this thesis aims at producing a solution to a particular problem: to inform distribution network operators about the thermal state of their network. The first objective of this research is to facilitate the connection of renewable energy plants, followed by allowing a more flexible management of the network also in situations where thermal limits have been reached because of load growth. As seen previously the connection of distributed generation to the electric network presents numerous aspects and challenges, but is expected also to produce additional benefits for society in general and the electric industry in particular. The system described in this thesis, would allow the limit imposed by conservative static ratings to be replaced with more realistic ratings assessed in real-time. This is expected to be part of a portfolio of solutions, currently under development in public and private research centres to face most of the difficulties present today in the electric industry.

1.2 Current research trends

Along with research aimed at improving traditional power system components, the main research effort for the electric power industry and in particular for distribution networks aims at developing frameworks and tools for integrating the action of all of its users in order to improve quality of supply whilst reducing the cost of the electricity transferred. In Europe a specific technology platform, the “SmartGrids European Technology Platform for Electricity Networks of the Future” (1) was created under the supervision of the General Directorate for

Research of the European Commission with the aim of carrying out high quality research and mobilising private and public investments. Similarly, in the United States, different initiatives have been launched in this sector such as the allocation of a combined public and private fund of $8 billion to spur the transition to a smart energy grid (2).

Although there is not a unified definition of smart grid, a series of characteristics are unanimously accepted as being peculiar of a smart grid:

- Accommodate distributed generation
- Active control
- Monitoring network state
- Communication through the network

One of the main reasons for interest in this approach is its ability to accommodate distributed generation and variable distributed generation from renewable energy without or with reduced expensive network reinforcements. This also means to make the transition from a vertical structure with a top-down flow of energy from the highest voltages levels, to a horizontal structure with local exchanges between actors of the network at a low or medium voltage level. Another key characteristic of the smart grid is the presence of active control for increasing power quality, reducing losses and disruptions and controlling a series of parameters currently considered as static or as an external condition, such as line rating or customers load. The distribution network was conceived for passive operation with limited control and monitoring. An extensive monitoring of the state of the distribution network is difficult and expensive because of the networks large size, but reductions in cost of the monitoring equipment and the application of estimation techniques are expected to overcome, at least in part, this problem. Finally, in order to coordinate the different actors of the network, and to provide centralised or distributed active controls with the necessary information,

communication across the network must be available, either through third party communication companies or through the same network.

Real-time rating, the technology described in this work, is a technology aimed at solving specific distribution network problems in the framework of the current research stream. Real-time rating in particular makes use of distributed sensors, specific algorithms and communications between the sensors and the computer where the algorithm runs for estimating maximum component rating. The interest in this technology arises from the observation that currently static power system components are based on conservative assumptions, as explained in detail in Chapter 3. On the other side, real component current carrying capacity is variable and influenced by environmental conditions such as air temperature or wind speed. Therefore monitoring component real-time rating would allow a greater amount of energy to be transferred through the network, without requiring expensive network reinforcements, which could also require new permissions that may be difficult to obtain.

1.3 Active network management based on component thermal properties

Considering the interesting opportunities offered by the dynamic thermal rating technology, a research consortium was formed with the objective of developing and testing a distributed generator power output controller informed by network components real-time ratings in the project, called “Active Network Management Based on Component Thermal Properties”. The members of the research consortium are: Durham University, ScottishPower EnergyNetworks, AREVA-T&D, PB Power and Imass, and the project benefited from the partial funding of the Department for Innovation Universities and Skills.

ScottishPower EnergyNetworks, a distribution network operator, is interested in the development of active network management in order to increase asset utilisation and to facilitate the connection of distributed generation on its own network. In the project, this company provided a network suitable for study in an area where the development of new wind farms is expected to create thermal overloads in different parts of the network. The company provided access to its infrastructure for the installation of monitoring equipment and of the test system. Thanks to this research, the company has an improved understanding of the thermal behaviour of its own network and of the potential benefits offered by this technology. Thanks to the positive outcomes of this research, ScottishPower EnergyNetworks has expressed further interest for a new research in the area of real-time rating with Durham University.

AREVA-TD, a manufacturer of components and controls for transmission and distribution networks, is interested in active network management in order to offer to its customers, primarily transmission and distribution network operators, the most advanced technologies for dealing with the new scenarios identified in Section1.1. In the research, this company provided the hardware necessary for the practical implementation of the system and the installation in two substations of the network mentioned above. Thanks to this research, AREVA-TD broadened its portfolio of active network management tools and is currently working on the integration of the codes developed in the project and its substation automation computers.

PB Power, a management consultancy firm, is interested in broadening its portfolio of technical expertise in developing technologies such as dynamic thermal rating. It acted as the project manager of the research project and provided valuable technical advice. This company is currently developing a planning tool for assessing the impact of dynamic thermal rating on

the distribution network as a method for alleviating thermal overloads caused by the connection of distributed generation.

Imass, an IT consultancy firm, is specialised in geographical based information management for utilities and is interested in broadening its portfolio of expertise. It acted mainly as a consultant during the development of the code, providing valuable technical advice.

The reasons that convinced these companies, among the most important national and international players in the power systems industry, represents a confirmation of the expected relevance of this technology in the future of distribution network. Furthermore, the interest in utilising and developing internally other tools based on the algorithms realised during this research, is considered as a confirmation of the appreciation and quality of the work done.

Inside the consortium, Durham University was in charge of the development of the algorithm, acting also as a scientific consultant and providing drive during the project. The work undertaken at Durham University is divided in two separate work streams: the development of the real-time rating estimator and the development of the distributed generators output controller. The work described in this Thesis is relative to the first work stream, carried out by the author, whilst the second work stream was carried out by S. C. E. Jupe, another PhD student at Durham University. Because of the close link between the two works, however, the distributed generator output control algorithm is frequently mentioned in this work, and a description of its behaviour is also provided.

1.4 Dynamic line ratings

1.4.1 Statement of the problem

Currently, static ratings are applied to power system components such as overhead lines, electric cables or power transformers. The rating of these components depends on their ability to dissipate to the environment the losses generated by the Joule effect. In turn, this is dependent on the external environment, and parameters such as air and soil temperature or wind speed and direction. Due to the variability of these environmental conditions and to the fact that they are usually not monitored by distribution network operators, conservative static seasonal values are used for calculating static ratings. The development of methods for exploiting variable ratings is expected to introduce greater flexibility in distribution network management and to facilitate distributed generation connection. This is dependent on the availability of cost effective, accurate, precise and reliable real-time estimation of power system component rating, with an acceptable spatial and temporal resolution.

In summary they are:

Accuracy: The system must be able to provide rating estimates with the lowest possible error.

Precision: The system must be able to assess the error associated with the estimate given and this error should be reduced as much as possible.

Reliability: The system must be able to provide real-time rating also in case of measurement or communication failures, reducing gradually its performance. An in-depth description of these points, necessary for providing the necessary confidence for a practical adoption of the real-time rating system, is given in Section 6.1.

Spatial resolution: The system must be able to provide estimates with a spatial resolution sufficient for the identification of hot spots and thermal bottlenecks. Electric

circuits made by overhead lines and electric cables can be extended over long distances and different environmental conditions such as line orientation, soil surface roughness or soil composition. Therefore, the rating of the conductor will change along the path and it is necessary not to exceed the rating of the most constrained component.

Temporal resolution: The system must be able to provide estimates within an acceptable time limit, in order to prevent the insurgence of potentially dangerous situations created by reduced component thermal capacitance, environmental conditions variability and electric power transfer variability.

Cost effectiveness and ease of deployment: The cost of the system must be justified by the economical return in terms of enhanced network reliability or power transfer capability. Furthermore, the deployment of the system should not be too invasive, possibly without requiring outages.

1.4.2 Possible solutions

Since component rating can not be measured with a device, alternative parameters should be used for assessing the amount of power that can be transferred through the component. The considered possible solutions are listed below:

- Temperature measurement
  - Local measurement
  - Resistance measurement
  - Distributed temperature sensing
- Environmental condition monitoring and rating estimation

Temperature measurement: consists of measuring directly or indirectly the temperature of the component, in order to compare it with its maximum rating operating temperature. The

main advantage of this method is that only one parameter is measured and this parameter is relative to the conductor, giving a measurement of part of its state. The main disadvantage is that component temperature is not a measure of component rating and this second parameter would be more useful in a real-time control, therefore additional approximations would be necessary in order to exploit this measurement. Each of the three possible methods of temperature measurement listed above presents advantages and disadvantages:

Local temperature measurement is carried out with temperature sensors on the component's surface. The sensor is coupled with a transmitter (usually radio or GPRS) usually powered by induction with the magnetic field around the overhead line conductor. This solution is suitable for the measurement of a few hot-spots, but its cost tends to increase linearly with the spatial resolution required and the length of the line. Furthermore, in order to measure the temperature on the three phases, it is necessary to install a measurement device on each conductor. An example of this approach can be found in (3).

Resistance measurement consists of measuring the resistance of the conductor through the measurement of electrical parameters such as voltage drop, current and phase. The temperature is then calculated from the relation between resistance and temperature. The main advantages of this system are that electrical parameters are usually already measured in the network and that usually resistance measurement is very precise. The main disadvantage is that this system provides only an averaged measurement of the temperature and is not able to identify hot-spots. An example of this approach can be found in (4).

Distributed temperature sensing allows overcoming the problems of these two technologies, providing a number of temperature measurements along a whole circuit. The measurement is carried out through an optical fibre built into the conductor (new models) or wrapped around (already installed equipment). An example of this approach can be found in (5).

An alternative option is environmental condition monitoring and rating estimation. Local meteorological stations are used for measuring environmental conditions in selected locations in the network area. Data are then sent through radio or GPRS to a database where software uses them for calculating component temperatures or component ratings in the meteorological station location thanks to component thermal models. Additional algorithms can be used for calculating environmental conditions in areas not directly instrumented with meteorological stations. The main advantage of this system is its scalability and cost effectiveness, since with few meteorological stations it could be possible to cover a large area with different circuits at different voltage levels. The main disadvantage is that the system does not provide a measurement of a state of the component, but, an estimation based on mathematical models and on the measurement of their variable inputs. This is likely to reduce system accuracy and precision. An example of this approach can be found in (6).

In Table 1 a summary of the different solutions is provided. For each one of the six parameters identified a grade between 1 (minimum) and 3 (maximum) has been given to each solution and the distributed temperature sensing along with the rating estimation from environmental condition monitoring were found to be the most promising technologies. Finally, considering that the negative effects of reduced accuracy and precision in rating estimation from environmental condition monitoring can be mitigated by improved algorithms and selectively placed local temperature measurements, this technology is considered the most promising one.

Table 1: Technologies comparison against main performance parameters

	local temperature measurement	temperature estimation from resistance measurement	distributed temperature sensing	rating estimation from environmental condition monitoring
Accuracy	*3*	*1*	*3*	*2*
Precision	*3*	*1*	*3*	*2*
Reliability	*2*	*2*	*2*	*2*
Spatial resolution	*1*	*1*	*3*	*3*
Temporal resolution	*3*	*3*	*3*	*3*
Cost effectiveness	*2*	*3*	*1*	*3*
Ease of deployment	*3*	*2*	*1*	*3*
TOTAL	*17*	*13*	*16*	*18*

As shown in Table 1, component state estimation through environmental condition monitoring is the technology which best performs against the seven parameters chosen for characterising the potential of a real-time rating system. The solution developed in this project is therefore based on this methodology, while at the same time trying to overcome its main disadvantages. A schematic view of the solution developed is shown in Figure 1.

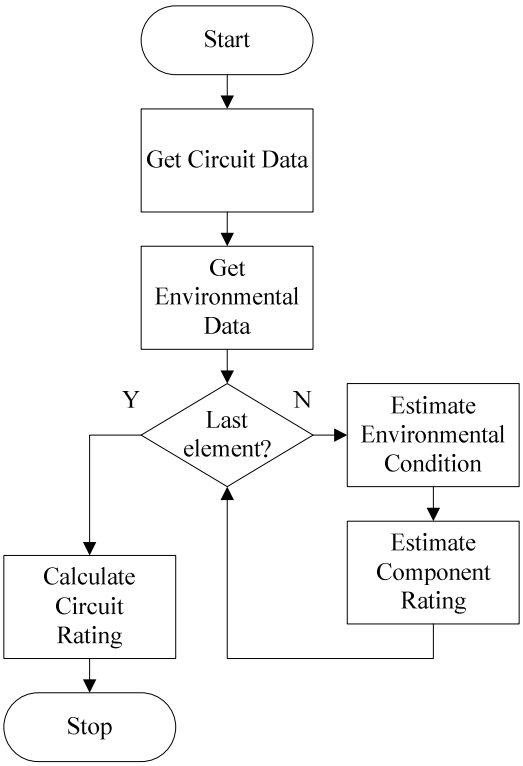

Figure 1: Circuit thermal rating algorithm, flow chart

The algorithm is based on a network model where each circuit is divided in several components characterised by uniform conditions, such a same conductor type or same environment or orientation. When the rating of a circuit is done, the algorithm load data relative to the circuit and real time environmental condition from meteorological stations. Environmental conditions are then interpolated in each component location and the rating for each component is calculated. Each rating is not represented by a single number, but by a probability distribution taking into account inputs variability and the effect of possible measurement and communication failures. The different probability distributions are then combined in order to identify the probability distribution of the rating of the whole circuit, and finally a single value is selected in function of a predetermined level of risk.

1.5 Research Objectives

The research described in this work aims at developing a power system real-time rating system based on component thermal properties and suitable for implementation on a real world application. In order to do so, the solution developed must be cost effective and allow safe operation of the network along the technical specifications summarised in the list below, developed after consultations with distribution network operators and design and protection engineers of different firms of the research consortium.

- To be cost effective, to require little maintenance and little running cost.
- Not to infringe statutory clearance limits for overhead lines
- Not to endanger secure network operation, in particular:
    - In the case of sudden drops in wind speed that would leave an overhead line with a power flow greater than the real-time rating.
    - In the case of inaccurate estimation of the network's thermal state

    - In the case of thermal overloads not relieved because of the temporal or the spatial resolution of the real-time rating system.
    - In the case of thermal overloads generated on non-monitored components
- Not to inflict permanent damage to the component
- Not to reduce component lifetime
- To provide safe estimations in case of measurement or communication failures

The development of the real-time rating system must also be supported by studies highlighting potential benefits and issues arising from a practical implementation. A summary of the questions that this research aims to answer is provided in the list below.

- To identify previous projects on power system component thermal monitoring, assessing strength and weaknesses of the approach followed.
- To identify the most suitable architecture for the real-time rating system able to satisfy the points identified in this list.
- To quantify the impact of the implementation of a real-time rating system on renewable energy integration.
- To quantify the impact of the active network management system developed in the consortium when informed by real-time ratings.
- To identify situations where real-time ratings could be applied and should not be applied.
- To quantify the increased component rating (in MVA) and the increased power transmission capacity (in MWh) obtainable with the use of real-time rating.

1.6 Thesis overview

The present work is structured in the following way:

Chapter 2 presents a review of previous work undertaken in the research area covered by this study. In Section 2.1 a short description of real-time rating systems deployed or conceived is given. The literature regarding the power system component thermal models used for real-time rating is reported in Section 2.2. Section 2.3 describes literature regarding environmental conditions modelling and Section 2.4 describes work in the area of electrical and thermal state estimation in power systems. Finally, in Section 2.5 the existing literature is analysed and the research area of this work is clearly defined and positioned in the context of the existing research on the topic.

Chapter 3 describes the models used in the state estimation algorithm for power system component rating and environmental condition interpolation and correction. Section 3.1 contains power system component models description, whilst environmental conditions models are described in Section 3.2. Finally in Section 3.3 conclusions on the models developed for the real-time rating algorithm are drawn.

In Chapter 4 the state estimation technique used for real-time power system component rating is described. A review of the possible techniques is given in Section 4.1 and following to the selection of the Monte Carlo method, in Section 4.2 a detailed description of this method is given. Finally in Section 4.3 main conclusions on the state estimation technique adopted for the real-time rating algorithm are drawn.

Chapter 5 presents a description of the actual algorithm developed for carrying out real-time rating estimation of power system components. The algorithm is described generically in Section 5.1, while in Section 5.2 the seven classes developed for describing methods and data structures of the problem are described. Section 5.3 provides a description of the databases used and in Section 5.4 the structure of the algorithm and the flow of information during the rating estimation of a component are described. Finally, in Section 5.5 the main aspects of the algorithm developed are summarised, analysed and conclusions are drawn.

In Chapter 6 the state estimation algorithm validation against field data is presented. Firstly, in Section 6.1 the validation strategy adopted is described: Section 6.2 presents the validation of the analytical models used. Section 6.3 presents the validation of the whole real-time state estimation algorithm, whilst in Section 6.4 the results of the validation process are discussed.

In Chapter 7 a study on the influence of environmental condition on power system components is presented. The datasets used for the simulations are introduced in Section 7.1 and in Section 7.2 the simulation results are presented. Finally, conclusions regarding the expected increased headroom obtainable in consequence of the installation of the real-time rating system developed in the research are drawn and exposed in Section 7.3. Finally, in Chapter 8 the findings of the research are discussed, and in Chapter 9 conclusions are drawn and scope for further work is identified.

1.7 Author's publications

A list of the author's publications published in scientific journals, conferences or books is provided below:

Journal papers

1) A. Michiorri, P. C. Taylor, S. C. E. Jupe and C. J. Berry, "Investigation into the effect of environmental conditions on power system ratings", *Proc. IMechE Part A: J. Power and Energy*, vol. 277(7), pp. 743-757, 2009;
2) A. Michiorri, P. C. Taylor and S. C. E. Jupe, "Overhead line real-time rating estimation algorithm: description and validation", *Proc. IMechE Part A: J. Power and Energy*, vol. 224(3), pp. 293-304, 2010;

3) S. C. E. Jupe, P. C. Taylor and A. Michiorri, “Coordinated output control of multiple distributed generation schemes”, *IET Renewable Power Generation*, vol. 4(3), pp.283-297, 2010;

Book chapter

4) S. C. E. Jupe, A. Michiorri and P. C. Taylor, “Increasing the energy yield of generation from new and renewable resources, in *Renewable Energy*. Vienna, Austria: IN-TECH, 2009, chapter. 1, pp. 1-26;

Conference proceedings

5) H. T. Yip, C. An, G. Lloyd, P. C. Taylor, A. Michiorri, S. C. E. Jupe, M. Bartlett and A. Beddoes, “Dynamic thermal rating and active control for improved distribution network utilisation”, 10th IET International Conference on Developments in Power System Protection, 2010
6) A. Michiorri, P. C. Taylor, “Forecasting Real-time Ratings for Distribution Networks Using Weather Forecast Data”, CIRED, 2009, Prague.
7) D. Roberts, P. C. Taylor, A. Michiorri, “Dynamic thermal rating for increasing network capacity and delaying network reinforcements”. CIRED Smart Grids, 2008, Frankfurt, Germany,
8) S. C. E. Jupe, P. C. Taylor, A. Michiorri, and C. J. Berry, “An evaluation of distributed generation constrained connection managers,” in Proc. 6th

Mediterranean Conference on Generation, Transmission and Distribution, Thessaloniki, Greece, 2008

9) A. Neumann, P. C. Taylor, S. C. E. Jupe, A. Michiorri, A. Goode, D. Curry and D. A. Roberts, “Dynamic thermal rating and active control for improved distribution network utilization,” in Proc. PowerGrid, Milan, Italy, 2008

10) P. C. Taylor, P. Trichakis, S. C. E. Jupe, A. Michiorri and P. Lyons, “Active management of MV and LV distribution networks”, in Proc CIGRE NGN, Paris, France, 2008

Chapter 2 Literature review

2.1 Related work

Active network management is a broad research topic in the academic and industrial environment. The reasons for this are twofold: firstly due to the planned development of DG and secondly due to the attempt to delay network investments forced by the rise of the energy demand. It is important to note that the European Union Research Commission on Energy considers the development of active network management as important for the future of energy as the development of renewable technologies such as photovoltaic or fuel cells. It is in fact a prerequisite for their diffused interconnection. For this reason, it was one of the key actions during the FP7 Programme (7).

It can be demonstrated (8) that for loads up to 11kV a voltage rise limit is usually met before thermal constraints are violated, whereas for greater voltages it is the thermal limit that typically constrains the capacity for the connection of DG. Being interested in the higher voltage part of the distribution network, attention will be focused on the thermal behaviour of the components and on the research carried out on them. This is a research topic that covers different branches of engineering: electrical, mechanical, control and it is also a promising area for IT applications. This complexity dramatically reduces the possibility to develop complete systems, and this can also be seen in the published literature, where work about a complete real-time rating system are a minority. As it is one of the most economic and more

effective methods for overhead lines uprating (9), (10) the interest on it has continued to increase in the last years, being concentrated almost entirely on the transmission network, due to its strategic importance and its minor extension. According to (11), in the year 2000 there were more than 50 electricity companies using some transmission lines monitoring system for evaluating its thermal limitations, and most of them were based on a tension measurement method. A quite different method, requiring a thermal state evaluation, was developed by Red Electrica de Espana and IBERDROLA in 1998 (6). Here a minimal number of meteorological stations are used to gather real-time data. The data is then processed using a meteorological model based on the Wind Atlas Analysis and Application Program (WAsP) (12), taking into account the effect of obstacles and ground roughness, and finally the rating is calculated. These works have been developed by electricity companies and they cover generally only overhead transmission lines.

There are two other works, describing quite different and more complex projects. EPRI's work on this subject is described in (13) and (14), whilst in (9) the project started by NUON in 2004 is described. In these papers, methods for measurement and real-time rating of overhead lines, electric cables and power transformers are described, respectively for transmission and for the distribution networks. Research in the area of state estimation techniques for component rating proved the necessity of reliable and accurate environmental condition monitoring in order to obtain accurate component rating estimates.

Other work is more specifically centred on one of the power system components. They describe the possible gains achievable using a real-time rating system on them and the related problems. Overhead lines are the most studied, such as the work by Henke and Sciacca (15), where they describe the possible gains and the avoided dangers in using real-time rating on an overhead line. Work by Belben and Ziesler (16) and Helmer (17) study the interesting correlation between wind farm output and overhead lines and power transformer rating. With

regards to electric cables, the work by Bascom (18) can be cited, even if their rating can not be easily related to renewable energy output.

2.2 Component modelling

2.2.1 Overhead lines

The most common model used for overhead line conductors rating is described in (19) and has been adopted by the IEEE for the thermal rating of overhead lines (20). Another model is proposed by the IEC in (21), even if this standard is quite general and covers not only the thermal behaviour, but also the methods to calculate other mechanical parameters for the calculation of the sag. An additional suggested standard is the one proposed by CIGRE (22): in this paper an accurate thermal model is proposed, enabling calculation with different levels of precision, depending on the information availability. The IEEE model has been tested and challenged several times as in (23) or (24) in wind tunnel and in both a mismatch between the calculated and measured values has been found for the dependence of convective heat transfer on wind direction.

Elsewhere, in (25) and (26) the temperature distribution inside conductors is studied, with an analytical and a numerical approach respectively. Finally it is important to mention (27) where many aspects concerning the conductor design are considered and different software that is used in this field are cited; it is also a valuable source of reference for further investigation on the design topic. Fundamental work for the thermal rating of overhead lines is reported by Davis (28) and (29), where the model used for the thermal rating, the heat exchange, and a statistical analysis of the environmental conditions relevant for the thermal rating itself are analysed, describing also a correlation between wind speeds and air

temperature. In particular, it analyzes the air temperature and the wind speed and direction for a period of over 25 years at Detroit Airport. In (30) the thermal ratings for overhead transmission lines have been calculated using weather measurements in ten places in the Rocky Mountains for one year, the data has been used to calculate a cumulative probability for the conductor's ampacity. Furthermore, it has been identified in the low wind speed measurement the greater source of error between calculated and measured conductor temperature values. In another work (31) by Foss and others, the same measurements are conducted in three different places in New England, measuring not only the environmental conditions but also the real temperature and the current carried by the conductor. In (32) an interesting method to select the transmission lines suitable for real-time ratings is presented. The load cumulative frequency is an independent field of study and it is linked with the thermal rating, for this reason it would be important to cite at least one work on this topic: (33) in particular compares the load on eight lines registered over a period of one year in three different continents.

The presence of data uncertainty is studied in (34) where the IEEE model is used to calculate the current carrying capacity of an overhead conductor, underlining the effects of the lack of information, and showing how it can result in an error of 50% on the determination of the temperature of the cable. In (35) another study on dynamic line rating is presented, in this work the thermal rating is assessed with measured weather data, exploring also the possibilities for a line rating forecast.

Overhead lines are not characterized only by their thermal behaviour: being conductors exposed to the environment they have to withstand atmospheric loads like wind and ice. Moreover, the sag of the catenary and the clearance from the ground or from other objects is a fundamental aspect of line design, concerning also legislation. Therefore, even if it is not a central topic of this research, it is important to consider it. The basic relation to calculate the

sag of an overhead line can be found in (36) or (37) where the attention is focused on the limitations of the ruling span method used for the line design. Other aspects on the sag calculation are quoted also in (38), (39), (40) and (41), focused particularly on different methods to increase the precision of the calculations. On a normative point of view (here only the IEC international standards are considered), (21) can be used not only to calculate the current carrying capacity of the conductor, but also its capacitance and inductance and the elongation parameters. Those last parameters can be used in the temperature-tension relation described in (36) or (37), rather than the external loads (wind, ice) can been found in (42) and (43)

2.2.2 Electric cables

The basic thermal model for the calculation of the current carrying capacity of electric cables was developed by Neher and McGrath in 1957 (44); in this work the cable is considered as a series of concentric layers composed of insulators (thermal resistances) and conductors (heat production). Methods to calculate the thermal resistances and the dissipations inside the metal sheaths are given in the document, with tables and formulae to consider the effect of multiple cables. Other work was developed in more recent years by Anders (45), considering a greater number of particular cases and improving part of the calculations, even if the structure of the modelling was not changed. These researches are the main source of the relevant international standard used in the UK (46).

Furthermore British distribution network operators refer for practical purposes also to the engineering recommendation ENA ER17 (47). In this document rating values are given in tables for each cable type, with correction values considering the effect of different external conditions. In time, work has been produced to improve the calculation method of different

parts of the model cited above without bringing modifications to the basic model. Anders in (48) proposes several improvements, refining the calculations of losses and cable temperature considering the real power flow. Finally, in (49) a new analytical model is suggested for considering the dynamic behaviour of multiple cables in different configurations, comparing it with other existing models.

The method for calculating the external heat exchange with or without the presence of solar radiation is challenged by Haskew (50) who suggest a Newton Raphson method instead of the currently used Gauss-Siedel one. A comparison between the two methods is provided showing the advantages of the proposed method. A model for cables wrapped in fireproof material, used in nuclear power plants, is proposed by Figueiredo (51). The results of this analytical model were compared with experimental results, suggesting how to improve the precision of the method. Sellers in (52) suggests improvements in three different parts of the IEC standard cited above: an improved method for calculating the effect of mutual heating of differently loaded cables, and reviewed models for the thermal resistance of fluid layer of pipe type cables and for the external thermal resistance of concrete-ducts banks. Finally, Bontempi (53) exposes a semi-physical model of the cable and discuss its implementation in a learning control for the DTR, completing the work with a case study on medium voltage cable.

Currently numerical simulations are becoming particularly popular in the electric cables industry especially for calculating particular cases that can represent hot spots able to reduce the rating of an entire line. A particularly complete work in this sector is the one of Aras (54) where results from finite element simulation are compared with results from the IEC standard analytical results and with laboratory experiment results. Work by Hanna (55) and (56) is focused on cables in multi layered soil. The model and the solution algorithm are shown in the first paper and a particular application considering three cables in a trench is presented in the second. A numerical simulation to calculate cable ampacity was carried out by Freitas (57)

focusing in particular on external conditions: firstly, developing a model describing soil heat and moisture migration, and then solving it with a finite element technique.

A general numerical simulation, concerning cable losses and external thermal resistance calculation is described in the work by Garrido (58), where a system of three cables in steady-state and in a short circuit situation is considered. A variable step discretization is used in order to reduce the points. An attempt to give a generalized way to solve the problem of the rating of cables systems is shown in the work by Hiranandani (59) based on a two dimensional finite differences model considering both cables touching and cables separated by an insulator medium. Another finite element model is proposed by Hwang (60) for the rating calculation of cables in duct. In particular, numerical methods are used for calculating both the electromagnetic field causing losses in the conductor and in the sheets, and the heat exchange between cable and duct, which is non-linear because of the irradiative heat transfer. Finally, it is important to cite the work by Kovac (61) where the problem of the evaluation of the losses is solved numerically, along with the external heat exchange through the ground. In particular, this model is applied for touching cables in flat formation and a re-examination of the IEC standard is proposed.

Another field of study concerning the rating of electric cables is the study of the external parameters influencing the ampacity. The heat exchange at the soil/air interface for the rating of buried cables systems is studied in the work by Buonanno (62) where different radiation sources (direct and indirect) are considered. Lyall (63) describes the results of ground parameters measurements (thermal resistivity and diffusivity) and their dependence on the rainfall. Then optical fibre DTS measurements inside the insulation sheet and outside the insulation are compared. Another work concerning the measurement of ground parameters is (64) by Milun, where the use of a spherical probe is described, describing how it can be used both in field measurements and in limited samples of soil. Finally, Dang (65) presents a study

on the thermal ageing of the dielectric insulation comparing data and models from more than 200 papers, and selecting the model of Simoni and Montanari (66) as the one that best suits with experimental data. The application of measurement devices for temperature measuring in electric cables systems is a developing research area, usually called Distributed Temperature Sensing (DTS). Built-in sensors would help to rate dynamically the cables, but these extensions of distribution systems and the cost of the instruments, the necessary frequency and the precision of the instruments are object of continued studies. A comparison between optical fibre measurements and predicted values is described in the work by Yilmaz (67) where the greater accuracy of DTS compared to mathematical models is highlighted, especially for recording the effect of external parameter variations. In the work by Kawai (68), a DTS system realized with a built-in optical fibre is used for locating faults, illustrating in field tests better performance in terms of measurement accuracy in comparison with thermocouples.

The possibility to estimate external parameters for cables rating, considering the data from a distributed temperature sensing system is explored by Li (69). The methodology was used also for hot spot location and validated by laboratory experimental tests. Finally, the work by Nakamura (70) focuses on measurements of joint temperatures, those points often representing the thermal bottlenecks of a whole line. The use of thermocouples and optical fibres for the measurement of joint external temperature is proposed, to calculate then conductor temperatures with differential equations.

2.2.3 Power transformers

The industrial standards (71) and (72) cover the entire field in its different parts and provide thermal models and parameters. Those two standards represent the state of the art in

thermal modelling for power transformers, even if their need to cover a large number of different models does not let them to be too specific. For this reason, they are continuously challenged by different research, and the availability of greater computational resources makes the use of numerical simulations more and more desirable. Preis and Biro present a complete work about thermal modelling in (73), where a finite element method for the magnetic and fluid dynamic field is applied to determine the temperature rise. Other research like (74), involve the numerical modelling only of the thermo fluid dynamic aspect of transformers. Most of the research is focused on the development of simple finite element thermal models, often with the use of iterative methods.

Those models present an intermediate complexity level between the one dimensional one proposed in the standards and the fully developed 3D one used in numerical simulations, requiring less design information than the last but yielding a greater accuracy than the first. A clear and exhaustive work in this sector is the one done by Susa introduced in (75) and summarised in (76), where an electrical analogy is used to simulate the dynamic thermal behaviour of a power transformer; the model was thereafter tested on a real asset and the results compared with the IEEE model in (72). After that, the proposed model was refined in (77), where the nonlinear resistance of the winding and the thermal capacitance were more carefully studied. An electrical analogy is used also in (78) and (79) by Ryder to calculate winding and core temperature rise. The results obtained were compared with measurements on two AREVA transformers obtaining limited errors. It is important to note that both the calculated and the measured values are smaller than the ones recommended in the standards for the rating and the calculation of the ageing.

Further work was done in Liverpool by Tang (80), (81), and (82) based on the thermal-electrical analogy. In those cases, the authors used a lumped parameter model (more or less refined depending on the publications) to calculate with greater accuracy the intermediate

parameters used in the standards. The model was tested on National Grid measured data. In (83) Radakovic and Feser suggest how to use a set of differential equations to calculate the hot-spot temperature. They suggest also how to calculate the necessary parameters with short circuit thermal measurements. Using differential equations, the model is strictly dependent on the initial hot-spot temperature, which is unknown in general; the same authors discuss this and other problems in (84).

An analytical model is proposed in (85) by Pradhan and Ramu. Aware of the need of design data, the authors suggest a method to calculate the necessary parameters from test measurements. Furthermore, in (85) they develop the model to introduce the effect of winding inhomogeniety. Some papers suggest improvements to the current used standards, focusing only on some particular aspect of the existing industrial models.

In (86) the dynamic behaviour under current step changes is studied: real measurements are compared with the IEEE model and an improved model consisting in a double time constant is suggested. In (87) Tojo uses a simple model for the calculation of the main parameters to suggest an improved loading guide. In the work by Lachman et al. described in (88), the model described in the IEEE relevant standard is used in an algorithm that not only considers the real-time state of the machine, but takes also into account any long term deterioration in the thermal performance. Finally, research has been carried out about transformers life and ageing. Among them Pandey (89) describes laboratory tests on the insulation paper, describing the ageing on the temperature.

2.3 Environmental condition modelling

In power systems, the modelling of environmental conditions is usually related to wind farm power output forecast or assessment. On the contrary, very little work was carried out

for assessing real-time component rating. Noteworthy exceptions are presented in (90) where meteorological readings from a few meteorological stations are used for calculating soil temperature over a large area to estimate electric cable real-time ratings. In order to do this, the authors suggest the use of a finite elements solution of Poisson's equation, with real-time boundary conditions determined at the soil surface. Similarly in (91) weather readings from a reduced number of meteorological stations are used for calculating atmospheric environmental condition values over a large area in order to calculate real-time overhead line ratings. The solution proposed is based on the inverse distance interpolation technique.

2.3.1 Wind speed and direction

Due to the complex nature of the problem and the number of possible applications, wind field modelling has attracted the attention of many researchers, both in the area of wind farm power output forecast and in general meteorology. A history of computational modelling techniques for wind resource assessment is given in (92) and a comparison of different wind field modelling techniques for wind energy applications is presented in (93). In (94) a nonlinear model for wind direction forecast is proposed and its improved performance over standard models is demonstrated through simulation analysis. The problem of turbine micro-siting is addressed in (95) where the linear model used in Wasp (described and tested in (96)) and the CFD nonlinear model are compared with wind measurements showing how CFD should be preferred to linear models in complex terrains. Other studies are not linked with wind farm power output prediction or assessment but are still interested in wind field modelling at a scale suitable for the real-time rating system developed.

In (97) a three dimension finite element code is developed for the wind field adjustment problem described in (98), providing accurate numerical solutions with low computational

cost and memory storage requirements. Another three-dimensional wind field modelling algorithm is described in (99) showing good agreement between calculated and measured data.

2.3.2 Air temperature and solar radiation

Air temperature presents a reduced variability with respect to wind direction and speed and therefore it is possible to obtain accurate and precise results with simple interpolation techniques. Therefore, the attention of researchers has been focused on the interpolation improvement through the introduction of correction for other parameters such as altitude, solar radiation and precipitations. A comparison of different spatial interpolation techniques, such as weighted averages or linear regression is presented in (100), finding highest errors for all the different models when estimating temperature at high elevation. Altitude correction is studied also in (101), where two different techniques for air temperature interpolation and altitude correction are compared. Between the two techniques: the authors identified temperature potential calculation from the hydrostatic equation as the most suitable method for air temperature correction.

Another fundamental parameter influencing air temperature is solar radiation. The study presented in (102) shows that the solar radiation influence correction methodology proposed is able to reduce air temperature interpolation error. An inverse distance exponential weighted average, coupled with a precipitation correction is presented in (103) and the comparison with two meteorological station datasets indicated a good coincidence between model predictions and observations. The application to air temperature interpolation of the geostatistical technique of Kriging is studied in (104) where seven different approaches are compared in terms of mean absolute error and bias. Regarding solar radiation, considerable research has

been undertaken in order to estimate it for renewable energy production, as in (105), or for use in agriculture, as in (106). They both use interpolation algorithms of locally measured solar radiation values. A different approach considering ground albedo and cloud effect and based on satellite images analysis is described in (107). Finally, a comparison between linear regression and different types of neural networks for solar radiation estimation is presented in (108), showing that linear regression is able to produce more precise results.

2.3.3 Soil temperature and thermal resistivity

Particular attention is given in power system engineering to soil temperature and thermal resistivity measurement and estimation, because of their direct influence on buried electric cable rating. In (90) for example a dynamic soil model is used for calculating soil temperature at cable burial depth, with an error of ±2°C at a distance of 25km. These parameters are also studied for applications in biological systems. In (109) two models based respectively on heat transfer, empirical observation and a third hybrid model developed by the authors are compared with measured data, showing how the hybrid model produces more accurate approximations. In another study (110), the traditional geostatistical technique of Kriging is modified in order to reduce error and results uncertainty in spatial-temporal soil temperature interpolation. Finally, in (111) a radial neural network is used for calculating both soil temperature and soil moisture at different depths.

2.4 Power System State estimation

Electrical state estimation is an established research branch in power systems. It makes use of real-time measures of the state of the network at regular intervals for producing a

representation of the state of the whole network. This is particularly important in distribution networks where most of the components are not monitored and the increase of distributed generation is likely to add new challenges to traditional operating practices. The estimation can be based on measurements of the topology of the network and on the solution of Kirchhoff's law on each node as suggested in (112). The author suggests the use of real-time voltage measurements at the distribution transformers and a probabilistic model of their load profile in order to reduce the number of necessary measurements while increasing estimation precision with the consideration of voltage phase angles.

The reduction of the estimation error is achieved considering the expected load profile at the transformer. A more comprehensive approach is described in (113) where generalised state estimation is described and its potential for estimating not only power flows and voltage excursion, but also network topology and even static network parameters is highlighted. The works summarises also fundamental techniques for identifying the observable part of the network and for processing bad data. Input uncertainty in power system state estimation is described also in (114), where a methodology based on linear programming is suggested for identifying input uncertainty consequences. The weighted least square method is used, as in previous work for calculating a "central" power flow solution at each node. Then linear programming is used for defining the boundaries of the confidence interval.

Currently power system component ratings are based on conservative assumptions based on historical environmental conditions, as described in (115) and (30). A similar approach is described in (116), where a methodology for calculating component rating considering the combination of historical environmental conditions, loads and expected costs related to thermal overloads is adopted. This approach is challenged in research showing the advantages for distribution network operators arising from the adoption of a real-time rating system. A quantitative estimation of the possible headroom unlocked by the adoption of real-

time ratings for overhead lines, electric cables and power transformers is presented in (117) and overhead lines are identified as the component type with highest possible gains. The effect of weather variability on the rating of power transformers is studied in (17) where it is shown that the rating of transformers positioned at the base of wind turbines may presently be oversized by up to 20%. A similar study described in (16) compares the power flow to the conductor real-time rating in an overhead line connecting a wind farm. In this research it was highlighted that high power flows resulting from wind generation at high wind speeds could be accommodated since the same wind speed has a positive effect on the line cooling. This observation makes the adoption of real-time rating systems relevant in applications where strong correlations exist between the cooling effect of environmental conditions and electrical power flow transfers. An application of real-time rating for wind farm connections in the UK is described in (3), where particular attention is given to the necessity to combine the real-time rating system with devices able to manage the non-firm connection of distributed generation.

In (34), (118), (119) the influence of component thermal model input errors on the accuracy of real-time rating systems is studied. The application of different state estimation techniques, such as affine arithmetic, interval arithmetic and Monte Carlo simulations was studied for overhead lines, electric cables and power transformers. Errors of up to ±20% for an operating point of 75ºC, ±29% for an operating point of 60°C and ±15% for an operating point of 65°C were found when estimating the operating temperature of overhead lines, electric cables and power transformers respectively. In order to reduce this error, the opportunity to use an expert system for enhancing rating estimation is explored in (53), where electric cable ratings estimated with physical models are refined with an expert system identifying the most suitable model according to past experience. In (5) a system combining distributed thermal sensing, physical models and learning algorithm is used for estimating

enhanced line rating forecasts. Another expert system informed by short term real-time ratings is described in (120) along with its indoor and outdoor test and its possible application during outages.

2.5 Conclusion

In light of the present literature review, the main research trends for the different relevant topics were identified. In the area of DTR, two main solutions are explored: component temperature measurements and component temperature estimation through external parameter measurements. It was verified that the first method is more precise and expensive, but not necessarily more reliable, due to the dependence on communications devices. Component temperature estimation through external parameter measurements was then confirmed as the most suitable for a practical application in the distribution network. Regarding overhead lines due to the extensive research carried out on overhead lines' thermal modelling and due to its simplicity, further work in this field is not considered necessary. In the area of electric cables, particular attention is given to the calculation of parasitic losses in the sheath or the armour, and to the determination of the external resistance. Numerical modelling is used to study the influence of particular configurations of cable banks and to determine the value of the external resistance.

Study of the transient and the behaviour during step changes and short circuits is also important. The study on the external conditions is probably the most important for this research. In the area of power transformers, studies were carried out in particular on the dynamic behaviour of the machine. Even if the majority of the models proposed are constituted of thermal-electrical analogies, numerical modelling is of great importance. The author's opinion is that more attention has to be given to the modelling of the external heat

exchange, in this case being the link between the machine and the external world. An analysis of the literature published on this topic shows the existence of several gaps and that work still has to be carried out in order to have the theoretical knowledge necessary for the creation of a working and secure real-time rating system. In particular, it was found that the electric network is not considered a “system” with regards to its thermal behaviour. Every component is considered by itself since conservative ratings are then adopted. The influence on the network management of components with different rating is not considered and no method is suggested to identify them. In addition it was found that the greatest part of the literature regarding component rating is focused on the thermal modelling but not on the determination of the external parameters influencing the rating itself. The result consists of a great number of very precise models that have to be used with conservative inputs.

Finally, very little literature was found on thermal state estimation and no complete system is described. The subsequent study on environmental condition estimation techniques highlighted the presence of different possible solutions for calculating the different parameters, mainly based on interpolation with weighted averages followed by corrections based on physical or empirical relations. Although these models can be applied directly for atmospheric parameters such as wind speed and direction, air temperature and solar radiation, a model able to calculate all the soil parameters necessary for buried electric cable rating was not found.

The research presented in this thesis adds to the work described above by describing the principles behind a different real-time rating system and its validation against field data. The proposed solution makes use of sophisticated estimation algorithms, which have threefold benefit: Firstly, the requirements for a large number of equipment installations in order to monitor large network areas are reduced. Secondly, the capital cost of the system is reduced. Thirdly, the estimation algorithm offers a robust solution, which maintains operational

security in the case of measurement or communication failures. Furthermore, the rigorous test carried out on different components in the same network for an extended period provides a detailed description of system behaviour under different operational conditions.

Chapter 3 Algorithm development: Modelling

3.1 Component modelling

3.1.1 Overhead lines

Overhead line ratings are constrained by a necessity to maintain statutory clearances between the conductor and other objects. Temperature rise causes conductor elongation, which, in turn, causes an increase in sag. The line sag (L_{sag}) depends on the span length (L_{span}), the tension (F_t), the perpendicular force applied to the conductor such as weight or wind pressure (F_p) inclusive of the dynamic force of the wind and the length of the span. The sag can be calculated as a catenary or its parabolic approximation, as given in Equation 1. To calculate the tension, it is necessary to solve the thermal-tensional equilibrium of the conductor, as shown in Equation 2. For calculating the conductor operating temperature at a given current, or the maximum current for a given operating temperature, it is necessary to solve the energy balance between the heat dissipated in the conductor by the current, and the thermal exchange on its surface, as given in Equation 3. This model is obtained omitting the effect of creep. General information on conductor rating can be found in (36).

$$L_{sag} = \frac{F_t}{F_p}\left[cosh\left(\frac{F_p L_{span}}{2F_t}\right) - 1\right] \cong \frac{F_p L_{span}^2}{8F_t} \quad (1)$$

$$E_c A_c \beta_c (T_{c,2} - T_{c,1}) + \left(\frac{F_{p_1}^2 L^2 E_c A_c}{24 F_{t_1}^2}\right) - F_{t_1} = \left(\frac{F_{p_2}^2 L^2 E_c A_c}{24 F_{t_2}^2}\right) - F_{t_2} \quad (2)$$

$$q_c + q_r = q_s + q_l \quad (3)$$

3.1.1.1 Detailed analysis of each term

In this section a detailed description of the most important terms of the equations described in Section 3.1.1 is given[1].

The term F_p in Equation 1 represents the force applied to the conductor. This is the sum of the gravity and the dynamic force applied by the wind and can be calculated as in Equation 4 (43). The first can be calculated as the sum of the weight of the conductor ($F_{p,g}$) and of the hypothetical ice ($F_{p,ice}$) present on it and the second is proportional to the conductor area and the kinetic energy of the air flow. These two forces are supposed to be applied in vertical and horizontal direction.

$$F_p[Nm^{-1}] = \left[\left(F_{p,g} + F_{p,ice}\right)^2 + \left(C_{drag} D_c \rho_{air} W s^2\right)^2\right]^{\frac{1}{2}} \quad (4)$$

The terms $E_c A_c$ and β_c in Equation 2 (21) (respectively the young modulus and the thermal expansion coefficient) are referred to the whole conductor and they can be calculated as in Equation 5 and Equation 6 for a steel core conductor.

---

1 In order to help the reader in understanding the thermal equations without using the nomenclature, a summary of the symbols used is given.

c_P $[J \cdot Kg^{-1} \cdot K^{-1}]$, specific heat
D $[m]$, conductor diameter
E $[Pa]$, Young's modulus
H $[N]$, conductor tension
k_f $[W \cdot m^{-1} \cdot K^{-1}]$, fluid thermal conductivity
w $[N \cdot m^{-1}]$, weight per unit length
w_f $[m \cdot s^{-1}]$, flow speed
β $[K^{-1}] \cong \frac{1}{T}$, volumetric thermal expansion coefficient
ΔT $[K]$, temperature gradient between the conductor and the environment
μ $[N \cdot s \cdot m^{-2}]$, dynamic viscosity
ρ $[Kg \cdot m^{-2}]$, fluid density

$$E_c A_c[N] = E_a A_a + E_s A_s \tag{5}$$

$$\beta_c[K^{-1}] = \frac{E_a A_a \beta_a + E_s A_s \beta_s}{E_a A_a + E_s A_s} \tag{6}$$

The effect of different environmental conditions on conductor sag is shown in Figure 2. It is possible to see how a real-time rating system limiting the current to the maximum design temperature, would prevent the conductor to exceed vertical and horizontal clearances. The simulation was carried out for a Lynx conductor with a maximum design temperature of 50ºC with perpendicular winds from 1 to 25m/s. For each point the relative wind speed is reported in brackets on the chart.

The two extreme points corresponds to extreme rating conditions: null wind speed and conductor temperature of 50ºC (completely vertical) and a wind speed of 25m/s on a conductor with an ice cover of 12mm, corresponding to an extreme winter storm, whilst the crosses represents conductor position for intermediate values of wind speed (without ice).

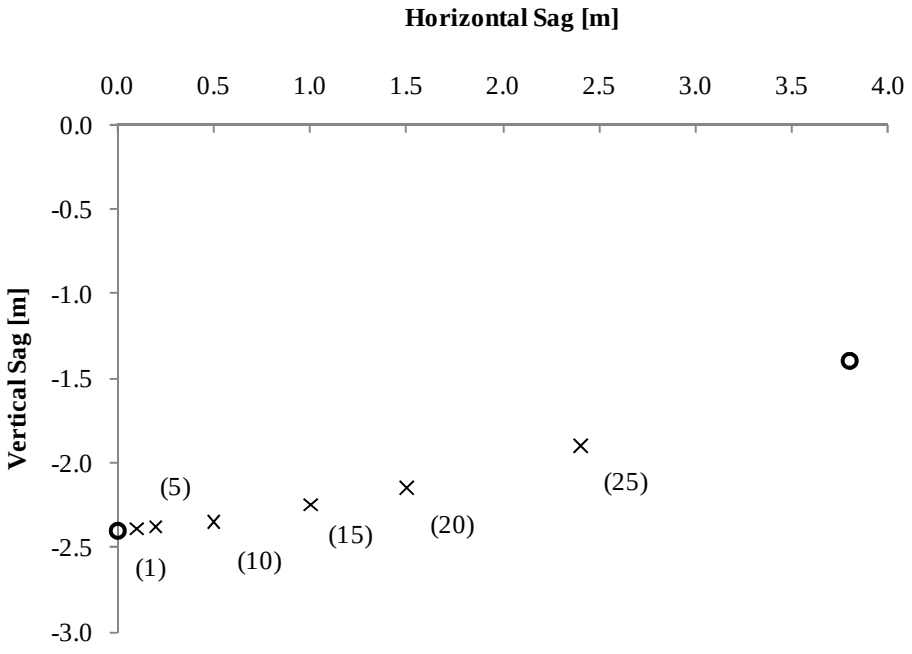

Figure 2: Maximum conductor sag under different wind speeds [2]

[2] A: $T_c = 50$°C, $w_f = 0\ ms^{-1}$, ice thickness = 0

The term q_s in Equation 3 takes into account the effect of solar radiation. This can be divided in direct solar radiation ($S_{r,dir}$) which transmit energy only on the surface directly exposed to the sun, and diffuse solar radiation ($S_{r,diff}$) which considers also other surfaces. The energy adsorbed by the conductor is proportional to those radiations, to the exposed areas and to an absorption factor (α_{abs}), as described in Equation 7. Even if diffuse radiation can be a considerable percentage of the total solar radiation, usually it is not considered in practical applications as the rating is calculated for worst case scenarios. Typical values for the parameter α_{abs} range from 0.3 to 0.9 for new and old conductors respectively.

$$q_s[Wm^{-1}] = \alpha_{abs}\left(S_{r,dir} \cdot D_c + S_{r,diff} \cdot \pi D_c\right) \tag{7}$$

The term q_r in Equation 3 takes into account the effect of irradiative heat exchange. This is proportional to the difference of the forth power of the temperatures (absolute) of the bodies through the Stephen-Boltzmann $\left(\sigma_{sb}\ \left[\frac{W}{m^2K^4}\right] = 5.67 \cdot 10^{-8}\right)$ constant and an empirical emission constant (α_{em}). Equation 8 describes the heat exchange between the conductor and the atmosphere. Typical values for the parameter α_{em} range from 0.23 to 0.91 for new and old conductors respectively.

$$q_r[Wm^{-1}] = \alpha_{em}\sigma_{sb}\left[{T_c}^4 - {T_a}^4\right]\pi D_c \tag{8}$$

The term q_l in Equation 3 takes into account the transformation of energy into heat in the conductor by Joule. This is proportional to the resistance $r(T_c, I)$ of the cable and the square of the current as in Equation 9.

$$q_l[Wm^{-1}] = r(T_c, I) \cdot I^2 \tag{9}$$

The term q_c in Equation 3 takes into account the convective heat exchange. This is proportional to the temperature difference between the conductor and the environment

B: $T_c = -6℃$, $w_f = 25\ ms^{-1}$, ice thickness = 12 mm
Conductor type: LYNX, span: 200 m

through the fluid thermal resistivity (ρth_a) and the Nusselt number (Nu), as reported in Equation 10. The Nusselt number is a dimensionless parameter defined as in Equation 11 depending on characteristics of the fluid such as viscosity, thermal conductivity, density, temperature and speed and characteristics of the surface, such as temperature or dimension. The Nusselt number is usually calculated as a function of other dimensionless parameters as in Equation 11, each one considering a particular aspect.

$$q_c[Wm^{-1}] = \frac{Nu \cdot (T_c - T_c)}{D_c \cdot \rho th_a} \tag{10}$$

$$Nu = h \cdot D_c \cdot \rho th_a = f(Pr, Re, Gr) \tag{11}$$

The Prandtl number (Pr) is defined as the ratio between the viscous diffusion and the thermal diffusion (heat transmission by convection or conduction) of the fluid as in Equation 12. The Grashof number (Gr), described in Equation 13, is defined as the ratio between the buoyancy and the viscous forces acting on the fluid. The Reynolds number represent the ratio between inertia and viscous forces, as described in Equation 14

$$Pr = \mu \cdot Cth_a \cdot \rho th_a \tag{12}$$

$$Gr = \frac{g \cdot \beta_{air} \cdot (T_c - T_c) \cdot D_c^3}{(\mu / \rho_a)^2} \tag{13}$$

$$Re = \frac{\rho_a \cdot D_c \cdot Ws}{\mu} \tag{14}$$

In natural convection ($Ws = 0$) the Reynolds number is null, and the Nusselt number can be written as a function only of the Grashof and Prandtl numbers, as shown in Equation 15. On the other hand in forced convection ($Ws \neq 0$) dynamic forces prevail and the Nusselt number can be written as function of the Prandtl and the Reynolds number, as in Equation 16. In addition, the Nusselt number can depend also on the direction of the flow; it is therefore possible to add a correction factor depending on the incidence angle of the flow on the conductor.

For the formulae used in industry and in the rest of the work, the reader is invited to consult Sections 3.1.1.2 and 3.1.1.3.

$$Nu = f(Pr, Gr) \tag{15}$$

$$Nu = f(Pr, Re) \tag{16}$$

3.1.1.2 Comparison of standards currently in use

This section presents a comparison of the methods for rating overhead lines currently accepted in industry. The need of this comparison and the decision of using industry accepted standards are driven by the necessity to implement the real-time rating system in a real network and the use of widely accepted and already used models will increase the confidence in the practical utility of the tool. The sources considered are:

- Energy Networks Association ER P27 (121)
- IEC TR 61597-1995 (21)
- CIGRE WG 22.12, ELECTRA No. 144, Oct. ’92 (22)
- IEEE 738-1993 (20)

The first document consists of a list of conservative static seasonal ratings for different overhead lines conductors, in pre and post fault conditions and for different maximum operating temperatures. These ratings, derived from (10) are calculated so that, with typical UK meteorological conditions, there is a 0.1% probability of exceeding the rated temperature, and a 0.01% probability of exceeding the rated temperature of more than 5°C.

In the other three documents, models for rating overhead line conductors are described. The structure is based on the energy balance described in Equation 3, but different formulae are used for calculating the different terms, in particular for the convective heat exchange, and input and intermediate parameters.

Regarding the electric resistance calculation, the three documents propose a linear correction with temperature as in Equation 17. In (21) and (22) values for the parameter α_R are suggested, however in (20), the use of tabular values for conductor resistance provided in (122) is suggested.

$$r(T)[\Omega m^{-1}] = r(T_0)[1 + \alpha_r(T_c - T_0)] \quad (17)$$

Regarding the skin effect, both (21) and (20) suggests the method described in (122) rather than (22) describe a correction of the final value of the current as reported in Equation 18, where the coefficients $C_j^{D/A}$ are given for different types of conductor shape.

$$I_{AC}[A] = I_{DC}\left(\sum_{j=0}^{6} C_j^{D/A} \cdot I^j\right)^{-\frac{1}{2}} \quad (18)$$

Regarding temperature distribution inside the conductor, only (22) provides a method for calculating the temperature inside the conductor, for steel core or aluminium conductors. The method is described in Equation 19 but considering the little temperature difference usually present between the core and the surface, it is suggested to assume a constant temperature equal to the surface one. In this formula q_{tot} represents the total heat gain and if the steel core is not present it is possible to assume $D_{core} = 0$.

$$T_{c,core}[K] = T_{c,surf.} + \frac{q_{tot}}{2\pi}\rho th_c\left(\frac{1}{2} - \frac{D_c}{D_c - D_{core}} ln\frac{D_c}{D_{core}}\right) \quad (19)$$

Regarding solar gain, the three sources report similar models, described in Equation 20, where only direct solar radiation is taken into account. In (20) and (22) a method for calculating a static value for solar radiation according to location latitude, altitude, atmosphere (industrial – non industrial) and time is given.

$$q_s[Wm^{-1}] = \alpha_{abs} D_c S_{r,dir} \quad (20)$$

Regarding irradiative heat exchange, the three models refers to the basic formula described in Equation 8.

Major differences appear when considering convective heat exchange, since different formulae are available for calculating the Nusselt number in different conditions. Firstly, it is necessary to divide between natural and forced convection, as said in Section 3.1.1.1 and then these two phenomena can be divided in turn in laminar and turbulent convection.

A division between laminar and forced natural convection is done in (22). This difference is not considered in (20) and the effect of natural convection is not considered at all in (21). Formulae for calculating the Nusselt number in natural convection are described in Equation 21 and Equation 22 for (22) and (20) respectively[3].

$$Nu = A_1(GrPr)^{B_1} \tag{21}$$

$$Nu/\rho th_a = A_2 \cdot \rho_a^{0.5} \cdot D_c^{0.75} \cdot (T_c - T_a)^{1.25} \tag{22}$$

Laminar and turbulent condition for forced convection are considered both in (22), where the roughness of the conductor is also considered, and in (20) but not in (21). Formulae for calculating the Nusselt number in forced convection are described in Equation 23, Equation 24 and Equation 25 for (21), (22) and (20) respectively[4].

$$Nu = A_{3,1} \cdot Re^{B_{3,1}} + A_{3,2} \cdot Re^{B_{3,2}} \tag{23}$$

$$Nu = A_4 \cdot Re^{B_4} \tag{24}$$

$$Nu = A_{5,1} + A_{5,2} Re^{B_5} \tag{25}$$

---

3 $A_1 = \begin{cases} 0.85 \\ 0.48 \end{cases}$ for $\begin{matrix} \mathrm{GrPr}[10^2 \cdot 10^4] \\ \mathrm{GrPr}[10^4 \cdot 10^6] \end{matrix}$, $B_1 = \begin{cases} 0.18 \\ 0.25 \end{cases}$ for $\begin{matrix} \mathrm{GrPr}[10^2 \cdot 10^4] \\ \mathrm{GrPr}[10^4 \cdot 10^6] \end{matrix}$, $A_2 = 0.283$

4 $A_{3,1} = 0.65$, $A_{3,2} = 0.23$, $B_{3,1} = 0.2$, $B_{3,2} = 0.61$,

$A_4 = \begin{cases} 0.641 & \mathrm{Re} < 2650 \quad \mathrm{R} = \mathrm{any} \\ 0.178 & \mathrm{Re} > 2650 \quad \mathrm{R} < 0.05 \\ 0.048 & \mathrm{Re} > 2650 \quad \mathrm{R} > 0.05 \end{cases}$, $B_4 = \begin{cases} 0.471 & \mathrm{Re} < 2650 \quad \mathrm{R} = \mathrm{any} \\ 0.633 & \mathrm{Re} > 2650 \quad \mathrm{R} < 0.05 \\ 0.8 & \mathrm{Re} > 2650 \quad \mathrm{R} > 0.05 \end{cases}$

The parameter R is the roughness of the conductor, defined as the ratio between the radius of the single wire and the diameter of the whole cable

$A_{5,1} = \begin{cases} 1.01 & \mathrm{Re} < 2000 \\ 0 & \mathrm{Re} > 2000 \end{cases}$, $A_{5,2} = \begin{cases} 0.371 & \mathrm{Re} < 2000 \\ 0.1695 & \mathrm{Re} > 2000 \end{cases}$, $B_5 = \begin{cases} 0.52 & \mathrm{Re} < 2000 \\ 0.6 & \mathrm{Re} > 2000 \end{cases}$

Forced convection Nusselt number is influenced also by flow direction. This is considered in (22) and in (20) but not in (21). Formulae for calculating the effect of wind direction are reported in Equation 26 and Equation 27 for (22) and (20) respectively. [5]

$$Nu(Wd) = Nu_{90}\left(A_{6,1} + A_{6,2}\, sin^{B_6}(Wd)\right) \quad (26)$$

$$Nu(Wd) = Nu_{90}\left(A_{7,1} - cos(Wd) + A_{7,2}\, cos(2Wd) + A_{7,3}\, sin(2Wd)\right) \quad (27)$$

Other difference between the models is represented by the calculation method of physical parameters such as air thermal conductivity or viscosity. In (21) constant values are given, in (22) linear functions for approximating parameters behaviour with temperature are given and in (20) polynomial approximations up to the 6th order are used. In the latter two documents, a correction of air density with the height is included.

3.1.1.3 Models implemented in the algorithm

For the practical implementation of the real-time rating in the state estimation algorithm, the model described in (21) was chosen, integrating it with parts taken from (22) when considered necessary. The main reason behind this decision is that this model tends to be more conservative than the other two, increasing the confidence in the security of the real-time rating system without reducing significantly its advantages.

Solar gain and irradiative heat exchange are calculated using Equation 8 and Equation 20 respectively. Convective heat exchange is calculated using Equation 23 and the wind direction correction described in Equation 26. For low wind speeds (Ws ≤ 0.5 m/s) the natural convection model reported in Equation 21 is used.

5 $A_{6,1} = 0.42$, $A_{6,2} = \begin{cases} 0.68 & \delta[0° \cdot 24°] \\ 0.58 & \delta[24° \cdot 90°] \end{cases}$, $B_6 = \begin{cases} 1.08 & \delta[0° \cdot 24°] \\ 0.9 & \delta[24° \cdot 90°] \end{cases}$, $A_{7,1} = 1.194$, $A_{7,2} = 0.194$, $A_{7,3} = 0.368$

3.1.2 Electric cables

Electric cables are made of a metallic conductor of copper or aluminium protected by a series of layers of insulating materials and metallic protections, each one with a different function. Insulating layers, in paper or plastic, reduces the ability of the conductor to dissipate in the environment the heat produced by Joule effect and metallic protections allow eddy currents resulting in additional heat to dissipate. Furthermore the media surrounding the cable: ground, air or water, introduces an additional thermal resistance.

The maximum operating temperature of the conductor is determined by the necessity of not damaging the insulation. Its mechanical properties reduce with age, and ageing is a process accelerated by the temperature[6]. In particular, cases, such as cables in galleries or in soil where drying-out must be prevented, cable surface temperature represents the limiting parameter.

Considering the thermal resistance of the layers (Rth), the conductor and soil temperatures (T_c, T_s) and the losses generated by Joule effect, a first linear approximation of an underground cable current carrying capacity can be calculated using the Fourier law described in Equation 28. Losses can be considered proportional to the losses by Joule effect in the conductor, with a multiplication (C_l) factor taking into account the losses due to eddy currents in protection metallic sheets as in Equation 29. The resulting cable ampacity is reported in Equation 30.

$$T_c[K] = T_c + Rth \cdot q_l \tag{28}$$

$$q_l[Wm^{-1}] = C_l \cdot r \cdot I^2 \tag{29}$$

$$I[A] = \sqrt{\frac{T_c - T_s}{C_l \cdot r \cdot Rth}} \tag{30}$$

[6] Material ageing can be seen as a chemical reaction, accelerated by the temperature. An example of ageing speed calculation is given in Section 3.1.3.2

This model can be refined considering the number of conductors present in the cable core (n), the dielectric losses in the insulation (q_d), the losses ratio between metallic sheet and conductor ($C_{c,1}$) and between armour and conductor ($C_{c,2}$) and different thermal resistances for each insulating layer (Rth_j) as shown in Equation 31.

$$I[A] = \sqrt{\frac{(T_c - T_a) - q_d\left[\frac{1}{2}Rth_1 + n(Rth_2 + Rth_3 + Rth_4)\right]}{r \cdot \left[Rth_1 + n(1 + C_{c,1})Rth_2 + n(1 + C_{c,1} + C_{c,2})(Rth_3 + Rth_4)\right]}} \quad (31)$$

The model described above requires detailed knowledge of the electric cable installation. However, this information may not always be available and therefore it is difficult to make practical use of the model. In these circumstances, an alternative model, described in (47) and summarised in Equation 32, may be used. The rated current of electric cables (I_0) is given in tables depending on the standardised cable cross-sectional area (A_c), conductor temperature (T_c), voltage level (V) and laying conditions (trefoil, flat formation; in air, in ducts or direct buried). The dependence of the cable ampacity on external temperature and soil thermal resistivity (ρth_s) is made linear through the coefficients (ξ_T) and ($\xi_{\rho th_s}$) respectively.

$$I = I_o(A, T_c, V, laying) \cdot \left[\xi_T \cdot \left(T_s - T_{s,0}\right)\right] \cdot \left[\xi_{\rho th_s} \cdot \left(\rho th_s - \rho th_{s,0}\right)\right] \quad (32)$$

Since this research concerns the influence of environmental conditions on component ratings, the effect of the voltage level, which influences the dielectric loss, is not considered. The effect of the heating given by adjacent components is also neglected as it is assumed that each cable has already been de-rated to take this effect into account.

3.1.2.1 Detailed analysis of each term

In this section a detailed description of the most important terms of the equations described in Section 3.1.2 is given.

The term q_d represents the dielectric loss per unit length for the insulation surrounding the conductor. This depends on current frequency (f), insulation capacitance (Cap), voltage to earth (V) and insulation loss factor (C_{ins}), and can be calculated as in Equation 33. Insulation capacitance can be calculated considering insulation relative permittivity (α_{cap}), and insulation internal (D_i) and external diameter (D_e), as shown in Equation 34.

$$q_d[W \cdot m^{-1}] = 2\pi f \cdot Cap \cdot V^2 \cdot C_{ins} \tag{33}$$

$$Cap[F \cdot m^{-1}] = \alpha_{cap} \cdot \left(18 \cdot ln\frac{D_e}{D_i}\right) \cdot 10^{-19} \tag{34}$$

Thermal resistances for the different insulating layers ($Rth_{j=1,3}$) can be calculated as in Equation 35 and depends on layer thermal resistivity (ρth_j) and layer internal (D_i) and external diameter (D_e). Regarding external thermal resistivity (Rth_4) different models have been proposed for different situations such as cables in air, buried in ground or in ducts, in trefoil or flat configuration. A complete description of such cases can be found in (46). Here the case of a cable buried in the ground in trefoil formation is reported in Equation 36 where soil thermal resistivity (Rth_4), cable external diameter (D_e) and cable burial depth (L_{burial}) are taken into account.

$$Rth_{i=1,3} = \frac{\rho th_i}{2\pi} ln\left(1 + 2\frac{D_e - D_i}{D_i}\right) \tag{35}$$

$$Rth_4 = \frac{\rho th_s}{2\pi} \cdot \left(ln\frac{4L_{burial}}{D_e} + 2 \cdot ln\frac{2L_b}{D_e}\right) \tag{36}$$

The electric resistance per length unit (r) is influenced by conductor temperature (T_c) through the resistance rise on temperature factor (α_r), current frequency (f) through a skin effect factor (C_{rs}) and conductor diameter (D_c) and axes distance (L_{axes}) through a proximity effect factor (C_{rp}) as in Equation 37. Formulae for calculating the intermediate parameters reported in Equation 37 are given in (46) for different cable architectures and laying conditions.

$$r(T_c, f, D_c, L_{axes})[\Omega \cdot m^{-1}] =$$

$$r_{20} \cdot \left(1 + \alpha_r (T_c - T_0)\right) \cdot \left(1 + C_{rs}(T_c, f) + C_{rp}(T_c, f, D_c, L_{axes})\right) \quad (37)$$

A complete description of calculating methods for the parameters C_{rs} and C_{rp}, with different cable architectures and laying conditions can be found in (46).

The value of the rated current (I_o) used in Equation 32, is not calculated but given in (47) in tables taking into account conductor material (copper or aluminium), cross sectional area (A_c) and temperature (T_c), cable architecture (single, dual or three-core), insulation type (paper or extruded) bonding, voltage level (V) and laying formation (trefoil or flat). Correction tables are given also for the spacing between cables and for installation (direct buried in ground, buried in ducts, in air). The same document (47) provides tabled values for the coefficients (ξ_T) and ($\xi_{\rho th_s}$), for different laying formation, installation and conductor rated temperature.

3.1.2.2 Comparison of standards currently in use

The two main industrial standards currently used for electric cables rating in the UK are:

- IEC 60287 (46)
- ENA P17 (47)

These two documents propose two different models, summarised in the ampacity calculation methods described in Equation 31 and Equation 32, therefore, it is not possible to carry out a complete analysis of the differences as in Section 3.1.1.2 and Section 3.1.3.2.

3.1.2.3 Model implemented in the algorithm

The detailed model described in (46) requires a considerable amount of information about the installed equipment. Furthermore, considering that the real-time rating system

should be used on existing networks with old equipment and that the state estimation algorithm used and described in Equation 31 requires reduced calculation time for component rating, the linearised ampacity calculation described in Equation 32 has been chosen. Tabular values reported in (47) have been used for calculating the intermediate parameters.

3.1.3 Power transformers

Power transformers are more complex than overhead lines and electric cables, therefore it is necessary to understand correctly their structure and cooling system to apply the thermal model used for their rating. Transformers are constituted by a magnetic circuit made of iron and an electric circuit made by insulated conductors wrapped around the core. These two basics component are called respectively “core” and “windings” in this document. These two parts are immersed in a tank of coolant oil, and a heat exchanger, more or less complex according to the size of the transformer, is connected to the tank. This coolant circuit is moved with natural convection, but pumps can be used in larger transformers. In Figure 3 an example of the coolant circuit is shown.

Transformer maximum operating rating is influenced by maximum oil temperature which, if exceeded, can damage the transformer in two ways. Firstly, a temperature exceeding of 120ºC-140ºC can induce the formation of bubbles in the coolant oil, which in turn is liable to cause an insulation breakdown due to the local reduction of dielectric insulation strength. Bubble formation is influenced also by moisture content, gas concentration and pressure, as described in (123). Secondly, high temperatures increase the ageing rate of the winding insulation.

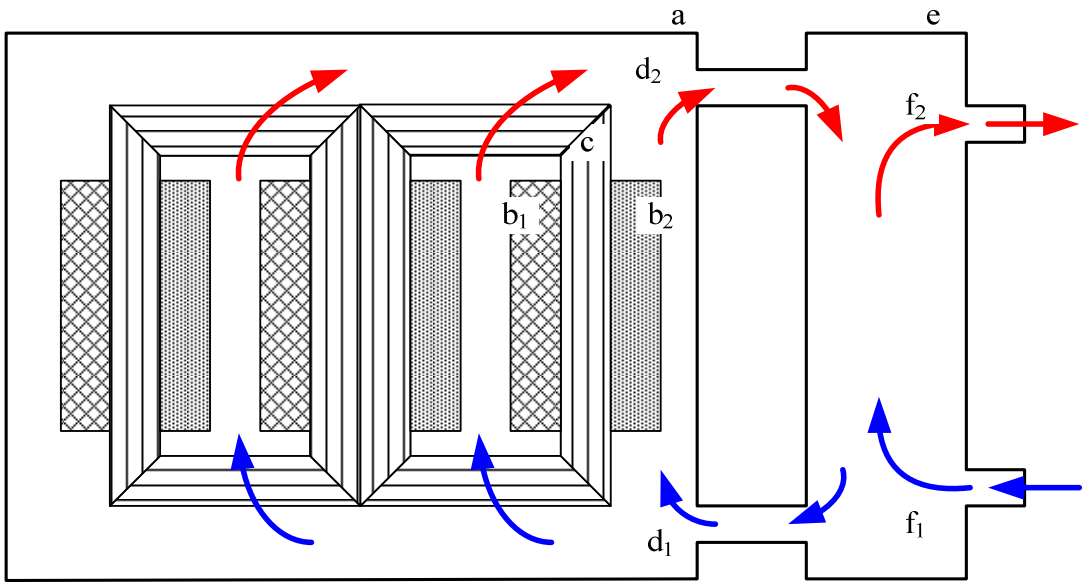

a	Oil tank	d_1 d_2	Coolant oil flow (cold, hot)
b_1 b_2	Windings (+-)	e	Heat exchanger
c	Ferromagnetic circuit	f_1 f_2	Refrigerating fluid (cold, hot)

Figure 3: Transformers: coolant circuit

In addition, this effect is influenced by the content of moisture and other chemicals as described in (124), but since these parameters are not influenced by the loading and external parameter history of the transformer, they are not taken into account in this research. Regarding the effect of ageing due to the temperature, this parameter accelerates chemical reactions leading to the oxidation of the insulation paper, as shown in Equation 38.

$$v = f(oil\ properties, T) \tag{38}$$

For these reasons maximum operating temperature should not exceed the rated value. The thermal model consists of a heat balance between the power dissipated in the winding and iron core, and the heat transferred to the environment via the refrigerating circuit. The model is then refined considering a temperature gradient between the bottom and the top of the windings, in order to consider the effect of the coolant oil being warmed while rising to the

entrance of the heat exchanger. An excellent description of a transformer thermal model can be found in (76).

Considering the thermal resistance between the winding and the oil (Rth_w), the thermal resistance between the heat exchanger and the air (Rth_{HE}) and the power dissipated into the core and the winding ($\dot{Q}_{cu+fe}$), it is possible to calculate the hot-spot temperature (T_{HS}) as in Equation 39.

$$T_{HS} = T_a + \dot{Q}_{cu+fe}(Rth_w + Rth_{HE}) \tag{39}$$

Usually the tank is fitted with a considerable quantity of oil in order to reduce temperature differences and provide a considerable thermal inertia, allowing short-time overloads to be withstood by the transformer without risk of failure. The dynamic behaviour of the transformer is usually modelled with a first order differential equation, resulting in an exponential passage between the initial and final state, as in Equation 40, where $T_{f,i}$ are the final and initial temperatures, and τ is the transformer thermal constant.

$$T_f = T_i + \left(T_f - T_i\right)e^{\frac{t}{\tau}} \tag{40}$$

3.1.3.1 Analysis of each term

In this section a detailed description of the most important terms of the equations described in Section 3.1.3 is given[7].

The term v in Equation 38 represents the insulation ageing speed. This can be considered as a chemical reaction involving the oxidation of winding insulation and can be calculated using the Arrhenius law, as in Equation 41.

[7] $\tau[s]$, time constant
$C\ [J \cdot kg^{-1}]$, thermal capacitance
$E_a\ [J]$, *reaction activation energy*
$\dot{Q}_x\ [W]$, *losses*
$R\ [J \cdot K^{-1}]$, *gas constant*
$R_{T,i}\ [K \cdot W^{-1}]$, thermal resistance

$$v = C_v e^{-\frac{Q_r}{RT}} \tag{41}$$

The losses in the core and in the windings, represented as $\dot{Q}_{cu+fe}$ in Equation 39, is usually written considering the ratio $\left(K_{loss} = \frac{\dot{Q}_{fe}}{\dot{Q}_{cu}}\right)$ between these two terms as in Equation 42, being the losses in the iron caused by eddy currents and correlated with the current (and so the losses) circulating in the windings.

$$\dot{Q}_{cu+fe} = \dot{Q}_{cu} + \dot{Q}_{fe} = \dot{Q}_{cu}(1 + K_{loss}) = I^2 R_w (1 + K_{loss}) \tag{42}$$

The thermal resistances Rth_W and Rth_{HE} in Equation 39 can be written as in Equation 43, where the heat transfer coefficient (h) depends on the Nusselt number, as in Equation 11. The Nusselt number in turn can be calculated as in Equation 15 considering natural convection.

$$Rth_j = (h \cdot A)^{-1} \tag{43}$$

Finally the time constant τ in Equation 40, can be calculated as the product of the thermal resistance and capacitance of the coolant circuit, as shown in Equation 44. The thermal capacitance Cth can be calculated as the sum of the thermal capacitance of the different part of the transformer, such as iron core, winding, oil and tank. The thermal resistance can be calculated as the ratio between the temperature difference at the ends of the thermal resistance (e.g. between oil and ambient temperature) and the thermal power flowing through it (e.g.: total losses as calculated in Equation 42).

$$\tau = Cth \cdot Rth \tag{44}$$

3.1.3.2 Comparison of standards currently in use

This section presents a comparison of the methods for rating power transformers currently accepted in industry. They have been chosen for the same reason discussed in Section 3.1.1.2: to inform the state estimation with models already used in industry for

facilitating the acceptance of the methodology developed in this research in real world applications. The sources considered are:

- IEC 60076-7 (71)
- IEEE C57.91 (72)
- ENA P15 (125)

In these documents models for calculating insulation ageing, hot spot temperature intermediate parameters and time response to changes are described. (72) and (71) reports models different in some part and (125) presents corrections to the model described in (71).

Regarding the dependence of ageing on temperature, in (72) a formula derived from the Arrhenius equation is used rather than in (71) and (125) where the Montsinger approximation is used. In Equation 45 and Equation 46 the relative ageing calculation method respectively for (72) and (71) is shown. Different reference temperatures are also considered: in (72) a maximum hot spot temperature of 108°C is used and in (71) and (125) a maximum operating temperature of 98°C is considered.

$$Ageing_r = e^{\left(\frac{1500}{383} - \frac{1500}{T_{HS}}\right)} \tag{45}$$

$$Ageing_r = 2^{\frac{T_{HS}-371}{6}} \tag{46}$$

Regarding the calculation of steady state hot-spot temperature (72) and (71) present the same method, even if in (71) the steady state value have to be obtained considering the limit of a transformation of the dynamic model. In (125) a temperature resistance correction factor is introduced. The difference between ambient temperature and hot-spot temperature is calculated as the sum of the maximum temperature gradient between environment and oil and the maximum temperature gradient between oil and windings as in Equation 47. The model considers a temperature gradient between the bottom and the top of the tank, with the highest temperatures in the upper part. The method for calculating maximum ambient-oil and oil-

winding temperature gradient is shown in Equation 48 and Equation 49 where the temperature gradient in standard condition $\Delta T_{i,R}$ is multiplied by a correction factor depending on the load ratio $\left(K_{load} = \frac{Load}{Load_0}\right)$ and the losses ratio in standard condition R_R.

$$T_{HS} = T_a + \Delta T_{a-O} + \Delta T_{O-HS} \tag{47}$$

$$\Delta T_{a-O} = \Delta T_{a-O,0} \left[\frac{1+K_{loss}K_{load}^2}{1+K_{loss,0}}\right]^{C_{T,o}} \tag{48}$$

$$\Delta T_{O-HS} = \Delta T_{O-HS,R} \cdot K_{load}^{C_{T,w}} \tag{49}$$

In (125) a correction factor (C) for winding resistance, and hence losses, dependence on winding temperature is introduced, as shown in Equation 50 and the correction factor can be calculated as in Equation 51. In this model, there is a distinction between the losses ratio in standard condition $K_{loss,0} = \frac{\dot{Q}_{fe}}{\dot{Q}_{cu,0}}$ with the average winding temperature (T_w) at 75°C and the real losses ratio $K_{loss} = \frac{\dot{Q}_{fe}}{\dot{Q}_{cu}}$.

$$\Delta T_{a-O} = \Delta T_{a-O,R} \left[\frac{1+C_{T,r}K_{loss}K_{load}^2}{1+K_{loss,0}}\right]^{C_{T,o}} \tag{50}$$

$$C_{T,r} = C_{T,r-0}K_{loss} + \frac{1-K_{loss}}{K_{loss}}, with\ C_{T,r-0} = \frac{507.5+T_w}{855} \tag{51}$$

Regarding the dynamic behaviour, (72) and (125) report the same model based on an exponential variation between two steady state conditions, as in Equation 40. In (71) a more complex model is used. This is reported in Equation 52 and considers the evolution of two different parts of the system: the oil and the metallic part constituted by windings and iron core. In Equation 52 the first function is for an increase in temperature, and the second for a decrease. The time dependant functions $\left(Y_i(t)\right)$ are reported in Equation 53.

$$\begin{cases} T_{HS}(t) = T_a + \Delta T_{a-O,i} + \left[\Delta T_{a-O,f} - \Delta T_{a-O,i}\right]Y_1(t) \\ +\Delta T_{O-HS,i} + \left(\Delta T_{O-HS,f} - \Delta T_{O-HS,i}\right)Y_2(t) \\ T_{HS}(t) = T_a + \Delta T_{a-o,f} + \left[\Delta T_{a-O,i} - \Delta T_{a-o,f}\right]Y_3(t) + \Delta T_{O-HS,f} \end{cases} \tag{52}$$

$$\begin{cases} Y_1(t) = 1 - e^{\frac{-t}{C_{T,11}\tau_o}} \\ Y_2(t) = C_{T,21}\left(1 - e^{\frac{-t}{C_{T,11}\tau_w}}\right) - \left(C_{T,21} - 1\right)\left(1 - e^{\frac{-t}{\tau_o / C_{T,22}}}\right) \\ Y_3(t) = e^{\frac{-t}{C_{T,11}\tau_o}} \end{cases} \quad (53)$$

3.1.3.3 Model implemented in the algorithm

The models described in Section 3.1.3.2 are used for the calculation of transformers hot spot temperature, and in order to obtain the corresponding rating, it is necessary to calculate iteratively the solution. In the algorithm, the Newton-Raphson method is used to find the solution of Equation 39 transformers: basic thermal model Equation 39, where each term is calculated using the steady state solution of Equation 52. The correction for resistance variation with temperature described in Equation 50 has not been used because of the additional information on transformers characteristics required. An initial function for calculating the maximum power allowable considering the thermal inertia and the possibility of allowing an increase of relative ageing for a given amount of time has been discarded because of the difficulties of integrating it into the rest of the control.

3.1.4 Sensitivity analysis

It can be seen from the work presented above that many diverse parameters affect the rating of power system components. These parameters may be categorized into component properties, geographical properties, and environmental conditions. For the purposes of the real-time rating estimation, component properties and geographical properties are assumed to be constants of the system. Therefore, the thermal models presented were underpinned by a sensitivity analysis that gave an indication of the influence of environmental conditions on power system component ratings. The sensitivity analysis was carried out such that one

parameter was varied at a time while all other parameters were maintained at their credible midrange values. A summary of the results of this analysis is presented in Table 2 and shows the percentage variation in component rating for a given percentage variation of environmental conditions from credible mid-range parameter values.

Table 2: Environmental condition sensitivity analysis (parameter variation versus rating variation)

		Overhead lines *(Lynx 50)*				**Electric cables** *(150mm²)*		**Transformers** *(ONAN 45)*
parameter *(credible mid-range value)*		***Ws*** *(8m/s)*	***Wd*** *($\frac{\pi}{4} rad$)*	***Ta*** [8] *(15°C)*	***Sr*** *(500W/m²)*	***R_T*** *(1.2WK/m)*	***Ts*** *(10°C)*	***Ta*** *(15°C)*
Variation from mid-range value	-50%	-23.86%	-11.38%	+10.80%	+0.72%	+31.46%	+3.00%	+6.11%
	-25%	-10.73%	-4.97%	+5.52%	+0.36%	+12.36%	+1.50%	+3.09%
	-10%	-4.07%	-1.85%	+2.24%	+0.15%	+6.18%	+0.60%	+1.24%
	10%	+3.84%	+1.66%	-2,29%	-0.15%	-4.49%	-0.60%	-1.25%
	25%	+9.22%	+3.82%	-5.81%	-0.36%	-8.99%	-1.50%	-3.16%
	50%	+17.40%	+6.54%	-11.96%	-0.73%	-16.48%	-3.00%	-6.40%

Moreover, in the sensitivity analysis, the soil thermal resistance is assumed to take into account the effect of rainfall. It can be seen that the rating of overhead lines is particularly sensitive to the environmental conditions of wind speed, wind direction, and ambient temperature, and that the rating of electric cables is particularly sensitive to the thermal resistance of the surrounding medium. Furthermore, a series of credible worst-case scenarios were selected to give an indication of the minimum component rating that would potentially result from the deployment of a real-time rating system. In this worst case analysis the following values were specified: *Ta* = 38.5 ◦C (the maximum temperature registered in England, August 2003) (126); *Ws* = 0,*Wd* = 0, *Sr* = 0W/m2 (from studies carried out at CERL, the highest conductor temperature excursions are recorded at times of low wind speed where there is negligible solar radiation) (115); *Ts* = 20 ◦C (46) and ρth_{s-T} = 3Km/W (47). The resulting rating multipliers of the standard static component rating were 0.81, 0.86, and 0.78 for overhead lines, electric cables, and power transformers, respectively.

[8] For *Ta* and *Tc*, the percentage variation is done considering a minimum temperature of 0°C

3.2 Environmental condition modelling

As described in Section 1.4 the real-time rating system developed in this project makes use of a limited number of meteorological measurements in selected areas of the network in order to estimate component ratings in a wide geographical area. It is therefore necessary to process this information for calculating environmental conditions for the location of every component of the network. This section describes the approach adopted to estimate, correct and interpolate environmental conditions to represent more accurately the actual environmental operating conditions for sections of the UK power system in different geographical areas.

3.2.1 Interpolation

The inverse distance interpolation technique (127) allows environmental conditions to be determined over a wide geographical area using a reduced set of inputs. This is attractive for situations where a large amount of installed measurements may be financially unattractive to the distribution network operator. The technique is also computationally efficient and allows the input locations to be readily adapted. Wind direction, air temperature and solar radiation values were included within interpolations but did not require the application of a correction factor. At each point in the geographical area (k) the value of the parameter (Z) representing the environmental condition can be estimated as a weighted average of the parameter values known at i points. The weighting factor is a function of the distance between the points as shown in Equation 54.

$$Z_k = \frac{\Sigma_i \left(\frac{1}{L_{i,k}^2} \cdot z_k \right)}{\Sigma_i \left(\frac{1}{L_{i,k}^2} \right)} \tag{54}$$

The wind speed correction process is described in Section 3.2.2. The soil parameter correction process is described in Section 3.2.3.

3.2.2 Wind speed correction

Ground roughness influences wind speed profiles and may lead to differences between the wind speed recorded by anemometers and the actual wind speed passing across an overhead line, particularly if the anemometer and overhead line are installed at different heights. This may be corrected using the wind profile power law given in Equation 55. The wind speed at two different heights is linked with the ground roughness through the exponent $Kshear$. Values of $Kshear$ for different ground types may be found in (43).

$$Ws = Ws_a \cdot \left(\frac{z_{ref}}{z_a} \right)^{Kshear_a} \cdot \left(\frac{z_c}{z_{ref}} \right)^{Kshear_c} \tag{55}$$

Using Equation 55, the anemometer wind speed (Ws_a) at the meteorological station height (z_a) is extrapolated to a reference height (z_{ref}, in this case 100 metres) to remove ground roughness dependence represented by the parameter $Kshear_a$. The values from different anemometer locations may then be interpolated, using Equation 54 as described in Section 3.2.1, to provide a wind speed estimate at the reference height for a particular geographical location. The ground roughness at this location is then taken into account through the coefficient $Kshear_c$ along with the conductor height (z_c) in Equation 55 to estimate the wind speed (Ws) across the overhead line. In Figure 4 a graphical example of the soil surface roughness effect on wind speed vertical profile is provided.

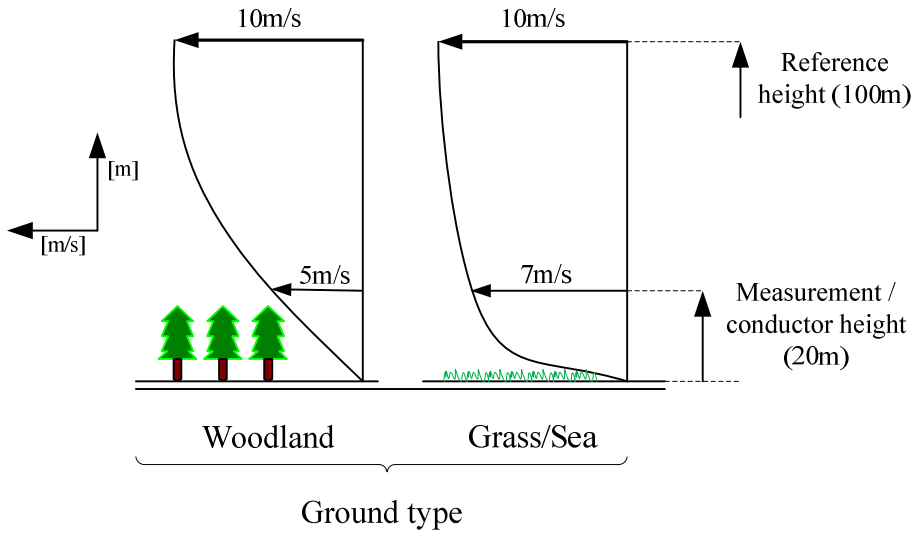

Figure 4: Soil surface roughness effect on wind speed vertical profile, example

Regarding wind direction, Equation 54 can be used for wind direction interpolation, although it can provide erroneous values for particular input datasets. In particular, when multiple meteorological stations record concurrent values of wind direction from North-North-West (NNW) and North-North-East (NNE). In this case the interpolation may produce distorted results because averaging wind direction values in the region of NNW to N (337.5°-360°) together with values in the region of N to NNE (0°-22.5°) produces wind direction estimates in the region SSW to SSE (157.5°-202.5°), which represents a 180° phase shift between real and calculated wind direction. This does not render equation (8) inappropriate to use because, due to the angular nature of the wind direction, a phase shift in wind-conductor angle of 180° has the same cooling effect as the wind-conductor angle without the phase shift. Therefore, an error of 200° in wind direction has the same effect on conductor temperature calculation as an error of ±20°.

3.2.3 Soil temperature and thermal resistance modelling

Electric cable ratings are dependent on soil temperature and soil thermal resistivity, as well as cable construction, burial layout and burial depth (which is typically 0.8–1 metre). Because of practical difficulties of measuring soil thermal resistivity, it was decided to measure the soil water content and to extrapolate the soil thermal resistivity (ρth_s) as in Equation 56 using the soil thermal diffusivity (δth_s), the dry soil density (ρ_s), and the soil thermal capacity (Cth_s). Soil thermal diffusivity (δ_{s-T}) and soil thermal capacity are influenced by soil composition (N) and water content (θ) and can be calculated using Equation 57 and Equation 58 according to (128).

$$\rho th_s = (\delta th_s \cdot \rho_s \cdot Cth_s)^{-1} \tag{56}$$

$$\delta th_s = -14.8 + 0.209 \cdot N + 4.79 \cdot \theta \tag{57}$$

$$Cth_s = -0.224 - 0.00561 \cdot N + 0.753 \cdot \rho_s + 5.81 \cdot \theta \tag{58}$$

Since Equation 57 and Equation 58 make use of location dependent parameters such as soil density and soil composition, first the soil water content is interpolated as in Equation 54 and then the soil thermal resistivity is calculated.

In addition to this, a series of dynamic soil models have been considered for different system configurations where the installation of temperature sensors at the depth of the cable or the measurement of ground water content was not possible, or previously installed meteorological stations should be used. Even if these models have not been used in the final algorithm, they are reported here. If it is not possible to measure soil temperature at cable burial depth, a depth-dependent soil temperature distributions may be calculated using the Fourier law, as explained in (129) and shown in Equation 59.

$$\frac{\partial T_s}{\partial t} = \frac{\partial}{\partial z}\left(\delta th_s \cdot \frac{\partial T_s}{\partial z}\right) \tag{59}$$

Boundary conditions can set up with a constant temperature of 10℃ at a depth of 2 metres for the lower layer and measured soil temperature readings for the upper layer. If it is no possible to measure the ground water content at the desired depth, it can be determined using the closed form of Richard's Equation (130) as described in Equation 60 after the calculation of the unsaturated hydraulic diffusivity ($\delta_{s-\theta}$) and the unsaturated hydraulic conductivity ($k_{s-\theta}$) as described in (131).

$$\frac{\partial \theta}{\partial t} = \frac{\partial}{\partial z}\left(\delta th_s \cdot \frac{\partial \theta}{\partial z} + k_{s-\theta}\right) \tag{60}$$

In order to solve Equation 60, boundary and initial conditions must be specified. A constant water content equal to the saturation value can be set at a depth corresponding to the water table. The ground-level water content can be calculated from rainfall values (lr) using the model described in Equation 61, where $Krain_1$ and $Krain_2$ can be calculated using (132)

$$\frac{d\theta}{dt} = -Krain_1 \cdot \theta(t) + Krain_2 \cdot lr(t) \tag{61}$$

3.3 Conclusion

Component thermal models widely used both in industry and in academia have been used for describing power system components thermal behaviour. This choice was driven by the intention to build the research on a solid base, building confidence in the suitability of the system developed in this research for field tests and to facilitate the development in commercial applications.

The model used for overhead lines conductor rating is based on the IEC standard (21) for overhead conductors rating, enriched by the wind direction correction proposed by the CIGRE Working Group 12 (22). The flexible algorithm structure allows manufacturers to apply the rating model preferred by each particular customer or even to implement their own

model. Between the three models considered, the CIGRE model is more detailed but it was discarded because of the greater number of parameters necessary while the IEEE (20) model was not used because UK overhead lines rating is based on the IEC method.

Also for electric cables available industrial standards were used. Of the two considered rating methods, the IEC (46) and the ENA (47) one, the second was chosen for a practical implementation in the code. The IEC standard requires an excessive number of cable construction parameters that were difficult to identify for the old components usually installed on the UK distribution network. Therefore the less detailed method based on tabulated rating values and tabulated correction coefficients for the different environmental conditions described in (47) was preferred.

The procedure of comparing different standard models for component rating and then selecting the most suitable was also followed for power transformers. The three models considered were the IEC loading guide (71), the IEEE loading guide (72) and the ENA loading guide (125). Very little differences exists between these three documents and the IEC method was chosen also in this case because of its use for transformer rating in the UK and in the network used for validation.

Regarding environmental conditions modelling there are no standard methods already used by the electric transmission and distribution industry that could be easily applied in this project. Furthermore, the complexity of the physical phenomena behind environmental conditions variation is often very complex, nonlinear and chaotic, requiring considerable computational resources. Considering these two constraints, but also the fact that currently no method is officially used for environmental condition calculation in the electricity distribution industry, the following approach was adopted. The value of each parameter is interpolated in each component location from the values measured in meteorological stations of known

location and corrections considering aspects of the natural phenomenon described are applied where possible. A list of possible improvements is provided in Section 8.5.

Wind speed and directions are strictly correlated parameters since they are used for describing the air flow and for this reason they are interpolated separately in the algorithm. Wind speed interpolation is corrected for taking into account the effect of soil surface roughness both on wind speed measurement at the meteorological stations and in each conductor location. This adds a possible source of error in the estimation of soil surface roughness parameters, but it is expected that this error is limited in comparison with the error of the simple interpolation.

Wind direction is simply interpolated and it was explained in Section 3.2 how the error generated by the algorithm for particular sets of data has a reduced effect on conductor temperature calculation and hence on conductor rating calculation. An alternative solution would have been to transform the wind description in polar coordinates (wind speed and wind direction) in a description in Cartesian coordinates (latitudinal and longitudinal wind speed) and then to interpolate these two values for calculating again in each conductor location the absolute value of wind speed and the angle relative to the conductor. This was not done in order not to influence wind direction calculation with the potential error generated by wrong soil surface roughness coefficient estimation. Air temperature and solar radiation calculation are based on simple inverse distance interpolation without additional correction.

The opportunity of introducing altitude correction for air temperature was considered but a practical implementation in the algorithm was discarded. The little altitude excursion in the test area would not have made a rigorous test possible and the correction could have become an additional non-measurable source of error. For the same reason the solar radiance is simply interpolated and no additional correction for local factors that could potentially modify readings value were implemented in the algorithm.

Regarding soil environmental conditions influencing electric cables rating, additional calculations were necessary in order to calculate the required parameters values. Initially only soil temperature readings at 5cms of depth and no soil thermal resistivity readings were available. Therefore, a complex soil dynamic model was developed for calculating soil temperature at electric cables burial depth and soil thermal resistivity from rainfall readings. Later, the test site was instrumented with a soil moisture sensor (linearly dependent with soil thermal resistivity) and a soil temperature sensor placed at cables burial depth. The interpolation of these values is expected to produce a reduced error with respect to the dynamic soil behaviour model developed in the first part of the project.

Chapter 4 Algorithm development: Estimation technique

4.1 Review of possible techniques

A review of other work carried out on the topic of power component real-time rating estimation is presented in Section 2.4. In this section, the estimation problem and the data structure is described. Then the main candidates for implementation into the algorithm are analysed, compared and the final candidate selected.

4.1.1 Data and models structure

Here the physical problem that is required to be solved and the logical passage to its solution are clarified.

- Output: N_C estimations of the state (rating) of N_C network components, with an estimation of the minimum, maximum and average probable value.
- Input: N_M measurements of N_P external parameters from N_M meteorological stations and N_T component temperature measurements.

The problem can be broken down in two parts:

- The $N_M x N_P$ measurements are used to calculate $N_M x N_C$ estimations of the N_P external parameters for the N_C components locations.

– Then for each component, the N_P parameters are used to calculate its state.

In order to carry out this thermal state estimation it is therefore necessary not only to know the physics of the problem, but also to have access to a number of intermediate calculations and possibly to store data. Finally, it is necessary to note that the methods to calculate the external parameters and the ratings are not only non-linear, but often iterative and numerical. Therefore, it will not be possible to act during the process of the calculation of the thermal stare estimation, but only on the calculated data.

4.1.2 State estimation techniques

The ideal state estimation technique used in the algorithm must satisfy a number of requisites often conflict with each other. The technique selected must produce precise and accurate estimation of component ratings. It must be able to carry out the calculations necessary for estimating the rating of different components such as overhead lines, electric cables and power transformers as described in Section 3.1. The technique selected must also be able to estimate environmental conditions using the models described in Section 3.2 and possibly to be able to integrate more complex models in the future. Furthermore it must be able to perform the estimation in real-time, and therefore it must not be excessively computationally intensive. A list of the requirements used for selecting the state estimation technique used is reported below:

– Use of non-linear models
– Open to accept further models development
– Reduced computational intensity requested

At first, analysis of the problem of the considerable number of nonlinear relations between the different parameters influencing power system component ratings suggested that

traditional estimation techniques based on linear algebra would not have been suitable for this problem. Considering the previous experiences reported in Section 2.4, the following techniques were considered for a practical implementation in the state estimation algorithm developed:

- Maximum Likelihood Method
- Weighted Least Square Method
- Interval Arithmetic
- Affine Arithmetic
- Monte Carlo Method

The Maximum Likelihood method is used for identifying the optimal set of function parameters to represent more precisely a set of data. A state estimation with this method would require the definition of parametric models for each parameter, followed by an estimation of the parameters with the use of measured data. A complete description of this method and its application can be found in (133) or (134). Given a probability density function $f(X;Q)$ where X is a set of n measured variables x_i and Q is a set of l parameters q_l, the likelihood function is defined as in Equation 62. The problem is then to search the set Q that maximise the likelihood function. For this task, Equation 63 or Equation 64 can be used.

$$L(X,Q) = \prod_{i=1,n} f(x_i;Q) \tag{62}$$

$$\frac{dL}{dq_j} = 0 = \prod_{i=1,n} f(x_i;Q)\,, \forall j = 1,l \tag{63}$$

$$\frac{dL}{dq_j} = 0 = \sum_{i=1,n} ln[f(x_i;Q)]\,, \forall j = 1,l \tag{64}$$

In addition, the Weighted Least Square Estimation is used for identifying the optimal parameters of a function previously defined for approximating the measured data. A complete description of this method and its application can be found in (133) or (134).

Considering a set of n measurements x_i and the parametric function used for their approximation $y = f(x; Q)$ the sum of squares function is defined as in Equation 65, where w_i is the relative weight for the i^{th} term. By solving the system of equations described in Equation 66, it is possible to find the set of parameters Q minimising Equation 65. The solution of this system can be done with a numerical method such as the Newton-Raphson and reciprocal of the variance is usually used as the weight w_i.

$$L = \sum_{i=1,n} w_i [y_i - f(x_i; q)]^2 \tag{65}$$

$$\frac{dL}{dq_j} = 0 = \frac{d}{dq_j} \sum_{i=1,n} w_i [y_i - f(x_i; q)]^2, \forall j = 1, l \tag{66}$$

Interval Arithmetic, like Affine Arithmetic, is a self validating method (118). This means that the computational algorithm can track the accuracy of the computed quantities, so that the amplitude of the error can be know *a posteriori* (135). In Interval Arithmetic, each quantity x is represented by an interval or by an array with the extremes value of the interval $\begin{bmatrix} x_{sup} \\ x_{inf} \end{bmatrix}$. The intervals are manipulated, subtracted or multiplied so that each computed interval contains the unknown value of the real quantity x. Examples of basic operations in Interval Arithmetic are described in Equation 67, Equation 68 and Equation 69. The main problem of this technique is that it tends to overestimate the amplitude of the interval, especially in iterative calculations.

$$x + y = \begin{bmatrix} x_{sup} + y_{sup} \\ x_{inf} + y_{inf} \end{bmatrix} \tag{67}$$

$$x \cdot y = \begin{bmatrix} min(x_{inf} \cdot y_{inf}; x_{inf} \cdot y_{sup}; x_{sup} \cdot y_{inf}; x_{sup} \cdot y_{sup}) \\ max(x_{inf} \cdot y_{inf}; x_{inf} \cdot y_{sup}; x_{sup} \cdot y_{inf}; x_{sup} \cdot y_{sup}) \end{bmatrix} \tag{68}$$

$$x^a = \begin{bmatrix} x^a_{sup} \\ x^a_{inf} \end{bmatrix} \tag{69}$$

In Affine Arithmetic (34) each partially unknown quantity x is represented by an affine form which is a polynomial as in Equation 70. In Equation 70, the terms ξ_i are known

coefficients and the terms $\varepsilon_i \in [-1; 1]$ are independent sources of uncertainty, called noise. Examples of basic operations in Interval Arithmetic are described in Equation 71, Equation 72 and Equation 73. Particular attention has to be given when it is necessary to obtain an affine form *Z* from a non-affine operation *f(x,y)*. In this case, a further term $z_k\varepsilon_k$ representing the residual approximation error has to be added.

$$x = \xi_0 + \xi_1\varepsilon_1 + \cdots + \xi_n\varepsilon_n \tag{70}$$

$$x + y = (\xi_0 + \eta_0) + (\xi_1 + \eta_1)\varepsilon_1 + \cdots + (\xi_n + \eta_n)\varepsilon_n \tag{71}$$

$$ax = a\xi_0 + a\xi_1\varepsilon_1 + \cdots + a\xi_n\varepsilon_n \tag{72}$$

$$x \pm a = (\xi_0 \pm a) + \xi_1\varepsilon_1 + \cdots + \xi_n\varepsilon_n \tag{73}$$

The Monte Carlo method consists of an iterative evaluation of results of deterministic models relative to randomly selected input values (136). Considering for example the function of two variables described in Equation 74, where the input variables are not completely known and they can assume random values in the intervals described in Equation 75. The Monte Carlo method calculates n times the value of the variable w with randomly selected values of the variables x and y as in Equation 76. The calculation can be refined with the use of probability density functions in order to select more often the more probable values of each input parameter.

$$w = f(x, y) \tag{74}$$

$$\begin{cases} x \in [x_{inf};\ x_{sup}] \\ y \in [y_{inf};\ y_{sup}] \end{cases} \tag{75}$$

$$\begin{cases} w_1 = f(x_1, y_1) \\ \cdots \\ w_n = f(x_n, y_n) \end{cases} \tag{76}$$

The analysis of these techniques, according to the requirements described at the beginning of this section, suggested that the Monte Carlo method was the most appropriate for the real-time state estimation system under development. The Maximum Likelihood

Method was discarded because it is not designed for giving information about the estimation error and another method should have been developed for this scope. For the same reason also the Weighted Least Square Method was not selected. The Interval Arithmetic technique was discarded because of its tendency to overestimate interval amplitudes especially in iterative calculations (34). This method would calculate every time the worst and best scenario only, giving excessive weight to extreme conditions with a limited probability to verify.

The Affine Arithmetic was discarded because it was felt that the transformation of the many non linear equations used in the models would have let to a reduction in the precision of the result of the estimation. Furthermore, the Monte Carlo method has the advantage of describing the probability structure of the results, allowing the controller or the distribution network operator to select a probability value for the rating when operating the network. Furthermore, a degree of customisation between the estimation precision and the estimation computational-time is allowed in the Monte Carlo method. This would allow the algorithm to be used in different applications such as the real-time distributed generator output controlled, with high computational speed and medium precision, and an off-line planning tool, with low computational speed but the possibility to simulate a considerable number of scenarios.

4.2 Monte Carlo simulation

4.2.1 Structure

As mentioned in 4.1.2, the Monte Carlo method consists of an iterative evaluation of results of deterministic models relative to randomly selected input values (136). These inputs are randomly generated from probability density functions describing parameter probabilistic structure and the results generated by the deterministic model in different trials can be

represented in turn by probability distributions. In Figure 5 a visual representation of a generic Monte Carlo simulation is given.

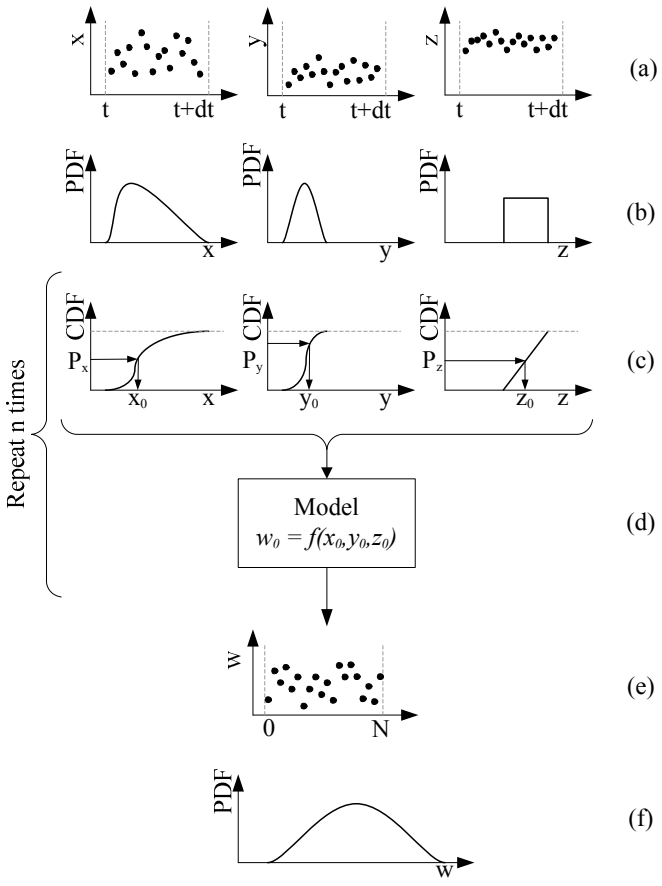

Figure 5: Monte Carlo method example

The simulation starts collecting parameter readings in a period *dt* (a). For each parameter (*x*, *y*, *z*), a probability density function is calculated from the measured data (b) as described in Section 4.2.3 and the cumulative density function is calculated by integration from the probability density function. At this point (c), a random value for the probability is generated for each parameter, and inverting the cumulative density function, the corresponding parameter value is selected, as described in Section 4.2.2. The random variate generated is then used (d) for calculating the output of a model. The different models used in this research are described in Section 3.1 and Section 3.2. The two steps (c) and (d) are

repeated N times, where N is calculated as described in Equation 77 and the model's results are stored (e) for further analysis. Finally, a probability density function for approximating the output is generated (f) from the N simulation results as in step (b). In a real-time rating system deployment the parameter w could be the wind speed across an overhead line conductor and the parameters x, y and z could be the wind speed in measured by three meteorological stations. Alternatively, the parameter w could be the conductor rating and the parameters x, y and z could be wind speed, wind direction and air temperature in the conductor location.

The thermal state estimation algorithm developed is divided in two steps: Firstly, environmental conditions measured in different meteorological stations are used for estimating environmental conditions in a single component location. This estimation is performed for wind speed, wind direction, air temperature, solar radiation, soil temperature and soil thermal resistivity, as described in Section 3.2. Secondly, when an estimation of the environmental conditions is available for the component location, the component thermal rating is estimated. The algorithm is able to estimate real-time thermal ratings for overhead lines, electric cables and power transformers, as described in Section 3.1. A graphical description of the complete state estimation for an overhead line conductor is described in Figure 6. Wind speed is measured in a time interval dt in three meteorological stations ($a_{1,2,3}$). At the same time, the same meteorological stations measures also wind direction (b), air temperature (c) and solar radiation (d) and these data are sent to a centralised server (currently through GPRS). At this point, the algorithm performs a Monte Carlo simulation (e), as described above and in Figure 5, in order to estimate wind speed in the conductor location (e_1). Monte Carlo simulations are carried out also for the other parameters (f, g, h). Environmental conditions estimations (e_1, f_1, g_1, h_1) for the conductor location are then used in another Monte Carlo simulation (i) which estimates conductor current carrying capacity (i_1).

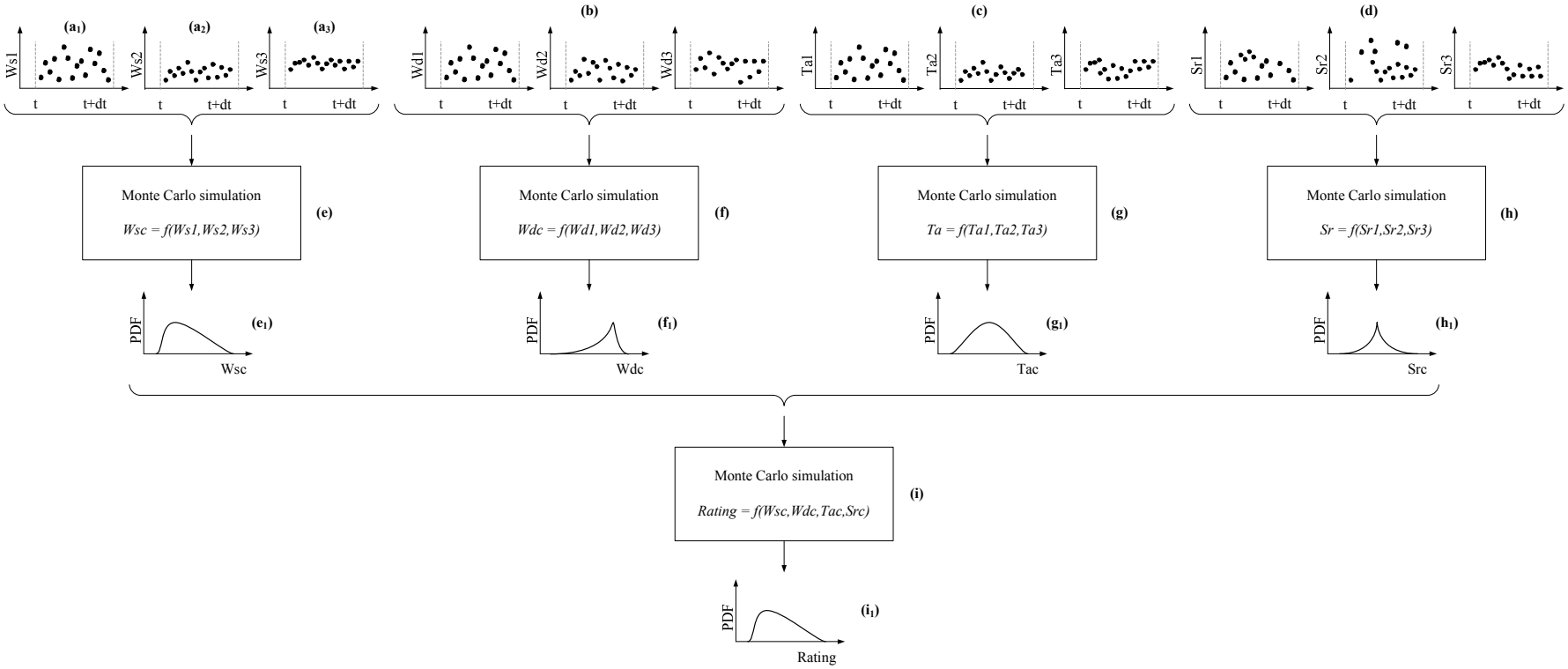

Figure 6: Example of overhead line rating estimation

Monte Carlo estimation precision depends on the number of simulations carried out. A limited number of simulations would reduce the computational-time since it is necessary to sample sufficiently the probability density function of every parameter and to consider a sufficient number of parameter combinations. In the algorithm developed the simulation number is calculated as in Equation 77 (137) which links together the number of samples (**N**), the standard deviation of the results ($\boldsymbol{\sigma_m}$) and a selected error value ($\boldsymbol{\epsilon_N}$).

$$\epsilon_N = \frac{3 \cdot \sigma_m}{x_m \cdot \sqrt{N_i}} \tag{77}$$

Equation 77 shows that the number of iteration is proportional to the square of the ratio between the dimensionless range of the results ($3\sigma_m/x_m$) and the accepted results' error (ϵ_N). This also means that if a higher precision is requested and the expected error is halved, the number of iterations and hence the estimation computational power will increase fourfold. Another consequence of Equation 77 is that the estimation of parameters with a broad relative range, such as wind speed, wind direction or solar radiation, would require more calculation than the estimation of less variable parameters such as conductor temperature, considering the same expected error.

4.2.2 Variate generation

In statistics, a variate is the random numerical value of a variable defined in a sample space. For each simulation, a random value in the sample range is selected for each input and used for calculating the model's output. One of the main principles behind the Monte Carlo method is to carry out for each parameter value in the range defined by its probability density, a number of random simulations proportional to its probability. In order to do so, probability density functions are used to describe the probabilistic structure of the parameter, and an adequate technique must be used for the selection of the particular parameter value from the

probability density function. The probability density function selected for the implementation of this algorithm, along with other potential candidates, is described in Section 4.2.3. The random number generation technique implemented in the algorithm along with other potential candidate techniques is described in Section 4.2.4. In this Section, the technique used for generating the variate for each simulation along with other potential candidates is described. The variate generation technique used in the algorithm must be precise and not computationally intensive. The two criteria used for selecting the variate generation technique are reported below:

- Simplicity
- Fast

Among the most common methods used for variate generation in Monte Carlo simulations, the following were initially selected for a possible implementation in the real-time rating estimation algorithm.

- Inverse transform method
- Composition method
- Acceptance-rejection method

The inverse transform method (136) consists of inverting the cumulative density function describing the probability structure of a parameter. Selecting a random value for the probability (P), the corresponding vale for the parameter (x) is calculated as in Equation 78.

$$x = CDF^{-1}(P; a_i) \tag{78}$$

The composition method is based on the assumption that is possible to represent a generic cumulative density function as a weighted sum of other cumulative density functions, as in Equation 79, where the coefficients a_i satisfy the conditions in Equation 80. In this way, is possible to split the range of the parameter x and to sample each interval with a simple cumulative density function.

$$CDF(x) = \sum_{i=1}^{n} a_i \cdot cdf_i(x) \tag{79}$$

$$a_i > 0, \sum_{1=1}^{n} a_i = 1 \tag{80}$$

The acceptance rejection method is based on a principle similar to the Monte Carlo integration. Considering a probability density function bounded on a finite interval [a,b] and with $c = sup\big(PDF(x)\big)$, as described in Figure 7. The method generates an independent pair of values x and y, with the conditions described in Equation 81. Then if $y < PDF(x)$, the value x is accepted and if $y > PDF(x)$ the value x is rejected. In the example in Figure 7 the couple (x_1, y_1) is rejected whereas the couple (x_2, y_2) is accepted.

$$\begin{cases} a < x < b \\ 0 < y < c \end{cases} \tag{81}$$

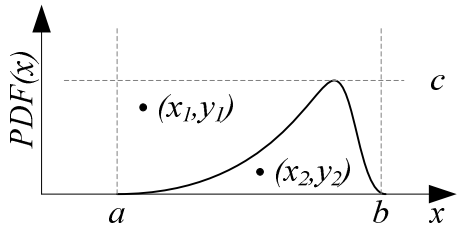

Figure 7: Acceptance rejection method

After considering these different techniques, the inverse transform method was chosen for the implementation in the algorithm. The composition method requires a more complex algorithm for taking into account the array of different cumulative density functions and its success depends on the methodology adopted for creating the different cumulative density functions. Therefore its implementation would be not simple, and potentially non precise. The acceptance-rejection method was discarded because in particular circumstances it can become computationally inefficient since the area below the probability density function can be many times smaller than the area outside. For these reasons, its implementation would have been simple, but would not have allowed the computational-time to be reduced in every situation.

The inverse transform method on the contrary presents intermediate characteristics, such as a moderately difficult implementation and a moderate computational-time, caused by the non closed form of the Beta function and the necessity of inverting iteratively the cumulative density function in Equation 78. The particular attention put in the inversion algorithm designed, based on the secant method (138), allowed to overcome this problem.

4.2.3 Probability density function

The probability density function of a random variable is a function describing the density of probability at each point in the sample space. It enables the calculation of the probability of the random variable falling within a given interval by calculating the integral, called cumulative density function of the probability density function in the given interval. In the Monte Carlo method, the probability density function is used to describe the probability structure of input and output variables and to increase the result precision, allowing a greater number of simulations to be carried out for the more probable values of each parameter.

Although the Monte Carlo method can work with different probability density functions, for the practical realisation of the algorithm it was decided to use only one. This decision was taken in order to reduce the complication of the algorithm in prevision of its use by third party developers. The selected probability density function must be defined in a bounded interval, since practical experience suggests that the environmental conditions recorded in a short period do not present infinite values or values particularly detached from the average. It must also be continuous in the defined interval, since it represents continuous phenomena. Finally, the probability density function must be flexible and all the possible phenomena involved in the thermal state estimation should be summarized using the same probability density function without losing accuracy. This is to make the thermal state

estimation algorithm less complex and moreover to facilitate the interface with other applications. A list of the requirements of the selected probability density function is provided below:

- Defined in a bounded interval
- Continue
- Flexibility

Among the probability density functions available in literature (139), (140), discrete distributions and distributions defined over an infinite interval were discarded. After a review of the remaining distributions, the elimination of monotone distributions such as the Exponential distribution or the Uniform distribution, the following were considered suitable for the implementation in the algorithm:

- Beta distribution
- Kumaraswamy distribution
- Triangular distribution
- Truncated Normal distribution

The Beta probability density function and cumulative density function for the interval [0,1] are given in Equation 82 and Equation 83 respectively. In these equations, the parameters p and q are the shape parameters and x is the variable. According to their values, the Beta probability density function can assume different shapes, as shown in Figure 8.

$$PDF_{\beta}(x;p,q)[[x]^{-1}] = \frac{(x)^{p-1}(1-x)^{q-1}}{\int_0^1 t^{p-1}(1-t)^{q-1}dw} \tag{82}$$

$$CDF_{\beta}(x;p,q) = \int_0^x \beta(w;p,q)dw = \frac{\int_a^x (w)^{p-1}(1-w)^{q-1}dw}{\int_0^1 t^{p-1}(1-t)^{q-1}dt} \tag{83}$$

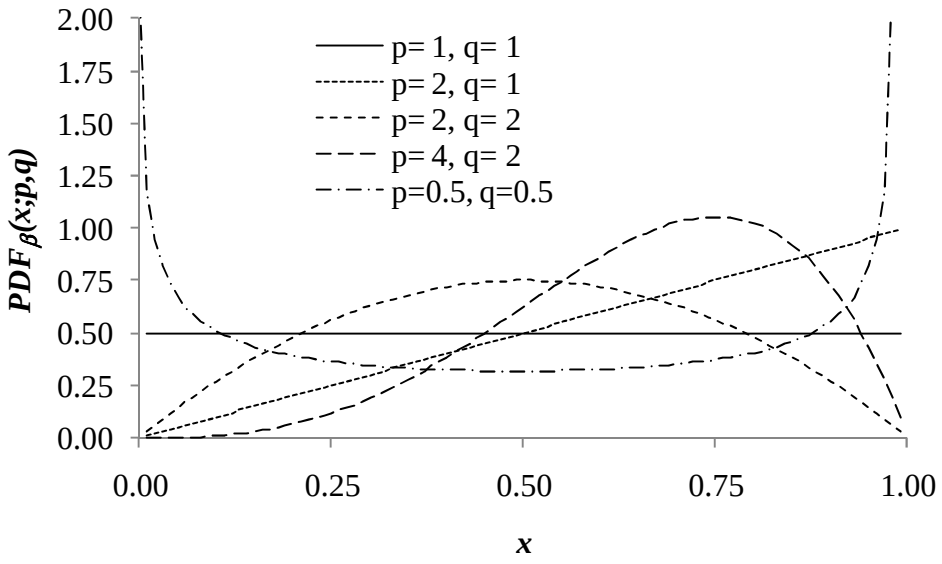

Figure 8: Beta distribution for different shape parameters values

The Kumaraswamy distribution is very similar to the Beta distribution, but easier to use thanks to its closed form as it is possible to see in the probability density function and cumulative density function for the interval [0,1] reported in Equation 84 and Equation 85 respectively. In these equations, the parameters p and q represents the shape parameters and x represents the variable. In Figure 9 different Kumaraswamy probability density functions with different combinations of the shape parameters are reported.

$$PDF_K(x;p,q) = pqx^{p-1}(1-x^p)^{q-1} \tag{84}$$

$$CDF_K(x;p,q) = 1-(1-x^p)^{q-1} \tag{85}$$

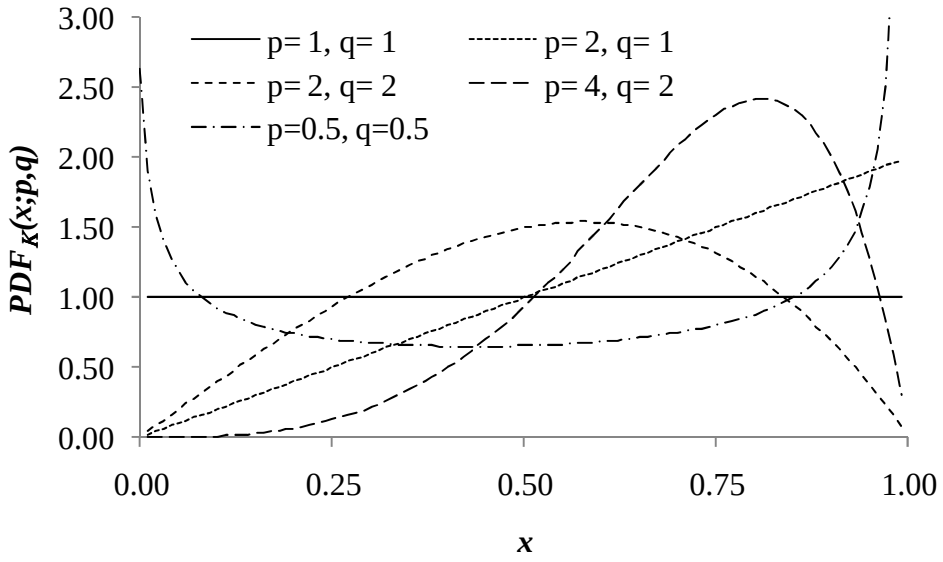

Figure 9: Kumaraswamy distribution for different shape parameters values

The triangular distribution approximates data probability density with a simple triangle as it can be seen from its probability density function and cumulative density function reported in Equation 86 and Equation 87 for the interval [0,1]. The parameter c is the only shape parameter of the equation and represents the mode of the distribution, as shown in Figure 10.

$$PDF_T(x;a,b,c) = \begin{cases} \frac{2x}{c} & 0 < x < c \\ \frac{2(1-x)}{(1-c)} & if \quad c < x < 1 \end{cases} \tag{86}$$

$$CDF_T(x;a,b,c) = \begin{cases} \frac{x^2}{c} & a < x < c \\ 1 - \frac{(1-x)^2}{(1-c)} & if \quad c < x < b \end{cases} \tag{87}$$

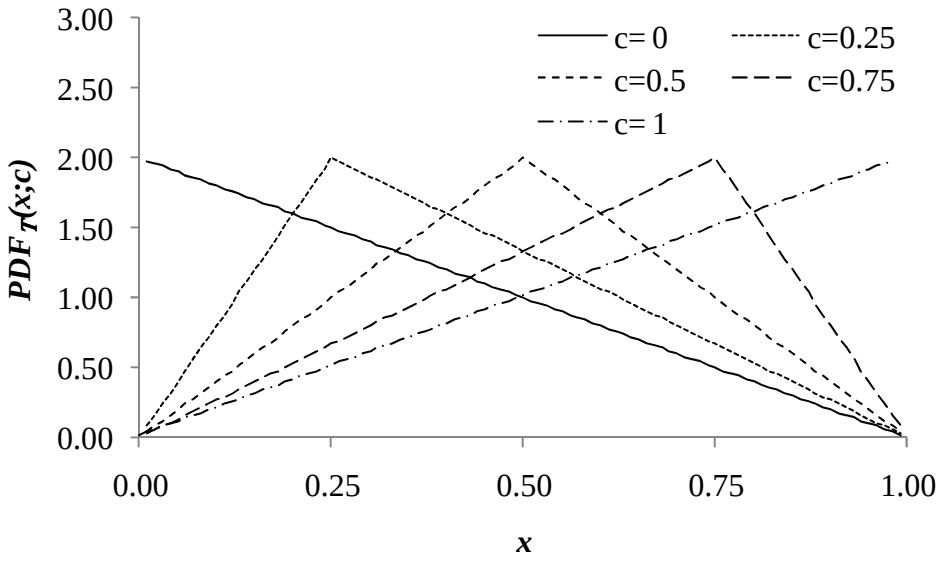

Figure 10: Triangular distribution for different shape parameter values

The truncated normal distribution is based on the normal distribution but it is defined over a bounded interval. Considering the normal distribution probability density function and cumulative density function reported in Equation 88 and Equation 89, where p and q represents the shape parameters, equivalent to the average and the standard deviation of the distribution. The truncated normal distribution probability density function and cumulative density function in the interval [0,1] can be obtained as in Equation 90 and Equation 91. The influence of the shape parameters can be seen in Figure 11.

$$PDF_N(x;p,q) = \frac{1}{p\sqrt{2\pi}} e^{-\frac{(q-\mu)^2}{2p^2}} \tag{88}$$

$$CDF_N(x;p,q) = \frac{1}{p\sqrt{2\pi}} \int_{-\infty}^{x} e^{-\frac{(q-\mu)^2}{2p^2}} du \tag{89}$$

$$PDF_{NT}(x;p,q) = \frac{PDF_N(x;p,q)}{CDF_N(1;p,q) - CDF_N(0;p,q)} \tag{90}$$

$$CDF_{NT}(x;\sigma,\mu) = \frac{CDF_N(x;p,q)}{CDF_N(1;p,q) - CDF_N(0;p,q)} \tag{91}$$

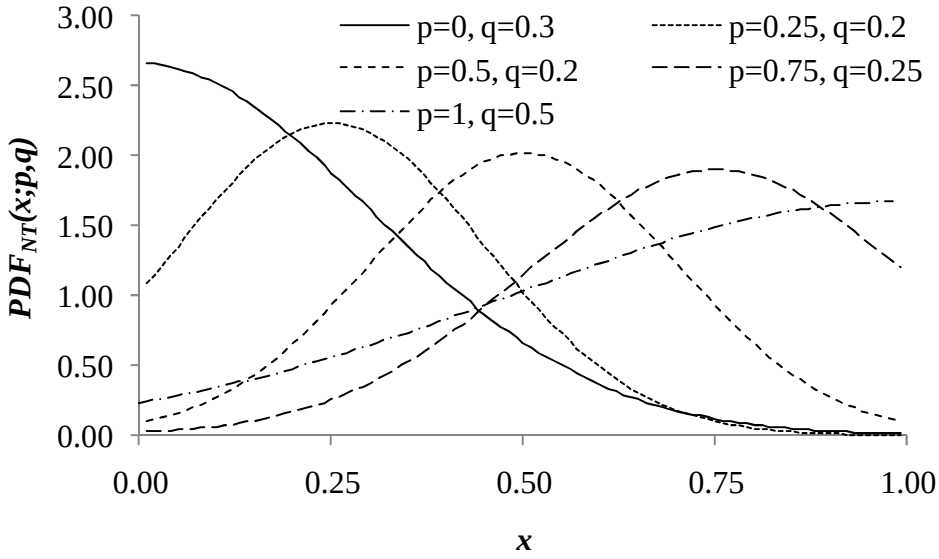

Figure 11: Truncated normal distribution for different shape parameters values

The comparison of these distributions is based on the objective concept of “flexibility”, representing the last point in the list of requirements for the general probability density function reported at the beginning of this section. This is a qualitative parameter, and the decision was based on the personal judgement of the author on the ability of each probability density function to describe the data available at the time of the decision. A revision carried out in a second phase, showed that it was not necessary to modify the selection or to introduce additional probability density functions for describing the available data. The triangular distribution was discarded because of its characteristic of increasing the weight of the “tale” of the distribution, and its inability to describe “u-shaped” distributions.

The Truncated normal distribution was discarded also because its inability to describe “u-shaped” distributions. Although it would have been possible to create new distributions based on these two able to overcome these limits, it was decided to use a distribution already existing and proven. For this reason, the Kumaraswamy and the Beta probability density function were finally selected to be implemented in the algorithm. This is because of their flexibility to represent symmetrical and asymmetrical distributions as well as bell-shaped or u-shaped distributions, as seen in Figure 8 and Figure 9. Finally the Beta distribution was chosen because of the possibility to use the simple method for estimating its parameters described in Equation 94-Equation 97. The main limitation of the Beta distribution is represented by its non-closed form, therefore particular attention was given to reducing the computational-time of the algorithm used for the calculation of its probability density function and cumulative density function. The Beta probability density function and cumulative density function are now reported in the more general case of the interval $[a, b]$ instead of the interval [0,1], along with the procedure used for calculating shape parameters from measured data.

$$PDF_{\beta}(x; p, q, a, b) = \frac{(x-a)^{p-1}(b-x)^{q-1}}{(b-a)^{p+q-1}\int_0^1 w^{p-1}(1-t)^{q-1}dw} \quad (92)$$

$$CDF_{\beta}(x;p,q,a,b) = \int_a^x \beta(w;p,q,a,b)dw = \frac{\int_a^x (w-a)^{p-1}(b-w)^{q-1}dw}{(b-a)^{p+q-1}\int_0^1 t^{p-1}(1-t)^{q-1}dt} \quad (93)$$

The shape parameters *p* and *q* can be calculated from data series analysis using Equation 94 and Equation 95 where $\bar{\mu}$ and $\bar{\sigma}$ can be calculated as in Equation 96 and Equation 97 and μ_m and σ_m are the average and the standard deviation of the data series.

$$p = \bar{\mu}\left(\frac{\bar{\mu}(1-\bar{\mu})}{\bar{\sigma}^2} - 1\right) \quad (94)$$

$$q = (1-\bar{\mu})\left(\frac{\bar{\mu}(1-\bar{\mu})}{\bar{\mu}} - 1\right) \quad (95)$$

$$\bar{\mu} = \frac{\mu_m - a}{b-a} \quad (96)$$

$$\bar{\sigma}^2 = \frac{\sigma_m^2}{(b-a)^2} \quad (97)$$

Due to the non-linearity and the closed form of Equation 93, its inversion for the inverse transform method is realised through an iterative algorithm based on the secant method (138).

4.2.4 Random number generation

Random numbers represent a fundamental part of the Monte Carlo method. Therefore, particular care is taken for the deterministic generation of random sequences presenting all the important statistical properties of true random sequences.

The two methods considered for using random numbers in the algorithm are:

- Physically generated random numbers
- Linear congruential generator

Physically generated random numbers are based on the measurement of phenomena such as atmospheric parameters variation, universal background radiation or the noise of a computer processor. These methods can be particularly slow, and of difficult application in an algorithm. A solution is represented by storing random numbers generated with such methods

in an array and using them scrolling consecutively through the array. This method would allow the use of real random numbers sacrificing memory.

The linear congruential generator is a simple algorithm based on Equation 98 (136).

$$P_n = \left(k_{R,1} \cdot P_{n-1} + k_{R,2}\right) mod\left(k_{R,3}\right) \tag{98}$$

The terms P_n and P_{n-1} in Equation 98 represent respectively the probability to calculate and the probability calculated at the previous step and the terms $k_{R,1}$, $k_{R,2}$ and $k_{R,3}$ are called respectively the multiplier, the increment and the modulus. Since the sequence P_0, P_1, …, P_n will repeat itself after at most $k_{R,3}$ steps, its value is selected as the large prime number that can be accommodated by the computer. The linear congruential random number generator was preferred in the practical implementation of the algorithm because of its speed and its wide use in a wide range of applications.

4.3 Conclusion

The real-time rating algorithm developed is not only composed by a library of component and environmental condition models but also by a framework for interpreting input and output data and for dealing with corrupted data caused by measurement or communication failures. The Monte Carlo method was preferred to other methodologies because of its ability to create a probabilistic description of models results. This was considered particularly important for interpreting the consequences of environmental conditions' uncertainty and variability. Furthermore, the probabilistic description of the results was considered fundamental for quantifying the risk associated with the single rating estimation with a twofold benefit: Firstly, real-time rating risk can be set as the same risk already adopted for seasonal static ratings but for a reduced observation period. Secondly, it

has a positive impact on estimation reliability with respect to measurement and communication failures, increasing gradually the confidence band.

Particular attention was given during the code development phase to the creation of a stable, fast and clearly structured algorithm. In order to avoid developing a particular solution for a particular case, a generic Monte Carlo method algorithm was built and then used with different models for component rating or environmental condition interpolation. This allowed flexibility in code realisation and is expected to facilitate future code improvements and model refinement. Attention also was given to estimation computational-time, a crucial factor in a real-time tool. Code architectures that would have resulted in a simpler but slower code have been discarded and the database was designed for facilitating data reading. Particular attention was given to the design of selected code areas such as random number generation and numerical function inversion of the probability density function.

Chapter 5 Software design and development

5.1 Introduction

The aim of this section is to describe the algorithm developed in order to perform the real-time rating estimation. This detailed description is conceived also as a reference for maintaining and improving the present code and for building new applications exploiting the whole algorithm or some of its parts. The algorithm is firstly conceived for use in a real-time distributed generator power output controller, and secondly as an off-line planning tool.

The requirements of the algorithm to develop can be summarised as follows:

- The algorithm must carry out the real-time rating estimation as described in the sections 3.1, 3.2 and 4.2.
- The rating estimation for a circuit must be carried out in a time compatible with the necessity of the distributed generator power output controller (15-30 min)
- The algorithm must be easy to maintain and improve, and comply with relevant industrial standards where necessary.
- The algorithm must be called by third party software independently from their programming languages or machine operating systems

A schematic view of the Real-time thermal rating algorithm in the general architecture of the control is given in Figure 12.

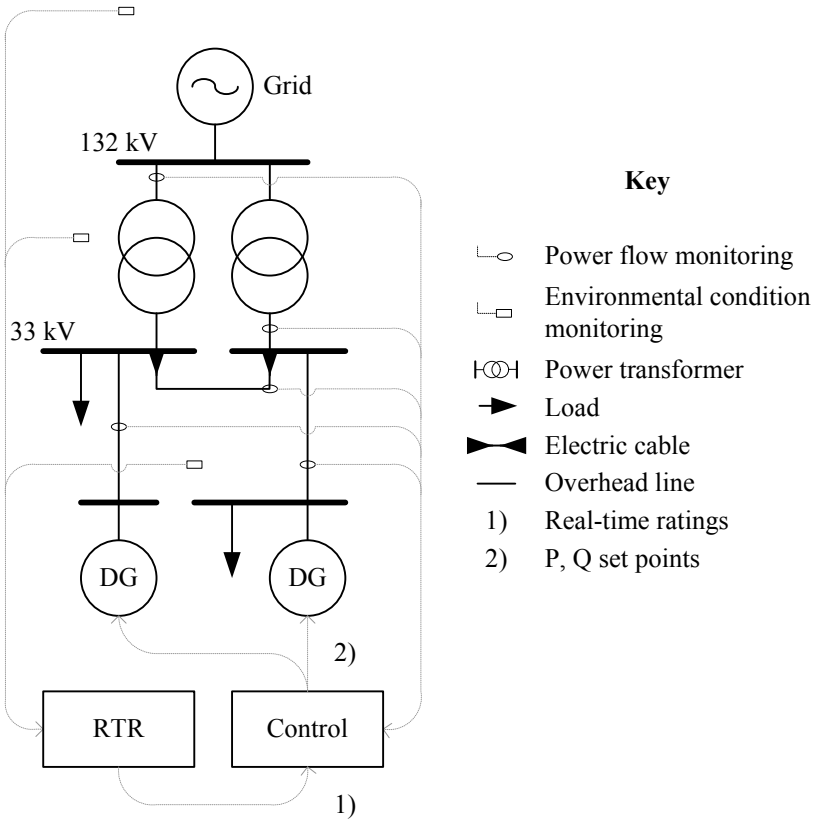

Figure 12: Real-time thermal rating algorithm in the control architecture

The programming language chosen for the development of the algorithm is VB.Net. There were several reasons in favour of this choice: the possibility to use the professional and user friendly development platform MS Visual Studio that allowed creating web services and web sites, as well as the possibility to use with minimal changes macros previously developed for MS Excel. Furthermore applications developed with this programming language would be able to run on every computer where the Microsoft .NET Framework 2.0 is installed. This was advised by Imass, an IT consultancy firm and member of the research consortium, and the firm provided support for the development in this language. Other choices would have been the use of Java, especially for creating web applications or of C++, for the wide

availability of existing open source libraries. Considering the advantages and disadvantages of the different programming languages and the resources available, the programming language chosen was VB.Net.

The database used in the development phase of the project is Microsoft Access. This is because it is particularly straightforward to create applications that make use of this database management software, while it is not necessary to have it installed on the machine where the algorithm is running, (the database management is included in the .NET framework 2.0). Furthermore, its practical graphical user interface allows analysis of partial results, facilitating the debugging and validation process.

For the program, three different programming paradigms were used according to their suitability for each particular task: service oriented architecture, object oriented programming and imperative programming. Although several definitions exist for the different programming paradigms, the differences between the three are clear and can be summarised as follows: Service oriented architecture is based on the concept of creating a series of interoperating services, sharing a common interface protocol. Object oriented programming uses collections of attributes and methods for describing real-world objects. Imperative programming consists of a series of instructions for the computer to perform.

The service oriented architecture is present in the web service used as interface between the thermal state estimation algorithm and the distributed generation power output controller. The object oriented programming is present in the description of the real-world objects used in the algorithm. Finally, imperative programming is present in the code specifying the actions of the different methods. This allowed exploiting the potential of each paradigm: object oriented programming is an excellent tool for describing real world objects and their interactions, like the interaction between the environment and a conductor. But this is not the most appropriate solution for performing the mathematical passages for calculating

component rating or for carrying out the Monte Carlo simulation. For these tasks, the more traditional imperative programming was used. It is also necessary to note that, although only one web service for calculating circuit real-time rating estimation was created, the algorithm is built with a series of integrated functions describing the structure of a complex network of services. This would allow with the creation of adequate interface wrapping codes, the development of a family of web methods based on the algorithm and able to perform single tasks like the rating of a single component or the calculation of a random number, reducing the granularity of the web service.

In summary, the algorithm developed can be described as follows: a web service with a single method provides the interface between the algorithm and any other program or website with a standard interface protocol. The web service makes use of a complex algorithm based on the object oriented programming paradigm, divided in six classes and with access to several databases.

These are then used to describe respectively electric networks component thermal behaviour, environment and probability distributions respectively. The object oriented programming is also used for coding the thermal state estimation and the Monte Carlo simulation, although these two classes consist of lists of methods. A sixth class is used for providing active data storage and ancillary methods used in the whole algorithm. Databases are used for storing static information relative to network components and geographical data and dynamic real-time environmental readings.

5.2 Classes

The aim of this section is to describe each class of the algorithm, with its attributes and its methods. A scheme representing the static structure and the relations between different

classes is shown in Figure 13. For each class and its sub-classes an accurate description is given, specifying the type of each attribute and the function of each method. Classes are also described visually according to the unified modelling language (UML), with each class represented as a rectangle divided in three horizontal sections: in the top section, there is the name of the class, in the middle section there is a list of the attributes and in the bottom section there is a list of the methods. For each attribute and each method the type of the output is also given. For reasons of clarity and space, attributes and methods are not shown in Figure 13. A detailed description of each class is provided in the Appendix. The chart shows also class level and dependence relationships.

Class level relationships, represented with solid lines, indicate that one class inherits methods and attributes of the other. Dependence relationships indicate that a class makes use of another class and is represented with a dashed line. An example is given in Figure 14, where three classes developed in the algorithm are represented with their relationships. The class “Web Service” has no attributes and one method called “Circuit_TSE”. The class PDF has two attributes: “Name” and “Type” but no methods. Finally, the class “Beta” has six attributes and one method “Estimate Parameters”. The class Beta is a subtype of the class PDF since different PDFs could be created. Therefore, their relationship is represented with a solid line. The class “Web Service” is not similar to the class PDF, but it makes use of the class PDF for representing estimation outputs. Therefore, their relationship is represented with a dotted line. This example is purely explicative and for a complete description of each class, the reader is invited to consult the Appendix.

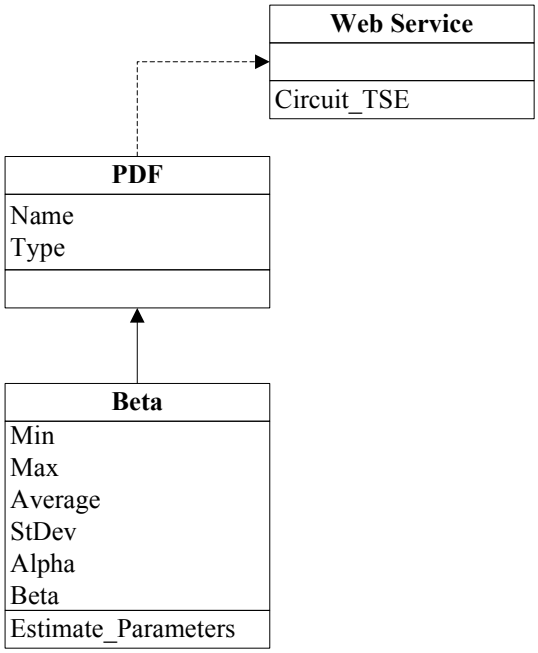

Figure 13: Class diagram, example

The algorithm makes use of the seven classes listed and described below. A visual description of their relations is shown in Figure 14.

- Web Service
- TSE (Thermal State Estimation)
- Monte Carlo Method
- PDF (Probability density Function
- Component
- Environment
- Auxiliary procedures

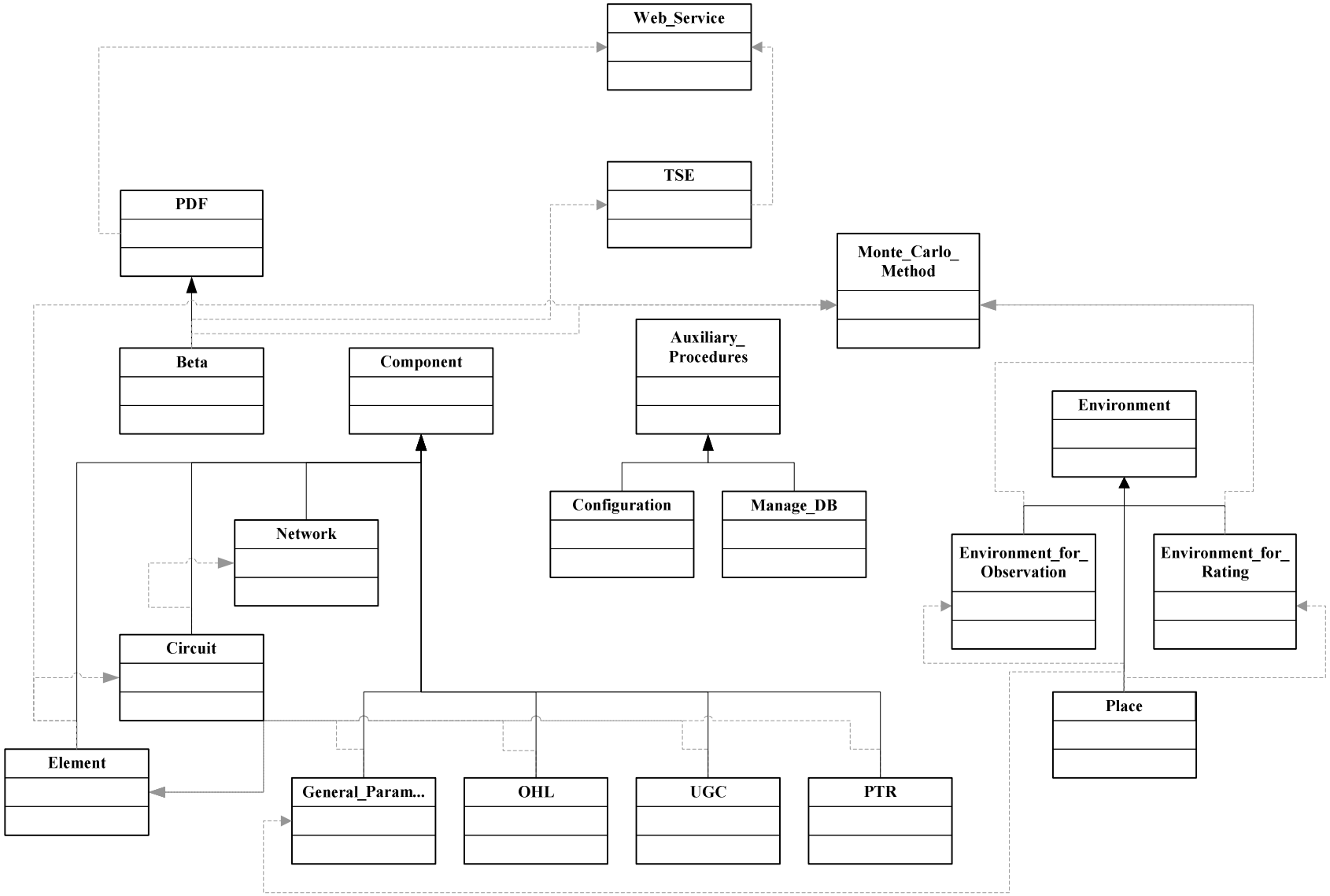

Figure 14: Whole system class static diagram

The task of the class “Web Service” is to act as an interface between the algorithm and other programs, such as the distributed generators power output controller developed in this research project. This class has a single method that calls in turn a method of the “TSE” class. The TSE class supervises the series of actions necessary to carry out the thermal state estimation of a single circuit, by using methods of the “Monte Carlo Method” class. The “Monte Carlo Method” class contains the method necessary for carrying out a single Monte Carlo estimation for environmental conditions or component rating. In this process, it uses methods and attributes of the classes “Environment”, “Component” and “PDF”, where the models and the methods necessary for modelling environmental conditions, power system components and probability density functions are implemented. Finally, the class “Auxiliary Procedures” contains attributes and methods of general utility that can be accessed in any part of the program, such as the access to databases. This solution allows a simpler algorithm structure and facilitates software maintenance and new features development.

5.3 Databases

This section describes the databases used by the thermal state estimation algorithm for storing static data regarding the electric network and its geographical area, and the real-time environmental parameters. Other two ancillary databases created in the software development and validation phases for storing errors logs and simulation results have been maintained for their expected utility in software maintenance and for the use of the algorithm as an off-line planning tool. The approach followed during the software development phase was to create an interface with the databases in each class. This allowed modifying the structure of each database, their number and the database software used without impacting on the whole

algorithm. The development started with MS Access because of its availability on the machine and later a MySQL database was introduced.

As introduced before, the algorithm makes use of the five databases listed and described below:

- Component
- Environment
- Geographical
- Errors
- Simulation output

The database “Component” is used for storing information regarding the network, with its circuits, circuit section and transformers. This database presents the most complex structure among the other databases used in the algorithm with a table describing the components as members of a network, tables describing the characteristics of the single component and finally tables describing the characteristics of the generic component type. A more detailed description of the database is provided in the Appendix. The database software currently used for this task is MS Access.

Environmental conditions are stored in the database “Environment”. This database presents a table listing the existing weather station on the network and a reference to their location, and one table for each weather station, with historical readings of the environmental condition recorded in the particular meteorological station. The database software used for this application is MySQL, in order to facilitate the integration with the on-line database used in the field trial.

Geographical information such as location coordinates, height and soil roughness are stored in the database “Geographical”. This database is composed by a single table listing all

the information mentioned above accessible using a location ID. The reason of two separate databases for geographical and network information is that this facilitates the utilization of existing databases in a future commercial version of the system.

The last two databases have been created during the development phase, but they have been maintained in the final version because of their utility. The database “errors” contains logs written by the program in case of errors and information on the decisions taken in consequence of these errors. Originally conceived for the phase of code debugging, the database and the associate functions are now used for keeping track of the decisions taken in coincidence of missing or bad data. The database “Simulation results” finally is used for storing long sequences of state estimations. Created for the algorithm validation, it was maintained in order to facilitate the development of an off-line planning tool.

5.4 Structure of the algorithm

The aim of this section is to describe the dynamic behaviour of the classes and the databases described in the previous sections and their methods. A detailed description of the process and the dataflow is reported in the Appendix.

The web service is used as the external interface of the algorithm. Its inputs are two strings corresponding to the time and the name of the circuit to be rated. The web service opens the connections with the databases and starts the circuit thermal state estimation. A flow chart describing the algorithm for the thermal rating estimation of a circuit is shown in Figure 15. Firstly, circuit data relative to the selected circuit are loaded from the off-line database and the instance of each circuit section is populated with these data. Then the most updated environmental condition readings at every meteorological station are loaded. The

data of each meteorological station are used for populating an instance of the class “Environment for Observation”. At this point, for each section of the circuit, the algorithm estimates environmental conditions in its location. The estimation is done for every environmental condition using the Monte Carlo Method algorithm described below. The environmental condition estimation produces an array of probability density functions describing the environment in the circuit section location. This is used for estimating component thermal rating, using again the same Monte Carlo Method algorithm described below. When thermal ratings for each circuit section have been estimated, the rating of the whole circuit is estimated by sampling the combined PDF of each section.

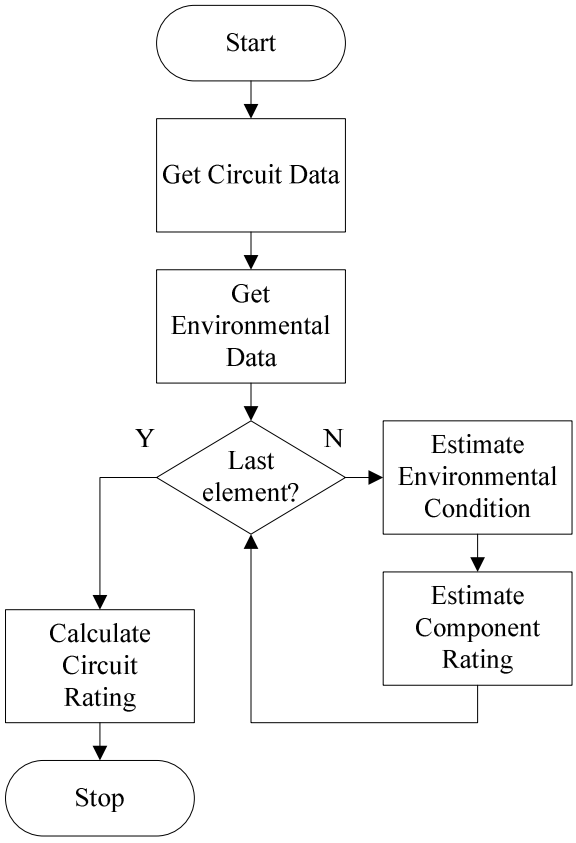

Figure 15: Circuit thermal rating algorithm, flow chart

Particularly important in the circuit state estimation algorithm is the Monte Carlo method algorithm described in the flow chart reported in Figure 16. At the beginning, a minimum number of iterations is fixed and an array for storing the results of the simulations is declared. Then the first set of iterations is carried out. At the first step a variate, containing a set of random values for each input parameter selected according to its PDF is generated. The random variate is then used for calculating the result of the particular model. At this stage, the model for interpolating environmental parameters or the component thermal models can be used.

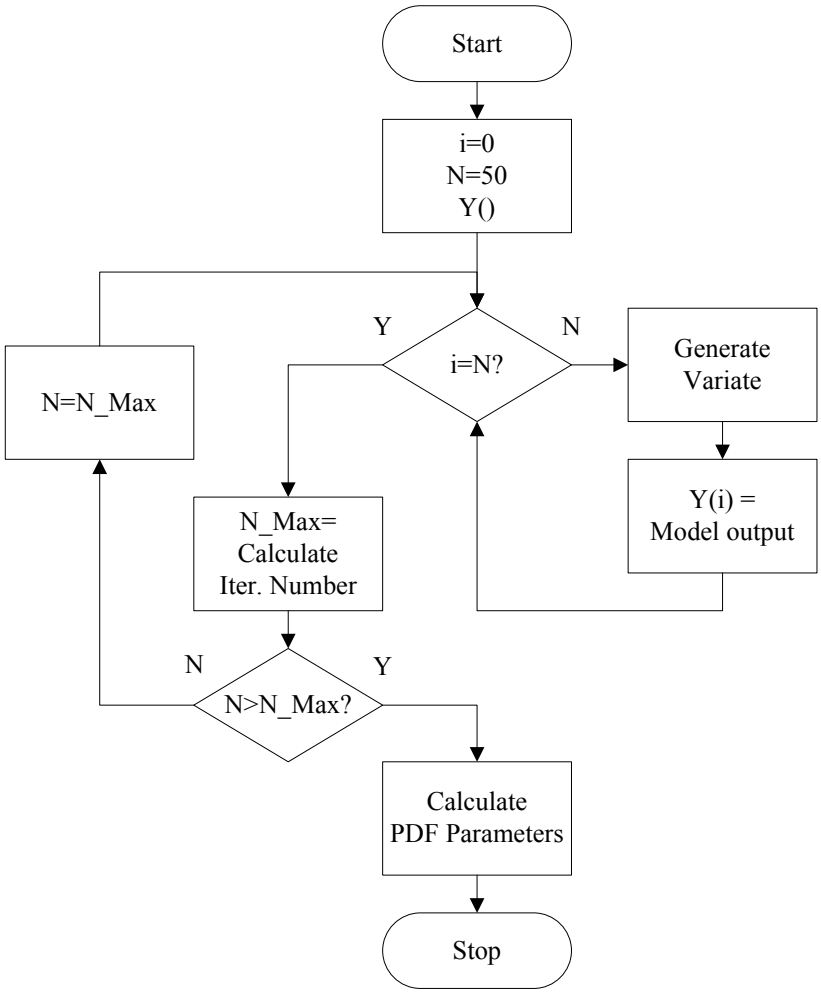

Figure 16: Monte Carlo method algorithm, flow chart

Model's results are stored in the array. When the fixed number of iterations is completed, the array with the stored values is used for calculating the minimum necessary number of iterations for the selected estimation precision. If this number is larger than the one previously used, the cycle is started again for a number of iteration equal to the difference between the two numbers. Finally, the array containing the simulations results is used for calculating the probability density functions' parameters. A detailed data flow of the algorithm, highlighting the different functions used and their dependence is reported in Figure 17 and a more detailed description of the algorithm is provided in the Appendix.

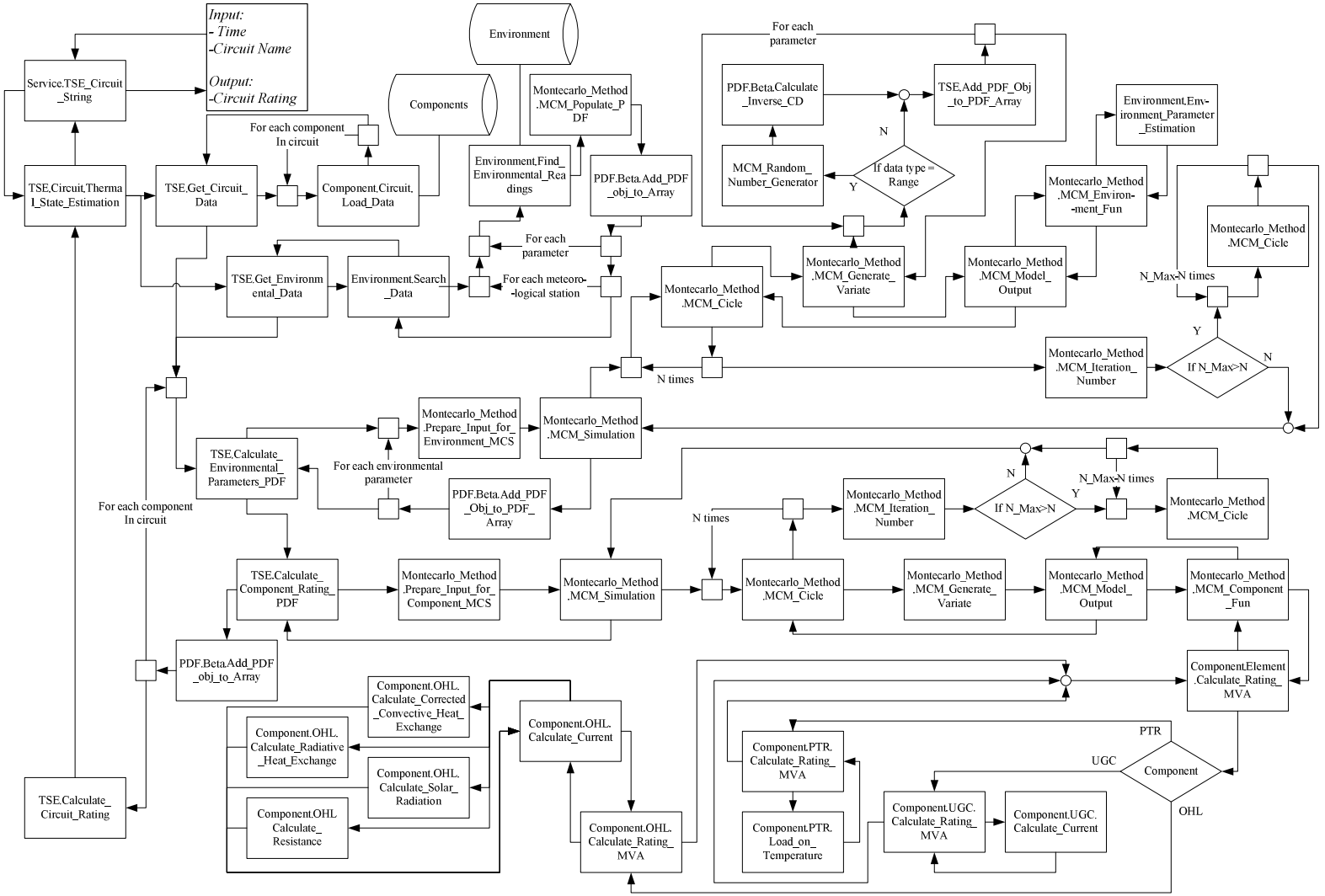

Figure 17: Circuit real-time rating estimation functions and data flow

5.5 Conclusion

This section described the power system real-time rating estimation algorithm developed in the framework of the research project aimed at realising a real-time distributed generator power output controller based on power system component thermal properties. The algorithm written in the language VB.Net is composed by a web service that acts as an interface with other programs. The actual code, written according to the object oriented programming paradigm, is divided in six classes. It uses three databases for storing static information such as network components and geographical related data and dynamic data such as real-time environment conditions readings. Each class is described carefully, specifying the nature of each attribute and the behaviour of each method. A description of the static structure of the classes and of the dynamic data flow during the estimation of the real-time rating is also provided. Initial algorithm requirements have been satisfied, a simplified version of the algorithm is installed in two relays in the test network where open and closed loop tests must be carried out. Furthermore, the whole algorithm is being implemented in commercial products by AREVA, a consortium partner. In order to carry out the real-time rating estimation, classes for describing the thermal behaviour of power system components and the environment have been developed. Furthermore the code necessary for performing generic Monte Carlo simulations and in particular environmental condition and component rating estimations have been written.

One of the main constraints for the algorithm was the ability to carry out the real-time rating estimation of a circuit in a time compatible with the exigencies of the of the distributed generator power output controller. The controller calculates distributed generators' set points

with a frequency of 30 minutes, therefore the estimation time should be a fraction of this time. Currently, as shown in Section 6.3, the estimation time for a single component is in the range of 2.3 seconds, a period that would allow the rating of a circuit made of 10 components to be estimated in less than 30 seconds, and the rating of the 10 most thermally vulnerable components in less than 3 minutes. Therefore, the computational-time has been found to satisfy the initial requirements.

This performance was obtained thanks to the general structure of the algorithm, the optimization of the code in particularly critical functions and to the choice of the precision accepted for the Monte Carlo simulation. This last parameter can be customised, and in further application of the code, it will be possible to increase estimation precision at the expenses of computational-time or vice versa. In order to ensure the possibility of improving and developing additional applications based on the code, the algorithm was written following a clear object oriented approach, assigning meaningful names to attributes and functions and providing extensive documentation. Furthermore, the dynamic structure of the algorithm, made of different functions calling each other allows simple improvements to be made to part of the code without touching other parts.

The presence of an object passed though the whole process, an instance of the "Auxiliary_Procedures.Configuration" class, and containing basic data and the connections to the databases, allows additional data to be passed to each function and each function to access any database in whatever part of the program. This is expected to facilitate improvements on the existing code. Finally, in order to allow third party applications to use the algorithm, a web service was developed for acting as interface. Web services are designed to support interoperable machine-to-machine interaction over a network. A second web service was realised for allowing the distributed generator power output controller to interrogate the

databases used by the real-time rating estimation algorithm. This is an example of the interoperability allowed by web services: since the first code does not have a direct access to the “Environment” database, the creation of a web service wrapping an existing method, was considered the most efficient solution.

Chapter 6 Validation

6.1 Validation strategy

For practical applications, the state estimation algorithm must produce accurate and precise rating estimates, whilst being computationally efficient and robust to measurement and communication failures. Furthermore, the estimation is strongly influenced by the models used, which also have to be accurate and precise. Therefore a testing strategy aimed at evaluating each one of these characteristics was developed. A summary of the results of this study was published in (141)

6.1.1 What to measure

Four parameters suitable for defining the performance algorithm developed have been identified and the algorithm was divided in two parts to be separately studied. The parameters identified are:

- Accuracy. It can be defined as the degree of approximation of a calculated parameter to its true value; in this work accuracy is measured with the average error between estimated and measured values.

- Precision. It can be defined as the measure of agreement between independent calculations. In this work the precision of the estimation is measured with the estimation standard deviation.
- Robustness. It can be defined as the ability of the algorithm to provide estimates in case of measurement or communication failures. In this work robustness is measured with the change of the estimation average error and average standard deviation.
- Computational efficiency. It can be defined as the ability of the algorithm to perform estimations in a given timeframe. In this work the speed of the algorithm is measured with the average time necessary to produce temperature estimations for one component.

Often the terms “accuracy” and “precision” are confused and considered as synonyms, but they represents two different and fundamental concepts in errors and measurement theory. Therefore, a brief clarification is given here with the help of Figure 18.

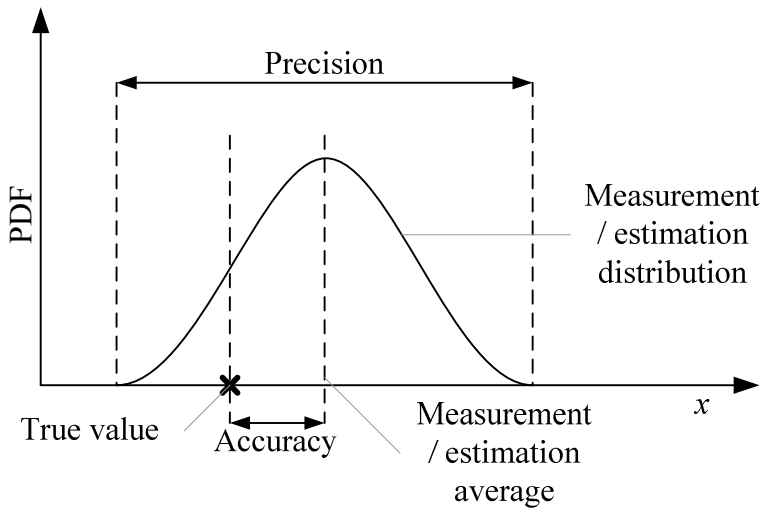

Figure 18: Accuracy and precision

It is important to remember that accuracy and precision are two qualitative and not quantitative terms, therefore it is important to define the method used to measure them (142). Furthermore the Monte Carlo method used and described in Section 4.2, provides an estimate with a probability distribution. Therefore, each estimation is given with a measure of its own precision.

The algorithm was then divided in two main parts:

- Models. Described in Section 3.1 and Section 3.2 they are used for calculating the value of non measured parameters and they are based on empirical or theoretical approximations of physical phenomena. They can be divided in turn in two parts:
  - Component models
  - Environmental conditions models

  The value of the models used is measured calculating the accuracy and precision.
- State estimation. This part of the algorithm is described in Section 4.2 and is used for estimating the rating of the conductor taking into account input uncertainties and measurement and communication failures. This part of the algorithm is validated through all the four parameters listed above. Furthermore, since each estimation is given with an interval and a probability density function, the precision of each estimation is also measured.

6.1.2 Datasets for validation

The thermal state estimation algorithm developed has been validated on measured data from a portion of ScottishPower network where meteorological stations and conductor temperature measurement devices were installed. The network is composed of 132kV overhead lines with Lynx conductors with a maximum operating temperature of 50ºC. A schematic view of the network and a map of the monitored area are given in Figure 19. The circuits shown in the map are highlighted in the schematic network view.

The 132kV network in this area comprises two circuits: one built in the east-west direction connecting the distribution network to local loads; the other built in the north-south direction connecting a local substation and a distributed generator. From a geographical point of view, the area is characterised by hills, valleys and the coast line running in the east-west direction. The different soil roughness of these areas was estimated observing satellite images. The prevailing wind direction is north to south. It is anticipated that this will considerably influence the rating of the circuits described above in the following manner: over the course of the year, the east-west running circuit will experience greater cooling than the north-south circuit.

Weather measurements for the period 07/12/2008-18/02/2009 were used for carrying out the validation. For each meteorological station five minute averaged values of wind speed, wind direction, air temperature and solar radiation were available. Furthermore, in each meteorological station location, five minute averaged readings for conductor temperature and current were available. A summary of the environmental conditions recorded during the observation period is given in Table 3. Average wind speed is the parameter presenting the greatest variation in the different locations, passing from a value of 5.4m/s in MS 5 to a value

of 2m/s in MS 3. The distance between these two meteorological stations is 11km, but differences in ground roughness between the urban and rural environment of MS 3 and MS 5 respectively influence wind speed as described in Equation 55.

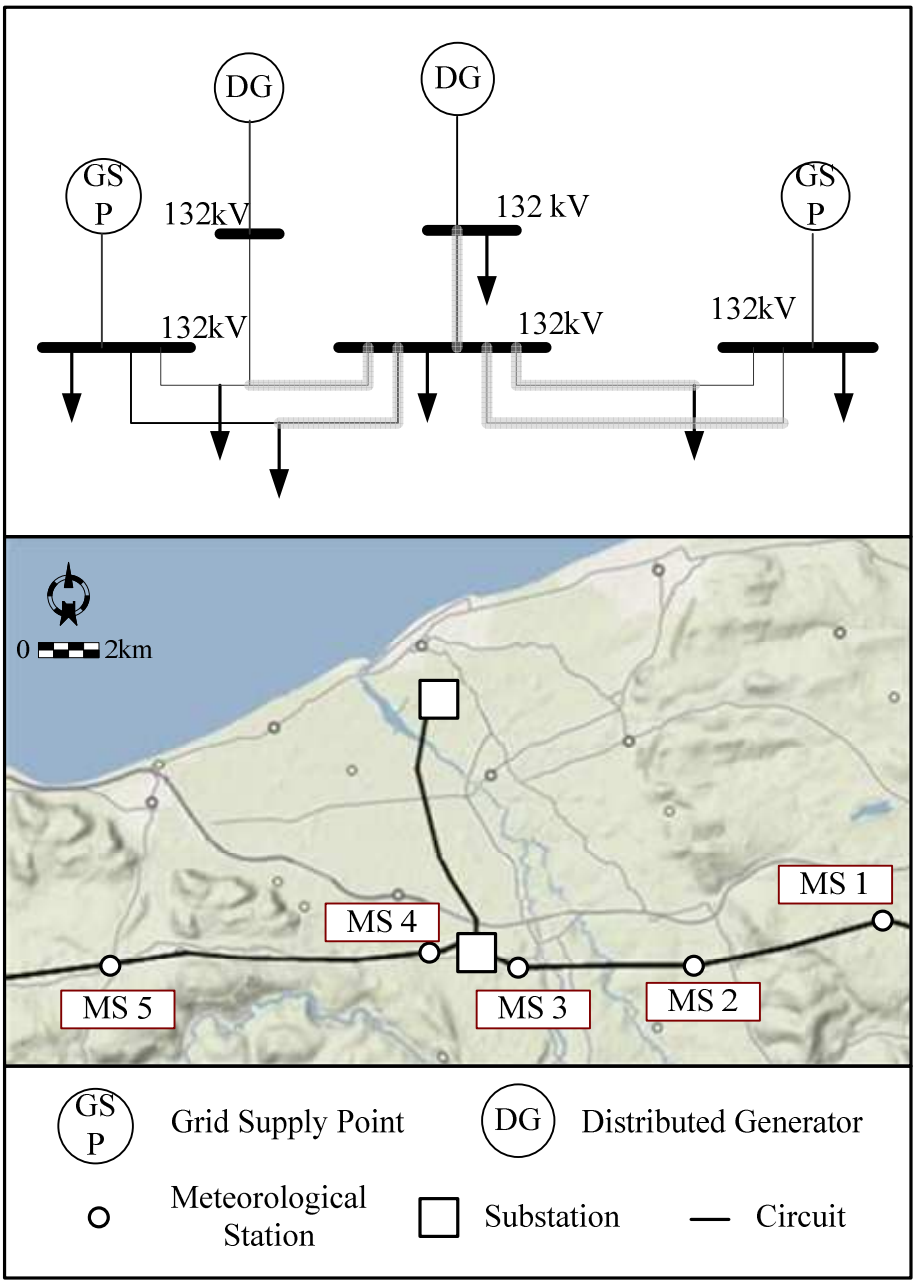

Figure 19: Monitored network area

Table 3: Frequency percentages of measured environmental conditions at the five meteorological stations and measured current flowing in the conductor in the same locations for the period 07/12/2008-18/02/2009.

Ws [m/s]		**0≤Ws≤0.4**	**0.4<Ws≤4.6**	**4.6<Ws≤8.8**	**8.8<Ws≤13**	**13<Ws≤17.2**	**17.2<Ws≤21.4**
	MS 1	12.6%	61.2%	13.1%	1.4%	0.0%	0.0%
	MS 2	8.5%	58.1%	19.0%	0.6%	0.0%	0.0%
	MS 3	12.6%	34.2%	4.5%	0.0%	0.0%	0.0%
	MS 4	10.0%	57.7%	20.3%	2.9%	0.3%	0.0%
	MS 5	1.5%	42.6%	40.9%	9.4%	2.4%	1.2%
		0≤Wd≤5	**5<Wd≤76**	**76<Wd≤147**	**147<Wd≤218**	**218<Wd≤289**	**289<Wd≤360**
Wd [deg]	**MS 1**	0.9%	9.2%	26.3%	37.0%	14.7%	11.4%
	MS 2	0.5%	4.7%	32.2%	36.0%	14.1%	12.0%
	MS 3	0.6%	6.1%	31.2%	26.3%	24.6%	10.8%
	MS 4	0.2%	2.8%	43.7%	28.3%	15.2%	9.5%
	MS 5	0.4%	4.4%	16.0%	41.7%	25.9%	11.3%
		Ta≤-3	**-3<Ta≤0.5**	**0.5<Ta≤4**	**4<Ta≤7.5**	**7.5<Ta≤11**	**11<Ta≤14.5**
Ta [°C]	**MS 1**	1.9%	15.6%	32.1%	33.3%	15.4%	1.0%
	MS 2	2.5%	12.7%	29.6%	30.9%	20.4%	3.5%
	MS 3	4.2%	15.8%	29.1%	29.9%	17.7%	2.8%
	MS 4	1.8%	10.7%	26.4%	33.9%	22.0%	4.7%
	MS 5	0.0%	12.6%	33.4%	37.7%	14.9%	1.1%
		0≤Sr≤5	**5<Sr≤112**	**112<Sr≤219**	**219<Sr≤326**	**326<Sr≤433**	**433<Sr≤541**
Sr [W/m^2]	**MS 1**	2.3%	46.9%	10.2%	4.8%	0.8%	0.1%
	MS 2	2.1%	55.2%	6.3%	0.4%	0.0%	0.0%
	MS 3	2.1%	57.6%	5.3%	1.0%	0.1%	0.0%
	MS 4	1.8%	48.0%	11.0%	4.2%	0.6%	0.1%
	MS 5	2.1%	50.3%	9.8%	3.8%	0.6%	0.1%
		0≤I≤20	**20<I≤64**	**64<I≤108**	**108<I≤152**	**152<I≤196**	**196<I≤240**
I [A]	**MS 1**	1.7%	28.6%	38.8%	21.8%	8.3%	0.4%
	MS 2	1.3%	19.9%	38.4%	23.7%	13.1%	3.0%
	MS 3	1.6%	26.7%	37.0%	21.1%	8.0%	0.5%
	MS 4	14.2%	50.4%	16.4%	13.4%	0.5%	0.0%
	MS 5	23.3%	46.5%	22.4%	1.6%	0.0%	0.0%

6.1.3 How to measure it

Different methods were developed for validating the different parts of the algorithm. The validation was also possible thanks to data provided by ScottishPower EnergyNetworks

and described in Section 6.1.2. The data available influenced the procedure used for the validation and limited the number of parameters that was possible to measure. In particular only overhead lines temperature and environmental conditions influencing this parameter were monitored. Therefore no validation was possible for electric cables and power transformers rating models and for soil temperature and soil thermal resistivity estimation. In order to test the analytical models used for environmental condition estimations, meteorological readings in each of the five locations were compared with values estimated in the same place. In each case, the simulation was performed without considering the data for the location studied and analytical models were populated with directly measured environmental conditions as given in Section 3.2, without using the Monte Carlo state estimation algorithm.

For example, the air temperature at location MS 1 was calculated using Equation 54 and measured values from MS 2 to 5. These values were then compared with data measured in MS 1, the latter measurement being considered as the true value of the parameters. Component ratings can not be directly measured, but rather calculated from standard based models. Therefore, conductor temperature was used for validation purposes since conductor operating temperatures can be directly measured and estimated values can be directly compared with measured values. In order to validate the model used for conductor rating, measured conductor temperatures were compared with conductor temperature calculated using the environmental conditions recorded in the same location. In this case, only the analytical models given in Section 3.1.1 were used.

This process was repeated in order to validate conductor rating models for each meteorological station location. For example, the conductor temperature in location MS 1 was calculated using Equation 3 and measured environmental conditions local to MS 1. This value

was compared to the monitored conductor temperature at location MS 1. An analysis of the model validations studies is given in Section 6.2. In order to validate the thermal state estimation algorithm, estimated conductor temperatures in each of the five locations were compared with measured conductor temperatures. For example, conductor temperature in location MS 1 was estimated as described in Section 3.1.1.3 measured values from MS 2 to 5 and compared to the measured conductor temperature at MS 1. An analysis of the state estimation validation study is given in Section 6.3. In this case, the Monte Carlo state estimation algorithm described in Section 6.3 was used. Results are presented with a chart comparing estimated and measured conductor temperature and a table reporting, for each monitored conductor, average error and standard deviation. The average estimation standard deviation is also given, along with the average standard deviation of the measured conductor temperature over a period of 30 minutes.

6.2 Model validation

6.2.1 Overhead line conductor rating model validation

The model described in Section 3.1.1.3 was tested on the five measurement points MS 1-5 with the methodology exposed in Section 6.1: For each measurement, point environmental conditions over the period 07/12/2008-18/01/2009 were used for calculating conductor temperature and these results were compared with conductor temperature readings in the same location. Figure 20 shows the comparison between calculated and measured values for the first week of simulation for the location MS 2. Figure 20 shows good agreement

between calculated and measured values, with the greatest error associated with spikes in measured conductor temperature not present in the trace produced by calculation.

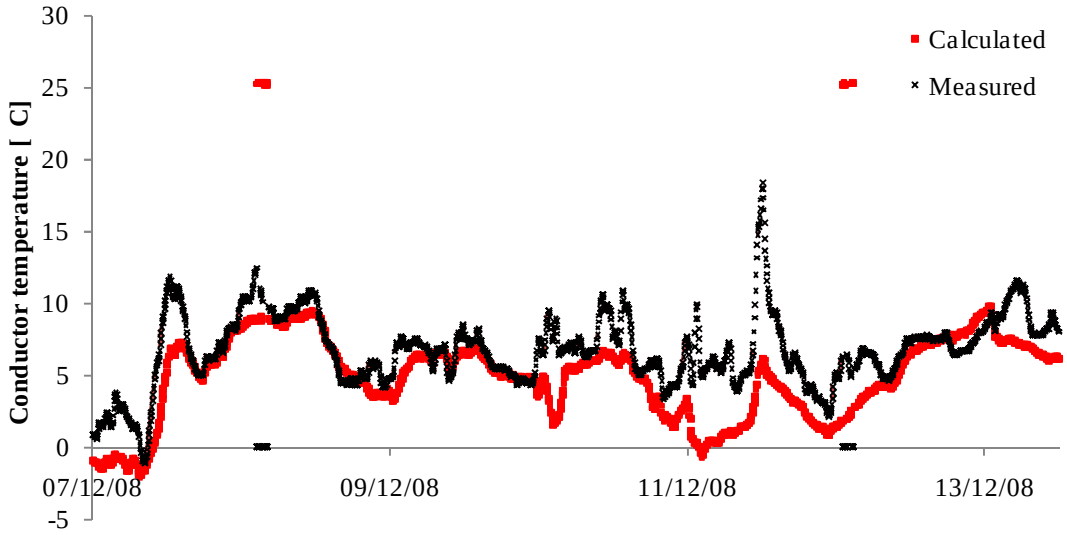

Figure 20: Conductor temperature, comparison between calculated and measured values in MS 2 for the period 07-13/12/2008

The comparison between conductor temperature measurements and conductor temperature calculation for the other four measurement points is reported in Figure 21.

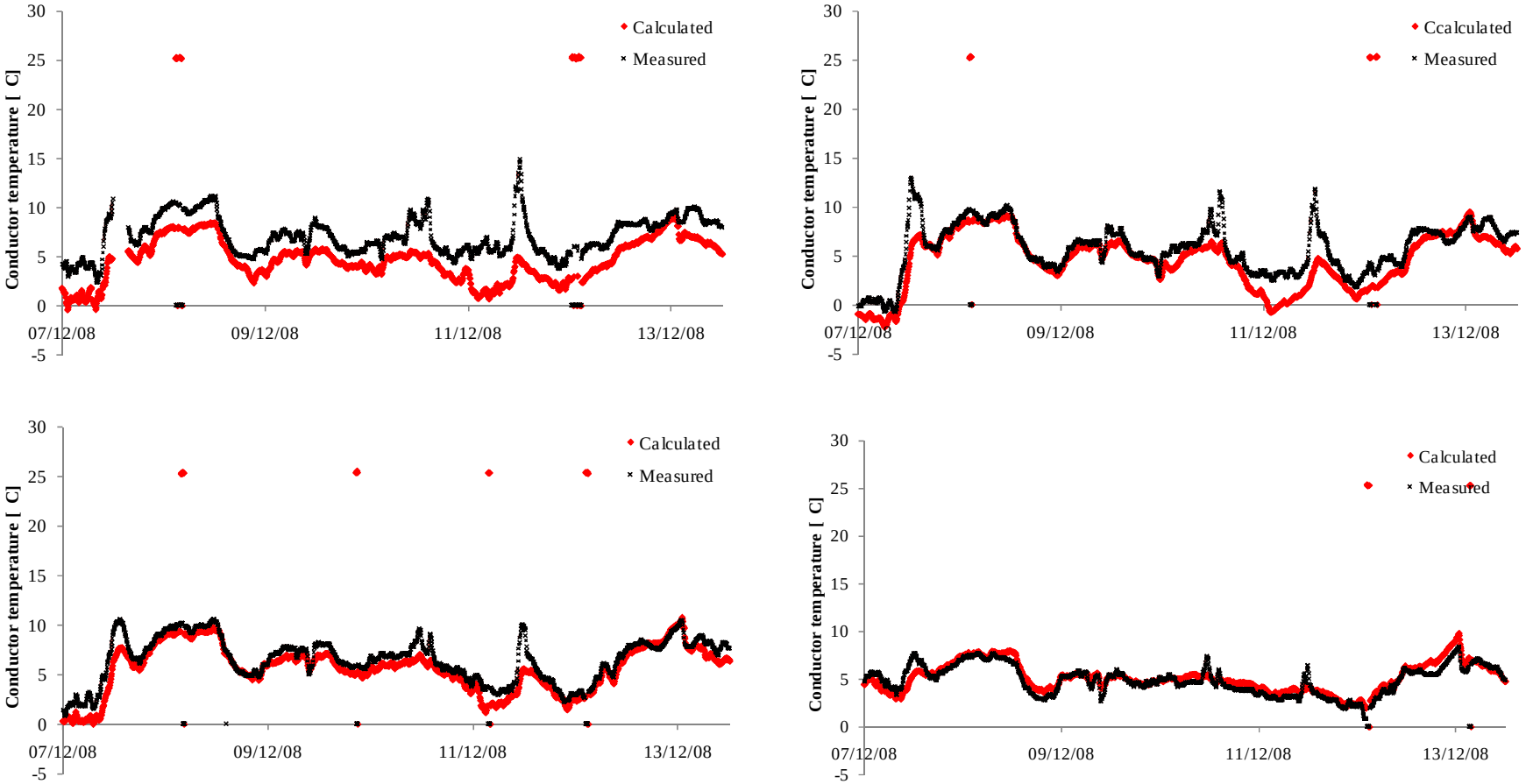

Figure 21: Conductor temperature, comparison between calculated and measured values in MS 1, MS 3, MS 4 and MS 5 (clockwise) for the period 07-13/12/2008

The error average value and the error standard deviation relative to the whole observation period for the five measured location are reported in Table 4. MS 1 and MS 2 reports the greatest values for these two parameters. This is most likely due to the wrong estimation for fixed inputs values such as line orientation and conductor absorption and emission coefficients. MS 5 register on the contrary a null average error, and an error standard deviation of 1.2°C, representing the more accurate result of the whole test.

Figure 22 shows the error probability density function and cumulative density function relative to the whole period for the location MS 2, chosen because of its largest error standard deviation, more suitable for highlighting particulars. It is possible to see that negative errors are more probable than positive errors. This means that the model tends to underestimate conductor temperature and therefore to overestimate conductor rating, with potential dangerous consequences in practical applications.

Finally, in Table 5, a study on the correlation between the error in conductor temperature calculation and the environmental conditions for the five measurement locations is reported. In general, this correlation is small or very small, also because the five parameters act together in influencing the conductor temperature. From this table, it is possible to make hypotheses on the main sources of error. Considering wind speed, the correlation between error and wind speed is positive in all the five locations.

Table 4: Conductor temperature, error average and standard deviation

	MS 1	**MS 2**	**MS 3**	**MS 4**	**MS 5**
Err. Average [°C]	-2.4	-1.8	-1.5	-1.0	0.0
Err. St. Dev. [°C]	2.1	2.6	1.7	0.9	1.2

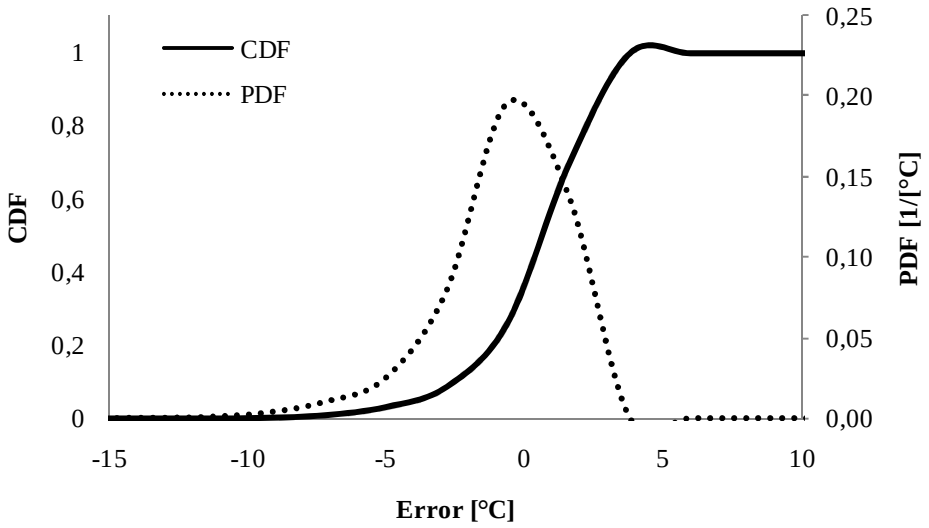

Figure 22: Conductor temperature, error PDF and CDF

This means that the calculated temperature tends to be lower that the measured temperature in case of higher wind speeds, therefore the effect of wind speed is generally overvalued by the model described in Section 3.2, at least in the average range considered in this experiment. From the table it is also possible to make a hypothesis on the reason of the lowest accuracy and precision in conductor temperature calculation in MS 2. In this location, the correlation between error and wind direction is considerably higher than in any other location. This would suggest an error in conductor direction estimation for that location. Thus, since wind direction acts in a multiplying parameter for the cooling effect of wind speed and then of air temperature, also the correlations between error and these two parameters are higher than in other locations. Considering the correlation between error and solar radiation, this is negative in all the five locations. This means that its effect is underestimated by the model, or that incorrect values for the conductor absorption factor were chosen. Conductor absorption factor can range between 0.3 and 0.9, and an average value of 0.5 was used as

suggested in (22). However, this value tends to increase with ageing; therefore, a higher value could have been used in these cases.

Finally, it is not possible to obtain particular information from the analysis for the correlation between error and current, since current values tend to be very similar in the five locations. This is true especially in MS 4 and MS 5. Furthermore, the resistance considered for the conductors is the same. Therefore, differences in the correlation parameter have to be considered as the consequence of errors caused by other parameters. A difference between standard conductor electrical resistance per unit length and the actual value could influence this parameter, but its change in sign for different locations and the lack of information on the installed equipment, do not allow hypotheses to be carried out in this direction.

Table 5: Correlation between conductor temperature calculation and environmental condition values. Absolute values greater than 0.1 are highlighted

	Ta	Ws	Wd	Sr	I
MS 1	0.12	0.15	-0.01	-0.18	0.04
MS 2	0.29	0.31	0.14	-0.19	-0.19
MS 3	0.14	0.08	0.08	-0.24	-0.01
MS 4	0.07	0.09	0.02	-0.21	0.09
MS 5	0.03	0.03	-0.06	-0.20	0.09

6.2.2 Environmental conditions models validation

6.2.2.1 Wind speed

Wind speed calculation is described in Section 3.2, and here the results of the test carried out as described in Section 6.1 are reported. In Figure 23 the comparison between calculated and measured wind speed values for the measurement location MS 2 in the period

07-14/12/2008. According to the description of the methodology in Section 6.1 this means that calculations were carried out using both the interpolation method described in Section 3.2 and the soil roughness correction method described in Equation 56, using wind speed measurements from the other four locations MS 1, MS 3, MS 4 and MS 5. Figure 23 shows in general good agreement between calculated and measured values, with highest error values in correspondence of spikes or periods of higher measured wind speed standard deviation.

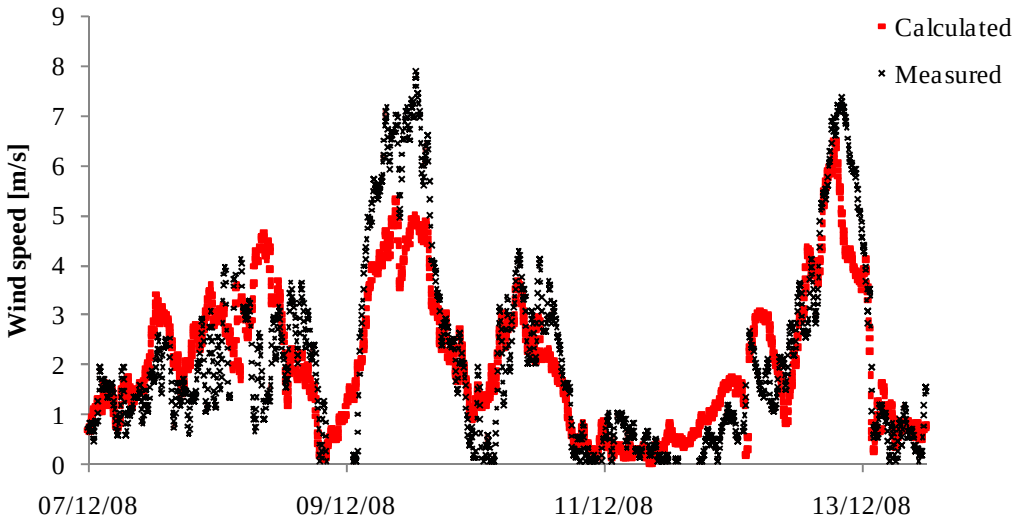

Figure 23: Wind speed, comparison between calculated and measured values for MS2 in the period 07-13/12/2008

The comparison between wind speed measurements and wind speed calculation for the other four measurement points is reported in Figure 24.

The error average and standard deviation relative to all the five measurement points and the whole studied period are reported in Table 6. In this case, the location with the greatest error is MS 3, probably because it position very close to an urban environment where turbulence is expected to be higher. On the other hand, MS 1 registers the lowest average error and also the lowest error standard deviation. This table allows hypothesis to be done on

the accuracy of the estimation of ground roughness parameters in the different locations. In the calculation of the average error, an error in ground roughness coefficient estimation in a measured location has a weight considerably higher than the same error in another location. Therefore, a negative average error would suggest that wind speed tend to be underestimated, so an excessive ground roughness was considered for that location. This would suggest also that in MS 3 the ground roughness was underestimated and that a higher value should be used.

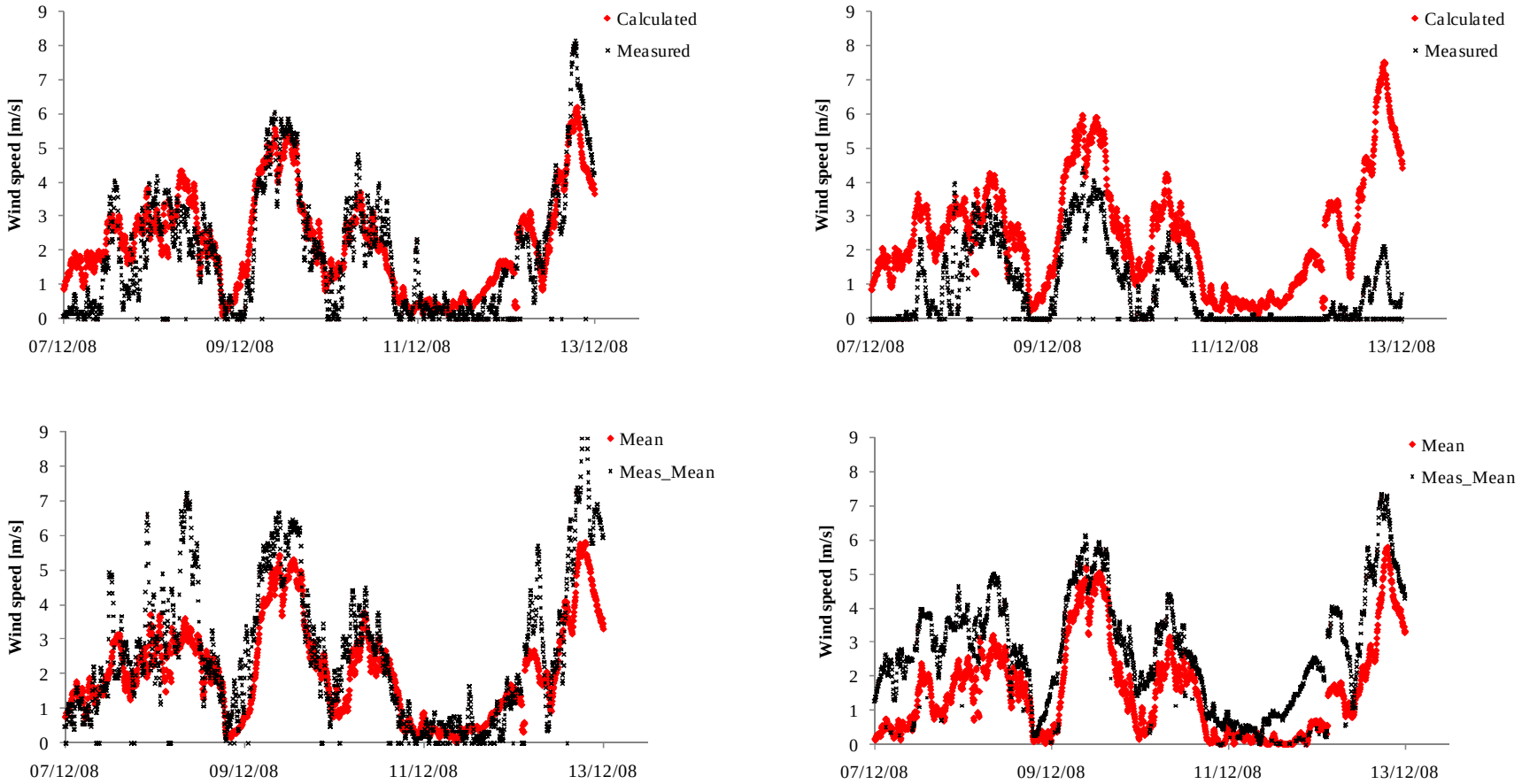

Figure 24: Wind speed, comparison between calculated and measured values for MS 1, MS 3, MS 4 and MS 5 (clockwise) in the period 07-13/12/2008

In Figure 25, where the error probability density function and cumulative density function for wind speed calculation in MS 2 are reported, it is possible to see that the mode tends to correspond with the average and it is close to zero, as the average error value of -0.3 m/s reported in Table 6 suggests.

Table 6: Wind speed, error average and standard deviation

	MS 1	MS 2	MS 3	MS 4	MS 5
Err. Average [m/s]	0.0	-0.3	1.8	-0.8	-0.8
Err. St. Dev. [m/s]	0.9	1.4	1.5	1.3	1.3

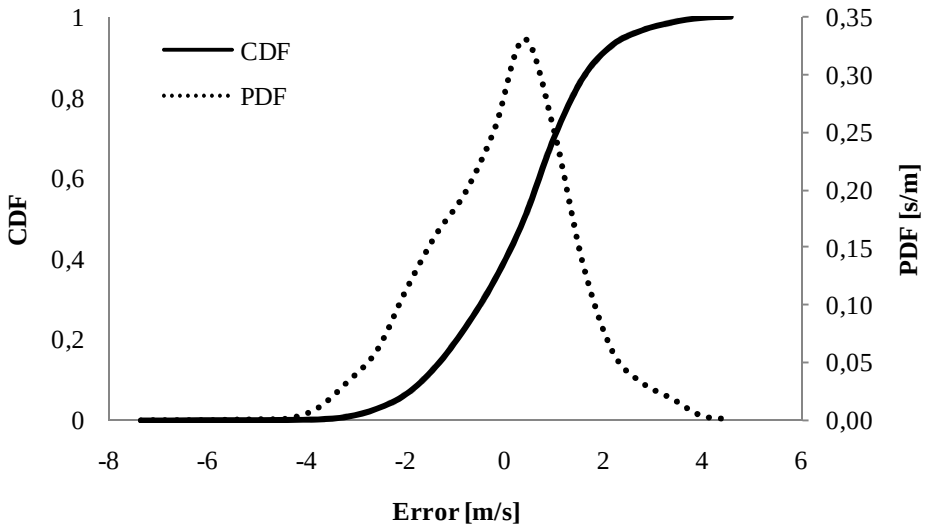

Figure 25: Wind speed, error PDF and CDF

In Table 7 the correlation between the error in wind speed calculation in each of the five measurement points and the value of wind speed in the other four measurement points used as inputs for the calculation are reported. It is expected that this crossed comparison will allow conclusions to be drawn on the sensitivity for wind speed calculation of one location on the others. In doing so, it is necessary also to consider the conclusions drawn from Table 6. Firstly, it is possible to notice that the line corresponding to MS 3 (horizontal highlighted

row) is the only presenting positive values. In that line there are also the highest values of the column, because of the highest error measured in that location. On the contrary when the influence of this measurement point on the others is considered (vertical highlighted column), the correlation parameter is the lowest of the each row.

This is because, wind speed measurements in MS 3, filtered with the ground roughness coefficient, gives values that are the less accurate of the whole series. It is possible to see that in general the correlation parameter tend to be higher for measurement locations that are next to each other, as for example MS 1 and MS2.

Table 7: Correlation between wind speed calculation error and wind speed measurement in the other locations

	Ws 1	**Ws 2**	**Ws 3**	**Ws 4**	**Ws 5**
Ws 1		-0,31	-0,08	-0,11	0,12
Ws 2	-0,39		-0,27	-0,24	-0,02
Ws 3	0,61	0,57		0,61	0,58
Ws 4	-0,37	-0,34	-0,32		-0,37
Ws 5	-0,25	-0,19	-0,16	-0,38	

6.2.2.2 Wind direction

The ability of the inverse distance interpolation to calculate wind direction was tested with the same technique used for wind speed calculation validation. A first qualitative analysis can be done analysing Figure 26 where calculated wind direction values for the first week in location MS 2 are compared with wind direction readings in the same location. Figure 26 shows that values calculated with the inverse interpolation technique can represent a good approximation of real conditions and can also follow very rapid wind direction changes, like on 13/12/2008. On the other hand, Figure 26 shows also periods with considerable error, like on 09-10/12/2008, where calculations produced a considerable error in

correspondence of a relatively constant measured wind direction. No measurement errors were identified in the other meteorological stations and in the same period, considerable error was measured also for wind speed calculation (see Figure 23).This suggests that there is room for improving the model used for air flow calculation.

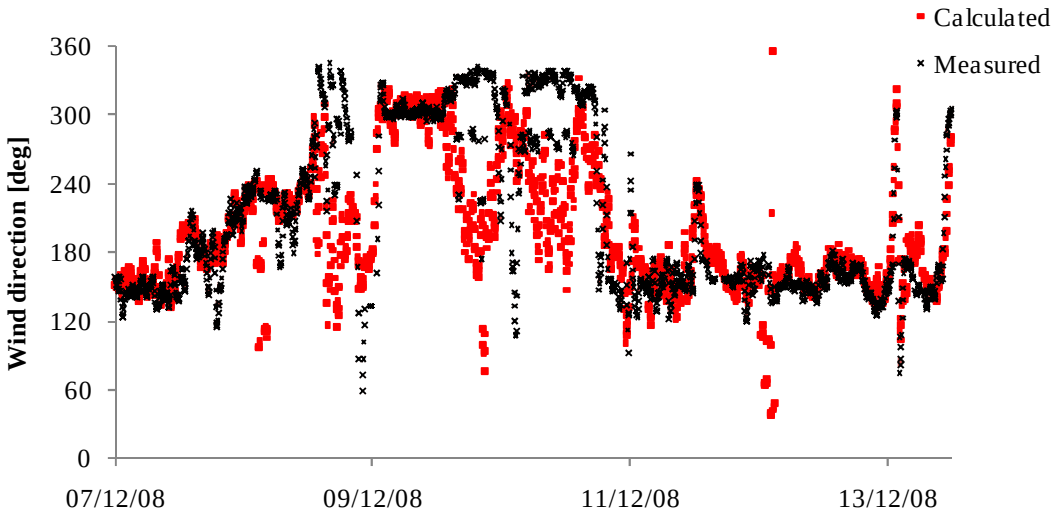

Figure 26: Wind direction, comparison between calculated and measured values

The comparison between wind direction measurements and wind direction calculation for the other four measurement points is reported in Figure 27.

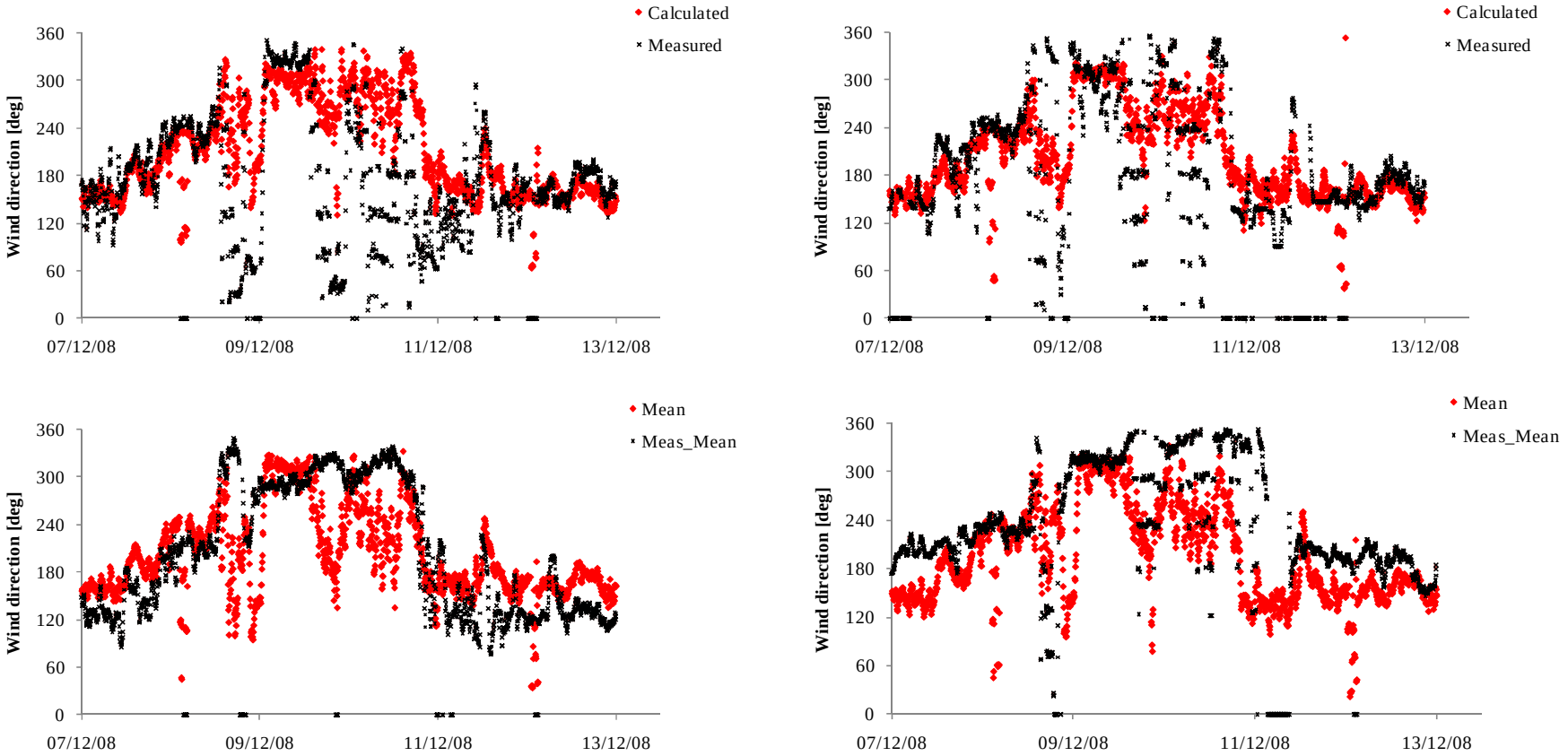

Figure 27: Wind direction, comparison between calculated and measured values for MS 1, MS 3, MS 4 and MS 5 (clockwise)in the period 07-13/12/2008

A quantitative analysis of wind direction calculation validation is given in Table 8 where the error average and standard deviation relative to the whole validation period are reported for each measurement location. The average error absolute value is below 15 degrees in each location except MS 5, and the error standard deviation range between 39 degrees in MS 2 and 54 degrees in MS 1. In Figure 28 the error probability density function and cumulative density function for MS 2 are reported, highlighting the considerable spread of the results. Considering that the effect of wind direction on conductor rating described in Equation 26 has a period of 90 degrees, error values reported in Table 8 and Figure 28 are excessive.

Table 8: Wind direction, error average and standard deviation

	MS 1	MS 2	MS 3	MS 4	MS 5
Err. Average [deg]	8	3	-7	12	-23
Err. St. Dev. [deg]	54	39	47	51	46

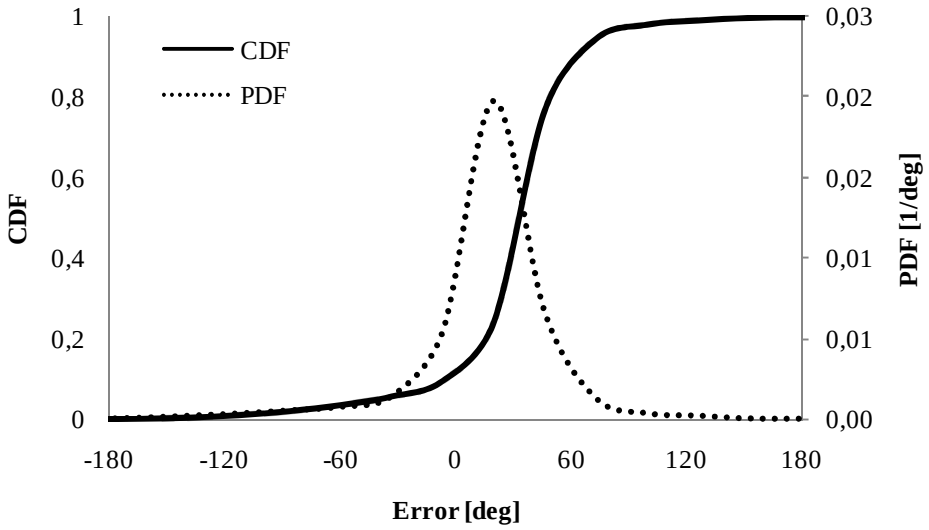

Figure 28: Wind direction, error probability density function and CDF

The correlation between the error in wind direction calculation in each location and wind direction measurement in the other locations used as inputs is reported in Table 9. Considering the high value for error standard deviation, the correlation parameter tends to be low in most of the cases. An exception is represented by MS 4, which presents the highest values for the correlation parameters, especially in reference to MS 1 and MS 2. On the other hand, MS 5 has very low correlation parameter value compared to the other measurement points. But because of the considerable average error reported in Table 8 this must be attributed to the fact that in that location wind direction tends to be less correlated with wind direction compared to other locations. Another distinctive feature is the fact that the correlation parameters in the column of MS 1 and MS 2 tend to have the same absolute value but sometimes with different sign. Even if this is most likely not a coincidence, an explication for this phenomenon was not found.

Table 9: Correlation between wind direction calculation error and wind direction measurement in the other locations

	Wd 1	**Wd 2**	**Wd 3**	**Wd 4**	**Wd 5**
Wd 1		0,34	0,08	0,47	0,17
Wd 2	0,26		0,03	-0,47	0,02
Wd 3	-0,10	0,10		0,18	0,09
Wd 4	0,32	-0,33	0,11		-0,15
Wd 5	0,26	0,26	0,23	0,11	

6.2.2.3 Air temperature

The application to air temperature calculation of the inverse distance interpolation was carried out as described in Section 6.1. From the qualitative analysis of Figure 29 where calculated values for MS 2 over the first week are compared with measured values, it is possible to see a good agreement between the two time series. The main error here is

represented by conservative assumptions made by the algorithm in correspondence of measurement or communication failures. This phenomenon is particularly clear on the 7th and the 12th of December 2008.

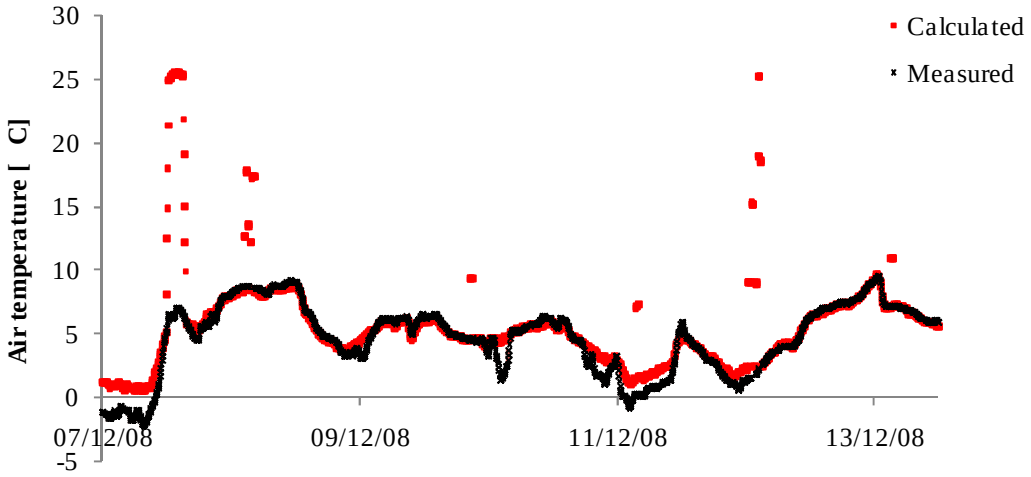

Figure 29: Air temperature, comparison between calculated and measured values

The comparison between air temperature measurements and air temperature calculation for the other four measurement points is reported in Figure 30.

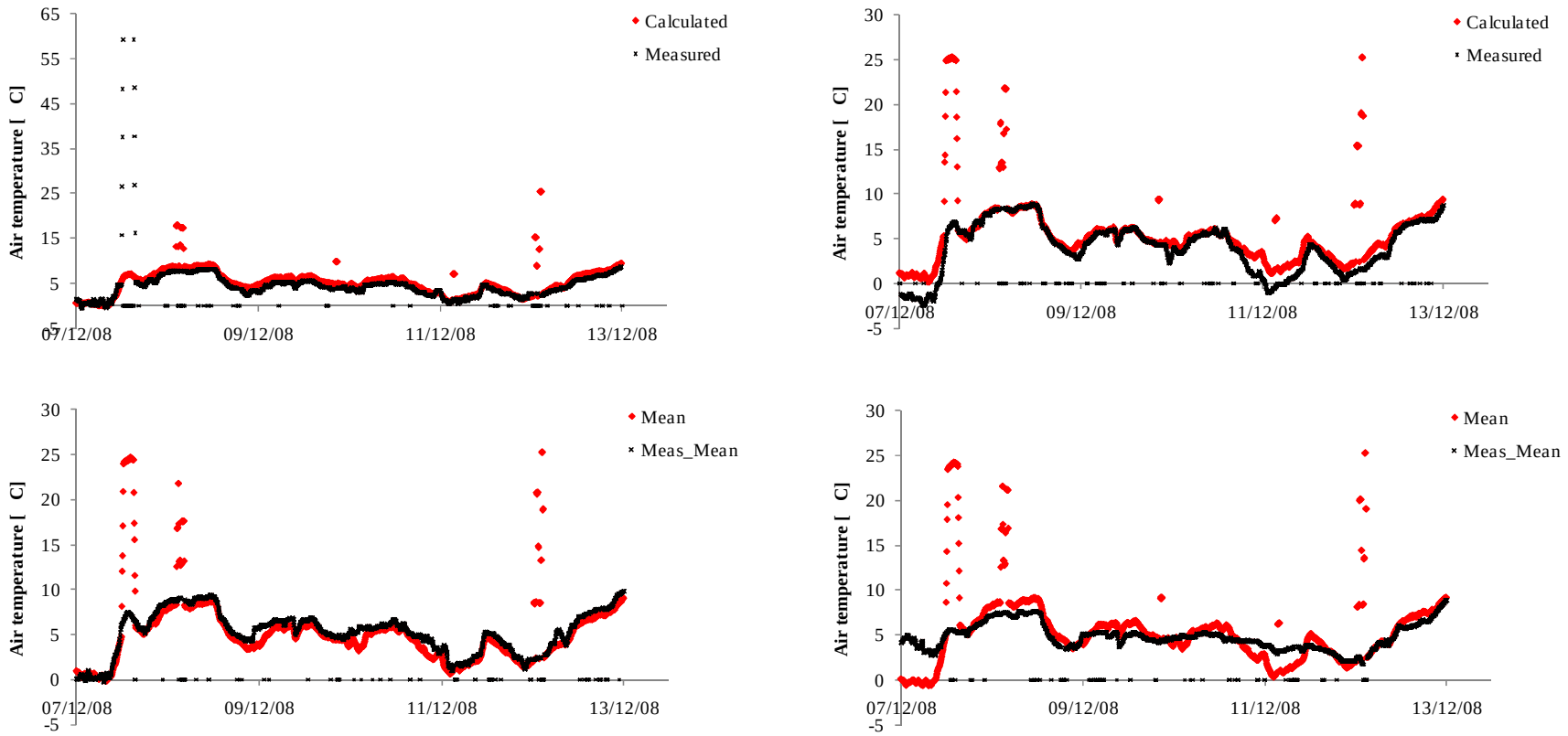

Figure 30: Air temperature, comparison between calculated and measured values for MS 1, MS 3, MS 4 and MS 5 (clockwise)in the period 07-13/12/2008

A quantitative analysis of the results is reported in Table 10, where the error average and standard deviation for air temperature estimation are shown for the five measurement points. The model produces the most accurate and precise results in MS 2 and MS 4 while in MS 1 and MS 5 the greatest average error and error standard deviation are recorded. When these error values are compared with air temperature range in Table 3, air temperature calculation results the one with the smallest relative error. In Figure 31 error probability density function and cumulative density function are reported for air temperature estimation in MS 2, highlighting the tight error spread for this parameter.

Table 10: Air temperature, error average and standard deviation

	MS 1	MS 2	MS 3	MS 4	MS 5
Err. Average [°C]	0.8	0.2	0.9	-0.3	0.4
Err. St. Dev. [°C]	1.5	1.4	1.8	1.6	2.0

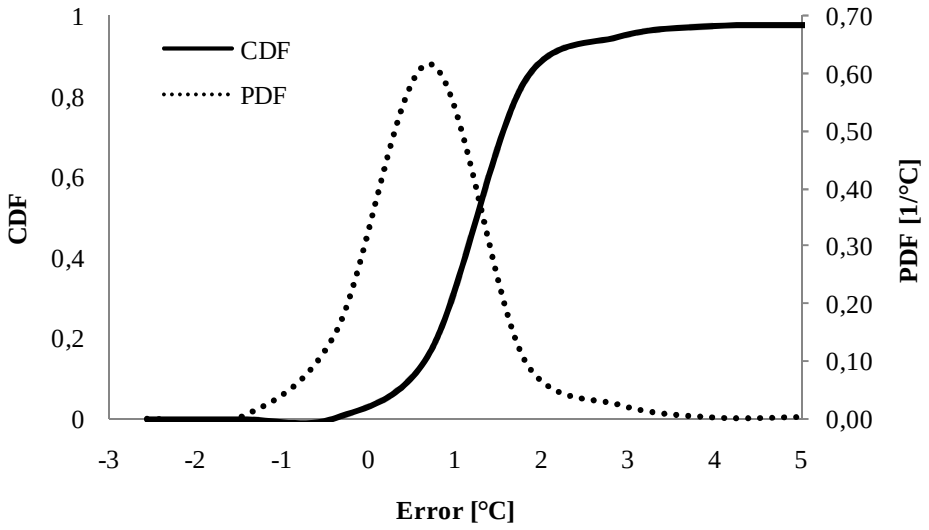

Figure 31: Air temperature, error PDF and CDF

Finally, in Table 11 the correlation parameters between air temperature calculation in each measurement location and the value of air temperature readings in the other measurement locations used as input is reported. In general, there is little correlation between these parameters. On the other hand cells relative to MS 1 and MS 5, the measurement locations with the lowest accuracy and precision according to Table 10, presents particularly high or low values. This is probably due to the fact that they are at the boundaries of the measurement area and the interpolation technique used reduces its accuracy when extrapolating data. This observation could be used in future when studying the optimal placement of meteorological stations.

Table 11: Correlation between air temperature calculation error and air temperature measurements in the other locations

	Ta 1	**Ta 2**	**Ta 3**	**Ta 4**	**Ta 5**
Ta 1		0,05	0,07	0,07	0,03
Ta 2	0,79		-0,13	-0,11	-0,09
Ta 3	0,79	-0,11		-0,11	-0,07
Ta 4	0,83	0,08	0,07		0,00
Ta 5	0,76	0,48	0,47	0,42	

6.2.2.4 Solar radiation

The application to solar radiation calculation of the inverse distance interpolation was carried out as described in Section 3.2. From the qualitative analysis of Figure 32, where calculated values for MS 2 over the first week are compared with measured values, there is a considerable difference between estimated and measured data. This is due to local cloud coverage or other local conditions such as local soil reflection not taken into account in the model described in Section 3.2.

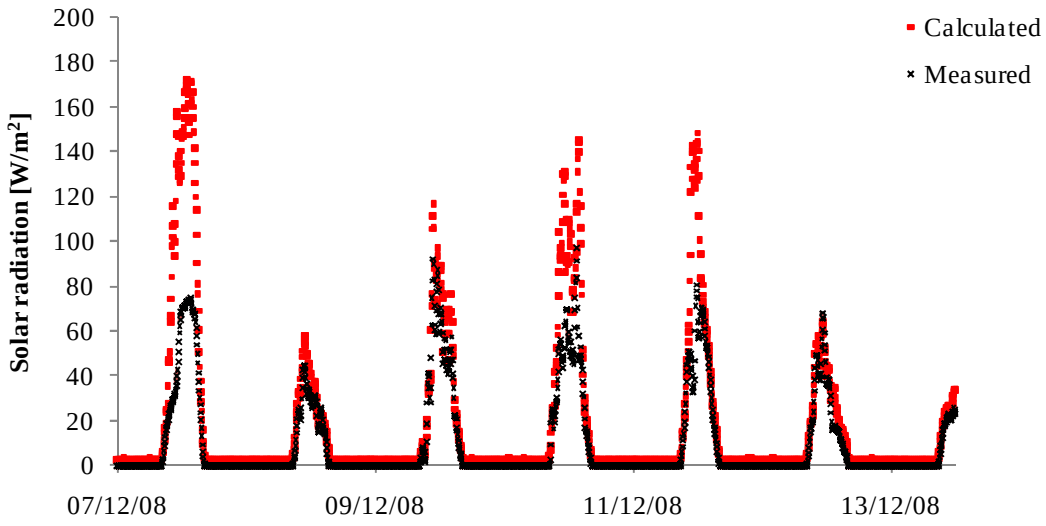

Figure 32: Solar radiation, comparison between calculated and measured values

The comparison between solar radiation measurements and wind speed calculation for the other four measurement points is reported in Figure 33

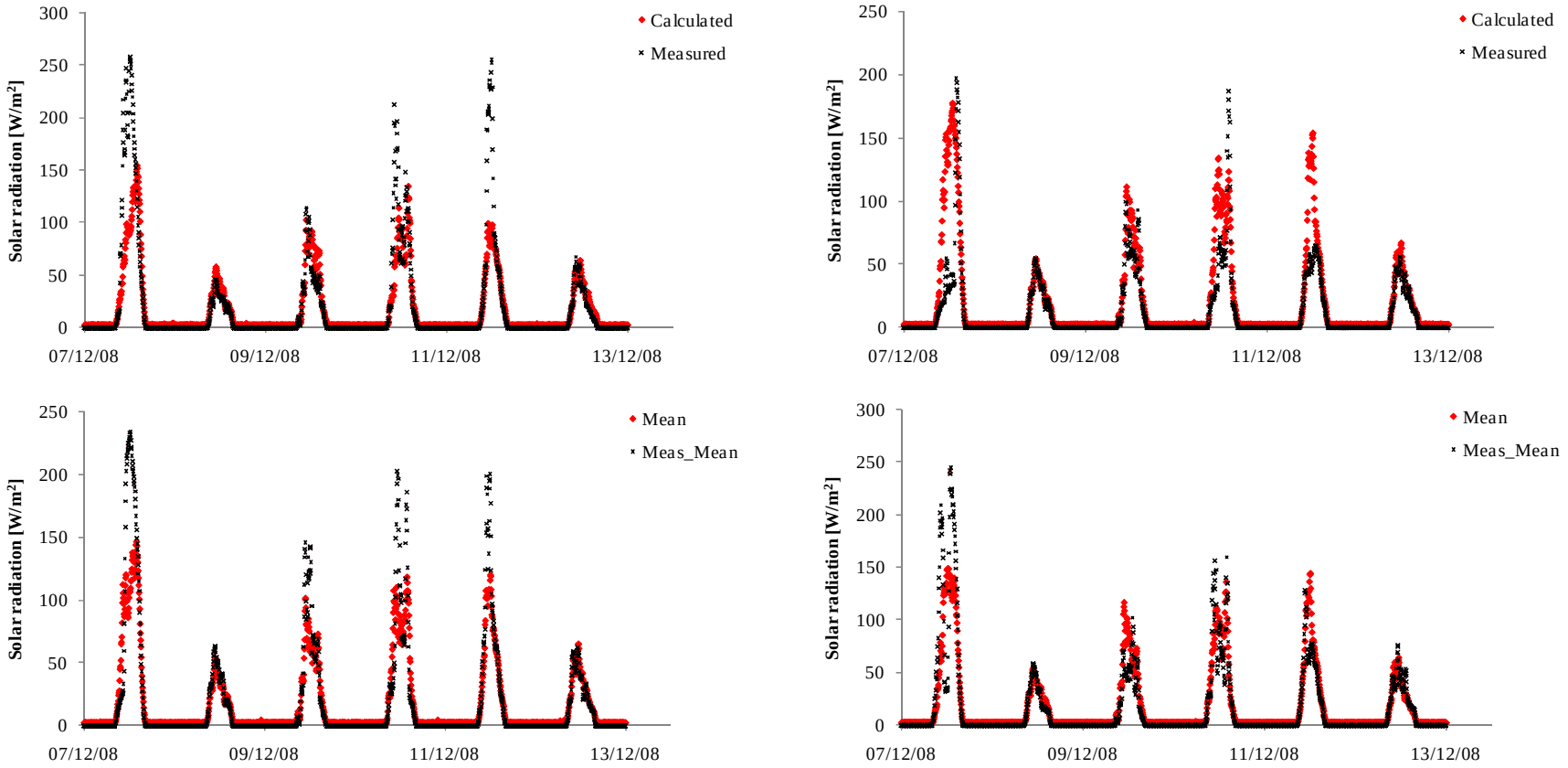

Figure 33: Solar radiation, comparison between calculated and measured values for MS 1, MS 3, MS 4 and MS 5 (clockwise) in the period 07-13/12/2008

The considerable error can be seen in Table 12 where the error average and standard deviation relative to the whole observation period are reported for the five measurement points. In location MS 2, the highest error average and the lowest error standard deviation are recorded. In this case, the observation of the error probability density function shown in Figure 34 along with error cumulative density function, provides valuable information. The probability density function in Figure 34 can be considered as composed by two different probability density functions: the main one has an average close to zero and a reduced standard deviation, the second has the average around 50 W/m^2 and a larger standard deviation. The presence of this second "component" of the error suggests the existence of another phenomenon not considered in the model.

Table 12: Solar radiation, error average and standard deviation

	MS 1	MS 2	MS 3	MS 4	MS 5
Err. Average [W/m^2]	-10	21	20	-11	-7
Err. St. Dev. [W/m^2]	44	27	43	39	42

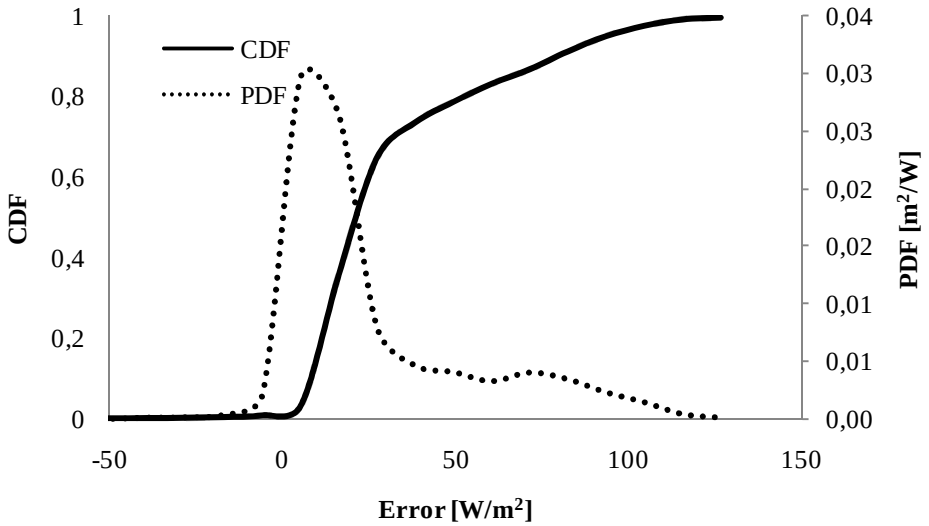

Figure 34: Solar radiation, error PDF and CDF

Finally, the analysis of the correlation between calculation error in each measurement point and the value of measured solar radiation in the other four measurement points is reported in Table 13. Correlations parameters related to MS 1 are the ones with the highest absolute values and the ones related to MS 5 have the lowest absolute values of the table.

Table 13: Correlation between solar radiation calculation error and solar radiation measurement in the other locations

	Sr 1	**Sr 2**	**Sr 3**	**Sr 4**	**Sr 5**
Sr 1		-0,32	0,02	-0,54	-0,39
Sr 2	0,52		-0,13	-0,02	-0,07
Sr 3	0,20	-0,17		-0,14	-0,11
Sr 4	-0,37	-0,17	-0,09		-0,06
Sr 5	-0,21	0,16	0,09	0,08	

6.3 State estimation validation

The Monte Carlo based state estimation algorithm described in Chapter 4 was tested as described in Section 6.1: conductor temperatures in each of the five locations, estimated with the method described in Section 4.2, were compared with measured conductor temperatures. Figure 35 shows the comparison between estimated conductor temperature and measured conductor temperature in location MS 2 during the first week of simulations. This chart displays strong similarities with Figure 20. However, the main differences in estimated conductor temperatures arise from missing data at MS 1, 3, 4 and 5. At these points in time the algorithm makes conservative assumptions of the environmental conditions local to MS 2 and therefore the predicted conductor operating temperature is higher.

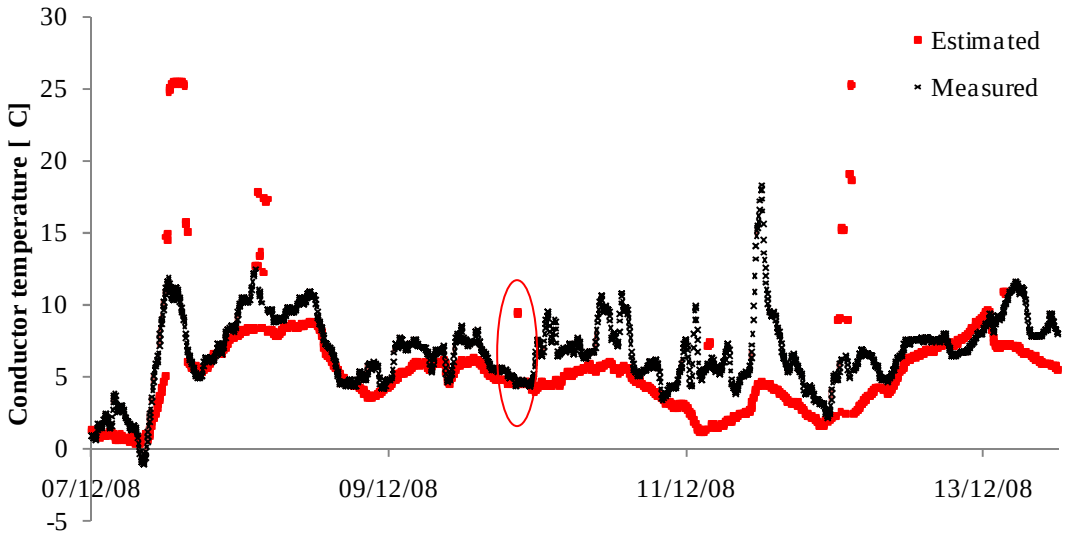

Figure 35: Conductor temperature estimation, comparison between estimated and measured values for MS2 in the period 07-13/12/2008

The same data can be represented also through a box plot, as in Figure 36, where the minimum, first quartile of the error, error median, third quartile of the error and maximum error for each hour are shown. The chart show clearly how the error is within a band of around 5°C through all the day, except than in the evening, when it rises suddenly. From a comparison between Figure 35 and Figure 36, this corresponds to the moment where the algorithm produces a single estimate considerably higher than the measured temperature value, probably in consequence of the presence of bad data. The phenomenon is highlighted in the two charts.

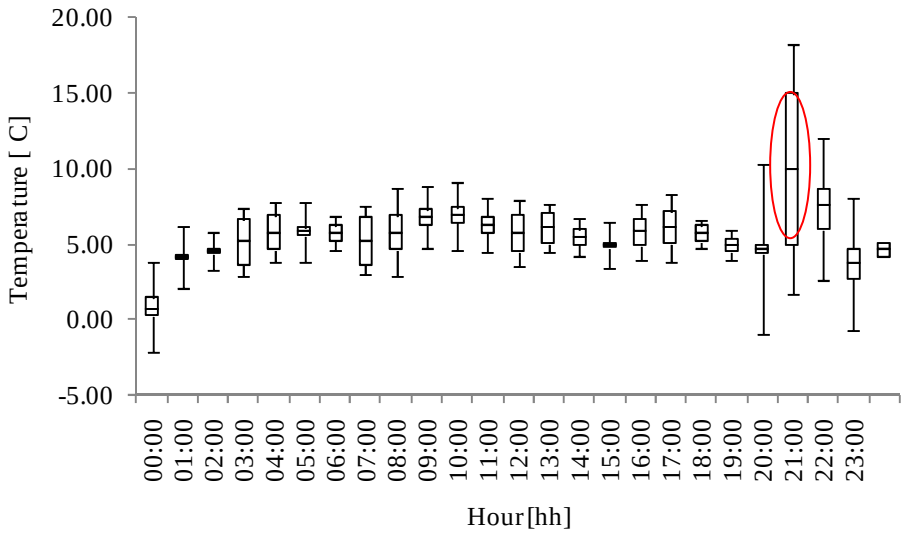

Figure 36: Conductor temperature estimation and error in MS2 for the day 09/12/2008

The comparison between conductor temperature measurements and conductor temperature estimation for the other four measurement points is reported in Figure 37.

A quantitative analysis of the parameters described in Section 6.1.1 is reported in Table 14 for the five measurement points. Particular attention was given to reducing the estimation computational-time, and in all the five examples, the average computational-time is between 2.16 and 2.24 seconds. This simulation was carried out using a 0.625GHz processor and the computational-time can be considerably reduced by increasing the parameter ϵ_N, currently set at 5% for every parameter. Regarding the estimation average error, its value is in line with the model average error reported in Table 4 but the standard deviation tends to be higher. The estimation standard deviation is also compared to the standard deviation of the measured temperature over a period of 30 minutes.

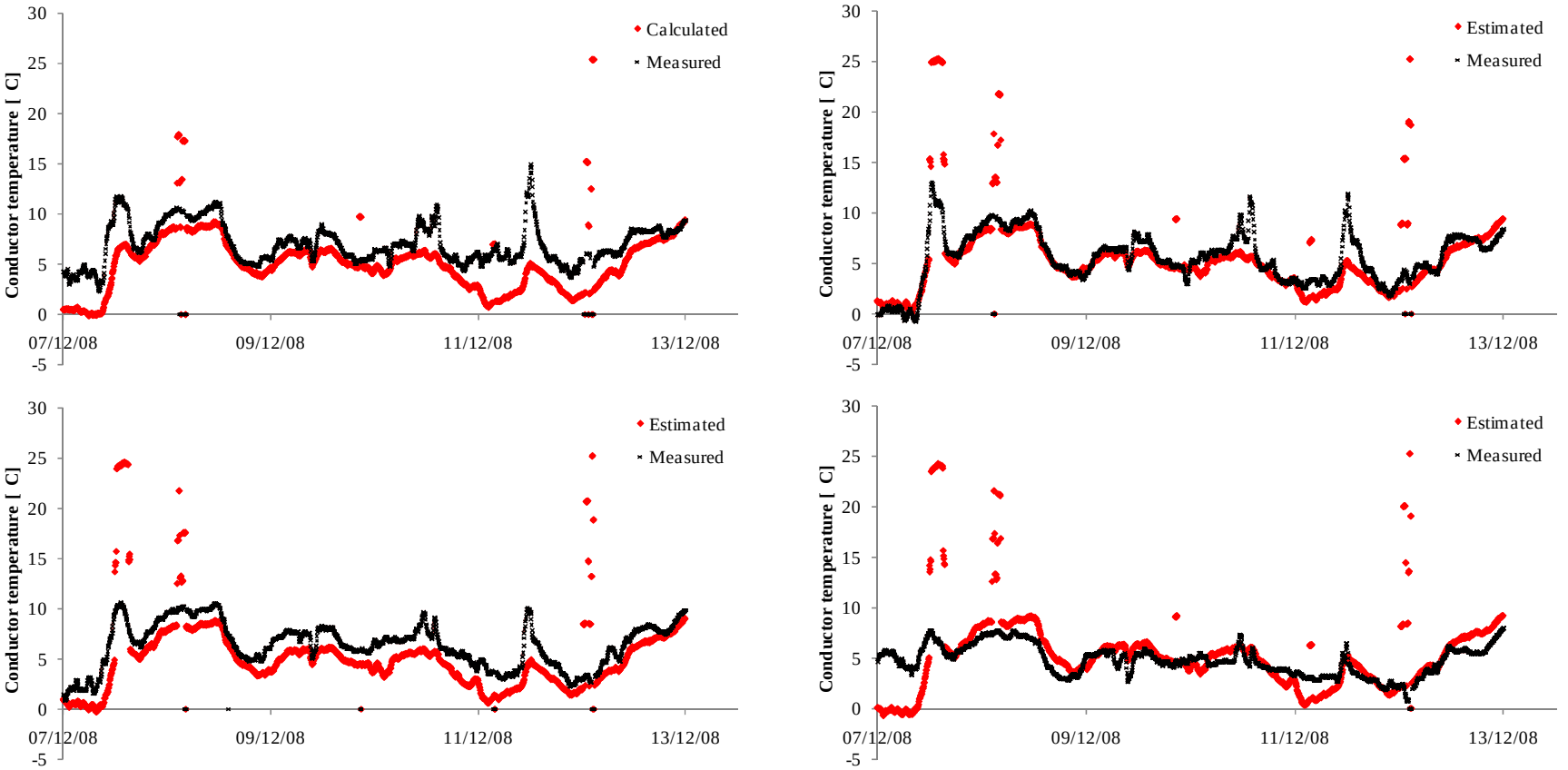

Figure 37: Conductor temperature, comparison between estimated and measured values for MS 1, MS 3, MS 4 and MS 5 (clockwise) in the period 07-13/12/2008

An optimal value for the estimation standard deviation would be similar to the measured standard deviation but here it is roughly one third. This can be explained in two ways: Firstly, the steady state model used for conductor temperature calculation does not take into account the dynamic behaviour of the conductor, producing a less variable estimation, as seen in Figure 35. Secondly, this parameter is influenced by the number of simulations carried out, but this number is voluntarily kept low in order to reduce the computational-time because of the use of this algorithm in an online controller.

Table 14: Conductor temperature estimation, average computational-time, error average and standard deviation, estimation average standard deviation

	MS 1	**MS 2**	**MS 3**	**MS 4**	**MS 5**
Time [s]	2.24	2.16	2.23	2.21	2.23
Error Average [°C]	-2.2	-1.9	-1.2	-1.9	1.4
Error St.Dev. [°C]	2.2	2.4	2.3	1.9	1.9
Estimated St.Dev. [°C]	0.118	0.120	0.121	0.119	0.121
Measured St.Dev. [°C]	0.355	0.355	0.355	0.447	0.447

The behaviour of the state estimation algorithm for measurement and communication failure was studied at location MS 2 by introducing a variable percentage of missing data into the input parameters of MS 1, 3, 4 and 5. Figure 39 shows changes in estimation average error and estimation standard deviation for different percentages of missing data. The meaningful observation occurs when 1% or more of the data is missing. Considering the average error in the region of 1% to 5% of data missing, the estimation average error increases linearly from 2.6ºC to 5.4ºC. Considering the standard deviation in the region of 1% to 5% of data missing, a similar linear behaviour is displayed and the standard deviation of conductor temperature estimates increases from 0.12 ºC to 0.14 ºC.

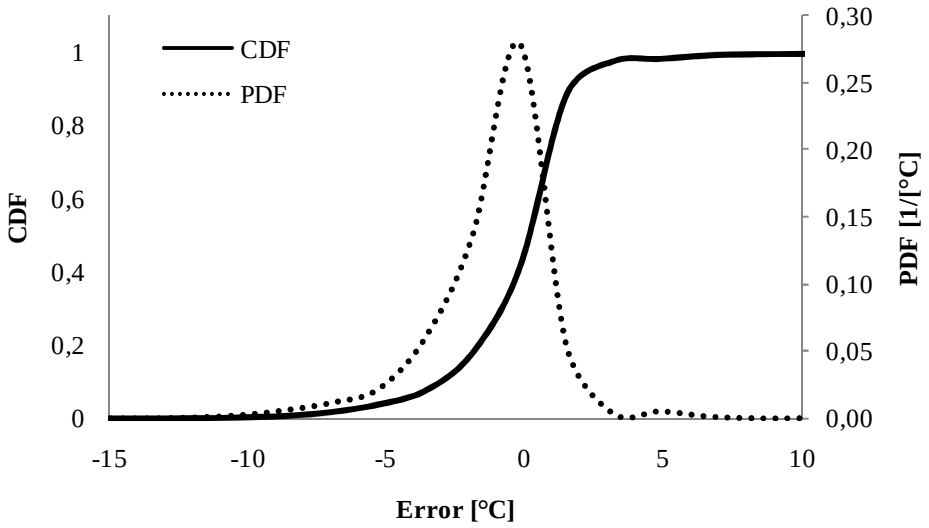

Figure 38: Conductor temperature estimation, error PDF and CDF

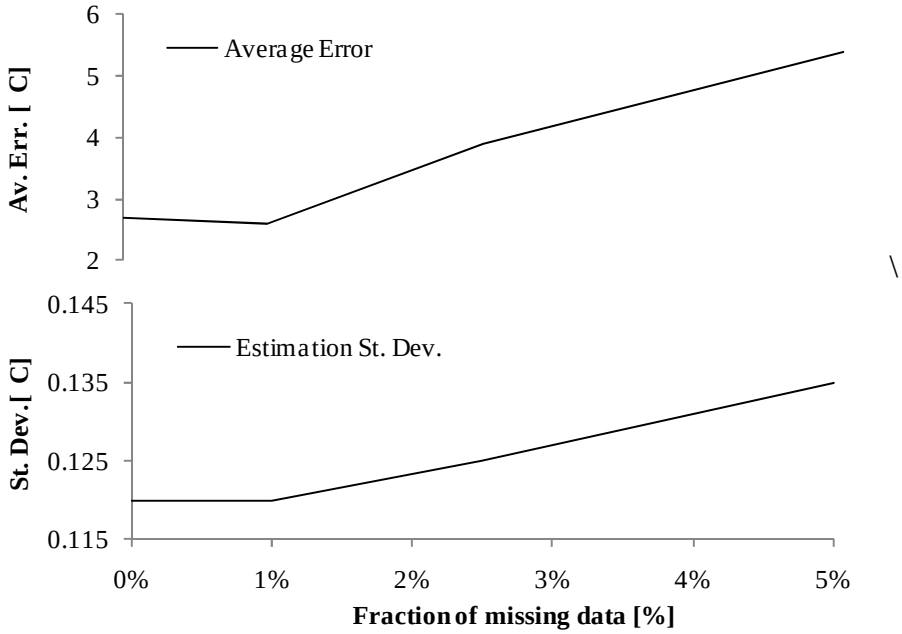

Figure 39: Performance degradation in consequences of measurement or communication failures

6.4 Discussion

Considering that, at present, distribution network operators have limited knowledge of the actual operating temperatures of overhead lines conductors, the results presented in this thesis are very encouraging and demonstrate the potential for the adoption of sophisticated state estimation algorithms in future network operation. In order to reduce the risk of a localised hotspot, when making an assessment of the real-time thermal rating for a long overhead line circuit, the overhead line can be divided into sections to represent the variation of external parameters such as line orientation or soil roughness.

The section of overhead line with the lowest rating represents the weakest point of the overhead line system and therefore this lowest rating can be adopted as the real-time rating for the entire overhead line. The simulation results reported in Section 6.3 confirms that the thermal state estimation algorithm developed is able to estimate conductor temperature, and therefore line rating, with a good degree of accuracy. Considering that typical overhead line design operating temperature in UK ranges from 50°C to 75°C, the maximum average error measured (-2.2°C) represents maximum average errors of -4.4% and -2.9% for the respective conductor operating temperatures.

Furthermore, the extensive tests carried out on the algorithm allow sources of error to be identified. In light of this, the following suggestions for estimation error reduction are made. Regarding environmental conditions, the interpolation method used has proven efficient for air temperature estimation. However, it was less successful in estimating wind speed and wind direction in all operating conditions. A more accurate estimation of the soil roughness parameters used in Equation 55 (they have been estimated observing satellite images) and a more complex wind flow modelling algorithm with computational fluid dynamics is likely to

increase the accuracy of environmental condition estimations. Commercial or open source software packages such as the ones used for wind farm design could easily be integrated in the algorithm, although this solution would be more computationally intensive. Since this state estimation algorithm was developed to inform an online control algorithm for the power output of distributed generation, computational efficiency was one of the main priorities.

Regarding solar radiation estimation, the model proposed does not consider the effect of cloud coverage or local environmental factors such as reflection from surfaces in proximity to the meteorological station. Regarding conductor temperature, a correct measurement of conductor parameters and in particular of conductor resistance and line direction, would help to increase the accuracy of the model. Work is ongoing at Durham University for improving the quality of the estimation produced by the thermal state estimation algorithm in light of these findings.

6.5 Conclusion

The real-time rating estimation algorithm developed for the project “active network management based on components thermal properties” was extensively tested with field data in order to assess its performance in terms of accuracy, precision, computational-time and behaviour toward measurement and communication failure. This was considered an important step in anticipation of the open and closed loop trials expected to conclude the project in 2010. A methodology for quantifying the qualitative parameters describing the performance of the algorithm was developed and described in Section 6.1. Environmental conditions recorded in five points on the test network where the active network management system will be deployed were used for the validation, along with overhead line conductor temperature

measured at the same points. The time series used cover a period of 71 days, from 07/12/2008 to 18/02/2009. Unfortunately, the data sets used did not included measurement of power transformers hot spot temperature and load, or measured of buried electric cable temperature along with surrounding soil temperature and thermal resistivity. This prevented testing of the rating estimation performance for these other fundamental components of the electric network. An average error of −2.2°C, −1.9°C, −1.2°C, −1.9°C, and 1.4 °C was measured for the estimation of conductor temperature in the five locations when comparing estimates to measured results. The main source of error was ascribed to the physical models used for describing overhead line conductor thermal behaviour, in particular the use of a steady state model. Uncertainty in weather stations installation information and on estimated values for parameters such as ground roughness were also identified as potential sources of error. Finally, suggestions on possible future development that could lead to improvements in algorithm performance were given, identifying further research areas.

Chapter 7 Real-time rating impact quantification

The aim of this study is to provide quantitative evaluation of real-time rating potential. Simulations were carried out calculating, for each component location, environmental condition values, as described in Section 3.2. These values were then used for calculating component real-time ratings using the models described in Section 3.1. Results were analysed to investigate the influence of environmental conditions on overhead lines, electric cables and power transformer ratings. Simulation results were analysed in three different ways: (i) comparing the rating cumulative probabilities of different component types against one another within the same network and environmental conditions, (ii) comparing the GWh headroom of four different overhead line types subjected to four different UK climates and (iii) assessing the increased energy throughput from DG that may be accommodated by using real-time ratings, as opposed to seasonal ratings, for a single overhead line.

7.1 Datasets

MetOffice datasets were used, referring to four British airports: Bishopton (Glasgow), Valley (Anglesey), Woodford (Manchester) and Heathrow (London). The data comprised

hourly averages of wind speed, wind direction, air temperature, solar radiation and soil temperature throughout the calendar year 2005.

In Figure 40 it is possible to observe the different site characteristics for the wind speed: Valley, on the west coast of Wales, is the windiest area with the highest maximum wind speed values and a probability distribution (PD) with the lowest peak. Heathrow, which is located in an urban environment, has wind speeds that are generally lower and more concentrated in the range between 2-7 m/s. As seen in Figure 41, air temperature appears to be the least variable parameter. Different sites may be differentiated by average temperature values. In Figure 42, the behaviour of the soil temperature is illustrated. Whereas the air temperature shows a variation with one peak across the year, soil temperature appears to vary with multiple peaks. Regarding wind direction, the presence of prevalent winds from the West and the North-West in the range 180°-360° was noted for all areas. Some areas also exhibited site-specific prevalent wind directions, for example from the South-West in Woodford and from North-North-West in Bishopton. Regarding solar radiation, no significant differences between the four sites were found.

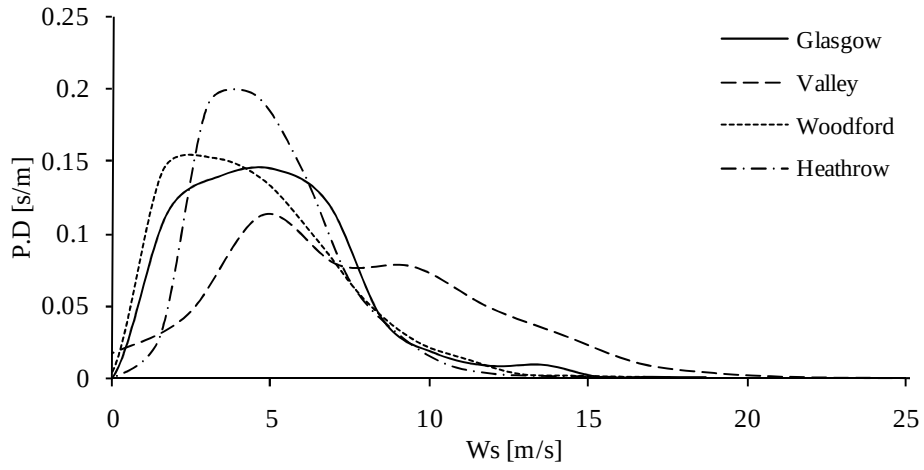

Figure 40: Wind speed probability distribution

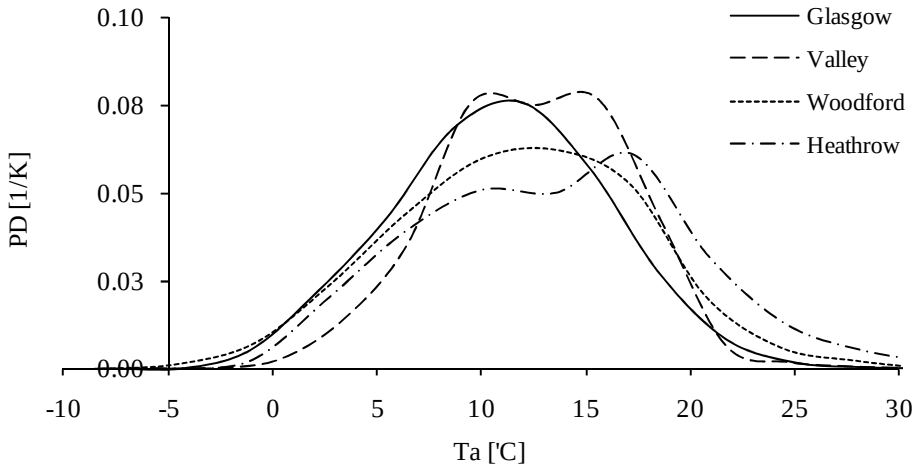

Figure 41: Air temperature probability distribution

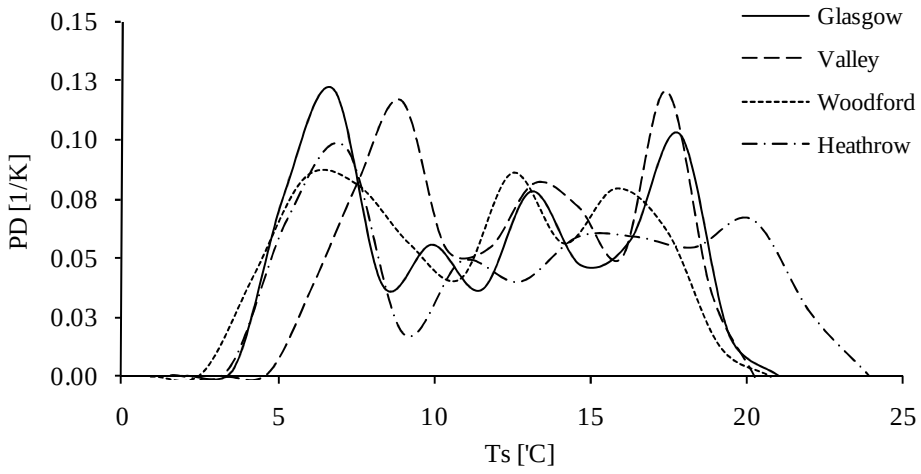

Figure 42: Soil temperature probability distribution

In order to simulate in a rigorous manner the influence of environmental conditions on power system ratings, three network models were adapted from the United Kingdom Generic Distribution Systems (UKGDSs) (143), each of which contain the three component types considered in this thesis. Moreover, a portion of the ScottishPower EnergyNetworks distribution network was included in simulations, as this will be instrumented in the near

future for real-time rating validation purposes. Voltage levels in the four networks studied vary from 6.6kV to 132kV. The ScottishPower EnergyNetworks Site network is shown in Figure 43 and has a meshed topology, with a prevalence of Lynx 175mm^2 overhead lines.

The network also has eleven electric cable circuits of 150mm^2 at the 33kV level and thirteen power transformers rated at 45MVA, 60MVA, 90MVA and 240MVA. UKGDS A, shown in Figure 44, has six overhead line circuits with Zebra and Lynx conductors rated at 50°C, 65°C and 75°C, twelve electric cables circuits with 150mm^2 and 240mm^2 conductors, and sixteen transformers with ratings from 14MVA to 500MVA. UKGDS B, shown in Figure 45, consists of six overhead lines with Zebra and Lynx conductors, eight electric cable circuits with 150 mm^2 conductors and thirteen power transformers, with ratings from of 21MVA and 500MVA. UKGDS C, shown in Figure 46, is characterized by a prevalence of electric cable circuits and power transformers. It comprises two overhead lines with Zebra conductors, twelve electric cable circuits with 150mm^2 and 240mm^2 conductors and eighteen power transformers with ratings from 14MVA to 500MVA. Electrical parameters for modelling the UKGDSs may be found in (143) and technical characteristics for the overhead lines may be found in (121).

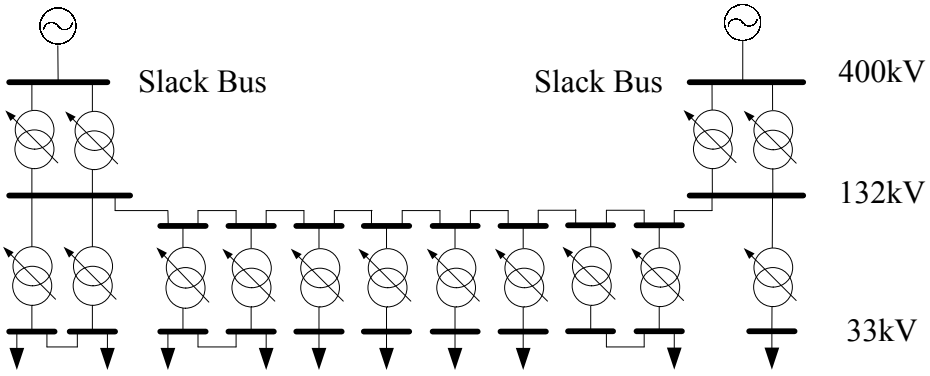

Figure 43: Site trial

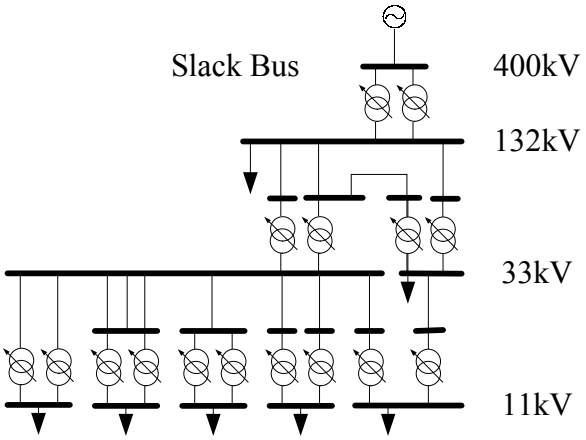

Figure 44: UKGDS A

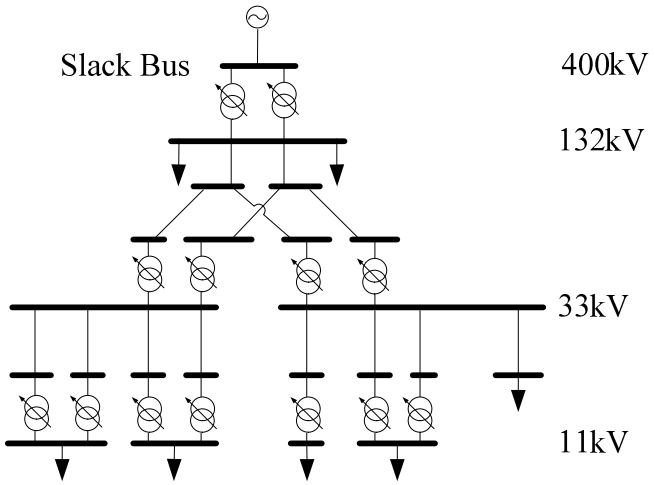

Figure 45: UKGDS B

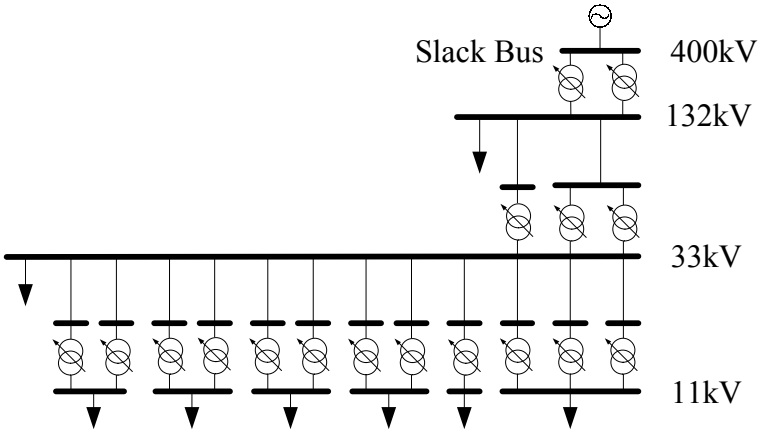

Figure 46: UKGDS C

Finally, a summary of the components present in each network is provided in Table 15.

Table 15: Network components

Network	Component	Number of components
SITE	Overhead line (Lynx 50)	11
SITE	Electric cable (150mm^2)	11
SITE	Power transformer (OFAF 240)	5
SITE	Power transformer (ONAN 45)	5
SITE	Power transformer (ONAN 60)	2
SITE	Power transformer (ONAN 90)	1
UKGDS_A	Overhead line (Lynx 50)	1
UKGDS_A	Overhead line (Lynx 65)	3
UKGDS_A	Overhead line (Zebra 75)	2
UKGDS_A	Electric cable (150mm^2)	4
UKGDS_A	Electric cable (240mm^2)	10
UKGDS_A	Power transformer (ODAF 500)	1
UKGDS_A	Power transformer (ONAN 23)	1
UKGDS_A	Power transformer (ONAN 60)	6
UKGDS_A	Power transformer (ONAN 90)	2
UKGDS_A	Power transformer (ONAN 14)	2
UKGDS_B	Overhead line (Lynx 65)	4
UKGDS_B	Overhead line (Zebra 75)	2
UKGDS_B	Electric cable (150mm^2)	7
UKGDS_B	Electric cable (240mm^2)	1
UKGDS_B	Power transformer (ODAF 500)	2
UKGDS_B	Power transformer (ONAN 100)	1
UKGDS_B	Power transformer (ONAN 21)	2
UKGDS_B	Power transformer (ONAN 23)	5
UKGDS_B	Power transformer (ONAN 45)	2
UKGDS_B	Power transformer (ONAN 90)	1
UKGDS_C	Overhead line (Zebra 50)	2
UKGDS_C	Electric cable (150mm^2)	1
UKGDS_C	Electric cable (240mm^2)	9
UKGDS_C	Power transformer (ODAF 500)	1
UKGDS_C	Power transformer (ONAN 60)	1
UKGDS_C	Power transformer (ONAN 14)	1
UKGDS_C	Power transformer (ONAN 23)	10
UKGDS_C	Power transformer (ONAN 60)	1
UKGDS_C	Power transformer (ONAN 14)	2
UKGDS_C	Power transformer (ONAN 23)	1

7.2 Results

In order to quantify the influence of environmental conditions on power system ratings, simulations were carried out on the networks described in Section 7.1 subjected to a range of UK climatic conditions. For each scenario, the minimum, maximum and average rating values together with additional potential annual energy throughput (in GWh) were calculated and the results are tabulated in Table 16. This data may be summarised as follows: The average rating of overhead lines ranged from 1.70 to 2.53 times the static rating with minimum and maximum ratings of 0.81 and 4.23 respectively. The average rating of electric cables ranged from 1.00 to 1.06 times the static rating with minimum and maximum ratings of 0.88 and 1.23 respectively. The average rating of power transformers ranged from 1.06 to 1.10 times the static rating with minimum and maximum ratings of 0.92 and 1.22 respectively.

Table 16: Simulation results, component ratings and theoretical headroom

Component	Static rating [MVA]	RTR Av. [MVA]	RTR Min. [MVA]	RTR Max. [MVA]	RTR Headroom [GWh/year]
Overhead line (Lynx 50)	89	213	84	419	988.48
Overhead line (Lynx 65)	108	220	94	390	898.94
Overhead line (Zebra 50)	154	328	125	595	1359.66
Overhead line (Zebra 75)	206	402	178	731	1576.20
Electric cable (150mm^2)	21	21	18	25	2.94
Electric cable (240mm^2)	30	32	27	37	13.33
Power transformer (ODAF 500)	500	532	469	580	282.41
Power transformer (OFAF 240)	240	258	223	284	154.75
Power transformer (ONAN 100)	100	108	92	120	70.80
Power transformer (ONAN 90)	90	97	83	108	63.72
Power transformer (ONAN 60)	60	65	55	72	42.48
Power transformer (ONAN 45)	45	49	41	54	31.87
Power transformer (ONAN 23)	23	25	21	28	16.28
Power transformer (ONAN 21)	21	23	19	25	14.87
Power transformer (ONAN 14)	14	15	13	17	10.80

7.2.1 Rating comparison of different component types

In Table 17, the simulation results for the Site network exposed to the Valley climatic scenario are given. For each component type, the average, minimum and maximum real-time rating is given, and the additional headroom theoretically obtainable with real-time ratings (as opposed to seasonal ratings) is quantified. The additional headroom was calculated by summing the difference between the real-time rating and the seasonal ratings across the year in hourly intervals.

Table 17: Simulation results for SITE network components exposed to the Valley climatic scenario

Component	Static rating [MVA]	RTR Average [MVA]	RTR Min [MVA]	RTR Max [MVA]	Additional RTR headroom [GWh/year]
Electric cable (150mm^2)	21	21	19	23	1.83
Power transformer (ONAN 45)	45	48	44	52	30.7
Power transformer (OFAN 240)	240	257	235	276	149.1
Overhead line (Lynx 50)	89	253	107	419	1342

For overhead lines, the seasonal ratings reported in (121) were used for this calculation. In Figure 47, the rating cumulative probabilities for the four components described in Table 17 are shown. Real-time ratings have been normalized using the static component rating. From inspection of Figure 47 it is evident that overhead lines show the greatest potential for rating exploitation. As seen in Table 16, electric cable and power transformer ratings have a limited variability. This is because soil temperature, soil thermal resistivity and air temperature are much less variable than wind speed and direction and it is these latter parameters that greatly influence the rating of overhead lines. By representing component ratings as cumulative probabilities, the potential comparison with power transfer duty (PTD) curves is facilitated. Moreover, distribution network operators are able to specify a probability

with which they are comfortable to operate a particular component and an assessment of the corresponding rating may be made.

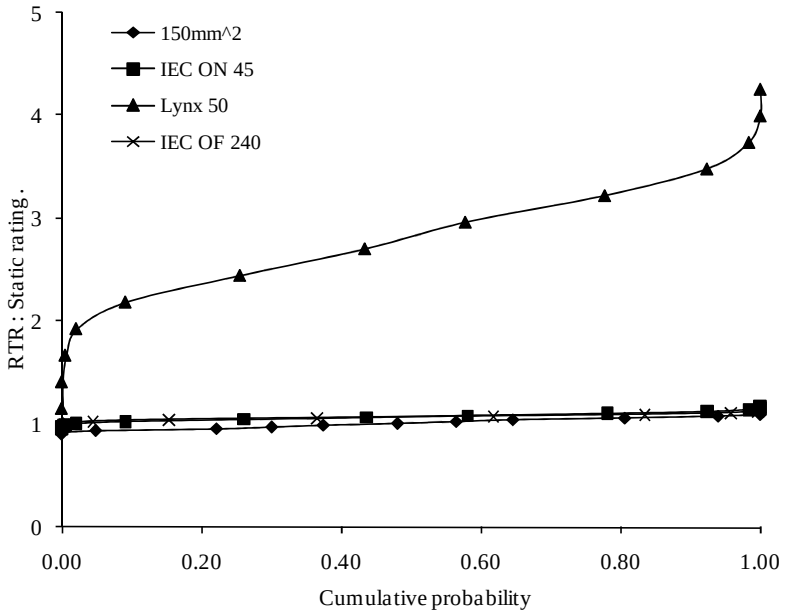

Figure 47: Rating cumulative probability for SITE network components exposed to the Valley climatic scenario

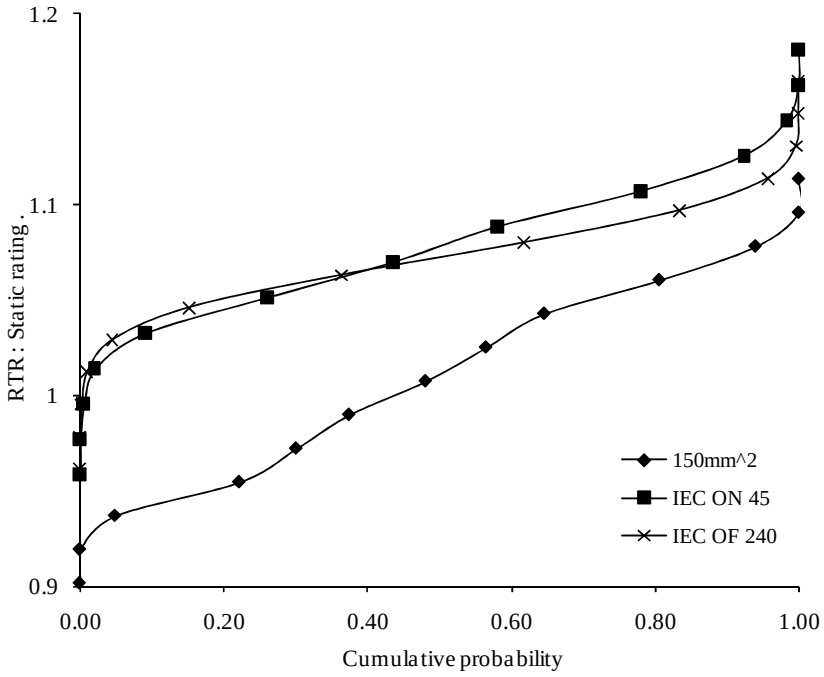

Figure 48: Magnified rating cumulative probability for SITE network components exposed to the Valley climatic scenario

7.2.2 Rating comparison of overhead line types

It was shown in Section 7.2.1 that overhead lines exhibit the greatest potential for real-time rating exploitation. Therefore, in Figure 49 the average headroom for different overhead line types, exposed to different climatic scenarios, is compared. For each case, the average headroom is given along with the minimum and maximum headroom. Headroom variations exist since differences in component orientation and component location result in rating variations. Variation bars are representative of the possible headroom ranges simulated. The size of the variation band is determined by the number of components existing within each case study network. A large variation band represents a frequently occurring component.

By inspecting the position of the lower variation band, it is evident that the additional headroom is greater for conductors with a greater initial static rating, and this effect is accentuated by conductor rated temperature. This is because the conductor temperature rise above ambient temperature multiplies the heat exchange coefficient as seen in Equation (6). Regarding the influence of the climates, Valley exhibits the highest average wind speed values and Bishopton the lowest average temperatures as seen in Figure 40 and Figure 41. Since overhead line ratings are more sensitive to wind speed than air temperature, the climate of Valley leads to the greatest overhead line power transfer headroom. Clearly, from this evidence the value of adopting a real-time rating system is dependent on geographical location.

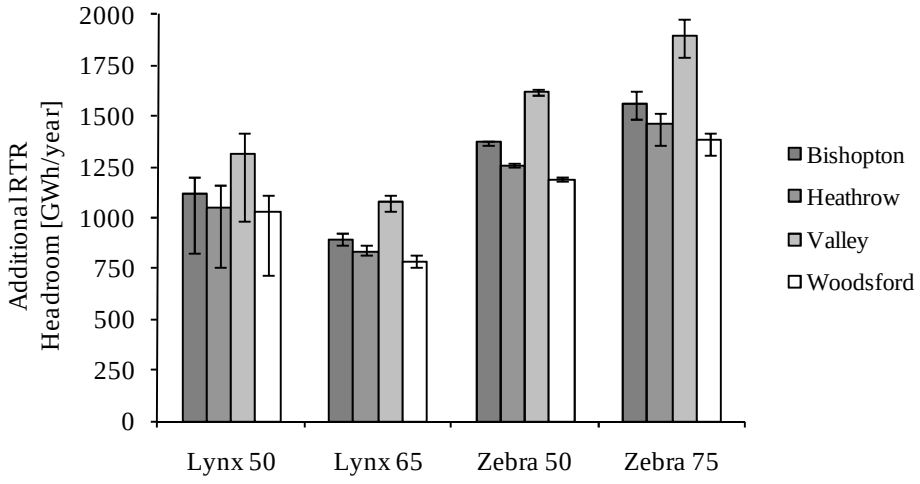

Figure 49: Influence of different UK climates on overhead lines power transfer headroom

Therefore, any utility interested in deploying a real-time rating system should conduct a site specific study to assess the value of real-time ratings as the output varies according to climate, and therefore the economic value is different. Furthermore, the quantification assessment presented in Section 7.2 allows a conservative approach to be adopted in

developing real-time rating systems since an investor may choose to utilise the rating seen at the bottom of the variation band.

7.2.3 Power transfer accommodation assessment

This section presents a methodology for quantifying the practically exploitable headroom for the specific case of a 132kV Lynx overhead line conductor with a maximum operating temperature of 50°C subjected to the Valley climate in the Site network. This location was selected since it is an area attractive to prospective wind farm development. The practically exploitable headroom was quantified as follows: Meteorological wind data from the Valley site was used together with the GE 3.6MW wind turbine power curve (144) to assess the power generated throughout the year and transferred through the overhead line conductor.

Clearly, the exposure of the overhead line conductor to environmental conditions varies as a function of line orientation and ground roughness. Therefore when making an assessment of the real-time thermal rating, the overhead line was divided into sections to represent the variation in these parameters. The section of overhead line with the lowest rating represents the weakest point of the overhead line system and therefore this lowest rating was adopted as the real-time rating for the entire overhead line. By comparing the power transfer across the year with the overhead line rating, for both seasonal and real-time rating regimes, the wind farm installed capacity was sized to correspond to a line cumulative overload probability of $^{1}/_{1000}$ (8.76 hours/annum).

Results are summarized in Figure 50, where the line real-time rating cumulative probability, along with the inverse cumulative probability for two different power transfer duties, seasonal and switchgear ratings are represented. The cumulative probability curve (the real-time rating distribution) may be interpreted by selecting an acceptable probability at which the component may be operated, for example 0.1 (10%). This corresponds to a rating of 149 MVA. Therefore there is the probability of 10% that during the course of the year the rating is less than or equal to 149 MVA (conversely there is a 90% probability that the rating is greater than 149 MVA). Similarly, the inverse cumulative probability (curves 1 and 2) may be interpreted by selecting a power transfer duty value, for example 76 MVA on the power transfer duty 2 curve. This corresponds to a probability of 10%. Therefore, there is a probability of 10% that during the course of the year power transfer duty 2 is greater than or equal to 76 MVA (conversely there is a 90% probability that the power transfer duty is less than 76 MVA).

For the seasonal rating regime an installed capacity of 89 MW (25 turbines) could be accommodated and an annual energy yield from the wind farm of 245 GWh could be attained. For the real-time rating regime, an installed capacity of 137 MW (38 turbines) could be accommodated and an annual energy yield from the wind farm of 377 GWh could be attained. This represents an increase in installed capacity and annual energy yield of 54% which is specific to the weather data used, the type of conductor, the risk at which the distribution network operator is prepared to operate the asset and the type of turbine selected. An annual energy yield increase of 54% would significantly enhance the revenue stream of a wind farm developer, demonstrating the value of a real-time rating approach. However, this is only 10% of the theoretical average additional headroom for this type of overhead line conductor exposed to the Valley climate, as seen in Figure 49.

Installing a larger capacity of distributed generation together with the adoption of an online power output controller (145) could allow a greater percentage of the theoretical average additional headroom to be realised whilst maintaining an acceptable level of risk to the distribution network operator. An estimation of the losses associated with the two PTD curves was carried out in the following way: From the average environmental conditions at the Valley site and from the average value of the power transfer, the average conductor temperature was calculated. From this, the average conductor resistance was calculated and, using the hourly values of the power transfer, it was possible to obtain the losses arising from Joule effect for the whole year. Loss values of 0.12% and 0.19% of the entire annual energy throughput were obtained for PTD 1 and PTD 2 respectively.

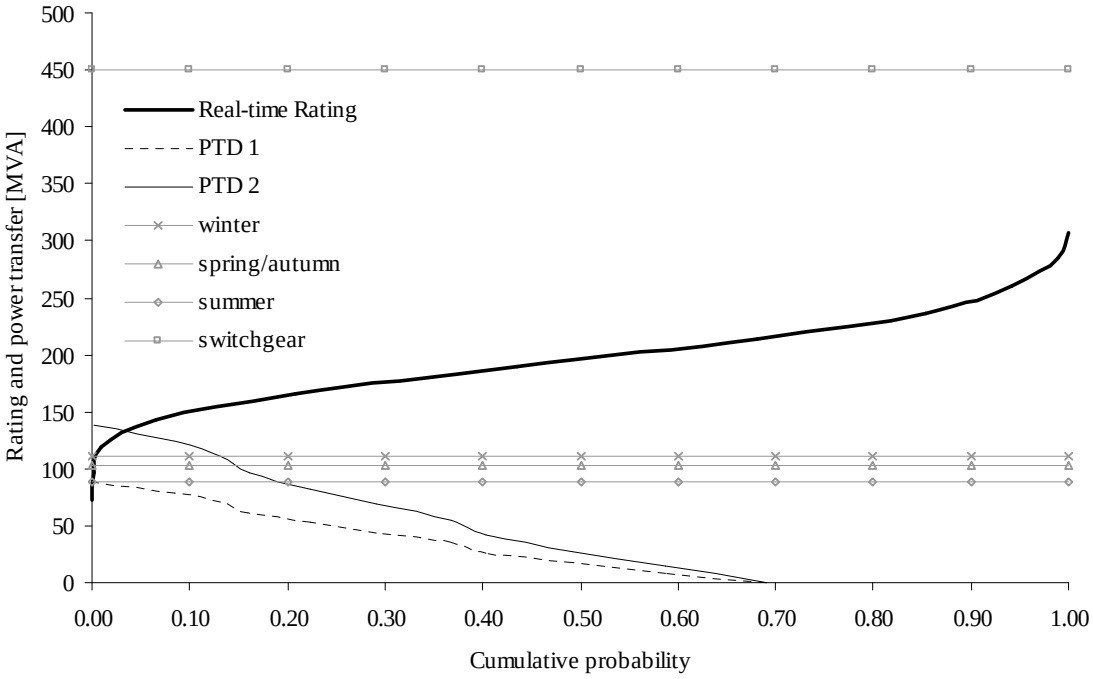

Figure 50: Cumulative probability comparison for a Lynx conductor in the Valley scenario

7.2.4 Impact of different control strategies

This last case was analysed in greater detail in order to assess the economical advantage of the implementation of a real-time rating-based distributed generation control respect of a static-rating-based distributed generation control or traditional network reinforcement. This was done in a joint research with S. C. E. Jupe, the other PhD student in Durham working on the same projects, and these results have been published in (145). The simulation results presented in this section considers a 150 MW off shore wind farm connected to the 7 km overhead line described above in order to create the necessity of a constraint. A degree of conservatism was added considering daily minimum ratings instead of the hourly ratings used for the study in Section 7.2.3. The other cases considered were: the use of the minimum static seasonal rating (89 MVA) of the existing line through the year, the use of continuous seasonal ratings on the existing line (89, 103 and 111 MVA for summer, spring/autumn and winter respectively), and the construction of a new line with an UPAS conductor (summer rating 176 MVA).

The five solutions for controlling the distributed generation output considered in this analysis are:

1) Tripping based on static yearly rating
2) Tripping based on static seasonal ratings
3) Control based on static seasonal ratings and load demand
4) Control based on real-time ratings and load demand
5) Network reinforcement for unconstrained connection

The tripping solution implemented in the cases 1 and 2 consists of reducing the distributed generator output to a value corresponding to the rating of the line (static yearly or

seasonal) plus the base load of an eventual local load. This solution, particularly simple, does not require excessive measurement or communication infrastructure and the cost of the local relay necessary to carry out the operation is estimated at £10k. The control solution, implemented in the cases 3 and 4, consists of constraining the distributed generator with a more complex system taking into account real-time local demand and, respectively in case 3 and 4, static seasonal or real-time rating, approximated here with the daily minimum. The estimated cost for the monitoring and regulation equipment used in case 3 is estimated at £50k, and the cost of the demand-following distributed generator output control based on real-time ratings is estimated at £100k. Finally, the case of network reinforcement able to remove any thermal constraints to the generator is simulated with the construction of a new overhead line equipped with 300mm^2 UPAS conductors with a maximum operating temperature of 75°C and with a minimum summer rating of 176 MVA. The cost of this reinforcement is estimated at £2M.

The annual energy yield at the DG connection busbar was calculated for each solution, by integrating the real power output of the DG scheme across the year in 30 minute intervals. The per unit electrical losses (I^2R) resulting from each solution implementation were calculated using the current flowing in the overhead line with per unit resistances of 0.0070 and 0.0041 for the 'Lynx' and 'UPAS' conductors respectively. These were then summated across the year on a half-hourly basis to produce annual energy loss figures. For each solution the net annual revenue was calculated by multiplying the annual energy yield at the distributed generator connection bus by £101.43/MWh (£52.15/MWh wholesale electricity price (146) + £49.28/MWh 'Renewables Obligation Certificate' sale price (147)) and making an adjustment for the cost of the losses incurred by transferring this energy to the slack busbar (calculated as the annual energy losses multiplied by the wholesale electricity price).

The basic tripping scheme based on summer static ratings (Case 1) was taken as the datum solution with a capital cost of £10k and net annual revenue of £42.35M (based an energy yield at the DG connection busbar of 418.1GWh and 1.3 MWh lost through power transfer to the slack bus). The estimated marginal costs (due to additional network costs), predicted marginal revenues (due to additional energy yield) and marginal losses (resulting from electrical power transfer to the slack busbar and changes in electrical resistance of the line) were compared to this solution. This allowed a basic Net Present Value comparison of the alternative solutions, based on their relative marginal costs and marginal revenues. A 10% discount rate and 20 year economic life was assumed (148).

The capital cost of the wind farm itself was neglected as this would be constant across each solution. Furthermore, because the wind farm is connected at via a single overhead line, any faults or scheduled maintenance on this line will cause it to shut down. Since such events have an equal constraint on the energy yield of each solution this effect was neglected. All the costs within the financial evaluations are estimates of equipment costs, based on the most appropriate data available at the time of consideration.

The results from the quantification methodology are summarised in Table 18.

Table 18: Quantification methodology results

Solution	1	2	3	4	5
Marginal Cost [£k]	0	0	40	90	1990
Marginal Annual Energy Yield [%]	0	4.93	5.24	10.75	10.76
Marginal Annual Energy Losses [%]	0	18.41	18.99	43.39	-16.31
Marginal Net Annual Revenue [£M]	0	2.08	2.21	4.53	4.58
Marginal 20 Year NPV at 10% dcf [£M]	0	17.71	18.76	38.46	36.97

For this case study, it appears that controlling DG output to follow load demand based on a single summer static rating (Case 3) yields greater revenue for the developer than switching ratings on a seasonal basis and tripping DG as a result (Case 2). DG tripping based on seasonal thermal ratings (Case 2) requires a lower initial investment, however, the risk on the part of the DNO is greater if seasonal ratings are utilised. This is due to the possibility of an anomalous hot day occurring when ratings have been relaxed. This risk may be mitigated by investment in a dynamic thermal ratings system to provide accurate knowledge of the current thermal status of the network.

Economically, the most attractive solution to the developer is the CCM based on component dynamic thermal ratings and load demand (Case 4). The annual revenue of the project is increased by £4.53M and shows the highest marginal net present value at £38.46M. For this case study, this solution appears to be more attractive than the alternative reinforcement option (Case 5). This provides an unconstrained energy yield (and hence maximum annual revenue) but would require an extra capital investment of £1.99M to upgrade the overhead line. Network reinforcement (Case 5) would reduce network losses relative to the other solutions since the larger cross-sectional area of the conductor would reduce the electrical resistance to power flow. However, despite increasing electrical losses through implementing the constrained connection management solution described in case 4, the cost of capital for the DG developer is likely to make the active management solutions, with lower upfront costs, a more attractive investment.

7.3 Conclusion

In this study, it was found that overhead lines exhibit the greatest potential real-time rating exploitation since they exhibit the greatest rating variability. Furthermore, it was found that power transformers and electric cables have a lower real-time rating exploitation potential relative to overhead lines. The analysis showed that the average rating of overhead lines, electric cables and power transformers ranged from 1.70 to 2.53, 1.00 to 1.06 and 1.06 to 1.10 times the static rating, respectively. The value of adopting a real-time rating system is dependent on geographical location, with the average ratings for the networks exposed to the climate of Valley and Glasgow exceeding the average rating of the networks exposed to the climates of Woodford and Heathrow. Therefore, any utility interested in deploying a real-time rating system should conduct a site specific study to assess the value of real-time ratings as the output varies according to climate, and therefore the economic value is different.

The increase in power transfer from DG that could be accommodated through a real-time thermal rating system implementation was investigated. For a Lynx overhead line conductor with a maximum operating temperature of 50°C it was found that a GWh energy throughput increase of 54% could be accommodated by operating the line with a real-time rating regime as opposed to a seasonal rating regime. It was also demonstrated that a constrained connection manager informed by dynamic thermal ratings was the most cost effective solution for facilitating wind generation access to the case study network when compared to alternative solutions. In particular it was found that in the case considered, a real-time rating system would allow a power transfer comparable with the one of a new line with a rating equal or greater than the wind farm capacity, but with a front investment twenty times smaller.

Chapter 8 Discussion

This work describes the real-time thermal state estimation system for power system components of the distribution network realised at Durham University. This was developed within the framework of the project “Active network management based on component thermal properties”, partially funded by the Department for Business Innovation and Skills and involving Durham University, ScottishPower EnergyNetworks, AREVA-T&D, PB Power and Imass.

The system is developed for estimating, in real-time, the rating of overhead line conductors, electric cables and power transformers over a wide geographical area from a minimum number of meteorological stations located in the same geographical area. The system automatically identifies thermal bottlenecks and for each circuit in the network provides a real-time rating based on the rating of its most vulnerable component. Furthermore, the algorithm follows a probabilistic approach in rating calculation, integrating environmental condition variability and measurement uncertainty in order to provide a range of ratings characterised by their own probability. This allows the distribution network operator to operate the network at a selected risk level and reproduce in real-time the probabilistic approach already used for power system components static seasonal rating. The description of the real-time rating algorithm is followed by a quantification of the potential advantages arising from the installation of a real-time rating system on a portion of distribution network. This helped to quantify the potential exploitable headroom of each power system component

type and to quantify the actual extra amount of power that it could be possible to transfer on an overhead line connecting a wind farm. The work also presents a validation of the algorithm developed and of the models used for environmental conditions interpolation and for component rating against field data.

8.1 Real-time rating system

8.1.1 Modelling

Component thermal models widely used both in industry and in academia have been used for describing power system components thermal behaviour. Behind this choice, there was the desire of building the rest of the research on solid bases, building confidence on the suitability of the system developed in this research for field tests and facilitating the development of commercial applications.

The model used for overhead lines conductor rating is based on the IEC standard (21) for overhead conductors rating, enriched by the wind direction correction proposed by the CIGRE Working Group 12 (22). The flexible algorithm structure, allows manufacturers to apply the rating model preferred by each particular customer or even to implement their own model. Between the three models considered, the CIGRE model is more detailed but it was discarded because of the greater number of parameters necessary, while the IEEE (20) model was not used because UK overhead lines rating is based on the IEC method. Also for electric cables, available industrial standards were used. Of the two considered rating methods, the IEC (46) and the ENA (47) one, the second was chosen for a practical implementation in the code. The IEC standard requires an excessive number of cable construction parameters that were difficult to identify for the old components usually installed on the UK distribution network. Therefore the less detailed method based on tabulated rating values and tabulated

correction coefficients for the different environmental conditions described in (47) was preferred. The procedure of comparing different standard models for component rating and then selecting the most suitable was followed also for power transformers. The three models considered were the IEC loading guide (71), the IEEE loading guide (72) and the ENA loading guide (125). Very little difference exists between these three documents and the IEC method was chosen also in this case because of its use for transformer rating in the UK and in the network used for validation.

Regarding environmental conditions modelling there are no standard methods already used by the electric transmission and distribution industry that could be easily applied in this project. Furthermore, the complexity of the physical phenomena behind environmental conditions variation is often very complex, nonlinear and chaotic, requiring often considerable computational resources. Considering these two constraints, but also the fact that currently any method is officially used for environmental condition calculation for conductor rating calculation in the electricity distribution industry, the following approach was adopted. The value of each parameter is interpolated in each component location from the values measured in meteorological stations of known location and corrections, which consider aspects of the natural phenomenon described, are applied where possible. Wind speed and directions are strictly correlated parameters since they are used for describing the air flow and for this reason they are interpolated separately in the algorithm. Wind speed interpolation is corrected for taking into account the effect of soil surface roughness, both on wind speed measurement at the meteorological stations and in each conductor location. This adds a possible source of error in the estimation of soil surface roughness parameters, but it is expected that this error is limited in comparison with the error of the simple interpolation. Wind direction is simply interpolated and it was explained in Section 3.2 how the error generated by the algorithm for

particular sets of data has a reduced effect on conductor temperature calculation and hence on conductor rating calculation. An alternative solution would have been to convert the wind description given in polar coordinates (wind speed and wind direction) to a Cartesian coordinates (latitudinal and longitudinal wind speed). These values would then have been interpolated for calculating again in each conductor location the absolute value of wind speed and the angle relative to the conductor. This was not done in order not to influence wind direction calculation with the potential error generated by wrong soil surface roughness coefficient estimation.

Air temperature and solar radiation calculations are based on simple inverse distance interpolation without additional correction. The opportunity of introducing altitude correction for air temperature was considered but a practical implementation in the algorithm was discarded. The presence of little altitude excursion in the test area would not have made a rigorous test possible, and the correction could have become an additional non-measurable source of error. For the same reason the solar radiance is simply interpolated and no additional correction for local factors that could potentially modify readings value were implemented in the algorithm. Furthermore, air temperature is dependent also on wind direction, since winds from different directions would bring in an area air from areas with potentially different environmental conditions. An example could be a costal area, where a change in wind direction could expose the network to air from the sea, with different a different temperature from the air from the mainland. Another example could be that in general in the UK southern winds tend to be warmer than northern winds.

Regarding soil environmental conditions, influencing electric cables rating, additional calculations where necessary in order to calculate the necessary parameters values. Initially only soil temperature readings at 5cms of depth and no soil thermal resistivity readings were

available. Therefore, a complex soil dynamic model was developed for calculating soil temperature at electric cables burial depth and soil thermal resistivity from rainfall readings. Later, the test site was instrumented with a soil moisture sensor (linearly dependent with soil thermal resistivity) and a soil temperature sensor placed at cables burial depth. The interpolation of these values is expected to produce a reduced error with respect to the dynamic soil behaviour model developed in the first part of the project.

In conclusion, it is necessary to highlight that these models have been developed and tested considering a network area of a typical British rural network supplied by a substation. This was estimated in an average of 400 km^2, roughly equivalent to a square with an edge of 20 km. The flexible structure of the algorithm makes possible to increase the number of meteorological stations, both to increase the density of measurement on the area, and to increase the area observed. Therefore it would be easy to increase the scale of the are monitored, although it is reasonable to expect that for considerably larger areas more refined meteorological models would be necessary.

8.1.2 Thermal state estimation

In order to make an appropriate use of the models described in Chapter 3, a suitable estimation technique was studied. The development of an estimation technique for the real-time rating of power system components is a consequence of the interest in developing a system able to deal with input uncertainty and measurement and communication failures, with the ability of estimating the thermal state of a wide network area. A first analysis of the problem shows that the considerable number of nonlinear relations between the different parameters which influence power system component ratings, suggests that traditional estimation techniques based on linear algebra would not have been suitable for this problem.

After a comparison of estimation techniques previously tested for power system components thermal rating, the Monte Carlo method was finally selected and appropriate methodologies were defined for each part of the method. The Monte Carlo method is a methodology with a series of steps, but different approaches and techniques can be adopted at each step and for linking the different passages. A single probability density function, the Beta distribution, was used for describing the probability density of all of the variable parameters of the problem. This decision was taken in order to reduce the complication of the algorithm in provision of its use by third party developers.

Attention was given also to the selection of a suitable variate generation method, in order to have precise and fast sampling of different parameters probability distributions. Finally, the inverse transform method was selected. During the development of the research, possible improvements were identified and Section 8.5 describe the ones that have not been implemented because they would have required additional studies or because their possible positive outcomes where not clearly defined.

8.1.3 Software design and development

In order to produce real-time rating estimation for the power system components comprised in a wide network area, an algorithm integrating static and dynamically updated databases and the models described in Chapter 3 were developed. The development process started with the definition of fundamental requirements of the algorithm, along with the definition of the expected output and the available inputs. The algorithm for power system component real-time rating was written in the language VB.Net and is composed by: a web service, the actual code and three databases.

The web service acts as an interface with other programs. The code is written according to the object oriented programming paradigm and divided into six classes describing the methods and the data structure of the problem. The databases are used for storing static information, such as network components and geographical related data, and dynamic data, such as real-time environment conditions readings. Initial algorithm requirements have been satisfied, a simplified version of the algorithm is installed in two relays in the test network, where open and closed loop tests must be carried out and the whole algorithm is being implemented in commercial products by AREVA, a consortium partner. A critical part of the development was represented by the necessity of carrying out the rating estimation in a period of time compatible with the exigencies of the active distributed generator power output controller.

The controller calculates distributed generators set points with a frequency of 30 minutes, therefore the estimation time should have been a fraction of this time. Currently, as shown in 6.3, the estimation time for a single component is in the range of 2.3 seconds, a period that would allow the rating of a circuit made of 10 components in less than 30 seconds, and the rating of the 10 most thermally vulnerable components in less than 3 minutes. Therefore the computational-time satisfy the initial requirements. This performance was obtained thanks to the general structure of the algorithm, the optimization of the code in particularly critical functions and to the choice of the precision accepted for the Monte Carlo simulation.

This last parameter can be customised, and in further applications of the code it will be possible to increase estimation precision at the expense of computational-time or vice versa. In order to assure the possibility of improving and developing additional applications based on the code, the algorithm was written following a clear object oriented approach, with a

dynamic structure of the algorithm, made of different functions calling each other. This allows improvements to be made in single parts of the code, without influencing other parts. Finally, in order to allow third party applications to use the algorithm, a web service was developed to act as an interface. Web services are designed to support interoperable machine-to-machine interaction over a network. During the development of the code, several possible improvements were identified. They are reported in Section 8.5.

8.1.4 Validation and impact quantification

The validation, described in Chapter 5 was only carried out on overhead line conductors because of the lack of available data for electric cables and power transformer temperatures. Furthermore, because of the impossibility to measure the conductor rating directly for a particular conductor maximum operating temperature, the component thermal model was used for calculating the conductor temperature corresponding to the measured current. The comparison showed good agreement between calculated and measured overhead line conductor temperatures, with an average error for the five points considered from 0°C to -2.4°C and an error standard deviation from 0.9°C to 2.6°C, over a period of 71 days. This error value is considered encouraging and it is expected that a revision of the thermal model used, especially regarding the values of constants used for heat exchange calculation, would improve these values considerably.

The validation described in Chapter 5 was carried out for the four atmospheric environmental condition considered: wind speed, wind direction, air temperature and solar radiation. Soil parameters such as soil temperature and soil thermal resistance have not been validated because the network area was not instrumented with sensors for these environmental conditions.

Regarding wind speed calculation, the comparison between measured values in each meteorological station location with wind speed calculated with the interpolation of wind speed measurements from the other four meteorological stations presents an average error range between -0.8 m/s and 1.8 m/s and the average standard deviation ranges from 0.9 m/s to 1.5 m/s. These values are considered satisfactory for the use in the real-time rating system developed, although an improved airflow model and a better knowledge of local environmental conditions, such as surface soil roughness, are expected to reduce the calculation error. Regarding wind direction, the comparison between calculated and measured data presents good agreement. As explained in Section 3.2, the algorithm used produces a result shift of about 180° in correspondence of input values corresponding to winds from the north. Although this is reflected in the considerable nominal average errors, which ranges from -23° to 12° and in the considerable average error standard deviation, which ranges from 39° to 54°, its influence in conductor temperature estimation is considerably smaller.

Conductor temperature is influenced by wind-conductor relative angle and not by the absolute wind direction, and this parameter has a period of 180°. Regarding air temperature, the comparison between measured and calculated values in the five meteorological stations presents an average error ranging from -0.3°C to 0.9°C with an average error standard deviation ranging from 1.4°C to 2.0°C. These values are considered satisfying and it is not expected to considerably reduce these error values without considerably increasing the number of meteorological stations. Finally, regarding solar radiation, the validation of the inverse distance interpolation technique calculation with measured data presents mixed results. The average error ranges from -11W/m^2 to 20W/m^2, with an error standard deviation, which ranges from 27W/m^2 to 44W/m^2. These errors are presumably caused by local conditions, such as shading or reflection from local surfaces not taken into account in the

model. In particular since the meteorological stations used for validation were mounted on overhead line towers, if they are not facing the south it is probable that the solar radiation sensor is shaded for part of the day, altering in this way both the initial data used for simulation and the readings used for comparison.

The validation presented in Chapter 5 represents a quantification of the ability of the real-time state estimation algorithm to produce accurate, precise, reliable and fast component rating estimations. As for the component model validation it was not possible to directly measure the real-time rating, conductor temperature calculated considering the measured current flowing in the conductor was compared with the conductor measured temperature. From a quantitative point of view average error range from -2.2°C to 1.4°C and average error standard deviation range from 1.9°C to 2.4°C in correspondence of the five temperature measurement points. These values are in line with component model errors, this means that additional errors introduced with the environmental conditions estimation does not have an particularly negative impact on the final conductor temperature (and hence conductor rating) estimation.

The real-time rating algorithm validation also shows that the algorithm is able to carry out the temperature estimation for a conductor in a period between 2.16s and 2.24s. This means that the algorithm can rate an overhead line circuit divided in 10 sections in less than 30s, a result in line with the requirements of a real-time controller. Considering that the Monte Carlo based system developed provides a confidence range for the results, its standard deviation at every rating was compared with the measured conductor temperature standard deviation relative to the same time period. This comparison shows that the estimated standard deviation ranges between the 27% and the 33% of the measured standard deviation.

The reason for this difference must be found in the structure of the Monte Carlo method and in particular in the method used for assessing the simulation precision: In order to reduce the computational-time, this was set to a fixed value of 5% for every parameter, both for environmental conditions estimation and in conductor temperature estimation. However, since these two estimations are in series, the error is increasing. This value was chosen as a compromise between estimation precision and computational-time. This was done considering also that improved precision would considerably increase the number of necessary simulations and that extreme results present in the “tale” of the distribution are likely to represent volatile conditions not representative of the state of the conductor over the period of 30 minutes considered.

On the other hand, the comparison between the simulation standard deviation, influenced by input variability, and the simulation error, influenced by model’s errors, shows that the errors in the models used for environmental condition and conductor temperature calculation represent the main source of error in the algorithm. In the following section, a possible methodology for taking into account model errors is suggested. The real-time rating algorithm validation measured also expected performance degradation in correspondence of missing data relative to measurement or communication failures. The test shows that rating accuracy and precision decrease linearly with a linear increase of the percentage of missing inputs. This is in line with the requirements of the real-time state estimation algorithm.

Finally, studies were also carried out in order to assess the possible outcomes in term of increased network transmission capacity arising from the implementation of a real-time rating system. The study confirmed that overhead lines exhibit the greatest potential real-time rating exploitation since they exhibit the greatest rating variability and that power transformers and electric cables have a slight real-time rating exploitation potential relative to overhead lines. It

was confirmed that the value of adopting a real-time rating system is dependent on geographical location. Therefore, any utility interested in deploying a real-time rating system should conduct a site specific study to assess the value of real-time ratings with respect to climate variation.

The increase in power transfer from DG that could be accommodated through a real-time thermal rating system implementation was investigated. For a Lynx overhead line conductor with a maximum operating temperature of 50°C it was found that a GWh energy throughput increase of 54% could be accommodated by operating the line with a real-time rating regime as opposed to a seasonal rating regime. It was also demonstrated that a constrained connection manager informed by dynamic thermal ratings was the most cost effective solution for facilitating wind generation access to the case study network when compared to alternative solutions.

Validation results are clearly influenced by the test site location and by the measurement timeframe. The test location, on the north coast of Wales and close to wind farm perspective areas is characterised by high wind speeds. The meteorological station of Valley is in fact the one with the highest average wind speed and lowest average air temperature of the four meteorological stations used in Chapter 7. It is reasonable to expect that the same test real time rating system would have behaved in a different way if deployed in a site close to the weather station of Heathrow, with the highest average temperature and lowest average wind speed. However, it is also reasonable to expect that the different behaviour of the thermal state estimation algorithm would not have altered the measured performance in terms of estimation accuracy and precision. These two parameters in fact do not depends on macroscopic yearly meteorological site characteristics, but on meteorological parameters behaviour in a timeframe of about half hour. The test site and timeframe anyway, do not allow

reproducing a complete series of conditions to what the thermal state estimation algorithm can be faced. High air temperature and low wind days are not included, as they are not included periods with high power flows in the circuits. As a result conductor temperature was often considerably below the maximum design operating temperature.

8.2 Real-time rating system for distributed generation control

A description of the distributed generation output control informed by component thermal properties developed in parallel with the real-time rating algorithm is described in this section.

The controller aims to maximise the power output of distributed generators taking into account the real-time ratings of the network area where the generators are connected and dispatching real and reactive power set points to each generator. This involves solving two problems: to identify the generators contributing to the thermal overload of a particular network component and to curtail them according to a suitable scheme. The controller must also to keep voltages within their operating limits and consider measurement and communication failures for providing a graceful and conservative degradation in control performance.

The control methodology developed in order to maximise power output from multiple distributed generators schemes considering real-time component rating is summarised in Figure 51. The real-time control is based on a previous network analysis, which assesses the power flow sensitivity of each component relative to each generator. A list of the most thermally vulnerable components is then realised and used for establishing the priority of the circuits to monitor. The priority list is also used to reduce the number of components for what is necessary to estimate a real-time rating. The first step of the algorithm is to check the

integrity of the network through the analysis of the position of the switchgears. If the algorithm identifies the presence of outages, safety values for distributed generators set points are applied.

Once this security check is passed, the algorithm runs a power flow simulation and calls the real-time rating estimations for the components resulting overloaded. At this point, if the control identify thermal overloads, necessary constraints are calculated according to the selected curtailment strategy. Otherwise, the algorithm verifies the possibility to relax existing constraints if additional capacity became available.

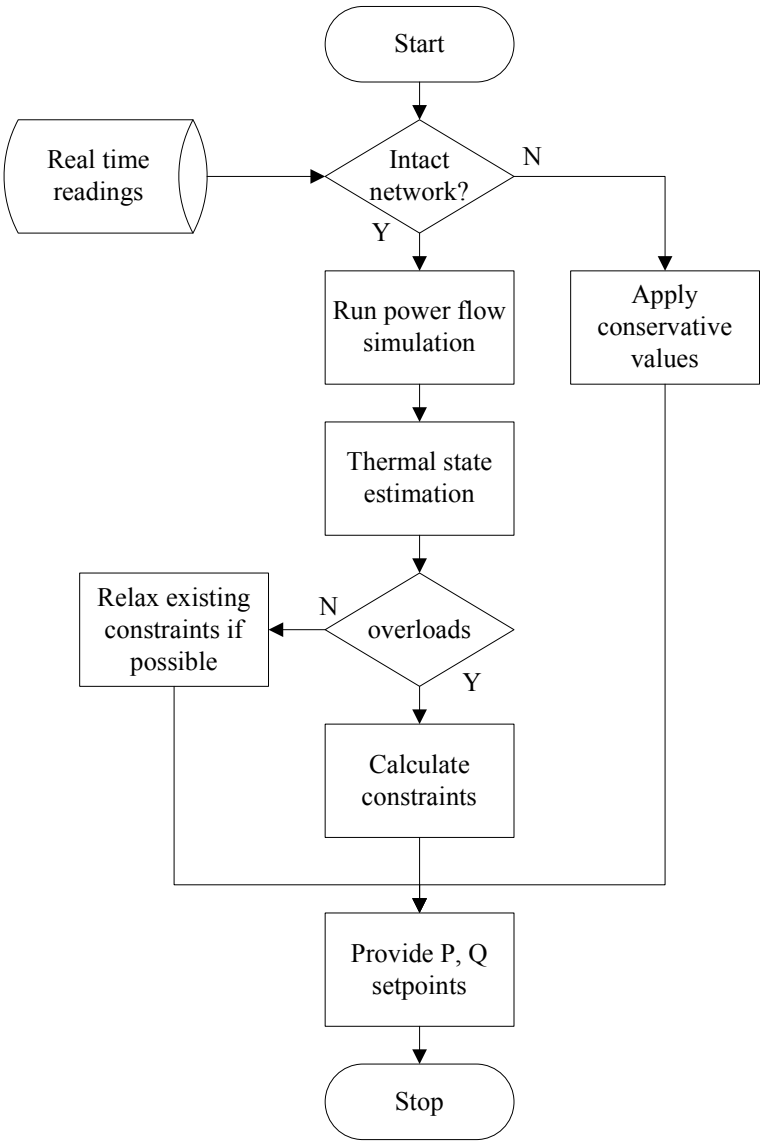

Figure 51: Control algorithm flowchart

Different strategies have been studied in this project for curtailing single or multiple schemes of distributed generator in presence of thermal overloads in their proximity or in other areas of the network. Regarding multiple distributed generation schemes, the following strategies have been studied for possible implementation, all based on the power flow sensitivity factor methodology, in order to solve thermal problems occurring in network locations far from the generation connection:

– Last in first off curtailment

– Egalitarian curtailment

– Technically most appropriate curtailment

The first approach consists of curtailing distributed generators schemes in reverse order respect to their connection to the network. In this way, the generator installed first, will not be constrained because of the excessive power flow generated by another generator installed later in time. This solution can be applied with simple contractual agreements between distribution network operators and generator developers. Two other methodologies have been studied in order to maximise multiple generator output. The egalitarian approach consists of reducing of a similar percentage, the output of all the generators involved in the creation of a thermal overload. This approach has the advantage to broadcast a single signal to all the generators, and since a reduction in percentage terms is given, generators producing more power and for this reason contributing more to the thermal overload, are constrained more.

Finally, in the technically most appropriate approach, generators are ranked according to their sensitivity factor with respect to the circuit experiencing the thermal overload and are constrained in this order. In this way, the generator in the position to contribute more directly to the solution of the problem is called to solve it first. It is important to note that, although particularly interesting from a technical and economical point of view, the last two approaches, would need a compensation scheme to be instituted amongst the different generators connected to the network, in order to compensate the generators with the highest priority connection of the eventual losses in production.

8.3 Real-time rating system site trial

In Figure 52 an overview of the real-time rating system developed is reported, and the figures from Figure 53 to Figure 55 show particular aspects of the practical implementation.

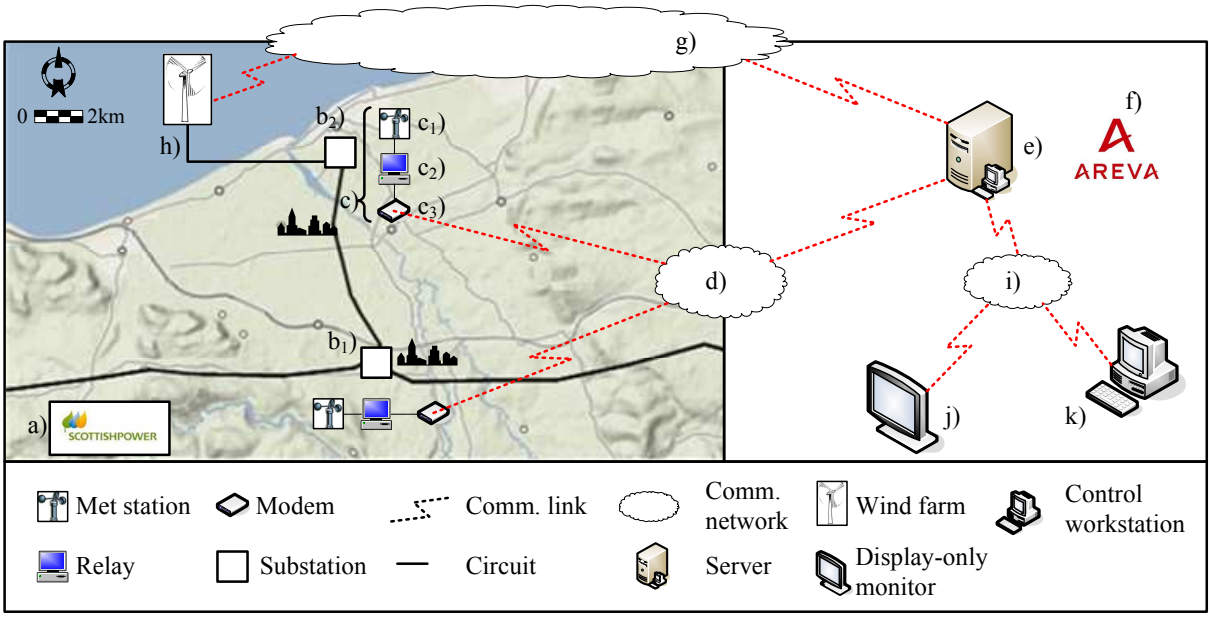

Figure 52: Schematic representation of the real-time rating system developed

A portion of ScottishPower EnergyNetworks distribution network (a) where thermal overloads are expected in consequence of the connection of new wind farms was used for installing and testing the equipment. In two substations ($b_{1,2}$) a kit (c) composed of a meteorological station (c_1) and a control relay (c_2) with a simple rating algorithm installed. Thanks to a modem (c_3) the relay is able to communicate through the internet (d) with a remote server (e) (currently located in AREVA-T&D's laboratories (f)). In the remote server, there is a more complex real-time rating estimation algorithm (which is the result of the research described in this work) and a distributed generator power output control algorithm, which can send optimized set-points to a remote wind farm (h). The server can also communicate information regarding the thermal state of the distribution network through an internal network (i) or the public internet to display only screen (j) in control rooms or to an operator (k).

As previously mentioned the distributed generator power output control informed by the real-time thermal rating algorithm is installed in the delocalised server. This algorithm considers the inputs from the meteorological stations installed in the two substations and calculate real-time ratings for different sections of each line, in order to identify potential thermal bottlenecks. Furthermore, the algorithm provides a range of possible component ratings, each one characterised by its own probability. Selecting a defined probability allows the operator to quantify and maintain network operational risk within accepted values.

The two relays installed in the substations have the role of final protection for the equipment of the network and they are not related to the distributed generation power output control. A simpler version of the real-time rating algorithm is installed in the substation relays and the ratings calculated in the delocalised server are compared in real-time with the calculations that consider the readings from a single meteorological station. A rating calculated in this way is more variable and typically higher than a rating calculated by the server, which interpolates environmental conditions in order to identify local hot-spots on the network. If for some reason the rating calculated by the relay is lower than the rating calculated by the server, or there is no signal from the server, the control relay takes the necessary measures in order to prevent damages to the installed network components.

The following figures show different characteristics of the solution implemented in the test site. Figure 53 shows the meteorological station in one of the two substations (a) and the three visible sensors (b) for wind speed and direction, solar radiation and pressure. Wind speed and direction are measured with a two axes ultrasonic anemometer: a solution without moving parts and thus reduced maintenance costs. The air temperature sensor is in the main body of the station. Two other sensors, for soil temperature and soil thermal resistivity measurement, are not visible and are buried in the ground in the proximity of the monitored

electric cable. In Figure 54 the user interface of the control relay is displayed and in Figure 55 the input-output doors are shown. Figure 55 (a) shows the connections with the environmental condition sensors and Figure 55 (b) shows the modem used for the connection with the outside world. The system developed makes wide use of existing technologies such as remote controlled meteorological stations, flash memory PCs and existing telephone lines (usually available in a substation environment and interchangeable with GPRS). This considerably reduced the installation cost, focusing resources on the algorithmic and experimental part of the project. Finally, in Figure 56 a portion of overhead line in the test area is shown.

Figure 53: Meteorological station in a distribution substation and particular. a) pressure sensor, b) solar radiation sensor, c) wind speed and direction sensor

Figure 54: Substation relay user interface

Figure 55: Substation relay: a) input from meteorological station (Figure 1). b) modem for communication to the outside world

Figure 56: 132kV overhead line in the site trial area

Chapter 9 Conclusion and Further Work

9.1 Conclusion

This work described the real-time thermal state estimation system for distribution network power system components realised at Durham University in the framework of a partially Government-funded research and development project. The system involves the use of a limited number of meteorological stations, a series of analytical models for estimating component ratings and a Monte Carlo based algorithm. This takes into account input uncertainty and provides safe estimations in case of measurement or communication failure.

The system was realised for meeting fundamental requisites identified after consultations with distribution network operators and design and protection engineers from different firms of the research consortium. These requisites have been listed in Section 1.5 and particulars of their implementation are reported in the list below.

- Cost-effective installation and maintenance is obtained thanks to the system structure, based on a limited number of meteorological stations. The cost of the whole active network management solution was estimated in the region of £100k.
- Maintenance of statutory clearings is satisfied maintaining conductor operating temperature below the line design maximum operating temperature, as explained in section 3.1.1. The error in conductor temperature estimation identified in

Chapter 6 must be taken into account in further developments preceding a commercial application.

- In order to not inflict permanent damage to the components, the system prevent the temperature of each part of each component of the network to exceed it's maximum continuous operating temperature.
- Maintaining component operating temperature within design limits prevent also to reduce significantly its operating life. On the other hand the study shown that increased power flows are likely to increase electrical cable and power transformer insulation ageing speed but this can be seen as a sign of a more efficient asset's utilisation.
- Safe estimation in case of measurement or communication failures is provided thanks to a series of filters applied to input data. The extensive algorithm validation described in Chapter 6 shown how algorithm performance degradation, in terms of accuracy and precision, advances linearly with the proportion of missing or corrupted data and without a sudden fall in performance.

A series of possible dangerous situations were identified in section 1.5 and the solutions identified are here listed.

- In order to prevent that a sudden drop in wind speed would leave an overhead line with a power flow greater than its real time rating, rating estimation time was reduced in order to allow more frequent estimations to be carried out. An appropriate interface with the power flow control scheme is also necessary for this cope.

- A non secure network operation due to inadequate network thermal state estimation is prevented thanks to the extensive validation carried out and described in Chapter 6. The test showed an average error between -2.2°C to 1.4°C in overhead line conductor temperature estimation over a period of 71 days and identified in component thermal model used for rating calculation the main source of error.
- To prevent the case of thermal overloads not relieved because of the temporal or the spatial resolution of the real-time rating system, a series of approaches have been developed. Firstly, component thermal state estimation time vas reduced to an average of 2.16-2.24 seconds. Secondly, in order to allow the system to detect local hotspot in a circuit, each circuit was divided into several sections characterised by uniform line direction and environment. The rating of each section is then calculated separately and the rating of the most constrained component is used as the rating of the whole circuit.
- The event of a thermal overload on a non-monitored components is avoided thanks to the system architecture based on the estimation of component rating, and not on direct component thermal measurement.

The development of the real-time rating system was also supported by studies highlighting potential benefits and issues arising from a practical implementation. A summary of the point that the researched answered is provided in the list below.

- Previous project on power system thermal monitoring have been identified and discussed in Section 2.4. The most relevant were identified in (6) and (9).

- A suitable architecture for the real-time rating system able to satisfy the points identified in the research objectives listed in Section 1.5 was identified. The solution proposed is described in detail in Chapter 5.
- The impact of the implementation of a real-time rating system on renewable energy integration was studied and the results are reported in Chapter 7. The research showed that, in the case of a wind farm, the additional annual energy yield from distributed generation that could potentially be accommodated through deployment of a real-time thermal rating system was found to be 54% of the line static summer rating for the case considered.
- Situations where real-time ratings could be applied and should not be applied have been identified. Not heavily loaded circuits where limited hours of thermal overloads are expected belong to the first category, and the presence of a power flow control scheme was found essential for the application of real-time ratings.
- The increased component rating (in MVA) and the increased power transmission capacity (in MWh) obtainable with the use of real-time rating was also quantified as described in section 7.2. It was found that the average rating of overhead lines, electric cables and power transformers ranged from 1.70 to 2.53, 1.00 to 1.06 and 1.06 to 1.10 times the static rating, respectively. It was also fount that, considering the minimum rating uplift measured for each component type, the implementation of a real-time rating system could increase the energy transferred through overhead lines, underground cables and power transformers by the 70%, 0% and 6% respectively.

Although this research can be considered concluded, a number of further research areas have been identified and described in the following section.

9.2 Further work

9.2.1 Modelling

The validation described in Chapter 5 proved that the thermal model used for calculating overhead line conductor temperature and hence conductor rating represents a source of error. Although this error was considered acceptable, further studies correlating environmental condition and conductor temperature measurements could lead to improvements in the rating algorithm increasing its accuracy. Unfortunately, the dataset used for the real-time rating algorithm validation did not comprised buried electric cables temperatures and soil parameters measurements. Therefore, a similar study should be undertaken also for buried electric cables. As for electric cables, the power transforming rating model was not tested in the validation of the real-time rating algorithm. In addition, an extended validation of the thermal model used with field data would be useful.

Although these results are referred only to overhead line conductors, the assessment of the potential of a real-time rating system described in Section 7.2.1 shown that overhead line conductors, being the most exposed power system component type, present the largest possible headroom. Electric cables and power transformers, with their higher insulation and thermal capacitance, would present more accurate results with the use of dynamic models. Regarding wind speed and direction modelling, the algorithm realised could be improved in several ways.

Firstly, the direct interpolation of wind direction produces errors for a reduced inputs dataset. Although it is explained how the consequences of this error are reduced, it could be removed with a numerical data pre-processing. Instead of interpolating separately wind speed and direction, it is possible to decompose the wind in its longitudinal and latitudinal

components. These two components can then be interpolated in the component location and there used again for calculating wind speed and direction on the conductor. Computational fluid dynamics techniques could be also used for improving wind speed and direction estimation in overhead lines conductor locations.

Although this method is more computationally intensive than the interpolation technique used and it would not be possible to use it with the Monte Carlo estimation algorithm, the improved accuracy could justify the calculation of few samples. This can be done with a computational fluid dynamic algorithm specifically written for the real-time state estimation algorithm, or integrating commercial software packages.

Regarding air temperature, it could be possible to introduce an altitude correction factor to take into account the variation of air temperature at different altitudes. This would be necessary in a mountain region where components can be placed at considerably different altitudes. Regarding solar radiation, the interpolation used in the algorithm produced considerable errors in the estimation of peak values. It is therefore necessary first to carry out a site visit in order to assess the presence of shading from trees or other obstacles on the solar radiation sensor. Then it is necessary to improve the model for taking into account shading and reflection from local surfaces with different reflection coefficients. The system of models used for describing soil dynamic behaviour and for estimating soil temperature at cables burial depth and soil thermal resistance have not been tested against field data as for atmospheric parameters. Therefore, an extended validation such as the one carried out for wind speed, wind direction, air temperature and solar radiation estimation should be carried out in order to assess the accuracy of the models. This is a necessary step for a future deployment of the real-time rating algorithm for cable systems extended over large areas.

Finally, considering the similarities between the interpolation method used and a neuron of an artificial neural network, it would be worthy to investigate the possible use of a neural network for estimating all the environmental conditions in each component location. Such system would calculate first the optimal weighting for estimating environmental conditions in meteorological station locations for particular inputs datasets, for interpolating them in a second step to the component location. This is expected to improve environmental condition estimation accuracy.

9.2.2 Estimation technique

Possible improvements identified during this research regarding the estimation technique adopted have been implemented during the work. The Beta distribution used in the algorithm proved to be as flexible as expected in describing the probability distribution of different phenomena and it was not felt necessary to add additional distributions, also in order not to increase the algorithm complexity. Additional studies could be carried out on “extreme values theory” and its application for improving estimation performance.

9.2.3 Software design and development

A potential improvement identified during the algorithm validation described in Chapter 5 is the real-time rating accuracy and precision self assessment. This consists of comparing in real-time meteorological stations readings against environmental conditions estimated in the meteorological station location without the use of the readings from that meteorological station in order to assess in real-time the error introduced by the models. The error calculated at every meteorological station can then be interpolated and used for correcting environmental condition estimation in other component locations. The same can be done comparing

conductor temperature estimation with measured conductor temperature, taking into account the error given by the thermal model used for calculating the real-time rating. This is expected to improve considerably the accuracy of the algorithm, correcting in particular models' inaccuracies or errors.

9.2.4 Validation and impact quantification

Regarding the validation of the real-time rating system, further work should be carried out for testing the performance of the algorithm for electric cables and power transformers rating. The use of the system only for overhead lines conductor real-time rating does not allow exploiting fully the potential of the real-time state estimation developed, which allows network operators to monitor the thermal state of a wide network area. Although overhead lines are the most critical component because of their exposure to environmental condition and their rating dependence to the considerable variability of wind speed and direction, it is believed that tests should be carried out before utilising the algorithm on circuits comprising electric cables and power transformers.

Furthermore, the whole system is still in test and open- and closed- loop trials will take place in 2010. These tests would allow validation of the combined behaviour of the real-time rating system and the distributed generator power output controller, identifying possible improvements and further research areas. Additional work could also be carried out in the area of the quantification of the impact of real-time rating systems on the distribution network. In particular, it would be necessary to consider the effect of additional constraints such as voltage rise and fault level rise that could potentially limit the benefits described in Section 7.2.3. Finally, a study was carried out on the combined us of real-time rating and distributed generators power output control, but real-time rating can also be applied in

combination with other active network management techniques, such as demand side management or energy storage.

9.2.5 Off-line planning tool

The primary application for the algorithm developed in this research, is for calculating real-time ratings to be used in the active distributed generators control algorithm described in Section 8.2. However, it is felt that the work done could be used in applications regarding other aspects of the interaction between the power system and the environment.

The algorithm developed can be used with little modifications for carrying out real-time rating feasibility studies. This will be necessary before the installation of any real-time rating system, both based on component temperature monitoring and on environmental condition monitoring. An off-line planning tool based on the real-time rating algorithm could be used in several scenarios. A simple case, similar to the one analysed in Section 7.2.3 and Section 7.2.4, consists of the connection of a single wind farm on an existing line and in the estimation of the expected curtailment experienced by the wind farm before and after the installation of a real-time rating system. In another situation, it is possible to imagine a distribution network operator planning the construction of a new line for connecting a zone with new wind farms developments to the existing network.

Future connected generation can only be estimated roughly, since different wind farm developers could not be able or interested in completing the generation plant. In these cases, low estimates could prevent the potential of an area to be completely exploited. Alternatively, high estimates could result in assets underutilisation. A preliminary study assessing the impact of a real-time rating system would allow the distribution network operator to plan a

connection for a reasonable expected generation, being able at the same time to offer further non firm connections contracts based on the line real-time rating.

This kind of planning studies can be carried out both with the use of historical-time series of environmental data and with the use of the Monte Carlo method already implemented in the code or a combination of the two, according o the availability of existing data. In this case, the Monte Carlo method would be used with estimated probability distributions in the case of parameters for what historical-time series are difficult to find or are particularly corrupted. This could also be used to assist network operations during planned outages. The installation of a real-time rating system could unlock additional capacity in a network area stressed by the presence of work reducing the capacity of particular circuits. This would allow more flexible planning and if necessary, longer outages.

9.2.6 Rating forecast

Another possible implementation of the work carried out in this research is the development of a tool able to forecast component ratings with different time horizons. A similar application would be useful in an active controller similar to the one developed in this research project, or as an information tool for the control room. It is expected that the passage from a reactive to a predictive control methodology would allow a more secure operation of the network and moreover an improved management of the operating risk. It would not be difficult to adapt the probabilistic-based data structure of the algorithm to the wide variation of weather forecasts, that could be obtained from existing meteorological offices or though data series analysis. Figure 57, from the preliminary study reported in (149), shows an example of rating forecasts for the day 18/09/2008, represented from the reference time of midnight.

Two main considerations arise from the observation of these results: As expected, the error increases with the distance of the forecast from the reference time. At 6pm, the possibility to have a real time rating below the value of the static seasonal rating is forecasted. In this case, the minimum forecasted rating in the late afternoon corresponds with the daily peak for the power transfer on the line. If the line utilization increased because of an increased connection of distributed generation, this would create a problem and the necessity to curtail part of the generation. On the other hand, the ability to forecast this situation and to quantify its probability, would allow appropriate decisions for generation control to be taken. Considering the different precision found for different time horizons, it is recommended to take into account this parameter, along with the distance from the forecast reference time, when developing control strategies for power flow management.

Existing load forecast methodologies could be combined with rating forecast in order to improve network management. Rating forecast could be particularly useful for managing load growth where this causes the exceeding of the thermal capacity of a line or a transformer for a reduced number of hours per year. This phenomenon is more visible at higher voltage levels in the distribution network. Different techniques should be used for forecasting environmental conditions and component ratings at different time horizons.

In particular, time series analysis could be used for short range rating forecasting and commercial meteorological office forecasts can be used for long term rating forecasts. In summary, the work carried out in this research could have outcomes in other areas of the power system industry such as the ones mentioned above. For this reason, in the development of the real-time rating algorithm an open architecture that would have facilitated the integration possible future functionalities was adopted.

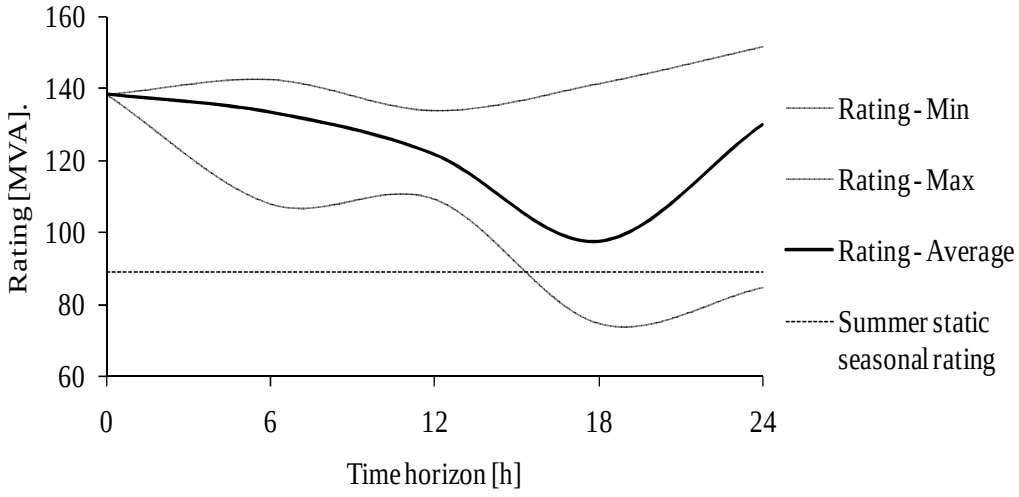

Figure 57: Rating forecast at different time horizons

References

[1] http://www.smartgrids.eu, accessed 10/10/2009

[2] http://www.energy.gov/news2009/8216.htm, accessed 10/10/2009

[3] Yip T, Chang A, Lloyd G, Aten M, Ferris B, "Dynamic line rating protection for wind farm connections", Electricity Distribution - Part 1, 2009. CIRED 2009. 20th International Conference and Exhibition on, 8-11 June 2009, Prague, Czech Republic, pp: 1-4

[4] Weibel M, Imohf K, Sattinger W, Etrans AG, Steinegger U, Zima M, Biedenbach G, "Overhead line temperature monitoring pilot project", ELECTRA B2-311, 2006

[5] Bernini R, Minardo A, Persiano G V, Vaccaro A, Villacci D, Zeni L, "Dynamic loading of overhead lines by adaptive learning techniques and distributed temperature sensing", 2007, IET Generation Transmission and Distribution, Vol. 1, pp.912–919

[6] Soto F, Latorre J, Wagensberger M, "Increasing the Capacity of Overhead Lines in the 400 kV Spanish Transmission Network: Real Time Thermal Ratings", 1998, ELECTRA, 22-211

[7] European Commission, EUR 22575 – European Electricity Projects – 2002/2006

[8] Masters C L, "Voltage rise: the big issue when connecting embedded generation to long 11 kV overhead lines", Journal of Power Engineering, 16(5), 2002

[9] Nuijten J M, Geschiere A, "Future Network Planning and Grid Control", 2005 International Conference on Future Power Systems, Amsterdam

[10] Stephen, D M, "Determination of the Thermal Rating and Uprating Methods for Existing Lines " ELECTRA, 22.301, 2000

[11] Seppa T O, Damsgaard-Mikkelsen S, Clements M, "Application of the Real Time Thermal Ratings for Optimizing Transmission Line Investment and Operating Decisions", ELECTRA, 22-301, 2000

[12] http://www.wasp.dk, accessed 10/10/2009

[13] Douglass, D.A. Lawry, D.C., Edris, A.-A., Bascom, E.C. III, "Dynamic Thermal Ratings Realize Circuit Load Limits ". 2000, IEEE Computer applications in Power, Vol. 13, pp. 38-44

[14] Douglass, D A, Edris, A A, "Real-time monitoring and dynamic thermal rating of power transmission circuits ", 1996, IEEE Transactions on Power Delivery, Vol. 11, pp. 1407-1418

[15] Henke R K, Sciacca S C, “Dynamic Thermal Rating for critical lines - a study of real-time interface requirements ”, 1989, IEEE Computer Applications in Power, Vol. 2, pp. 46-51
[16] Belben P D, Ziesler C D, “Aeolian Uprating: how wind farms can solve their own transmission problem”, 2002, World Wind Energy Conference and Exhibition, Berlin
[17] Helmer M, “Optimized size of wind power plant transformer and parallel operation”, 2000, Wind Power for the 21st century, Kassel
[18] Bascom E C, “Underground Cable Uprating and Upgrading Tutorial”, 2003, IEEE PES Transmission and Distribution Conference and Exposition, Dallas, 7-12 September 2003, pp: 1010-1016
[19] House, H E, Tuttle, P D, “Current Carrying Capacity of ACSR”, 1959, IEEE Transactions on Power Apparatus Systems, Vol. 78, pp. 1169-1177
[20] IEEE 738, “Standard for calculating the current-temperature relationship of bare overhead conductors” 1993
[21] IEC TR 1597, “Overhead electrical conductors - Calculation methods for stranded bare conductors” 1995
[22] CIGRE WG 22.12, “The thermal behaviour of overhead conductors Section 1 and 2”, 1992, Electra, 144, pp. 108-125
[23] Hall J F, Deb A K, Savoullis J, “Wind tunnel studies of transmission line conductor temperatures”, 1998, IEEE Transaction on Power delivery, Vol. 3(2), pp. 801-812
[24] Isozaki, M. Iwama, N., “Verification of forced convective cooling from conductors in breeze wind by wind tunnel testing”, 2002, Asia Pacific IEEE/PES Transmission and Distribution Conference and Exhibition, 6-10 Oct, pp:1890-1894
[25] Black W Z, Collins S S, Hall J F., “Theoretical model for temperature gradients within bare overhead conductors”, 1988, IEEE Transactions on Power Delivery, Vol. 3, pp. 707-715
[26] Minambres J F, Barandiaran J J, “Radial Temperature Distribution in ACSR Conductors Applying Finite Elements”, 1999, IEEE Transactions on Power Delivery, Vol 14(2), pp. 472-480
[27] Barrett, J S., “Optimization of Conductor Design”, IEEE Transactions on Power Delivery, Vol. 4, 1989, pp: 453 – 464
[28] Davis M W, “New Thermal Rating Approach – Real-Time Thermal Rating System for Strategic Overhead Conductor Transmission Lines. 1. General Description and Justification of Real Time Thermal Rating System”, 1977, IEEE Transactions on Power Apparatus and Systems, Vol. 96, pp. 803-809
[29] Davis M W, “New Thermal Rating Approach – Real-Time Thermal Rating System for Strategic Overhead Conductor Transmission Lines .2. Steady State Thermal Rating Program”, 1977, IEEE Transactions on Power Apparatus and Systems, Vol. 96, pp. 810-825
[30] McElvain F R, Mulnix S S, “Statistically determined static thermal ratings of overhead high voltage transmission lines in the Rocky Mountain region”, 2000, IEEE Transactions on Power Systems, Vol. 15, pp. 899-902
[31] Foss, S.D. Lin, S.H. Maraio, R.A. Schrayshuen, H., “Effect of Variability in weather Conditions on Conductor temperature and the Dynamic Rating of

transmission Lines", 1988, IEEE Transactions on Power Delivery, Vol. 3, pp. 1832-1841
[32] Chu, R F, "On Selecting Transmission lines for Dynamic Thermal Lines Rating System Implementation", 1992, IEEE Transaction on Power Systems, Vol. 7(2), pp. 612 - 619
[33] Morgan, V T., "Statistical Distribution of the temperature Rise of an Overhead Line Conductor Carrying Constant Current", 1992, Electric Power Systems Research, Vol 24(3), pp. 237-243
[34] Piccolo, A, Vaccaro, A and Villacci, D., "Thermal rating assessment of overhead lines by Affine Arithmetic", 2004, Electric Power Systems Research, Vol. 71, pp. 275-283
[35] Douglass, D A., "Weather-dependent versus static thermal line ratings", 1988, IEEE Transactions on Power Delivery, Vol. 3(2), pp. 742 -753
[36] Bayliss B. H. "Transmission and Distribution Electrical Engineering", Newnes, 2007
[37] IEEE Task Force "Bare Conductor Sag at High Temperature", "Limitations of the Ruling Span Method for overhead Line Conductors at High Operating Temperatures", 1999, IEEE Transactions on Power Delivery, vol. 14(2), pp. 549-560
[38] Rawlins C. B. (1) ; Douglass D., "Some Effects of Mill Practice on the Stress Strain Behaviour of ACSR", 1999, IEEE Transactions on Power Delivery, vol. 14(2), pp. 602-629
[39] Keshavarzian, M, Priebe, C H, "Sag and tension calculations for overhead transmission lines at high temperatures - Modified ruling span method", 2000, IEEE Transactions on Power Delivery, Vol. 15, pp. 777-783
[40] Seppa, T O., "Accurate Ampacity Determination – Temperature-Sag Model for operational Real-Time ratings", 1995, IEEE Transactions on Power Delivery, Vol. 10, pp. 1460-1470
[41] Alawar, E J, Nutt, S R., "A hybrid numerical method to calculate the sag of composite conductors", 2006, Electric Power Systems Research, Vol. 76, pp. 389–394
[42] IEC 61774, "Overhead lines - Meteorological data for assessing climatic loads"
[43] IEC 60826, "Loading and strength of overhead transmission lines", 1991
[44] Neher, M H, McGrath, J H., "The Calculation of the Temperature Rise and Load Capability of Power Systems", 1957, AIEE Transactions, Vol. 76, pp. 752-772
[45] Anders, G J., "Rating of Electric Power Cables, Ampacity Computations for Transmission, Distribution, and Industrial Applications", McGraw-Hill Professional, 1997
[46] IEC 60287, "Electric cables - calculation of the current rating", 1994
[47] ENA ER P17, "Current rating guide for distribution cables", 1976
[48] Anders, G J, Brakelmann, H., "Improvement in cable rating calculations by consideration of dependence of losses on temperature", 2004, IEEE Transactions on Power Delivery, Vol. 19, pp. 919-925
[49] Anders, G J, Elkady, M, "Transient Ratings of Buried Power-Cables - 1 – Historical Perspective and mathematical Model", 1992, IEEE Transactions on Power Delivery, Vol. 7, pp. 1724-1734

[50] Haskew, T A, Carwile, R F, Grigsby, L L, “An Algorithm for steady-State Thermal Analysis of Electrical cables with Radiation by Reduced Newton-Raphson Technique”, 1994, IEEE Transactions on Power Delivery, Vol. 9, pp. 526-532

[51] Figueiredo, R D, Carneiro, S, Cruz, M E., “Experimental validation of a thermal model for the ampacity derating of electric cables in wrapped trays” 1999, IEEE Transactions on Power Delivery, Vol. 14, pp. 735-742.

[52] Sellers, S M, Black, W Z., “Refinements to the Neher-McGrath model for calculating the ampacity of underground cables”. 1996, IEEE Transactions on Power Delivery, Vol. 11, pp. 12-30.

[53] Bontempi G, Vaccaro A, Villacci, D, “Semiphisical modelling architecture for dynamic assessment of power components loading capability”, 2004, IEE Proc. Gen transm. Distr, 151(4), pp: Generation, Transmission and Distribution, IEE Proceedings-, Vol. 151, No. 4. (2004), pp. 533-542.

[54] Aras F, Oysu C, Yilmaz G, “An assessment of the methods for calculating ampacity of underground power cables”, 2005, Electric Power Components and Systems, Vol. 33, pp. 1385-1402.

[55] Hanna M A, Chikhani A Y, Salama M M A, “Thermal-Analysis of power cables in multilayered soil – 1 – Theoretical model”, 1993, IEEE Transactions on Power Delivery, Vol. 8, pp. 761-771.

[56] Hanna M A, Chikhani A Y, Salama M M A, “Thermal analysis of power cable systems in a trench in multi-layered soil”, 1998, IEEE Transactions on Power Delivery, Vol. 13, pp. 304-309.

[57] Freitas D S, Prata A T, DeLima A J, “Thermal performance of underground power cables with constant and cyclic currents in presence of moisture migration in the surrounding soil”, 1996, IEEE Transactions on Power Delivery, Vol. 11, pp. 1159-1170.

[58] Garrido C, Otero A F, Cidras J, “Theoretical model to calculate steady-state and transient ampacity and temperature in buried cables” 2003, IEEE Transactions on Power Delivery, Vol. 18, pp. 667-678

[59] Hiranandani A, “Calculation of conductor temperature and ampacities of cable systems using a generalised finite element model”, 1991, IEEE Transactions on Power Delivery, Vol. 6, pp. 15-29.

[60] Hwang, C C, Jiang, Y H., “Extensions to the finite element method for thermal analysis of underground cable systems”, 2003, Electric Power Systems Research, Vol. 64, pp. 159-164

[61] Kovac N, Sarajcev I, Poljak D, “Nonlinear-coupled electric-thermal modeling of underground cable systems”, 2006, IEEE Transactions on Power Delivery, Vol. 21, pp. 4-14

[62] Buonanno G, Carotenuto A, Dell'Isola M, Villacci D, “Effect of radiative and convective heat transfer on thermal transients in power cables”, 1995, IEE Proceedings-Generation Transmission and Distribution, Vol. 142, pp. 436-444.

[63] Lyall J S, Barnewall G, “Analysis of temperatures and daily field data on the soil thermal parameters of operating circuits” ELECTRA. 2000, Vol. 21, 204e.

[64] Milun S, Kilic T, Bego O, “Measurement of soil thermal properties by spherical probe”, 2005, IEEE Transactions on Instrumentation and Measurement, Vol. 54, pp. 1219-1226.

[65] Dang C, Parpal J L, Crine J P, “Electrical aging of extruded dielectric cables - Review of existing theories and data” 1996, IEEE Transactions on Dielectrics and Electrical Insulation, Vol. 3, pp. 237-247.
[66] Montanari G C, simony L, “Aging phenomenology and modelling”, IEEE Transactions on Electrical Insulation, 28(5), Oct 1993, pp:755-776
[67] Yilmaz G, Karlik S E, “A distributed optical fiber sensor for temperature detection in power cables”, 2006, Sensors and Actuators a-Physical, Vol. 125, pp. 148-155.
[68] Kawai T, Takinami N, Chino T, Amano K, Watanabe K, Nakamura Y, Shiseki N, “A new approach to cable fault location using fiber optic technology”, 1995, IEEE Transactions on Power Delivery, Vol. 10, pp. 85-91.
[69] Li H J, Tan K C, Su Q, “Assessment of underground cable ratings based on distributed temperature sensing”, 2006, IEEE Transactions on Power Delivery, Vol. 21, pp. 1763-1769.
[70] Nakamura S, Morooka S, Kawasaki K, “Conductor temperature monitoring system in underground power transmission XLPE cable joints” 1992, IEEE Transactions on Power Delivery, Vol. 7, pp. 1688-1697.
[71] IEC 60076-7, “Power Transformers - Part 7: Loading guide for oil-immersed power transformers”, 2005
[72] IEEE C57.91, “Guide for loading mineral-oil-immersed transformers”, 1995
[73] Preis K, Biro O, Buchgraber G, Ticar I, “Thermal-electromagnetic coupling in the finite-element simulation of power transformers”, 2006, IEEE Transactions on Magnetics, Vol. 42, pp. 999-1002.
[74] Smolka J, Ingham D B, Elliott L, Nowak A J, “Enhanced numerical model of performance of an encapsulated three-phase transformer in laboratory environment”, 2007, Applied Thermal Engineering, Vol. 27, pp. 156–166.
[75] Susa D. “Dynamic Thermal Modelling of Power Transformers”, PhD thesis, Helsinki, 2005
[76] Susa D, Lehtonen M, Nordman H, “Dynamic thermal modelling of power transformers”, 2005, IEEE Transactions on Power Delivery, Vol. 20, pp. 197-204.
[77] Susa D, Lehtonen M, “Dynamic thermal modeling of power transformers: Further development - Part II”. 2006, IEEE Transactions on Power Delivery, Vol. 21, pp. 1971-1980.
[78] Ryder S A, Vaughan I J, “A simple method for calculating core temperature rise in power transformers”. 2004, IEEE Transactions on Power Delivery, Vol. 19, pp. 637-642.
[79] Ryder S A, “A simple method for calculating winding temperature gradient in power transformers”. 2002, IEEE Transactions on Power Delivery, Vol. 17, pp. 977-982.
[80] Tang W H, Wu Q H, Richardson Z J, “Equivalent heat circuit based power transformer thermal model”. 2002, IEE Proceedings-Electric Power Applications, Vol. 149, pp. 87-92.
[81] Tang W H, Wu Q H, Richardson Z J. “A simplified transformer thermal model based on thermal-electric analogy”. 2004, IEEE Transactions on Power Delivery, Vol. 19, pp. 1112-1119.
[82] Tang W H, Zeng H, Nuttall K I, Richardson Z, Simonson E, Wu Q H “Development of power transformer thermal models for oil temperature

prediction". 2000, Real-World Applications of Evolutionary Computing, Proceedings, pp. 195-204
[83] Radakovic Z, Feser K, "A new method for the calculation of the hot-spot temperature in power transformers with ONAN cooling". 2003, IEEE Transactions on Power Delivery, Vol. 18, pp. 1284-1292.
[84] Radakovic Z, Feser K, "Some important aspects of oil power transformer thermal protection". 2003, Electrical Engineering, Vol. 86, pp. 1-8.
[85] Pradhan M K, Ramu T S, "Estimation of the hottest spot temperature (HST) in power transformers considering thermal inhomogeniety of the windings". 2004, IEEE Transactions on Power Delivery, Vol. 19, pp. 1704-1712.
[86] Nordman H, Rafsback N, Susa D. "Temperature responses to step changes in the load current of power transformers". 2003, IEEE Transactions on Power Delivery, Vol. 18, pp. 1110-1117.
[87] Tojo S. "Proposition of individual loading guide for power transformers". 2006, IEEE Transactions on Power Delivery, Vol. 21, pp. 1383-1389.
[88] Lachman M F, Griffin P J, Walter W, "Real-time dynamic loading and thermal diagnostic of power transformers". 2003, IEEE Transactions on Power Delivery, Vol. 18, pp. 142-148.
[89] Pandey S B, Lin C, "Estimation for a life model of transformer insulation under combined electrical and thermal stress". 1992, IEEE Transactions on Reliability, Vol. 41, pp. 466-468.
[90] Williams G M, Lewin P L, LeBlanc M. "Accurate determination of ambient temperature at burial depth for high voltage cable ratings". 2004. IEEE International Symposium on Electrical Insulation, Indianapolis, 19—22 September 2004, pp:458-461
[91] Ringelband T, Lange M, Dietrich M, Haubrich H J, "Potential of Improved Wind Integration by Dynamic Thermal Rating of Overhead Lines". IEEE Bucharest PowerTech, 28 June – 2 July 2009, pp:1-5
[92] Ayotte, K W. "Computational modelling for wind energy assessment". 2008, Journal of Wind Engineering and Industrial Aereodynamics, Vol. 96, pp. 1571–1590.
[93] Finardi S, Tinarelli G, Faggian P, Brusasca G, "Evaluation of different wind fiel modeling techniques for wind energy applications over complex topography". 1998, Journal of Wind Engineering and Industrial Aerodynamics, Vol. 74, p. 283-294.
[94] Hirata Y, Mandic D, Suzuki H, Aihara K, "Wind direction modelling using multiple observation points". 2008, Philosophical Transactions of the Royal Society, Vol. 366, pp. 591-607.
[95] Palma J M L M, Castro F A, Ribeiro L F, Rodrigues A H, Pinto A P, "Linear and nonlinear models in wind resource assessment and wind turbine micro-siting in complex terrain". 2008, Journal of Wind Engineering and Industrial Aerodynamics, Vol. 96, pp. 2308– 2326.
[96] Walmsley J L, Troen I, Lalas D P, Mason P J, "Surface-layer flow in complex terrain: comparison of models and full-scale observations". 1990, Boundary-Layer Meteorology, Vol. 52, pp. 259-281.
[97] Montero G, Montenegro R, Escobar J M, "A 3-D diagnostic model for wind field adjustment". 1998, Journal of Wind Engineering and Industrial Aereodynamics, Vol. 74, p. 249-261.

[98] Winter G, Montero G, Montenegro R, “Adaptive strategies using standard and mixed finite elements for wind field adjustment”. 1995, Solar Energy, Vol. 54, pp. 49-56

[99] Ross D G, Smith I N, Manins P C, Fox D G, “Diagnostic wind field modeling for complex terrain: model development and testing”. 1988, Journal of Applied Meteorology, Vol. 27, pp. 785-796.

[100] Stahl K, Moore R D, Floyer J A, Asplin M G, McKendry I G, “Comparison of approaches for spatial interpolation of daily air temperature in a large region with complex topography and highly variable station density”. 3-4, 2006, Agricultural and forest meteorology, Vol. 139, pp. 224-236

[101] Dodson R, Marks D, “Daily air temperature interpolated at high spatial resolution over a large mountainous region”. 1997, Climate Research, Vol. 8, pp. 1-20.

[102] Chung U, Yun J I, “Solar irradiance-corrected spatial interpolation of hourly temperature in complex terrain”, 2004, Agricultural and Forest Meteorology, Vol. 126, pp. 129-139 .

[103] Hasenauer H, Merganicova K, Petritsch R, Pietscha S A, Thornton P E, “Validating daily climate interpolations over complex terrain in Austria”. 2003, Agricultural and Forest Meteorology, Vol. 119, pp. 87-107 .

[104] Benavides R, Montes F, Rubio A, Osoro K, “Geostatistical modelling of air temperature in a mountainous region of Northern Spain”. 2007, Agricultural and Forest Meteorology, Vol. 146, pp. 173-188.

[105] McKenneya D W, Pelland S, Poissant Y, Morris R, Hutchinson M, Papadopol P, Lawrence K, Campbell K, “Spatial insolation models for photovoltaic energy in Canada”. 2008, Solar Energy, Vol. 82, pp. 1049-1061.

[106] Bechini L, Ducco G, Donatelli M, Stein A, “Modelling, interpolation and stochastic simulation in space and time of global solar radiation”. 2000, Agriculture, Ecosystems & Environment, Vol. 81, pp. 29-42.

[107] Hammer A, Heinemann D, Hoyer C, Kuhlemann R, Lorenz E, Müller R, Beyer H G, “Solar energy assessment using remote sensing technologies”. 2003, Remote sensing of environment, Vol. 86, pp. 423-432

[108] Mohandes M, Balghonaim A, Kassas M, Rehman S, Halawani T O, “Use of radial basis functions for estimating monthly mean daily solar radiation”, 2000, Solar Energy, Vol. 68, pp. 161-168.

[109] Kang S, Kim S, Oh S, Lee D, “Predicting spatial and temporal patterns of soil temperature based on topography, surface cover and air temperature”. 2000, Forest Ecology and Management, Vol. 136, pp. 173-184.

[110] Snepvangers J J, Heuvelink G B, Huisman J A, “Soil water content interpolation using spatio-temporal kriging with external drift”. 2003, Geoderma, Vol. 112, pp. 253-271.

[111] Dos Santos Coelho L, Zanetti Freire R, Henrique Dos Santos G H, Mendes N, “Identification of temperature and moisture content fields using a combined neural network and clustering method approach”. 2009, International Communications in Heat and Mass Transfer, Vol. 36, pp. 304–313.

[112] Roytelman I, Shahidepur R S, “State estimation for electric power distribution systems in quasi rel time conditions”. 1993, IEEE Transactions on Power delivery, Vol. 8, pp. 2009-2015.

[113] Monticelli A. “Electric Power Systems State Estimation”. IEEE, Proceedings of, 2000, Vol. 88, pp. 262, 282.
[114] Al-Othman A K, Irving M R, “Uncertainty modelling in power system state estimation”. IEE Proc.-Gener. Transm. Distrib, 2005, Vol. 152, pp. 233-239.
[115] Price C, Gibbon R, “Statistical approach to thermal rating of overhead lines for power transmission and distribution”. 1983, IEE Proceedings, Vol. 130, pp. 245-256.
[116] Wan H, McCalley J D, Vittal V., “Increasing thermal rating by risk analysis”. 3, 1999, IEEE Transactions on Power Systems, Vol. 14, pp. 815-828.
[117] Michiorri A, Taylor P C, Jupe S C E, Berry C J, “Investigation into the influence of environmental conditions on power system ratings”, 2009, Proceedings of the Institution of Mechanical Engineers, Part A, Journal of Power and Energy, Vol. 223(7), pp. 743-757
[118] Villacci D, Vaccaro A, “Transient tolerance analysis of power cables thermal dynamic by interval mathematic”, 2007, Electric Power Systems Research, Vol. 77, pp. 308–314.
[119] Ippolito L, Vaccaro A, Villacci D, “The use of affine arithmetic for thermal state estimation of substation distribution transformers”. 2004, COMPEL: The International Journal for Computation and Mathematics in Electrical and Electronic Engineering, Vol. 23(1), pp.237 - 249
[120] Lee T L, Negnevitsky M, Piekutowski M, “Expert system application for the loading capability assessment of transmission lines”. 1995, IEEE transactions on power systems, Vol. 10(5), pp. 1805 – 1812
[121] ENA ER P27, “Current rating guide for high voltage overhead lines operating in the UK distribution system”. 1986.
[122] Walker, M. “Aluminum Electrical Conductor Handbook”. Aluminum Association, 1983.
[123] Fessler W A, Rouse T O, McNutt W, J, Compton O R, “A refined mathematical model for prediction of bubble evolution in transformers”, Jan 1989, Power Delivery, IEEE Transactions on, Vol. 4, pp. 391-404.
[124] Lundgaard L E, Hansen W, Linhjell D, Painter T J; “Aging of oil-impregnated paper in power transformers”, 2004, Power Delivery, IEEE Transactions on, Vol. 19, pp. 230- 239.
[125] ENA ER P15, Transformer loading guide. 1971
[126] www.metoffice.gov.uk, accessed 13/05/2008
[127] Shepard D. “A two-dimensional interpolation function for irregularly-spaced data”, 1968. Proceedings of the 23rd ACM national conference. pp. 517-524.
[128] Abu-Hamdeh N H, “Thermal properties of soil as affected by density and water content”. 2003, Biosystems engineering, Vol. 86, pp. 97-102.
[129] Nairen D, Qinyun L, Zhaohong F, “Heat transfer in ground heat exchangers with groundwater advection”. 2004, International Journal of Thermal Sciences, Vol. 43, pp. 1203-1211.
[130] Celia M, Boulotas E, Zarba R, “A general mass-conservative numerical solution for the unsaturated flow problem”. 1990, Water resources research, Vol. 26, pp. 1483-1496.
[131] Van Genuchten M, “A closed-form equation for predicting the hydraulic conductivity of unsaturated soils”. 1980, Soil science society of America Journal, Vol. 44, pp. 892-898.

[132] Rodriguez-Iturbe I, Isham V, Cox D R, “Space-time modelling of soil moisture: stochastic rainfall forcing with heterogeneous vegetation”. 2006, Water resources research, Vol. 42, pp. 1-11
[133] R. Deutsch. “Estimation Theory”. 1965
[134] Monticelli A. “State Estimation in Electric Power Systems – a generalized approach”. Boston 1999.
[135] Figuiredo L H, Stolfi J, “Self-validated Numerical methods and Applications”, Brazilian Mathematics Colloquium monograph, Rio de Janeiro, 1997.
[136] Rubinstein R Y, “Simulation and the Monte Carlo method”, Wiley-Interscience, 2007.
[137] Morris R D, Young S S, “Determining the Number of Iterations for Monte Carlo Simulations of Weapon Effectiveness”. Naval postgraduate school, Monterey, 2004, Monterey, Ca
[138] Mathews J H. “Numerical methods for computer science, engineering, and mathematics”, Prentice-Hall, 1987.
[139] Johnson N L, Kotz S, “Continuous univariate distributions”, John Wiley & Sons, 1978.
[140] Saralees N, “On the distribution of Kumaraswamy”. 2008, Journal of Hydrology, Vol. 348, pp. 568-569.
[141] Michiorri A, Taylor P C, Jupe S C E, “Overhead line real-time rating estimation algorithm: description and validation”, 2009, Proceedings of the Institution of Mechanical Engineers, Part A: Journal of Power and Energy, 224(3), pp. 293-304
[142] http://physics.nist.gov/Pubs/guidelines/appd.1.html “Guidelines for Evaluating and Expressing the Uncertainty of NIST Measurement Results - Appendix D”, accessed on 10/08/2009
[143] http://www.sedg.ac.uk/, “United Kingdom Generic Distribution System”, 12/01/2008
[144] GE Energy, “3.6 MW Offshore Series Wind Turbine”, datasheet. 2005.
[145] Jupe S C E, Taylor P C, Michiorri A, Berry C J, “An Evaluation of Distributed Generation Constrained Connection Managers”, 2008. MedPower – 6th Mediterranean Conference and Exhibition on Power Generation, Transmission and Distribution, 2-5 November 2008, Thessaloniki
[146] European Commission. “Quarterly Review of European Gas and Electricity Prices”. Luxembourg: 2005.
[147] Ofgem. “Renewables Obligation: Annual Report 2006-2007”. London, 2008.
[148] http://www.offshoresea.org.uk, “Wind Background – Cost of Wind Power Generation”, accessed on 12/04/2008
[149] Michiorri A, Taylor P C, “Forecasting Real Time Ratings for Distribution Networks Using Weather Forecast Data”, 2009, CIRED, Prague, pp.1-4

Appendix

Algorithm details

Classes

Component

The class “Component” is designed for describing the structure and the thermal behaviour of electric network component. It is the most complex class of the algorithm, compose by six sub-classes describing respectively an electric network, the electric circuit, the single element of the circuit, the general parameters of each element, overhead line conductors, electric cables and power transformers. The static structure of the class is described in **Error! Reference source not found.**.

The main idea behind the architecture of this class is that a network is modelled as a list of circuits and a circuit is modelled as a list of elements. Each element can be an overhead line, an electric cable or a power transformer. Substations can be modelled or as independent circuits, or the transformer can be considered the final or initial element of a circuit, replicating the same transformer for the high and low voltage circuit.

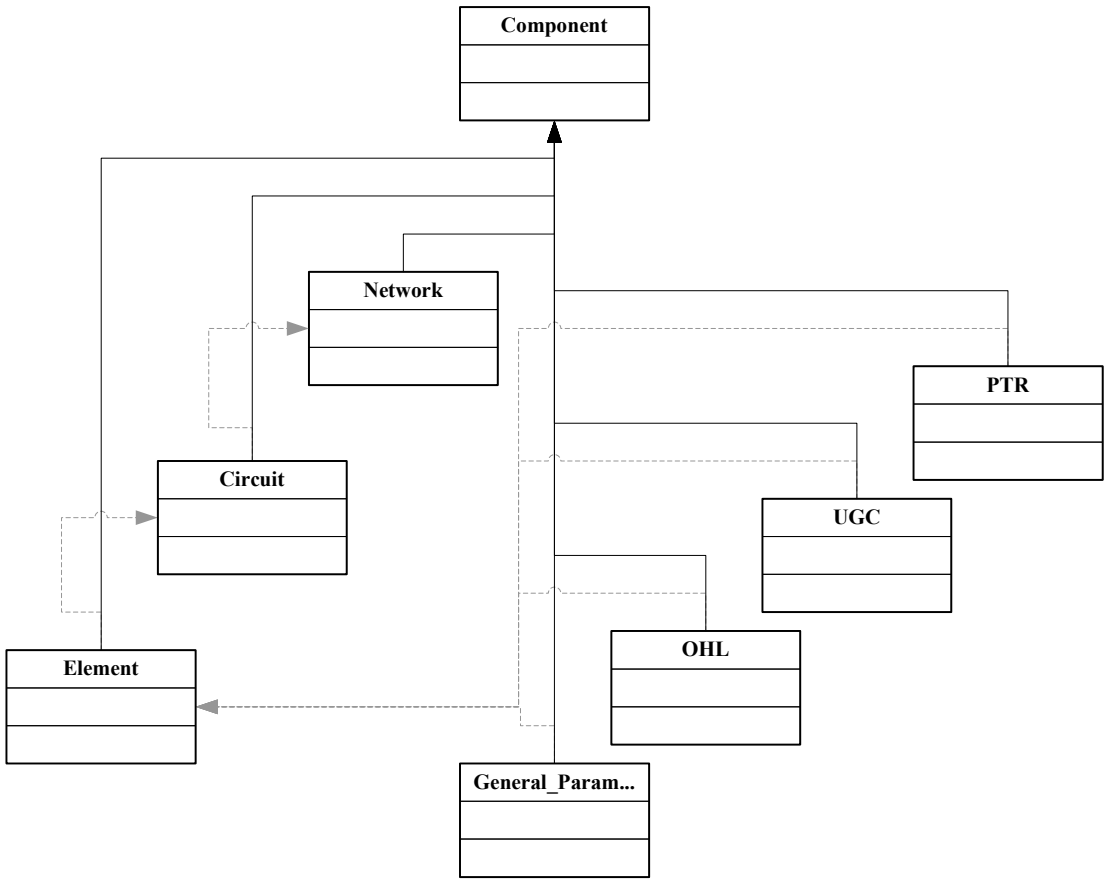

Figure A - 1: Component_Class static diagram

Component.Network

Error! Reference source not found. shows the graphical representation for the sub-class “Network”. This class has only two attributes:

- Name
- Network_Circuits

Whilst the name is a single string, the list of circuit is an array of instances of the “Circuit” class. The class has also two functions:

- Load_Data
- Find_Circuits_in_Network

The method “Load_Data” takes the network name as input and returns an instance of the “Network” class populated with the parameters read into the database. The method

“Find_Circuits_in_Network” return a list of the names of the circuits belonging to the network, and it is used in the method “Load_Data”

Table A - 1: Component.Network class

Component.Network	
Name Circuit_Components	String Component.Circuit()
Load_Data(Name, Configuration) Find_Circuits_in_Network(Name, Configuration)	Component.Network String()

Component.Circuit

The “Circuit” class has two attributes and three methods. The two attributes are:

- Name
- Circuit_Components

In this case too, the name is a string, whilst “Circuit_Components” is an array of instances of the class “Element”, described later. The three methods of the class are:

- Load_Data
- Find_Components_in_Circuit
- Circuit_Rating

The method “Load_Data” uses the circuit name as input and returns an instance of the “Circuit” class populated with the parameters read into the database. The method “Find_Components_in_Circuit” return a list of the names of the elements belonging to the circuit, and it is used in the method “Load_Data”. The method Circuit_Rating takes as input a Circuit object and the time, for returning a value of the rating of the circuit, calculated as the rating of the component with the lowest rating in the circuit. **Error! Reference source not found.** shows the representation for the sub-class “Circuit”.

Table A - 2: Component.Circuit class

Component.Circuit	
Name String Circuit_Components	String Component.Element()
Load_Data(Name, Configuration) Find_Components_in_Circuit(Name, Configuration) Circuit_Rating(Name, Configuration)	Component.Circuit String() Single

Component.Element

The “Element” class has four attributes and six methods. The four attributes are:

- General_Parameters
- OHL_Parameters
- UGC_Parameters
- PTR_Parameters

These attributes are instances of classes specifically designed for describing electric network component thermal properties and they are described later in this section. The six methods of the class are:

- Calculate_Rating_MVA
- Calculate_Static_Rating_MVA
- Get_Power_Flow
- Calculate_Temperature
- Get_Component_Type
- Load_Data

The method “Calculate_Rating_MVA” returns a single value for the rating in MVA of the single component, whilst the method “Calculate_Static_Rating_MVA” returns a single value corresponding to the static seasonal rating for that component in the period corresponding to the time of the request. This latter function is not longer used in the algorithm but was kept for possible future improvements. The function

"Calculate_Temperature" returns the temperature of the component. It makes use of the method "Get_Power"Flow" which obtains current readings from the observation database. If component power flow is not measured, the function returns the component rated maximum temperature. The method "Get_Component_Type" returns the type of component (between overhead lines, electric cables and power transformers) and is used in several parts of the algorithm for selecting the right method corresponding to the component type described by the object. Finally the function "Load_Data" returns the instance of the "Element" class corresponding to the component's name. A representation of the "Element" class is shown in **Error! Reference source not found.**.

Table A - 3: Component.Element class

Component.Element	
General_Parameters	Component.General_Parameters
OHL_Parameters	Component.OHL
UGC_Parameters	Component.UGC
PTR_Parameters	Component.PTR
Calculate_Rating_MVA(Component, Environment, Configuration)	Single
Calculate_Static_Rating_MVA(Component, Time, Configuration)	Single
Get_PowerFlow(Element, Date, Configuration)	Single
Calculate_Temperature(Load, Component, Environment, Configuration)	Single
Load_Data(Name, Configuration)	Component.Element
Get_Component_Type(Name, Configuration)	String

Component.General_Parameters

The class "General_Parameters" has no methods and thirteen attributes. The attributes are:

- Name
- Type
- Type_Specification

- Circuit
- Network
- Rating_MVA
- Rated_Voltage
- Real_Time_Rating
- Spring_Rating_MVA
- Summer_Rating_MVA
- Autumn_Rating_MVA
- Winter_Rating_MVA
- Place

These attributes represents a list of the attributes of every element independently from their type. The attributes “Name”, “Circuit” and “Network” are strings for the storage of the component’s name and the names of the circuit and the network to which it belongs. The attributes “Type” and “Type_Specification” are used for storing respectively the component type (overhead line, electric cable or power transformer) and an additional description relative to the component. The latter attribute is not used actively in the algorithm but was added for facilitating the offline data analysis. The attributes “Real_Time_Rating” and “Rating_MVA” are used for storing the real-time rating in Amperes if applicable (not for power transformers) and in MVA, whilst “Rated_Voltage” stores a value corresponding the component rated voltage (in this case too, not for power transformers) and is used for calculating the rating in MVA for the component. Component seasonal static ratings are stored in the attributes “Spring_Rating_MVA”, “Summer_Rating_MVA”, “Autumn_Rating_MVA”, and “Winter_Rating_MVA”. Although spring and autumn rating are currently the same, it was decided to leave an additional attribute in case of future modifications of the static rating or

the use of the algorithm in countries with different regulations. Finally the attribute “Place” is an instance of the class “Environment.Place” containing all the geographical information relative to the component location such as latitude, longitude or soil roughness.

A representation of the “General_Parameters” class is shown in **Error! Reference source not found.**.

Table A - 4: Component.General_Parameters

Component.General_Parameters	
Name	String
Type	-
Type_Specification	-
Circuit	-
Network	Single
Rating_MVA	-
Rated_Voltage	-
Winter_Rating_MVA	-
Spring_Rating_MVA	-
Summer_Rating_MVA	-
Autumn_Rating_MVA	-
RealTime_Rating	-
Place	Environment.Place

Component.OHL

The class “Component.OHL” (OHL is an acronym for “OverHead Line”) provides a representation of the thermal behavior of an overhead line conductor. The class has nine attributes and thirteen methods used mainly for calculating the component real-time rating. The nine attributes are:

- Conductor_Code
- Line_Dir_Nord
- Height
- Rated_Temperature

- Emissivity
- Absorbivity
- Diameter
- Resistance20
- Th_Res_Coeff

The attribute “Conductor_Code” is used for describing the type of conductor. “Line_Dir_Nord” describe the clockwise angle in degrees between the axis of the component and the north, “Height” describes the height of the conductor from the soil and “Rated_Temperature” is used for storing the value of the maximum design rated temperature. The attributes “Emissivity” and “Absorbivity” are used to store the value for the conductor’s surface emissivity and absorbivity factor used for calculating the radiative heat exchange and the solar gain. The attribute “Diameter” is used to store the value of the conductor’s diameter used in all heat exchange formulae. Finally the attributes “Resistance20” and “Th_Res_Coeff” represents respectively the conductor’s electrical resistance at 20°C and the conductor’s electrical resistance rate of change with the themperature.

The methods of the class “Component.OHL” are:

- Calculate_Rating_MVA
- Calculate_Static_Rating
- Calculate_Current
- Calculate_Component_Temperature
- Calculate_Resistance
- Calculate_Solar_Radiation
- Calculate_Radiative_Heat_Hexchange
- Calculate_Convective_Heat_Hexchange

- Calculate_Corrected_Convective_Heat_Hexchange
- Calculate_Nusselt_Forced
- Calculate_Nusselt_Natural
- Calculate_Angle_Correction
- Load_Data

These methods are mainly developed for calculating conductor rating, except for “Load_Data” and “Caclulate_Component_Temperature”. The first return an instance of the class “Component.OHL” populated with the data read in the static parameters database and corresponding to the component named in the input. The second returns component temperature, and can be used only if the current flowing in the conductor is monitored locally. The method “Calculate_Static_Rating” return the static seasonal rating of the conductor corresponding to the season, whilst the method “Calculate_Rating_MVA” returns the real-time rating in MVA. Because of the importance of this method in the whole algorithm, particular attention is given in its description. The method “Calculate_Rating_MVA” has for input one instance of the class “Component.OHL” and one instance of the class “Environment.Environment_for_Rating” and returns as output a single vlue for the component rating. It makes use of the method “Component.OHL.Calculate_Component_

_Current” and then converts the value in Amper given by this method in MVA thanks to the component rated voltage stored in the attribute “Component.OHL.Rated_Voltage”.

Table A - 5: Component.OHL class

Component.OHL	
Conductor_Code	String
Conductor_Old_Code	-
Line_Dir_Nord	Single
Height	-
Rated_Temperature	-
Emissivity	-
Absorbivity	-
Resistance20	-
Diameter	-
Th_Res_Coeff	-
Calculate_Rating_MVA(Component, Environment, Configuration)	Single
Calculate_Static_Rating(Component, Time, Configuration)	
Calculate_Current(Component, Environment, Configuration	
Calculate_Component_Temperature(Recorded, Component,Environment,Configuration)	
Calculate_Resistance(Component,Environment, Temperature, Configuration)	
Calculate_Solar_Radiation(Component, Environment, Configuration)	
Calculate_Radiative_Heat_Exchange(Component, Environment, Configuration)	
Calculate_Convective_Heat_Exchange(Component, Environment, Configuration)	
Calculate_Corrected_Convective_Heat_Exchange(Component, Environment, Configuration)	
Convective_Nusselt_Forced(Component, Environment, Configuration)	
Convective_Nusselt_Natural(Component, Environment, Configuration)	
Convective_Angle_Correction(Wind_Direction, Line_Direction,Configuration)	
Load_Data(Name, Configuration)	Component.Element

The method “Component.OHL.Calculate_Component_Current”, which uses the same inputs of the method “Component.OHL.Calculate_Rating_MVA”, calculates component rating with the energy balance described in Section 3.1.1 and calls the methods “Calculate_Resistance”, “Calculate_Solar_Radiation”, “Calculate_Radiative_Heat_Hexchange”, and “Calculate_

_Corrected_Convective_Heat_Hexchange" for calculating respectively conductor electrical resistance, solar radiation gain, radiative heat exchange and convective heat exchange. The method "Calculate_Corrected_Convective_Heat_Hexchange" calls in turn the methods "Calculate_Nusselt_Forced", "Calculate_Nusselt_Natural" and "Calculate_Angle_ _Correction".

Component.UGC

The class Component.UGC is designed for describing the thermal behaviour of electric cables. UGC is an acronym for UnderGround Cables, definition used in the first part of the project for defining insulated electric cable, in opposition with the bare conductors used in overhead lines. Lately the more common terminology "electric cable" was adopted, but the acronym UGC survived in this part of the code.

The class has twenty attributes and five methods, mostly used for calculating the real-time conductor rating. The twenty one attributes of the class are:

- Code
- Laying
- Configuration
- Bonding
- Drying_Out
- Area
- Rated_Current
- Corr(i)_(K) (i=1,4 – K=A,C)

The attribute "Code" describes cable characteristics and is used as a key for retrieving information from the database. The attribute "Laying" described the laying condition of the cable and is a string with three possible values: BGr (directly buried in the ground), BDu

(buried in duct), Air (laid in air). The attribute “Configuration” describes the geometrical configuration of the cable system and is a string with two possible values. Tr (trefoil) and Fl (flat). The attribute “Bonding” describes the bonding to earth of the metallic insulation, is a string with two possible values: S (single bounded) and B (bounded at both ends) although more possibilities could be considered. The attribute “Drying_Out” describes if it is admitted a drying out of the soil surrounding the cable or not, and it has two possible values: Y (yes) and N (no). The attribute Area represents in squared millimeters the conductor cross sectional area. The “Code” is composed by the series of the values of the fields “Area”, “Configuration”, “Laying”, “Bonding” and “Drying_Out”; for example a cable with a 150mm^2 conductor, laid directly in the ground in flat configuration, bounded at both sides and with no drying out allowed would be represented by the code “150BGrFlBN”.

Finally the attributes “Corr(*i*)_(K)” where *i* can assume the integer values from 1 to 4 and K can assume the values A, B or C, represents the coefficients of the cubic interpolation of the dependence between cable rating and respectively (for each value of the index i) soil temperature, soil thermal resistivity, air temperature and soar radiation.

The five methods of the class are:

- Calculate_Rating_MVA
- Calculate_Static_Rating
- Calculate_Current
- Calculate_Component_Temperature
- Load_Data

The method “Calculate_Rating_MVA” returns a single value of the component rating in MVA. In order to do this, it calls the method “Calculate_Current”, which calculates conductor rating considering the cubic interpolation of the dependence between rating and external

conditions summarised in the coefficients Corr(i)_(K) and the external conditions described in the object “environment” given as input. The method “Calculate_Static_Rating” returns the conductor seasonal static rating and the method “Load_Data” returns an instance of the object “Component.Element” populated with the parameters read in the database.

A representation of the class “Component.UGC” according to the unified modeling language is shown in Table A - 6.

Table A - 6: Component.UGC class

Component.UGC	
Code	String
Laying	-
Configuration	-
Bonding	-
Drying_Out	-
Area	Single
Rated_Current	-
Corr(i)_(K) (i=1,4 – K=A,C)	-
Calculate_Rating_MVA(Component, Environment, Configuration)	Single
Calculate_Static_Rating(Component, Environment, Configuration)	-
Calculate_Current(Component, Environment, Configuration)	-
Calculate_Component_Temperature(Component, Environment, Configuration)	-
Load_Data(Name, Configuration)	Component.Element

Component.PTR

Power transformer thermal behaviour is modelled in the class “Component.PTR” (PTR is an acronym for “Power TRansformer”), characterised by sixteen attributes and five methods. The sixteen attributes are:

- Code
- Voltage_Ratio
- Cooling
- Oil_Exponent

- Loss_Ratio
- Hot_Spot_Temperature
- Hot_Spot_Factor
- Oil_Time_Constant
- Rated_Ambient_Temperature
- Hot_Spot_Rise
- Average_Winding_Rise
- HotSpot_TopOil_Gradient
- Average_Oi_Rise
- TopOfWinding_Oil_Rise
- Bottom_Oil_Rise

The attribute “Component.PTR.Code” is used to describe the type of transformer, with information regarding the size and the cooling system, whilst “Voltage_Ratio” represent the voltage ratio at the ends of the transformers. The attribute “Cooling” is used for storing values regarding transformer cooling method and can have four values, according to (71) ON: for oil immersed transformers with natural convection, OF for oil immersed transformers with forced convection, OD for oil immersed transformers with direct convection and finally ONAN for small (<20MVA) oil immersed transformers with natural convection. The other attributes describe parameters cited in (71) and necessary for transformer thermal rating. Their value can be found in (71).

The five methods of the class “component.PTR” are:

- Calculate_Rating_MVA
- Calculate_Static_Rating
- Calculte_Hot_Spot_Temperature

- Calculate_Load_on_Temperature
- Load_Data

The method “Component.PTR.Calculate_Rating_MVA” returns a single value for the component rating in MVA using one instance of the “Component.PTR” class and one instance of the “Environment.Environment_for_Rating_Class” as input. In order to calculate transformer real-time rating, the method “Component.PTR.Calculate_Rating_MVA” calls the method “Component.PTR.Load_on_Temperature”, which returns a dimensionless value for the transformer rating that must be multiplied by the transformer static rating. Since in (71) a model for calculating transformer hot spot temperature depending on external condition and load is provided, this method finds a solution solving iteratively the equation provided in Section 3.1.3 calling the method “Component.PTR.Calculate_Hot_Spot_Temperature”. The method “Component.PTR.Calculate_Static_Rating” returns the static rating of the transformer. Finally the method “Component.PTR.Load_Data” returns a instance of the “Component.Element” class populated with the parameters read on the static database and corresponding to the component name taken as input.

A visual representation of the class “Component.PTR” is shown in Table A - 7.

Table A - 7: Component.PTR class

Component.PTR	
Code	String
Voltage_Ratio	-
Cooling	-
Oil_Exponent	Single
Winding_Exponent	-
Loss_Ratio	-
HotSpot_Temperature	-
HotSpot_Factor	-
Oil_Time_Constant	-
Rated_Ambient_Temperature	-
HotSpot_Rise	-
Average_Winding_Rise	-
HotSpot_TopOil_Gradient	-
Average_Oil_Rise	-
TopOfWinding_Oil_Rise	-
Bottom_Oil_Rise	-
Calculate_HotSpotTemperature(Component, Environment, Configuration)	Single
Load_on_Temperature(Component, Environment, Configuration)	-
Calculate_Rating_MVA(Component, Environment, Configuration)	-
Calculate_Static_Rating(Component, Environment, Configuration)	-
Calculate_Component_Temperature(Component, Environment, Configuration)	-
Load_Data(Name, Configuration)	Component.Element

Environment

The class “Environment”, shown in **Error! Reference source not found.** and **Error! Reference source not found.**, is designed for modelling environmental condition for component rating. It has no attributes, six methods and three sub-classes, designed to describe and to be appropriate data structure for the environment read in weather stations, the environment necessary for calculating component rating and the geographical location. The static structure of the class is described in **Error! Reference source not found.**.

The decision of creating two different sub-classes for the representation of the environment read in weather stations (Environment.Environment_for_Observation) and the environment use for component rating (Environment.Environment_for_Observation) was

taken after the following consideration: Component thermal models are already developed and describe clearly the environmental parameters necessary for the rating of each component type. On the other hand environmental conditions that are not directly involved in component rating can influence other environmental condition directly responsible for component rating changes. An example of this is the use of the rainfall for calculating soil thermal resistivity, or air pressure could be used for improving wind speed and direction calculation. Therefore, in order to facilitate further developments of the algorithm it was decided to create to separate the “Environment_for_Observation” class from the “Enironment_for_Rating” class, facilitating the future increasing of the number of measured parameters.

For practical reasons, The sub-class “Environment.Component_Reading”, containing the data structure describing component electrical and electrical parameters readings and necessary for conductor temperature estimation used in the code validation process, was created in the class “Environment” instead than the class “Component”. This is due to the fact that even if it is referred to an electrical component, its structure and its behaviour are much more similar to the class “Environment.Environment_for_Observation”. Furthermore the methods of this class are used to read in the real-time database and therefore they are called together with the methods of the class “Environment.Environment_for_Observation”. Therefore it was decided to create the sub-class “Component_Reading” inside the class “Environment”.

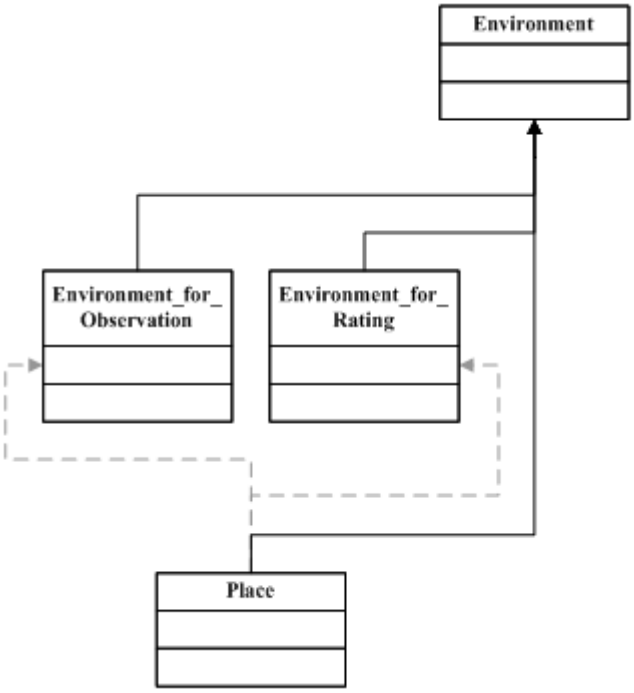

Figure A - 2: Environment class static structure

The six methods of the class “Environment” are:

- Search_Data
- Environment_Parameter_Estimation
- Find_Environmental_Readings
- Inverse_Distance_Interpolation_Fun
- Distance
- Refine_Wind_Speed

The methods “Search_Data” returns an array of probability distributions and is used directly by the class Thermal_State_Estimation. In order to read data from the weather stations, it calls the function “Find_Environmental_Readings” and converts the array of single values of this function in a probability distribution thanks to the method “Montecarlo_Method.MCM_Populate_PDF” for each environmental condition. The method “Environmental_Parameter_Estimation” returns a single vale for the estimated value of a

single environmental condition in the desired location. It makes use of the method "Inverse_Distance_Interpolation_Fun" which in turn makes use of the methods "Distance" and "Refine_Wind_Speed". This last method is called when the environmental condition interpolated is the wind speed. Thanks to the structure of the program, it is possible modify the model used for environmental condition calculation at the level of the method "Environmental_Parameter_Estimation", changing the input structure, and the methods called.

Table A - 8: Environment class

Environment	
Search_Data(Time, Configuration)	
Environment_Parameter_Estimation(Name, Parameters(), Latitude(), Longitude(), Place, Configuration)	PDF.Beta() Single
Find_Environmental_Readings(Station_Name, Parameter_Name, Time_Min, Time_Max, Configuration)	Single()
Inverse_Distance_Interpolation_Fun(Parameter(), Latitude(), Longitude(), Place, Configuration)	-
Distance(Lat1, Long1, Lat2, Long2)	Single
Refine_Wind_Speed(Wind_Speed_1, Height_1, Reference_Height, Ground_Type, Configuration)	-

Environment_for_Rating

The sub-class "Environment.Environment_for_Rating", represented in **Error! Reference source not found.**, is designed for representing the environment necessary for calculating component ratings. It has six attributes and two methods, although it is mainly used in the algorithm for its attributes.

The six attributes of the class are:

- Wind_Speed
- Wind_Direction
- Air_Temperature

- Solar_Radiation
- Soil_Temperature
- Soil_Thermal_Resistivity
- Place

Their names are descriptive of their function and they are all single values except the attribute “Place” that is an instance of the class “Environment.Place”.

The two methods of the class are:

- Calculate_Environment_for_Rating
- Season_for_Rating

The method “Calculate_Environment_for_Rating” reads environmental readings in weather stations and returns an instance of the “Environment.Environment_for_Rating” class with the calculated environmental condition in the component location. The difference between this method and the method “Environment.Read_Data” described in Section 0 is that the one belonging to this class reads and returns instantaneous values of weather readings, no probability distributions based on a period of readings. For this reason it is not used in the thermal state estimation: it was created to perform off-line simulations and it is maintained for future development of the algorithm as an off-line analysis tool. In order not to generate confusion this method is placed in this sub-class instead than the more general Environment class with other similar methods. The method “Season_for_Rating” return a string with the name of the season corresponding to the time given as input. This method is used for calculating component static seasonal rating.

Table A - 9: Environment.Environment_for_Rating class

Environment.Environment_for_Rating	
Wind_Speed	Single
Wind_Direction	-
Air_Temperature	-
Solar_Radiation	-
Soil_Temperature	-
Soil_Thermal_Resistivity	-
Place	Environment.Place
Calculate_Environment_for_Rating(Observation_Array(), Place, Configuration)	Environment.Environment _for_Rating
Season_for_Rating(Time)	String

Environment_for_Observation

The sub-class "Environment.Environment_for_Observation", represented in **Error! Reference source not found.**, is designed for representing the environment arising from meteorological stations observations. It has eight attributes and three methods. The Eight attributes of the class are:

- Station_Name
- Wind_Speed
- Wind_Direction
- Air_Temperature
- Solar_Radiation
- Soil_Temperature
- Soil_Thermal_Resistivity
- Place

Their names are descriptive of the parameters that they represent and they are all single values except the attribute "Place" that is an instance of the class "Environment.Place" and the attribute "Station_Name" that is a string. The three methods of the class are:

- Read_Environment_in_Station

– Find_Observations

– Load_Weather_Station_Data

These three functions are strictly linked between each other and work together in the following way: firstly the method “Load_Weather_Station_Data” is called. The method returns an array of instances of the class “Environment.Environment_for_Observation” populated only with the attributes “Station_Name” and “Place”. This array is then passed to the method “Find_Observations” which calls, for each element of the array, the method “Read_Environment_in_Station”. This method read in the database values for the environmental condition for a given period of time and populates the instance of the instance with the messing data relative to the weather.

Table A - 10: Environment.Environment_for_Observation

Environment.Environment_for_Observation	
Station_Name	String
Wind_Speed	Single
Wind_Direction	-
Air_Temperature	-
Solar_Radiation	-
Soil_Temperature	-
Soil_Thermal_Resistivity	-
Place	Environment.Place
Read_Environment_in_Station(Observation, Time, Configuration)	Environment.Environment_for_Observation
Find_Observations(Time, Observation_Array(), Configuration)	Environment.Environment_for_Observation()
Load_Weather_Station_Data(Configuration)	-

Place

The sub-class “Environment.Place” is designed for representing geographical locations for components and meteorological stations. It has five attributes and one method.

The five attributes are:

– GeoID

– Ground_Type_Turbulence

– Latitude

– Longitude

– Altitude

The attribute “GeoID” is a string defining the geographical location with an identification used as key to read information in the geographical database. The attribute “Ground_Type_Turbulence” is a string defining the roughness class of the soil used for refining the wind speed. The attributes “Latitude”, “Longitude” and “Altitude” represents the geographical coordinates of the location. “Latitude” and “Longitude” can be expressed in whatever Cartesian reference system but they must be coherent with the system used in the whole database.

The only method of the class “Environment.Place” is:

– Find_Place_Coordinates

This method returns an instance of the “Environment.Place” class populated with data read in the database and corresponding to the location specified by the field “geoID”.

A representation of the class “Environment.Place” is provided in **Error! Reference source not found.**.

Table A - 11: Environment.Place cass

Environment.Place	
GeoID	String
Ground_Type_Turbulence	-
Latitude	Single
Longitude	-
Altitude	-
Find_Place_Coordinates(GeoID, Configuration)	Environment.Place

Monte Carlo Method

The class Monte_Carlo_Method contains the methods necessary for performing the Monte Carlo simulation for environmental parameters interpolation and component rating. The methodology adopted is aimed at allowing the algorithm to be fast but at the same time applicable easily to any model. The methodology followed is described here:

Firstly, an array of probability distributions of the model's input is generated. Since the array is a linear structure but model's inputs can be contained in different objects, a specific function for creating the array for each particular model is necessary. The array is then passed to the Monte Carlo simulation function which, for a defined number of times, calculates a single value for each parameter from the probability distributions and then run the specific model. Since the Monte Carlo simulation reason with arrays but the single model reason with objects, an intermediate function for converting the list of values to the objects used in the models is necessary. When a fixed number of simulations are performed, the variance of the results is analysed and the necessary number of simulation necessary for achieving the expected precision of the simulation is calculated. The previous steps are then repeated for the calculated number of times. Finally, the results of each simulation, stored in an array of single numbers are used for calculating the probability distribution of the Monte Carlo simulation returned as the output of the method.

In order to perform this simulation, the class "Monte_Carlo_Method" has eleven methods but no attributes. The methods of the class are:

- MCM_Simulation
- MCM_Cicle
- MCM_Generate_Variate
- MCM_Model_Output

- MCM_Random_Number_Generator
- MCM_Iteration_Number
- MCM_Populate_PDF
- MCM_Environment_Fun
- MCM_Component_Fun
- Prepare_Input_for_Environment_MCS
- Prepare_Input_for_Component_MCS

The method “MCM_Simulation” is the front-end method responsible for coordinating the whole Monte Carlo simulation. It returns an instance of the PDF.Beta class with the probability distribution of the results using as inputs an array of instances of the PDF.Beta class representing the probability distributions of the inputs, the name of the model with which to carry out the simulation, and the precision error accepted. The method “MCM_Simulation” calls the method “MCM_Cicle”, “MCM_Iteration_Number” and “MCM_Populate_PDF”. The method “MCM_Cicle” in turn calls the methods “MCM_Generate_Variate” and “MCM_Model_Output” and the method “MCM_Generate_Variate” calls the method “MCM_Random_Number_Generator”. In “MCM_Generate_Variate” each component of the input array of probability distributions is analysed for extracting a single value which is used to populate another array of probability distributions but with single values.

This is done because of the flexibility of the class PDF.Beta which can contain probability distributions but also strings or single values for representing textual and constant inputs. For this reason each element is firstly scanned to identify to which type it belongs (text, constant number, probability distribution), then it simply pass constant numbers and

textual values to the output. If the element is a probability distribution the method firstly calls the method “MCM_Random_Number_Generator” and then the method “PDF.Beta.Calculate_

_Inverse_CD” which inverts the cumulative probability distribution and returns the value of the variable corresponding to the selected probability. The method “MCM_Random_Number_Generator” makes use of the built-in visual basic function for returning random numbers. But this function, which is based on the processor’s clock, can return a different random number only every one millisecond. This was not acceptable considering the number of parameters that must be processed in every simulation, the number of simulations to carry out and the real-time nature of the application designed. For this reason the seed of the random number generator is created with a combination of the processor’s clock time and a number updated every time that a function is called and passed by the Configuration object present in every function and method.

These methods represent the core of the Monte Carlo simulation, but other ancillary functions have been created to facilitate and standardize the input-output process. The method “MCM_Populate_PDF” returns a structured instance of the PDF.Beta class populated according to the input. The particularity of this function is that it can recognise the type of input and to perform the necessary operations, in particular it automatically calculates Beta PDF parameters for a generic array of single values given as input. The methods “Prepare_Input_for_Environment_MCS” and “Prepare_Input_for_Component_MCS” are used for converting the objects containing information necessary to run the models into arrays of probability distributions. Their structure is influenced by the information structure available in the class “Thermal_State_Estimation”, from where the function “MCM_Simulation” is called. Similarly the methods “MCM_Environment_Fun” and

"MCM_Component_Fun" are used for converting the array resulting from the method "MCM_Generate_Variate" into the objects used by the respective models.

A representation of the class "Monte_Carlo_Method" is shown in **Error! Reference source not found.**.

Table A - 12: Monte_Carlo_Method class

Monte_Carlo_Method	
MCM_Simulation(Input_Array(), Model_Name, Err, Configuration)	PDF.Beta
MCM_Cicle(Input_Array(), Model_Name, Configuration)	Single
MCM_Generate_Variate(Input_Array(), Configuration)	PDF.Beta
MCM_Model_Output(Variate(), Model_Name, Configuration)	Single
MCM_Random_Number_Generator(Configuration)	-
MCM_Iteration_Number(Data_Array(), err, Configuration)	Integer
MCM_Populate_PDF(Name, Type, Value, Configuration)	PDF.Beta
MCM_Environment_Fun(Variate(), Configuration)	Single
MCM_Component_Fun(Variate(), Configuration)	-
Prepare_Input_for_Environment_MCS(Parameter_Name, Environment_Observation(), Place, Configuration)	PDF.Beta()
Prepare_Input_for_Component_MCS(Environment(), Component, Configuration)	-

Thermal State Estimation

The "TSE" class (TSE is an acronym for "Thermal State Estimation") contains the methods necessary for carrying out the thermal state estimation of power system networks. It has no attributes and nine methods. The nine circuits are:

- Network_Thermal_State_Estimation
- Circuit_Thermal_State_Estimation
- Component_Thermal_State_Estimation
- Get_Circuit_Data
- Get_Component_Data
- Get_Environmental_Data
- Calculate_Environmental_Parameters_PDF

- Calculate_Component_Rating_PDF
- Calculate_Circuit_Rating
- Add_PDF_Obj_to_PDF_Array

The methods “Network_Thermal_State_Estimation”, “Circuit_Thermal_State_Estimation”, and “Component_Thermal_State_Estimation” coordinate the other methods for estimating respectively the rating of each circuit in the network, the rating of a single circuit and the rating of a single component. The method “Network_Thermal_State_Estimation” calls iteratively the method “Circuit_Thermal_State_Estimation”. But the method “Circuit_Thermal_State_Estimation” does not calls the method “Component_Thermal_State_

_Estimation” but uses autonomously the same functions in order to reduce repetitive executions of the same calculations and to reduce circuit estimation computational-time. This is because the active distribution generation output controller developed in this research project in parallel with the thermal state estimator will ask selectively for the rating of potentially vulnerable circuits.

Both “Circuit_Thermal_State_Estimation” and “Component_Thermal_State_Estimation” return an instance of the PDF.Beta class corresponding to the rating of the circuit or the component specified at the time specified. Even if the algorithm could autonomously identify the current time and find the most updated environmental condition readings, it was decided to let the user to specify the time for two reasons:

- The user can specify a time in the past, in this way the algorithm would search in the database for historical values of the environmental parameters and the algorithm can be used for off-line analysis.

– The user can specify a time in the future, and the algorithm would provide a forecast of circuit rating. Rating forecast aroused during the research as an interesting possible further research field and for this reason the algorithm was developed for facilitating the introduction of this improvement. Currently if a date for what they do not exist records is given, the algorithm returns a conservative and static value for the rating, that can be considered valid also for the future.

Both methods make use of the methods “Get_Environmental_Data” and respectively of the methods “Get_Circuit_Data” and “Get_Component_Data”. The first method returns an array of instances of the class “PDF.Beta” corresponding to the information necessary to perform the environmental condition estimation with the Monte Carlo method. This function is called only one time in the method “Circuit_Thermal_State_Estimation” and its output is used for the environment state estimation in the position of each component. This is done in order to reduce the number of queries to the database that can result particularly expensive in time. The other two methods return an instance respectively of the class “Component.Circuit” and “Component.Element”, used for the component rating estimation.

The method “Calculate_Environmental_Parameters_PDF” returns an array of instances of the class “PDF.Beta” that is used for component rating estimation and has already the structure necessary for the Monte Carlo simulation. The method “Calculate_Circuit_Rating” and "Calculate_Component_Rating” manage the different functions necessary for estimating circuit and component thermal rating respectively. In the method “Calculate_Circuit_Rating” in particular, the array of probability distributions of the components of the circuit is scanned for calculating the minimum rating corresponding to each probability. The results are then summarised in a final probability distribution representative of the rating of the whole circuit.

Finally the method “Add_PDF_Obj_to_PDF_Array” is simply used for facilitating the creation of array of probability distributions, a structure widely used in the algorithm.

A representation of the class “TSE” is reported in **Error! Reference source not found.**.

Table A - 13: Thermal State Estimation class

TSE	
Network_Thermal_State_Estimation(Name, Time, Configuration)	PDF.Beta()
Circuit_Thermal_State_Estimation(Name, Time, Configuration)	PDF.Beta
Component_Thermal_State_Estimation(Name, Time, Configuration)	-
Get_Circuit_Data(Name, Configuration)	Component.Circuit
Get_Component_Data(Name, Configuration)	Component.Element
Get_Environmental_Data(Time, Configuration)	PDF.Beta()
Calculate_Environmental_Parameters_PDF(Environment(),	PDF.Beta()
place, Configuration)	PDF.Beta
Calculate_Component_Rating_PDF(Environment(),Component Configuration)	PDF.Beta
Calculate_Circuit_Rating(Component_Rating(), Configuration)	PDF.Beta
Add_PDF_Obj_to_PDF_Array(PDF_Obj, Array(), Configuration)	PDF.Beta()

Probability Density Function

The class “PDF” (PDF is an acronym for Probability Density Function) is designed for describing data probability density function structures, with the necessary parameters and the functions necessary for creating and extracting the desired data from this non-standard type of data. Since probability distributions are widely used in the state estimation this class has a particular importance in the structure of the algorithm. The class is conceived as a container of sub classes representing different probability distributions, as shown in **Error! Reference source not found.**.

During the development of the program, the use of a single, well chosen probability distribution proved to give acceptable results and the development of other distribution was

suspended. The structure of the class was not modified and the development of new distribution can be seen as a possible further development of the work with low priority.

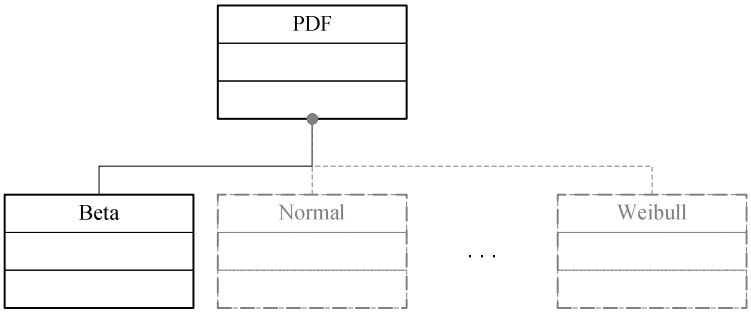

Figure A - 3: PDF class static structure

As said above, the algorithm uses exclusively the Beta probability distribution, encoded in the class “PDF.Beta”. The class has 10 attributes and five methods. Since only the Beta PDF is used, this class is conceived for describing also different types of data such as string and constant values. The ten attributes are:

- Name
- Type
- String_Value
- Min
- Max
- Alpha
- Beta
- Mean
- Variance
- Static_Value

The attribute “Name” is a string used for storing the name of the variable described by the PDF. The attribute “Type” is a string and can have three values: “Name”, “Constant” and “Range”, used respectively for describing textual variables, single numbers or probability distributions. The attribute “String_Value” is used for the textual values if the attribute “Type” value is “Name”, otherwise, this field is empty. The attribute “Static_Value” is used for storing the value of the variable when the attribute “Type” value is “Constant”, otherwise this field is empty. The attributes “Min”, “Max”, Mean” and “Variance” along with “Alpha” and “Beta” are used for storing information regarding the time series corresponding to the probability distribution and the shape parameters of the distribution. These fields are empty if the value of the attribute “Type” is not “Range”.

The five methods of the class are:

- Estimate_BetaPDF_Parameters
- Calculate_PD
- Calculate_Beta_Function
- Calculate_CD
- Calculate_Inverse_CD

The method “Estimate_BetaPDF_Parameters” uses an array of single numbers as input for calculating the parameters of the Beta PDF that are used to populate an instance of the “PDF.Beta” class returned as output. The method “Calculate_PD” calculate the value of the probability density of a particular PDF corresponding to a given parameter value, calling the method “Calculate_Beta_Function” during the process. The method “Calculate_CD” return the cumulative probability of a probability distribution corresponding to a given parameter value. Finally the method “Calculate_Inverse_CD” returns the value of the variable corresponding to the probability given as input calling iteratively the method “Calculate_CD”.

A summary of the class “PDF.Beta” is shown in Table A - 14.

Table A - 14: PDF.Beta class

PDF.Beta	
Name	String
Type	-
String_Value	-
Min	Single
Max	-
Alpha	-
Beta	-
Mean	-
Variance	-
Static_Value	-
Estimate_BetaPDF_Parameters(Data_Array())	PDF.Beta
Calculate_PD(Variable, PDF)	Single
Calculate_Beta_Function(Variable, PDF)	-
Calculate_CD(Variable, PDF)	-
Calculate_Inverse_CD(Probability, PDF)	-

Auxiliary Procedures

The class “Auxiliary_Proceures” has been designed for containing classes and methods used in the algorithm for data management but not necessary related to the thermal state estimation. This class is a container of two sub classes: “Auxiliary_Proceures.Configuration” and “Auxiliary_Procedures.Manage_DB”. The first one define the “Configuration” class as a list of parameters used in several part of the algorithm through an instance of this class created at the beginning of the simulation and passed in every function. The second one contains methods for opening, closing and writing into databases.

Originally also the function of reading into databases was present in this class, but in order to reduce component thermal state estimation computational-time, very specific methods for reading component properties and environmental parameters have been designed

and included in the most appropriate class. A visual representation of the class “Auxiliary_Procedures” and its sub-classes is shown in Figure A - 4.

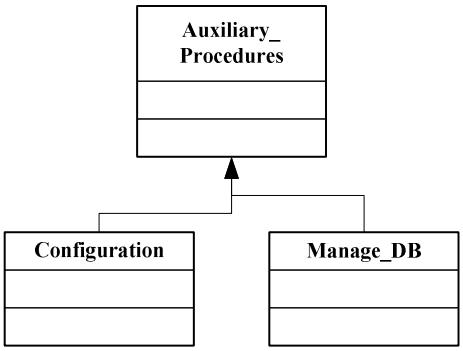

Figure A - 4: Auxiliary_Procedures class static structure

The class “Auxilary_Procedures.Configuration” is used for defining an object which, present in every step of the algorithm, allows basic information to be accessible in any point of the algorithm. The presence of this object is considered particularly useful in phases of software maintenance or upgrading, since would allow an easy method for testing new methods or procedures requiring different inputs without modifying completely the data flow structure of the whole algorithm. It is recommended to remove additional attributes in the class after the testing period when not strictly necessary in order to invalidate the future possibility of software improvements. The class has fourteen attributes and one method. The fourteen attributes are:

- Component_Connection
- Environment_Connection
- Geo_DB_Connection
- Output_Connection
- Errors_Connection

- Message_String
- Altitude_Ref_for_WS_Correction
- Alternative_WS
- Alternative_WD
- Alternative_TA
- Alternative_SR
- Alternative_TS
- Alternative_STR
- Count

The attributes “Component_Connection”, “Environment_Connection”, “Geo_DB_Connection”, “Output_Connection” and “Errors_Connection” are connections to the databases used in by the algorithm. The attribute “Message_String” is a string and is used for passing error messages between different methods, in particular to the method “Auxiliary_Class.Manage_DB.Write_Errors”. The attribute “Altitude_for_WS_Correction” contains the value for the reference height used for wind speed correction due to soil roughness. The attributes “Alternative_WS”, “Alternative_WD”, “Alternative_TA”, “Alternative_SR”, “Alternative_TS” and “Alternative_STR” are used for storing the emergency values for wind speed, wind direction, air temperature, solar radiation, soil temperature and soil thermal resistivity to be used in case of errors in data reading or calculations. Finally the attribute “Count” is an integer that is updated every time that a function is called and is used for improving the quality of the random number generator. The only method of the class is:

- Configuration

This method returns an instance of the class “Auxiliary_Procedures.Configuration” populated with the necessary parameters. In particular it calls the method “Auxiliary_Procedures.Manage_DB.Manage_DB” in order to open the connection with the databases and to store them in the attributes of the instance.

A representation of the class “Auxiliary_Procedures.Configuration” is shown in **Error! Reference source not found.**.

Table A - 15: Auxiliary_Procedures.Configuration class

Auxiliary_Procedures.Configuration	
Component_Connection	OleDbConnection
Environment_Connection	-
Geo_DB_Connection	-
Output_Connection	-
Errors_Connection	-
Message_String	String
Altitude_Ref_for_WS_Correction	Single
Alternative_WS	-
Alternative_WD	-
Alternative_TA	-
Alternative_SR	-
Alternative_TS	-
Alternative_STR	-
Count	Integer
Configuration(Action, Configuration)	Auxiliary_Procedures_ .Configuration

The class “Auxiliary_Procedures.Manage_DB” is contains the methods necessary for opening, closing and writing specific output into particular databases. The class has no attribute and three methods:

- Manage_DB
- Write_Ratings_PDF
- Write_Errors

The method “Manage_DB” open and closes the database specified in the input “DB_Name” according to the action specified in the input “DB_Action”. If the action is “Open” then the method returns the open connection and if the action is “Close” then the method closes the connection given as input and returns a closed connection. The method “Write_Ratings_PDF” is a subroutine specialised in writing in an output database designed for storing simulation results and used in the algorithm validation phase. This method was maintained because of its potential utility when using the algorithm as an off-line planning tool. The method “Write_Errors” is specialised in writing messages in the database “Errors” created for storing a log with the description of the error every time that an error arises in the running of the program. This method was created during the algorithm development phase, but it was not removed for its utility phases of software maintenance or improvement. A representation of the class “Auxiliary_Procedures.Manage_DB” is shown in **Error! Reference source not found.**.

Table A - 16: Auxiliary_Procedures.Manage_DB class

Auxiliary_Procedures.Manage_DB	
Manage_DB(DB_Name, DB_Action, Connection) Write_Ratings_PDF(Time, PDF, Configuration) Write_Errors(Description, Configuration)	OleDbConnection

Web Service

The role of the Web Service is to create a standard interface between the thermal state estimation algorithm and the distribute generator output controller. It allows also the algorithm to be installed on a server and to be consulted by remote applications and websites. The Web Service developed has two methods:

- NMS_Data

– TSE_Circuit_Rating_Single_String

The method “NMS_Data” was build for facilitating the distributed generation output controlle access to the MySQL database with real-time electrical readings. This algorithm in fact has no direct access to the database, but relies on this web service. The method returns a string with the value of the requested parameter value at the time requested. Both inputs are passed through textual values, for facilitating data tansfer between potentially different algorithm, programming languages and operating systems. The method “TSE_Circuit_Rating_Single_String” returns a sting with a single value corresponding to the real-time circuit rating relative to a selected probability, calculated by the thermal state estimation algorithm. Currelty, in anticipation of the distributed generation real-time output controller open and closed loop tests, the minimum circuit rating is returned. Also in this web method, inputs and outputs are excanged in the format of strings. A representation of the web service “Service” is shown in Table A - 17.

Table A - 17: Web service class

Service	
NMS_Data(Time, Parameter)	String
TSE_Circuit_Rating_Single_String(Time, Circuit_Name)	-

A module was created for demonstrating the possibility of accessing remotely to the thermal state estimation algorithm, arousing consortium partners’ interest in the technology. The module was installed on a server of Imass, a consortium partner, and allowed other members to consult the algorithm from their offices, building confidence for the practical implementation of this technology in practical industrial applications although it is based on meteorological historical data.

Databases

The table “Component_General” contains the parameters necessary for populating the attributes of the class “Component.General_Parameters” and can be accessed using the field “Component_Name” as key, although an indipendent numerical key is provided. The tables “Components_OHL” and “Components_OHL_Conductor” are used for storing data relative to the particular overhead line and to the conductor respectively and they can be accessed using the fields “Name” and “Code” respectively. The information contained in these two tables is used for populating the attributes of the class “Component.OHL”.

The tables “Components_UGC” and “Components_UGC_Cable” are used for storing data relative to the particular electric cable and to the conductor respectively and they can be accessed using the fields “Name” and “Code”. The information contained in these two tables is used for populating the attributes of the class “Component.UGC”. finally the tables “Components_PTR” and “Components_PTR_Transformer” are used for storing data relative to the particular transformer and to the transformer type respectively and they can be accessed using the fields “Name” and “Code”. The information contained in these two tables is used for populating the attributes of the class “Component.PTR”.

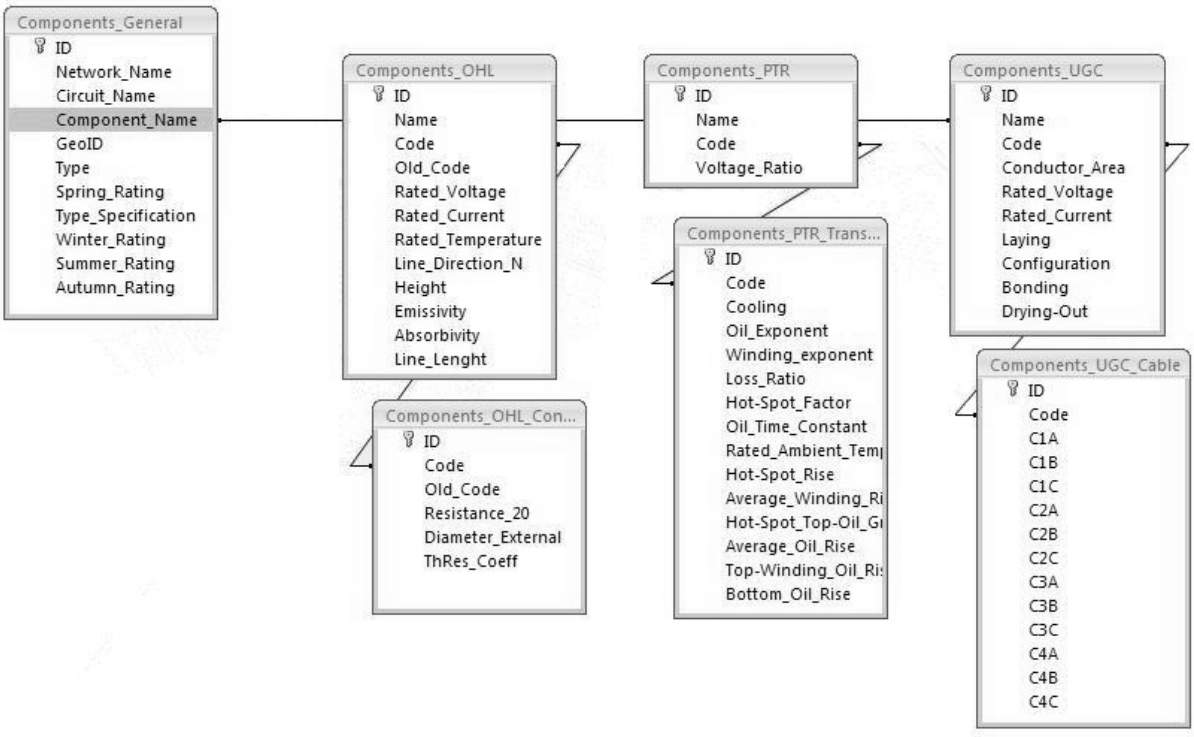

Figure A - 5: Database_Components tables and relations diagram

Historical environmental condition readings are stored in the “Environment” database. As said before, real-time environmental conditions are retrieved from an on-line MySQL database, but this is relative to a part of the project not yet ultimate, therefore here the first MS Access database is described. The database “Environment” has two and plus tables:

- Info_WS
- WS_(Name,i)

A diagram of the relations between the tables of the database “Environment” is shown in **Error! Reference source not found.**.

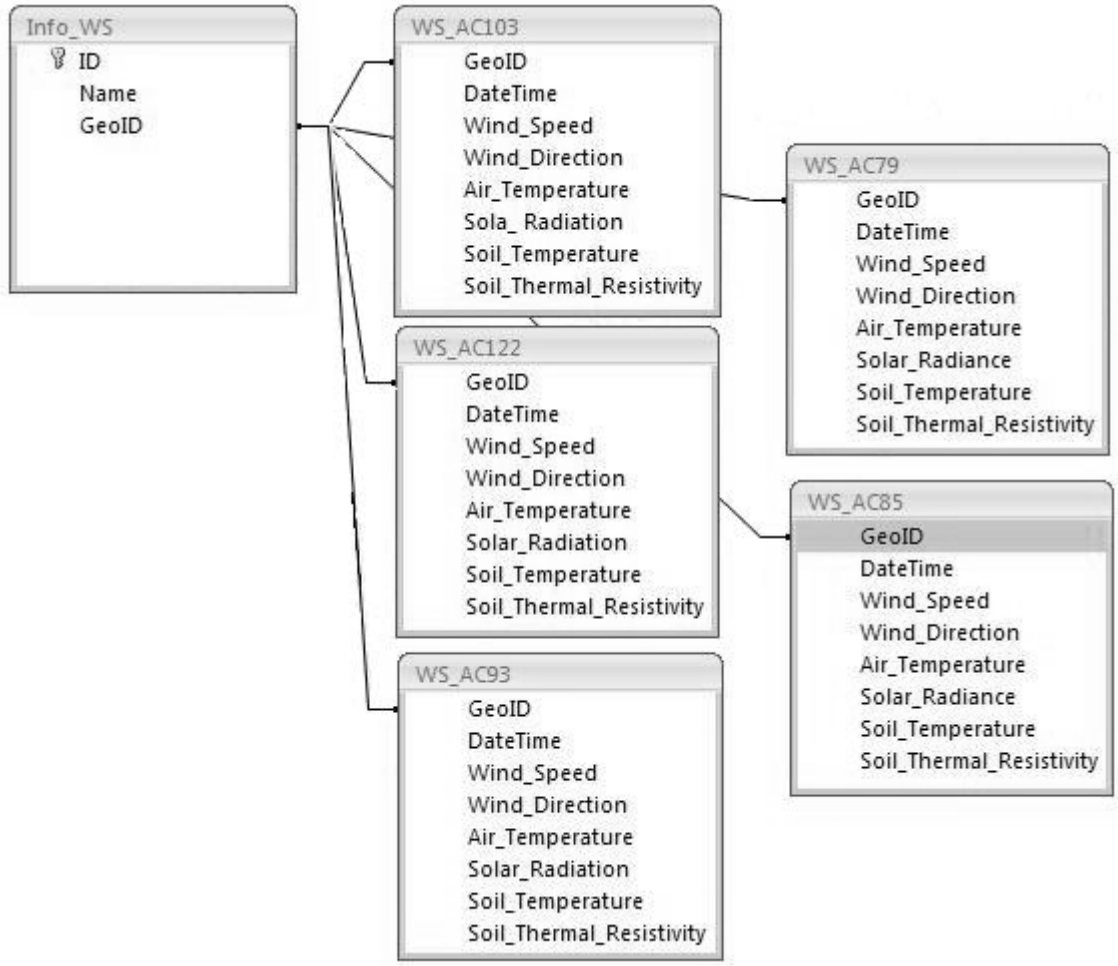

Figure A - 6: Database "Environment" tables and relations diagram

The table “Info_WS” contains a list of the meteorological stations installed in the area, whilst the tables “WS_(Name,i)”, one for each meteorological station, contains the readings of each environmental condition, along with a timestamp for the period when they have been recorded.

Geographical based information are stored in a separate database, currently a MS Access database, but in future it is expected to substitute it with the database of a professional GIS program. The table, called “Coordinates” is shown in Figure A - 7

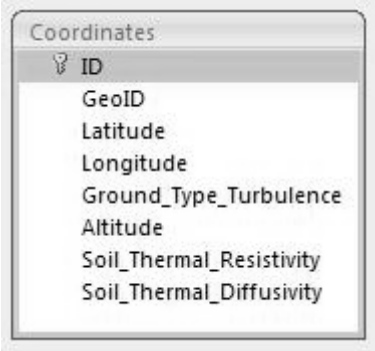

Figure A - 7: Database "Geo_DB" table "Coordinates" diagram

As said before other two databases have been created for software maintenance and validation purposes: the database “Errors” and the database “Output”. The database “Errors” has a single table “Errors” used for storing errors logs generated by the algorithm. Each entry is characterised by a timestamp and by a string, mentioning the function where the error appeared, the type of error and the decision taken by the algorithm. The most common error recorded is the lack of data in the “Environment” database for a particular time, error that is followed by the forced assumption of conservative static values for the corresponding environmental parameter. A visual description of the table “Errors” of the database “Errors” is shown in Figure A - 8.

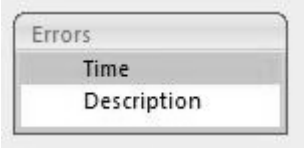

Figure A - 8: Database "Errors", table "Errors" diagram

The last database created for the algorithm validation process is the database “Output”, where the ratings for each component of the network can be stored for each timestamp in the table “Ratings_PDF”. This table has a field for storing the timestamp of the simulated output,

and all the fields necessary for storing the information contained in the attributes of the class “PDF.Beta”. A visual description of the table “Ratings_PDF” of the database “Output” is shown in Figure A - 9.

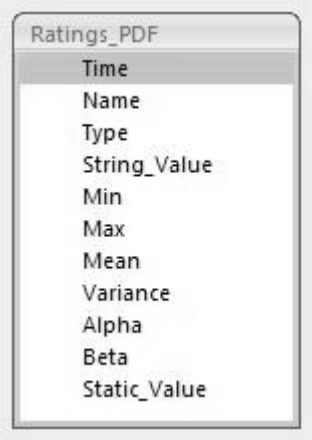

Figure A - 9: Database "Output", table "Ratings_PDF" diagram

Data Flow

Firstly, it calls the methods “TSE.Get_Circuit_Data”, for loading circuit static data from the “Components” database in an instance of the “Component.Circuit” class and “TSE.Get_Environmental_Data”, for loading the readings of environmental conditions in an array of probability density functions objects. After this, the method “TSE.Circuit_Thermal_State_Estimation” calls iteratively the method “TSE.Calculate_Environmental_Parameters_PDF”, “TSE.Calculate_Component_Rating_

_PDF” and “PDF.Beta.Add_PDF_Obj_to_Array” for each component in the circuit. These methods perform respectively: the estimation of environmental conditions in the component location, the estimation of the component real-time rating, the insertion of the real-time component rating probability distribution in an array.

Finally, the method “TSE.Calculate_Circuit_Rating” returns the probability distribution for the whole circuit real-time rating. This object is returned in turn by the method “TSE.Circuit_Thermal_State_Estimation” to the web method, which calculates the rating value corresponding to a selected probability, closes the connections with the databases and returns the single value as output.

The first two methods are now analysed in detail. The method “TSE.Get_Circuit_Data”, creates a list of the names of the components belonging to the circuit reading in the database “Components” with the circuit name given as input as a key. Then it calls iteratively the method “Component.Circuit.Load_Data” which reads component data into the database “Components” and populates with the correct values an instance of the class “Component.Element”. The method “TSE.Get_Circuit_Data” calls the method “Environment.Search_Data” which finds, in the database “Enironment”, name nd locations of the weather stations installed in the area. Then for each weather station and for each parameter, creates a PDF object populated with the values read in the “Environment” database, using the methods “Environment.Find_Environmental_Readings”, “Montecarlo_Method.MCM_Populate_PDF” and “PDF.Beta.Add_PDF_Obj_to_Array”.

The methods “TSE.Calculate_Environmental_Parameters_PDF” and “TSE.Calculate_

_Component_Rating_PDF” have a similar structure, but are specialised respectively in environmental condition estimation and component rating estimation.

The method “TSE.Calculate_Environmental_Parameters_PDF” calls iteratively for each environmental condition the methods “Montecarlo_Method.Prepare_Input_for_Environment_MCS”, “Montecarlo_Method.MCM_

_Simulation” and “PDF.Beta.Add_PDF_Obj_to_Array”. The array of PDF object generated is given as input to the method “TSE.Calculate_Component_Rating_PDF” which

calls in turn the methods “Montecarlo_Method.Prepare_Input_for_Component_MCS”, and “Montecarlo_Method..MCM_Simulation”. The method “Montecarlo_Method.Prepare_Input_ _for_Environment__MCS” and “Montecarlo_Method.Prepare_Input_for_Component_MCS” transform their inputs in a list of probability distributions that can be used directly by the method “Montecarlo_Method.MCM_Simulation”.

The method “Montecarlo_Method.MCM_Simulation” supervises the Monte Carlo simulation with the particular model selected and the inputs given. Firstly, it calls N times the method “Montecarlo_Method.MCM_Cicle”, then, with the method “Montecarlo_Method.MCM_Iteration_Number” verifies if the number of iterations N is acceptable for the precision requested; if the condition if verified the method returns the solution of the “Montecarlo_Method.MCM_Cicle”, otherwise it calls the method “Montecarlo_Method.MCM_Cicle” until the condition is not verified. The method “Montecarlo_Method.MCM_Cicle” calls in sequence the methods “Montecarlo_Method.MCM_Generate_Variate” and “Montecarlo_Method.MCM_ _Model_Output”.

The first method, transforms the list of probability distribution get as input in a list of constant parameters, whilst the second calls the appropriate method according to the model name given as input: for environmental parameters it calls the method “Montecarlo_Method.MCM_Environment_Fun” and for a component, it calls the method “Montecarlo_Method.MCM_Component_Fun”. The methods “Montecarlo_Method.MCM_ _Environment_Fun” and “Montecarlo_Method.MCM__Component_Fun” call respectively the methods “Environment.Environment_Parameter__Estimation” and

“Component.Element_Calculate_Rating_MVA” after converting the list of constant values given as input in the structured objects necessary for the models.

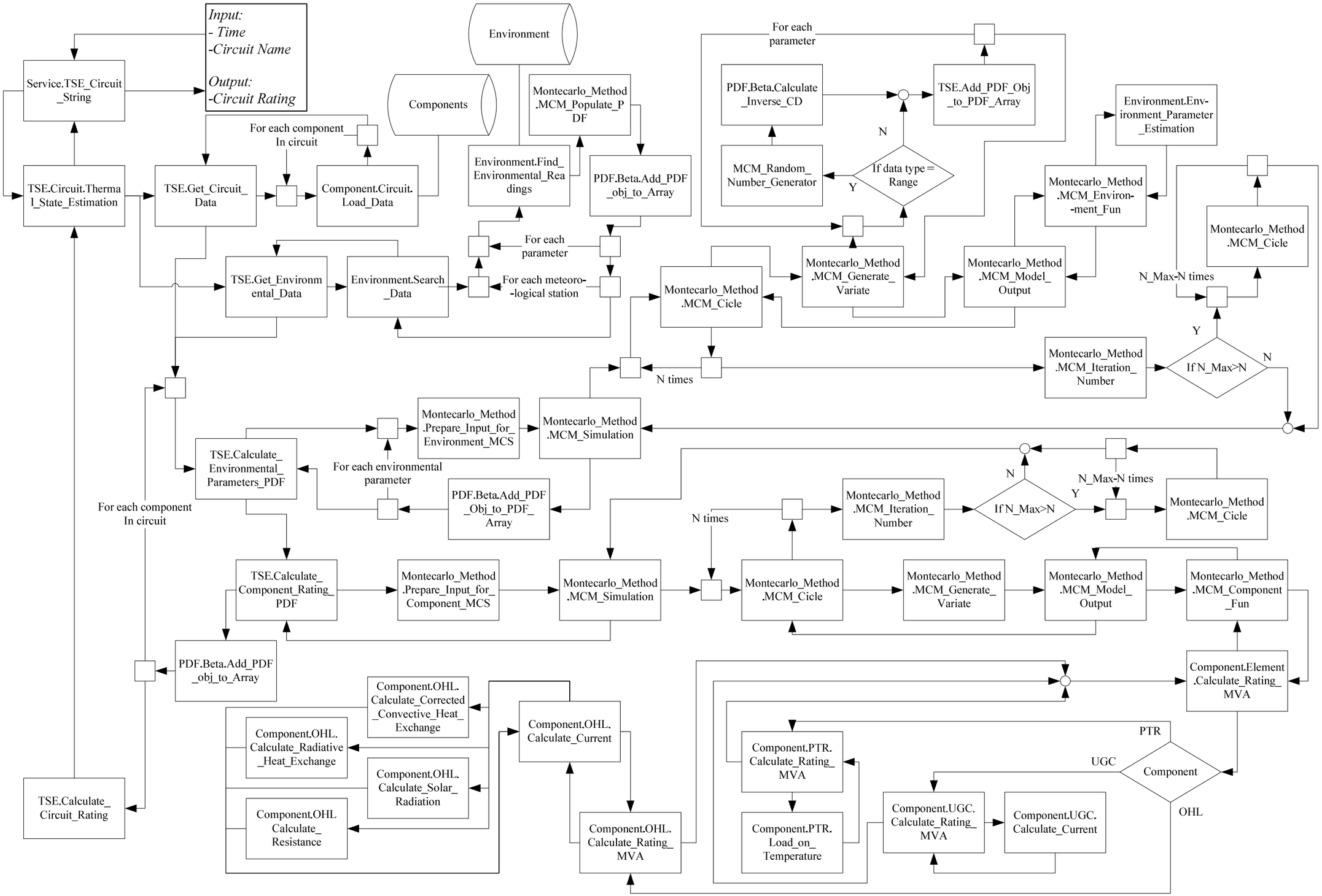

Figure A - 10: Circuit real-time rating estimation functions and data flow

Publications

The following articles were selected among the publications listed in Section 1.7 and are reproduced in the following pages.

A. Michiorri, P. C. Taylor and S. C. E. Jupe, “Overhead line real-time rating estimation algorithm: description and validation”, *Proc. IMechE Part A: J. Power and Energy*, vol. 224(3), pp. 293-304, 2010;

A. Michiorri, P. C. Taylor, S. C. E. Jupe and C. J. Berry, “Investigation into the effect of environmental conditions on power system ratings”, *Proc. IMechE Part A: J. Power and Energy*, vol. 277, no. A7, pp. 743-757, Nov., 2009;

A. Michiorri, P. C. Taylor, “Forecasting Real-time Ratings for Distribution Networks Using Weather Forecast Data”, CIRED, 2009, Prague.

S. C. E. Jupe, P. C. Taylor, A. Michiorri, and C. J. Berry, “An evaluation of distributed generation constrained connection managers,” in Proc. 6th Mediterranean Conference on Generation, Transmission and Distribution, Thessaloniki, Greece, 2008

Overhead line real-time rating estimation algorithm: description and validation

A Michiorri*, **P C Taylor,** and **S C E Jupe**
School of Engineering, Durham University, Durham, UK

The manuscript was received on 23 July 2009 and was accepted after revision for publication on 21 October 2009.

DOI: 10.1243/09576509JPE859

Abstract: This article describes research that aims to realize a real-time rating (RTR) system for power system components. The RTR technology is regarded with interest due to its potential to unlock network power transfer capacity, improve power flow congestion management flexibility, and facilitate the connection of distributed generation. The solution described in this work involves the use of a limited number of meteorological stations and a series of analytical models for estimating component ratings. The effect of data uncertainty is taken into account by an estimation algorithm based on the Monte Carlo method. Estimations of conductor temperature and environmental conditions have been validated against measured data in five different network locations. Average errors of −2.2, −1.9, −1.2, −1.9, and 1.4 °C were found for the five different network locations over a period of 71 days when comparing estimates to measured results. Results analysis identified that the models used were the main source of error. The estimation of wind direction and solar radiation was the most sensitive to errors in the models. Therefore, suggestions are made regarding the improvement of these models and the RTR estimation system.

Keywords: overhead line, real-time, rating, Monte Carlo, validation

1 INTRODUCTION

This article describes a real-time rating (RTR) estimation algorithm for overhead lines developed at Durham University and its validation against field data. The solution described in this work involves the use of a limited number of meteorological stations and a series of analytical models for estimating component ratings. The research builds on previous work [**1**], which quantified the influence of environmental conditions on power system ratings and identified overhead lines as the power system component with the greatest potential for RTR exploitation. Estimated values for conductor temperature and for the environmental conditions influencing component rating are compared with measured values and the estimation error is then analysed. Environmental conditions were assessed by processing the data monitored at five meteorological station locations. The number and location of the meteorological station installations were driven by physical constraints of the particular site. The concept behind RTR is that power system component ratings are influenced by environmental conditions such as wind speed, wind direction, air temperature, and solar radiation and are therefore continuously varying. Real-time monitoring of component temperature or environmental conditions allows the exploitation of additional headroom. This headroom is currently neglected by the prevalent use of conservative static ratings based on seasonal worst case scenarios. For the purpose of this research, RTRs are defined as a time-variant rating that can be practically exploited without damaging components or reducing their life expectancy. Actual measurements of environmental conditions are used as the input to steady-state thermal models. In order to calculate and exploit the RTR, it is assumed that a limited number of local environmental condition measurements are available and that there are no outages (planned or unplanned) present within the electrical power system. Short-term transients, taking into account the thermal capacitance of power system components, are not included within the RTR assessment. It is felt that this would not materially affect the GWh/annum throughput of energy within the electrical power system. The research described

* *Corresponding author: School of Engineering, Durham University, South Road, Durham DH1 3LE, UK.*
email: andrea.michiorri@durham.ac.uk

in this article forms part of a UK Government partly funded project [**2**] that aims to develop and deploy an online power output controller for distributed generation (DG) based on component RTRs. In this project, a DG power output controller compares RTRs with network power flows and produces set points that are fed back to the DG operator for implementation. The research consortium includes ScottishPower EnergyNetworks, AREVA T&D, PB Power, Imass, and Durham University. The article is structured in the following way: section 2 provides an overview of relevant work. In section 3, the estimation algorithm used for component RTRs is described. Section 4 describes the validation of the algorithm estimates against measured data, and in section 5, conclusions are drawn from the work carried out and the scope for further work is identified.

2 RELEVANT WORK

Currently, power system component ratings are based on conservative assumptions based on historical environmental conditions, as described in references [**3**] and [**4**]. A similar approach is described in reference [**5**], where a methodology for calculating component ratings considering the combination of historical environmental conditions, loads and expected costs related to thermal overloads is adopted. This approach is challenged in research showing the advantages for distribution network operators (DNOs) arising from the adoption of an RTR system. A quantitative estimation of the possible headroom unlocked by the adoption of RTRs for overhead lines, electric cables, and power transformers is presented in reference [**1**] and overhead lines are identified as the component type with the highest possible gains. The effect of environmental condition variability on the rating of power transformers is studied in reference [**6**], where it is shown that the rating of transformers positioned at the base of wind turbines may at present be oversized by up to 20 per cent. A similar study described in reference [**7**] compares the power flow to the conductor RTR in an overhead line connecting a wind farm. In this research, it was highlighted that high-power flows resulting from wind generation at high wind speeds could be accommodated since the same wind speed has a positive effect on the line cooling. This observation makes the adoption of RTR systems relevant in applications where strong correlations exist between the cooling effect of environmental conditions and electrical power flow transfers. An application of RTR for wind farm connections in the UK is described in reference [**8**], where particular attention is given to the necessity to combine the RTR system with devices able to manage the non-firm connection of DG. The application of an RTR system for the Spanish transmission grid is described in reference [**9**]. Here a minimal number of meteorological stations are used to gather real-time data. These data are then processed using a meteorological model based on the Wind Atlas Analysis and Application Program (WAsP) [**10**], taking into account the effect of obstacles and ground roughness, and finally the rating is calculated. The experience of the Dutch companies NUON and KEMA on temperature monitoring of overhead lines, electric cables, and power transformers is described in reference [**11**]. Research on the area of state estimation techniques for component rating proved the necessity for reliable and accurate environmental condition monitoring in order to obtain accurate component rating estimates. In references [**12**] to [**14**], the influence of component thermal model input errors on the accuracy of RTR systems is studied. The application of different state estimation techniques, such as affine arithmetic, interval arithmetic, and Monte Carlo simulations, was studied for overhead lines, electric cables, and power transformers. Errors of up to ± 20 per cent for an operating point of 75 °C, ± 29 per cent for an operating point of 60 °C and ± 15 per cent for an operating point of 65 °C were found when estimating the operating temperature of overhead lines, electric cables, and power transformers, respectively. In order to reduce this error, the opportunity to use an expert system for enhancing rating estimation is explored in reference [**15**], where electric cable ratings estimated with physical models are refined with an expert system identifying the most suitable model according to past experience. In reference [**16**], a system combining distributed thermal sensing, physical models, and learning algorithm is used for estimating enhanced line rating forecasts. Another expert system informed by short-term RTRs is described in reference [**17**] along with its indoor and outdoor test and its possible application during outages. The research presented in this article adds to the work described above by describing the principles behind a different RTR system and its validation against field data. The proposed solution makes use of sophisticated estimation algorithms, which have threefold benefits: first, the requirements for a large number of equipment installations in order to monitor large network areas are reduced. Second, the capital cost of the system is reduced. Third, the estimation algorithm offers a robust solution, which maintains operational security in the case of measurement or communication failures. Furthermore, the rigorous test carried out on different components of the same network for an extended period provides a detailed description of system behaviour under different operational conditions.

3 RATING ESTIMATION ALGORITHM

The estimation of the RTR of power system components is a problem characterized by non-linear models

and input uncertainty. Therefore the Monte Carlo method was considered the most appropriate solution both for the estimation of environmental conditions in each component location and for the estimation of component rating.

3.1 Analytical models

In these sections, the models used for calculating overhead line ratings and environmental condition values are described. For safe network operation, the line design operating temperature must not be exceeded in order to avoid damaging the component. For overhead lines in particular, a temperature rise leads to a reduction in conductor tension and to an increase in the sag. Typical values for maximum conductor temperature are between 50 and 90 °C. Component temperature is not a constant value but depends upon the energy balance between the heat produced inside the component and the heat exchange on its surface. However, the heat exchange is mainly influenced by the temperature difference between the cable and the environment and by other external factors such as wind speed or solar radiation. By considering the heat dissipated by the Joule effect (I^2R), the heat exchanged by convection (q_c) and radiation (q_r), and the solar radiation (q_s), the energy balance for an overhead line conductor is described in equation (1) taken from [**18**]

$$I^2R + q_s = q_c + q_r \tag{1}$$

The heat exchange terms in equation (1) are calculated according to equations (2), (3), and (4)

$$q_s[\mathrm{W/m}] = \alpha_{abs}\, S_r\, D_c \tag{2}$$

$$q_r[\mathrm{W/m}] = \alpha_{em}\, \sigma_{SB}\, [T_c^4 - T_a^4]\, \pi\, D_c \tag{3}$$

$$q_c[\mathrm{W/m}] = \frac{Nu\,(T_c - T_a)}{D_c\, \rho\, th_a} \tag{4}$$

The Nusselt number (Nu) in equation (4) is calculated according to equation (5), where the Reynolds number (Re) and the direction correction coefficient (K_{dir}) are calculated as in equations (6) and (7) taken from [**19**]

$$Nu = (0.65\, Re^{0.2} + 0.23\, Re^{0.61})\, K_{dir} \tag{5}$$

$$Re = 1.644 \times 10^9\, Ws\, D_c \left(\frac{T_c + T_a}{2}\right)^{-1.78} \tag{6}$$

$$K_{dir} = K_{dir-1} + K_{dir-2} \sin^{K_{dir-3}}(\delta) \tag{7}$$

Environmental condition values are read in real time at selected locations in the network area and are used for estimating environmental conditions in every component location. For this purpose, the inverse distance interpolation technique [**20**] described in equation (8) is used. At each point (k) in the geographical area, the value of the parameter (w) representing the environmental condition can be estimated as a weighted average of the parameter values known at i points. The weighting factor is a function of the distance between the points.

$$w_k = \frac{\Sigma_i[(1/l_{i,k}^2)w_i]}{\Sigma_i(1/l_{i,k}^2)} \tag{8}$$

This technique is used for the estimation of wind speed (Ws), wind direction (Wd), air temperature (Ta) and solar radiation (Sr). For wind speed estimation, the ground roughness effect is taken into account and an additional correction, based on the use of the wind profile power law [**21**] and described in equation (9), is used

$$\mathrm{Ws_c} = \mathrm{Ws_a} \left(\frac{h_{ref}}{h_a}\right)^{\mathrm{Kshear_a}} \left(\frac{h_c}{h_{ref}}\right)^{\mathrm{Kshear_c}} \tag{9}$$

The wind speed at two different heights is linked with the ground roughness through the exponent Kshear. Values of Kshear for different ground types may be found in reference [**1**].

Using equation (9), the anemometer wind speed ($\mathrm{Ws_a}$) at the meteorological station height (h_a) is extrapolated to a reference height (h_{ref}), in this case 100 m, to remove ground roughness dependence represented by the parameter Kshear. The values from different anemometer locations may then be interpolated, using equation (8), to provide a wind speed estimate at the reference height for a particular geographical location. The ground roughness at this location is then taken into account through the coefficient $\mathrm{Kshear_c}$ along with the conductor height (h_c) in equation (9) to estimate the wind speed ($\mathrm{Ws_c}$) across the conductor. Regarding wind direction, equation (8) can be used for wind direction interpolation although it can provide erroneous values for particular input datasets, in particular when multiple meteorological stations record concurrent values of the wind direction from north–north–west (NNW) and north–north–east (NNE). In this case, the interpolation may produce distorted results because averaging wind direction values in the region of NNW to N (337.5°–360°) together with values in the region of N to NNE (0°–22.5°) produces wind direction estimates in the regions SSW to SSE (157.5°–202.5°), which represents a 180° phase shift between the real and calculated wind directions. This does not render equation (8) inappropriate to use because, due to the angular nature of the wind direction, a phase shift in wind-conductor angle of 180° has the same cooling effect as the wind-conductor angle without the phase shift. Therefore, an error of 200° in the wind direction has the same effect on conductor temperature calculation as an error of ±20°.

3.2 The Monte Carlo method

The Monte Carlo method consists of an iterative evaluation of results of the deterministic models relative to randomly selected input values [**22**]. These inputs are randomly generated from probability density functions (PDF) describing parameter probabilistic structure and the results generated by the deterministic model in different trials can be represented in turn by probability distributions. In Fig. 1, a visual representation of the Monte Carlo-based solution used in this work is given. The simulation starts collecting parameter readings in a period dt (a). For each parameter (x, y, z), a PDF is calculated from the measured data (b) as described in section 3.2.1 and the cumulative density function (CDF) is calculated by integration from the PDF. At this point (c), a random value for the probability is generated for each parameter, and inverting the CDF, the corresponding parameter value is selected, as described in section 3.2.2. The random variates generated are then used (d) for calculating the output of a model. The different models used in this research are described in section 3.1. The two steps (c) and (d) are N repeated times, where N is calculated as described in section 3.2.3 and the model's results are stored (e) for further analysis. Finally, a PDF for approximating the output is generated (f) from the N simulation results as in step (b). In an RTR system deployment, the parameter w could be the wind speed across an overhead line conductor and the parameters x, y, and z could be the wind speed as measured by three meteorological stations. Alternatively, the parameter w could be the conductor temperature and the parameters x, y, and z could be the wind speed, wind direction, and air temperature in the conductor location. For conductor temperature estimation, the state estimation algorithm is used in two ways: first, for estimating environmental condition values in the conductor location from environmental condition measurements at the meteorological stations, and Second, for estimating conductor temperature from the estimated environmental conditions local to the conductor.

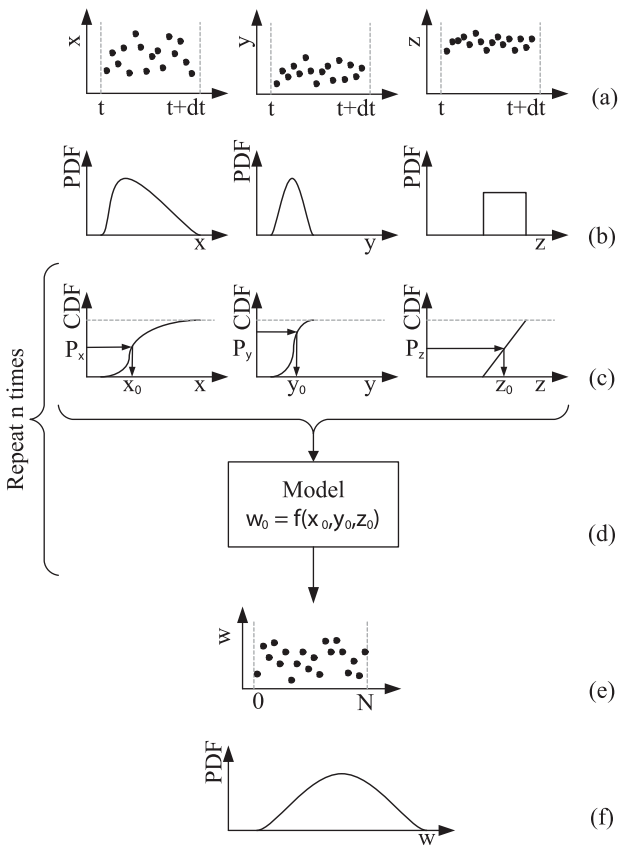

Fig. 1 Monte Carlo method example

3.2.1 *Probability density function*

The PDF of a random variable is a function describing the density of probability at each point in the sample space. It enables the calculation of the probability of the random variable falling within a given interval by calculating the integral, called CDF, of the PDF in the given interval. In the Monte Carlo method, the PDF is used to describe the probability structure of input and output variables and to increase the result precision, allowing a greater number of simulations to be carried out for the more probable values of each parameter. The most common PDFs are the constant and the normal, although in this work the Beta PDF was chosen because of its flexibility [**23**]. In equations (10) and (11), the Beta PDF and the Beta CDF are given. In these equations, the parameters a and b represent the lower and upper bounds, while the parameters p and q are the shape parameters and x is the variable. According to their values the Beta PDF can assume different shapes, as shown in Fig. 2

$$\mathrm{PDF}_\beta(x; p, q, a, b)[[x]^{-1}] = \frac{(x-a)^{p-1}(b-x)^{q-1}}{(b-a)^{p+q-1}\int_0^1 w^{p-1}(1-w)^{q-1}dw} \tag{10}$$

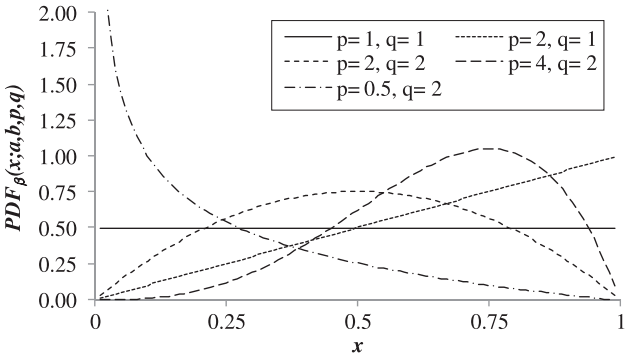

Fig. 2 Beta PDF for different values of the shape parameters

$$\mathrm{CDF}_\beta(x;p,q,a,b) = \int_a^x \beta(w;p,q,a,b)dw = \frac{\int_a^x (w-a)^{p-1}(b-w)^{q-1}dw}{(b-a)^{p+q-1}\int_0^1 w^{p-1}(1-w)^{q-1}dw} \quad (11)$$

The shape parameters p and q can be calculated from data series analysis using equations (12) and (13), where $\bar{x}$ and $\bar{\sigma}^2$ can be calculated as in equations (14) and (15) and x_m and σ_m^2 are the average and standard deviation of the data series [**23**].

$$p = \bar{x}\left(\frac{\bar{x}(1-\bar{x})}{\bar{\sigma}^2} - 1\right) \quad (12)$$

$$q = (1-\bar{x})\left(\frac{\bar{x}(1-\bar{x})}{\bar{\sigma}^2} - 1\right) \quad (13)$$

$$\bar{x} = \frac{x_\mathrm{m} - a}{b-a} \quad (14)$$

$$\bar{\sigma}^2 = \frac{\sigma_\mathrm{m}^2}{(b-a)^2} \quad (15)$$

3.2.2 *Variate generation*

For each simulation, a random value in the sample range is selected for each input and is used for calculating the model's output. In the algorithm developed, a pseudorandom linear congruential generator, described in equation (16) [**22**], is used for calculating a probability (P) in the interval [0,1]

$$P_{n+1} = (k_{R,1}P_n + k_{R,2})\mathrm{mod}(k_{R,3}) \quad (16)$$

In equation (16), the multiplier ($k_{R,1}$) and the increment ($k_{R,2}$) are calculated at each step considering the time of the processor's clock and the iteration number of the general algorithm, while the modulus ($k_{R,3}$) is constant. This was done to improve the ability of the algorithm to generate uncorrelated random numbers. The probability P_{n+1} is then used for calculating a variate for each input parameter with the inverse transform method. The CDF described in equation (11) is inverted in order to find the parameter value (x) corresponding to the given probability (P) as in equation (17). Because of the non-linearity of equation (11), its inversion is realized through an iterative algorithm based on the secant method [**24**]

$$x = \mathrm{CDF}_\beta^{-1}(P;p,q,a,b) \quad (17)$$

3.2.3 *Calculation of the required number of simulations*

Monte Carlo estimation precision depends on the number of simulations carried out. A limited number of simulations would reduce the computational time, since it is necessary to sample sufficiently the PDF of every parameter and to consider a sufficient number of parameter combinations. In this work the simulation number is calculated as in equation (18), which links together the number of samples (N), the standard deviation of the results (σ_m) and a selected error value (ϵ_N)

$$\epsilon_N = \frac{3\,\sigma_\mathrm{m}}{x_\mathrm{m}\sqrt{N_i}} \quad (18)$$

In the algorithm developed, first an acceptable value for the error is defined and a fixed number of simulations ($N_0 = 50$) is carried out and, then, from the average and standard deviation of the results the necessary number of iterations (N_i) is calculated. If $N_i > N_0$, then it is necessary to carry out $N_i - N_0$ more simulations.

4 VALIDATION

In this section, the methodology used for validating the algorithm is described and test results are reported and discussed, analysing the strengths and limitations of the proposed RTR algorithm.

4.1 Testing strategy

For practical applications, the state estimation algorithm must produce accurate and precise rating estimates while being computationally efficient and robust to measurement and communication failures. Furthermore, the estimation is strongly influenced by the models used, which also have to be accurate and precise. Therefore, a testing strategy aimed at evaluating each one of these characteristics was developed.

1. Accuracy can be defined as the degree of approximation of a calculated parameter to its true value; in this work, accuracy is measured with the average error between estimated and measured values.
2. Precision can be defined as a measure of agreement between independent calculations. In this work, the precision of the estimation is measured with the estimation standard deviation.
3. Robustness can be defined as the ability of the algorithm to provide estimates in the case of measurement or communication failures. In this work, robustness is measured with the change of the estimation average error and average standard deviation.
4. Computational efficiency can be defined as the ability of the algorithm to perform estimations in a given timeframe. In this work, the speed of the algorithm is measured with the average time necessary to produce temperature estimations for one component.

In order to test the analytical models used for environmental condition estimations, meteorological readings in each of the five locations were compared

with values estimated in the same place. In each case, the simulation was performed without considering the data for the location studied; and analytical models were populated with directly measured environmental conditions as given in section 3.1, without using the Monte Carlo state estimation algorithm. For example, the air temperature at location MS 1 was calculated using equation (8) and measured values from MS 2 to 5. These values were then compared with data measured in MS 1, the latter measurement being considered as the true value of the parameters. Component ratings cannot be directly measured, but rather calculated from standard-based models. Therefore, the conductor temperature was used for validation purposes since conductor operating temperatures can be directly measured and estimated values can be directly compared with measured values. In order to validate the model used for conductor rating, measured conductor temperatures were compared with the conductor temperature calculated using the environmental conditions recorded in the same location. Also in this case only the analytical models given in section 3.1 were used. This process was repeated in order to validate conductor rating models for each meteorological station location. For example, the conductor temperature in location MS 1 was calculated using equation (1) and measured environmental conditions local to MS 1. This value was compared to the monitored conductor temperature at location MS 1. An analysis of the model validation studies is given in section 4.3.1. In order to validate the thermal state estimation algorithm, estimated conductor temperatures in each of the five locations were compared with measured conductor temperatures. For example, the conductor temperature in location MS 1 was estimated using equations (1) and (9) and measured values from MS 2 to 5 and was compared to the measured conductor temperature at MS 1. An analysis of the state estimation validation study is given in section 4.3.2. In this case, the Monte Carlo state estimation algorithm described in section 3.2 was used.

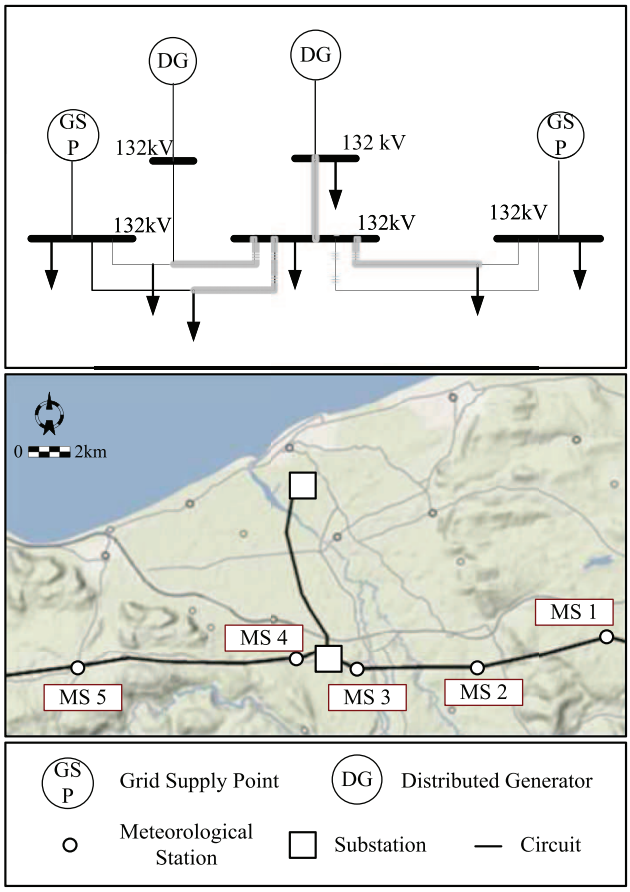

Fig. 3 Monitored network area

4.2 Case study

The thermal state estimation algorithm developed has been validated on measured data from a portion of ScottishPower network, where five meteorological stations and conductor temperature measurement devices were installed. The network is composed of 132 kV overhead lines with Lynx conductors with a maximum operating temperature of 50 °C. A schematic view of the network and a map of the monitored area are given in Fig. 3. The circuits shown in the map are highlighted in the schematic network view. The 132 kV network in this area comprises two circuits: one built in the east–west direction connecting the distribution network to local loads and the other built in the north–south direction connecting a local substation and a distributed generator. From a geographical point of view, the area is characterized by hills, valleys, and the coast line running in the east–west direction. The different soil roughnesses of these areas was estimated by observing satellite images. The prevailing wind direction is north to south. It is anticipated that this will considerably influence the rating of the circuits described above in the following manner: over the course of the year, the east–west running circuit will experience greater cooling than the north–south circuit. Meteorological measurements for the period 7 December 2008 to 18 February 2009 were used for carrying out the validation. For each meteorological station, five minute averaged values of wind speed, wind direction, air temperature, and solar radiation were available. Furthermore, in each meteorological station location, five minute averaged readings for conductor temperature and current were available. A summary of the environmental conditions recorded during the observation period is given in Table 1. Average wind speed is the parameter presenting the greatest variation in the different locations, passing from a value of 5.4 m/s in MS 5 to a value of 2 m/s in MS 3. The distance between these two meteorological stations is 11 km, but differences in ground

Table 1 Frequency percentages of measured environmental conditions at the five meteorological stations and measured current flowing in the conductor in the same locations for the period 7 December 2008 to 18 February 2009

Ws (m/s)	$0 \leqslant \text{Ws} \leqslant 0.4$	$0.4 < \text{Ws} \leqslant 4.6$	$4.6 < \text{Ws} \leqslant 8.8$	$8.8 < \text{Ws} \leqslant 13$	$13 < \text{Ws} \leqslant 17.2$	$17.2 < \text{Ws} \leqslant 21.4$
MS 1	12.6%	61.2%	13.1%	1.4%	0.0%	0.0%
MS 2	8.5%	58.1%	19.0%	0.6%	0.0%	0.0%
MS 3	12.6%	34.2%	4.5%	0.0%	0.0%	0.0%
MS 4	10.0%	57.7%	20.3%	2.9%	0.3%	0.0%
MS 5	1.5%	42.6%	40.9%	9.4%	2.4%	1.2%
Wd (°)	$0 \leqslant \text{Wd} \leqslant 5$	$5 < \text{Wd} \leqslant 76$	$76 < \text{Wd} \leqslant 147$	$147 < \text{Wd} \leqslant 218$	$218 < \text{Wd} \leqslant 289$	$289 < \text{Wd} \leqslant 360$
MS 1	0.9%	9.2%	26.3%	37.0%	14.7%	11.4%
MS 2	0.5%	4.7%	32.2%	36.0%	14.1%	12.0%
MS 3	0.6%	6.1%	31.2%	26.3%	24.6%	10.8%
MS 4	0.2%	2.8%	43.7%	28.3%	15.2%	9.5%
MS 5	0.4%	4.4%	16.0%	41.7%	25.9%	11.3%
T_a (°C)	$T_a \leqslant -3$	$-3 < T_a \leqslant 0.5$	$0.5 < T_a \leqslant 4$	$4 < T_a \leqslant 7.5$	$7.5 < T_a \leqslant 11$	$11 < T_a \leqslant 14.5$
MS 1	1.9%	15.6%	32.1%	33.3%	15.4%	1.0%
MS 2	2.5%	12.7%	29.6%	30.9%	20.4%	3.5%
MS 3	4.2%	15.8%	29.1%	29.9%	17.7%	2.8%
MS 4	1.8%	10.7%	26.4%	33.9%	22.0%	4.7%
MS 5	0.0%	12.6%	33.4%	37.7%	14.9%	1.1%
Sr (W/m^2)	$0 \leqslant \text{Sr} \leqslant 5$	$5 < \text{Sr} \leqslant 112$	$112 < \text{Sr} \leqslant 219$	$219 < \text{Sr} \leqslant 326$	$326 < \text{Sr} \leqslant 433$	$433 < \text{Sr} \leqslant 541$
MS 1	2.3%	46.9%	10.2%	4.8%	0.8%	0.1%
MS 2	2.1%	55.2%	6.3%	0.4%	0.0%	0.0%
MS 3	2.1%	57.6%	5.3%	1.0%	0.1%	0.0%
MS 4	1.8%	48.0%	11.0%	4.2%	0.6%	0.1%
MS 5	2.1%	50.3%	9.8%	3.8%	0.6%	0.1%
I(A)	$0 \leqslant I \leqslant 20$	$20 < I \leqslant 64$	$64 < I \leqslant 108$	$108 < I \leqslant 152$	$152 < I \leqslant 196$	$196 < I \leqslant 240$
MS 1	1.7%	28.6%	38.8%	21.8%	8.3%	0.4%
MS 2	1.3%	19.9%	38.4%	23.7%	13.1%	3.0%
MS 3	1.6%	26.7%	37.0%	21.1%	8.0%	0.5%
MS 4	14.2%	50.4%	16.4%	13.4%	0.5%	0.0%
MS 5	23.3%	46.5%	22.4%	1.6%	0.0%	0.0%

roughness between the urban and rural environments of MS 3 and MS 5, respectively, influence wind speed as described in equation (9).

4.3 Results and discussion

In this section, the results of the simulations carried out using the system described in section 3.2 are compared with the inputs described in section 4.1. The results are analysed according to the methodology described in section 4.1.

4.3.1 Model validation

Environmental condition models and conductor rating models were tested as described in section 4.1. The comparison between estimated and measured values for all the models is shown in Fig. 4 and a quantitative analysis of the error is shown in Table 2. For illustrative purpose, the data shown in Fig. 4 are relative to MS 2 and to the limited period 7 December 2008 to 13 December 2008. Regarding wind speed and direction estimation, there is generally good agreement between estimated and measured data, but on particular occasions the interpolation method described in equation (8) produces a considerable error. This is shown clearly in Figs 4(a) and (b) in the period 9 November 2008. Regarding the wind direction, the phase shift in results that potentially occurs when the interpolation in equation (8) is used may be seen for estimated values corresponding to measured values in the region of 360°. Regarding air temperature estimation, Fig. 4(c) shows good agreement between estimated and measured data. Here, the effect of conservative assumptions in the case of missing or unacceptable data is evident in the estimates produced for the days 7 December 2008 and 12 December 2008. Regarding solar radiation, there is a considerable difference between estimated and measured data, as shown in Fig. 4(d). This is due to local cloud coverage or other local conditions such as reflection from surfaces in proximity to the meteorological station that are not taken into account. Regarding conductor temperature, there is good agreement between estimated and measured values, with the greatest error associated with spikes in the measured conductor temperature not present in the trace produced by calculation. This is because the model used does not consider the dynamic behaviour of the conductor, which increases the error in cases where there is a response to rapid changes in current. In Table 2, the average error and the error standard deviation for each parameter in each location are reported for the period 7 December 2008 to 18 February 2009. Regarding wind speed, the estimation in location MS 3 presents an average error considerably higher than the others and

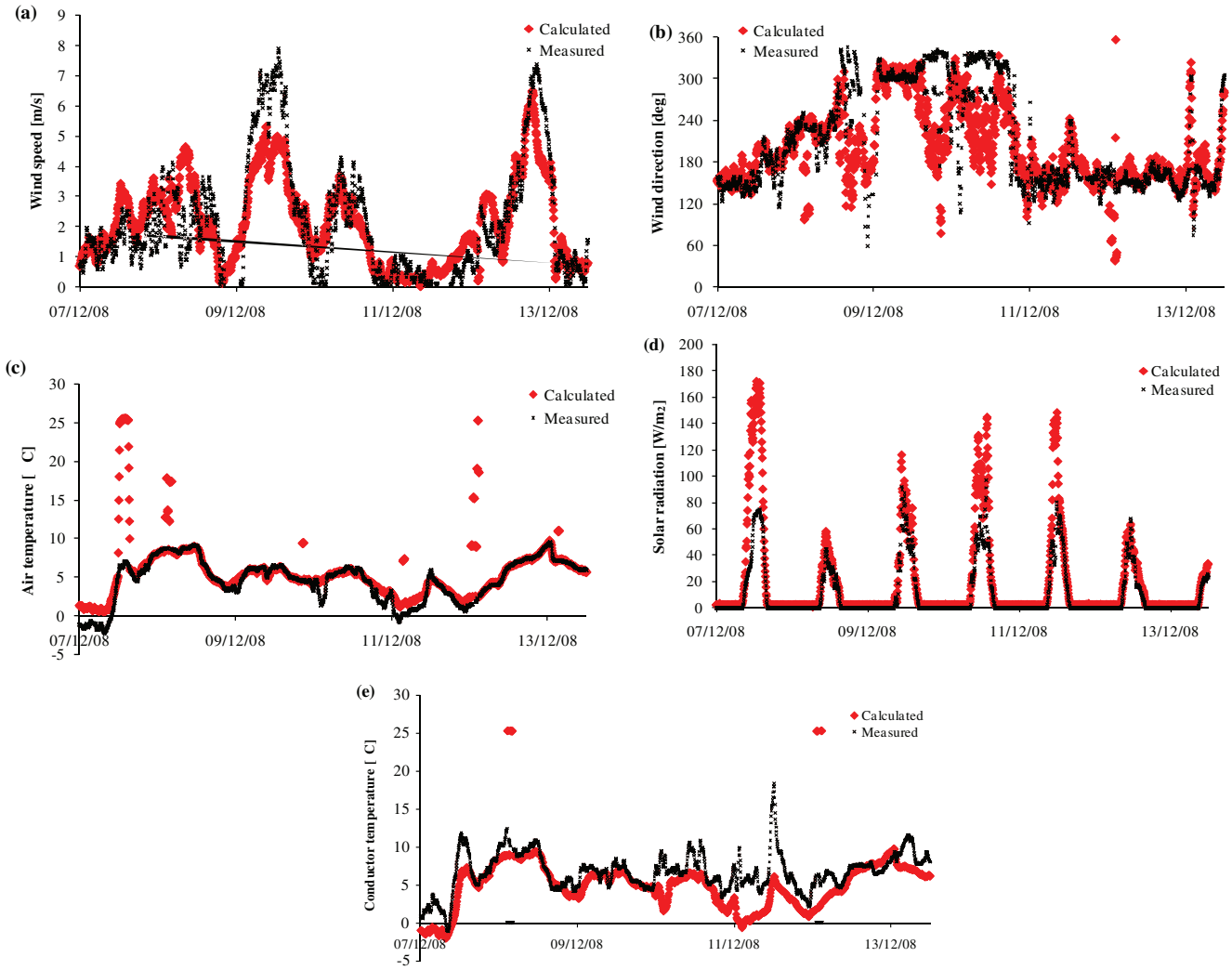

Fig. 4 Comparison between calculated and measured data in the period 7 December 2008 to 13 December 2008 for the location MS 2: (a) wind speed, (b) wind direction, (c) air temperature, (d) solar radiation, and (e) conductor temperature

error standard deviation is also the highest. This is expected to be caused by errors in ground parameter estimation. Imprecise values for conductor parameters such as line orientation or conductor resistance are expected to be the main causes for the high average error and high error standard deviation for the conductors in locations MS 1 and MS 2, respectively. Errors for the other parameters can only be associated with imprecision in the model used.

4.3.2 State estimation validation

The Monte Carlo-based state estimation algorithm described in section 3.2 was tested as described in section 4.1 and the results are summarized in Table 3. Particular attention was paid to reducing the estimation computational time, and in all the five examples, the average computational time is between 2.16 and 2.24 s. This simulation was carried out using a 0.625 GHz processor and the computational time can be considerably reduced by increasing the parameter ϵ_N, currently set at 5 per cent for every parameter. Regarding the estimation average error, its value is in line with the model average error reported in Table 2 but the standard deviation tends to be higher. The estimation standard deviation is also compared to the standard deviation of the measured temperature over a period of 30 m. An optimal value for the estimation standard deviation would be similar to the measured standard deviation, but here it is roughly one third. This can be explained in two ways: first the steady-state model used for conductor temperature calculation does not take into account the dynamic behaviour of the conductor, producing a less variable estimation, as seen in Fig. 4(e). Second this parameter is influenced by the number of simulations carried out, but this number is voluntarily kept low in order to reduce the computational time because of the use of this

Table 2 Error average and standard deviation for each model and each meteorological station for the period 7 December 2008 to 18 February 2009. The highest values for each parameter are highlighted

	Parameter	Ws (m/s)	Wd (°)	T_a (°C)	Sr (W/m^2)	T_c (°C)
MS 1	Error average	0.0	8	0.8	−10	−2.4
	Error standard deviation	0.9	54	1.5	44	2.1
MS 2	Error average	−0.3	3	0.2	21	−1.8
	Error standard deviation	1.4	39	1.4	27	2.6
MS 3	Error average	1.8	−7	0.9	20	−1.5
	Error standard deviation	1.5	47	1.8	43	1.7
MS 4	Error average	−0.8	12	−0.3	−11	−1.0
	Error standard deviation	1.3	51	1.6	39	0.9
MS 5	Error average	−0.8	−23	0.4	−7	0.0
	Error standard deviation	1.3	46	2.0	42	1.2

Table 3 Conductor temperature state estimation error analysis at the five meteorological stations for the period 7 December 2008 to 18 February 2009

	MS 1	MS 2	MS 3	MS 4	MS 5
Time (s)	2.24	2.16	2.23	2.21	2.23
Error average (°C)	−2.2	−1.9	−1.2	−1.9	1.4
Error standard deviation (°C)	2.2	2.4	2.3	1.9	1.9
Estimated standard deviation (°C)	0.118	0.120	0.121	0.119	0.121
Measured standard deviation (°C)	0.355	0.355	0.355	0.447	0.447

algorithm in an online controller. Figure 5 shows the comparison between estimated conductor temperature and measured conductor temperature at location MS 2 during the first week of simulations. This chart displays strong similarities with Fig. 4(e). However, the main differences in estimated conductor temperatures arise from missing data at MS 1, 3, 4, and 5. At these points in time, the algorithm makes conservative assumptions of the environmental conditions local to MS 2 and, therefore, the predicted conductor operating temperature is higher. The behaviour of the state estimation algorithm for measurement and communication failure was studied at location MS 2 by introducing a variable percentage of missing data into the input parameters of MS 1, 3, 4, and 5. Figure 6 shows changes in estimation average error and estimation standard deviation for different percentages of missing data. The meaningful observation occurs when 1 per cent or more of the data is missing. Considering the average error in the region of 1–5 per cent of data missing, the estimation average error increases linearly from 2.6 to 5.4 °C. Considering the standard deviation in the region of 1–5 per cent of data missing, a similar linear behaviour is displayed and the standard deviation of conductor temperature estimates increases from 0.12 to 0.14 °C. Finally, in order to give a qualitative and quantitative description of the error, conductor temperature error PDF and CDF are reported in Fig. 7. This helps us to see in greater detail the data summarized in Table 3. From Fig. 7, the error distribution is not symmetrical with the average lower than the mode. This means that the

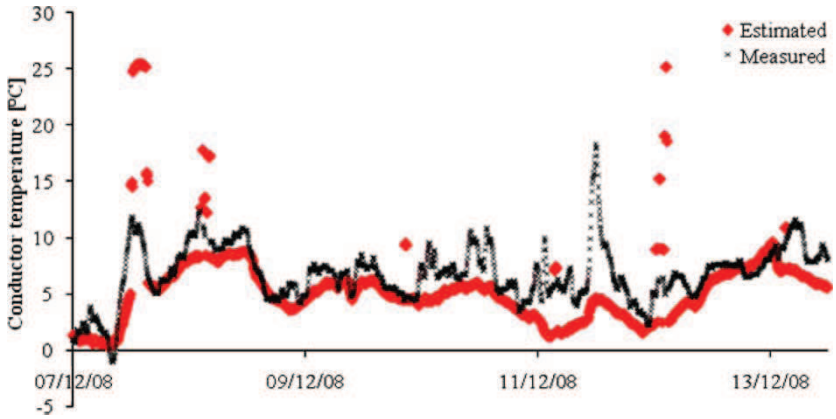

Fig. 5 Comparison between conductor temperature estimation and conductor measured temperature in location MS 2 for the period 7 December 2008 to 13 December 2008

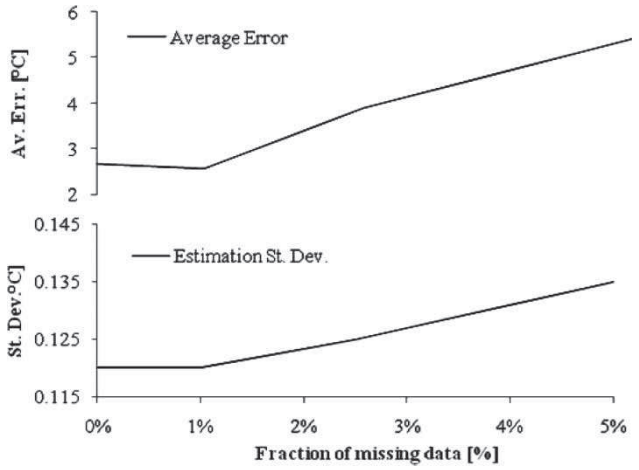

Fig. 6 Performance degradation in consequences of measurement or communication failures at location MS 2 for the period 7 December 2008 to 18 February 2009

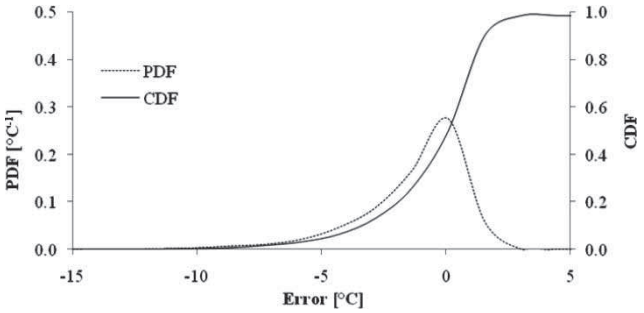

Fig. 7 Probability and CDF for the error in conductor temperature estimation. Location MS 2, period 7 December 2008 to 18 January 2009

system tends to underestimate conductor temperature and therefore to overestimate its current-carrying capacity.

4.3.3 Discussion

Considering that, at present, DNOs have limited knowledge of the actual operating temperatures of overhead line conductors, the results presented in this article are extremely encouraging and demonstrate the potential for the adoption of sophisticated state estimation algorithms in future network operation. In order to reduce the risk of a localized hotspot, when making an assessment of the real-time thermal rating for a long overhead line circuit, the overhead line can be divided into sections to represent the variation of external parameters such as line orientation or soil roughness. The section of the overhead line with the lowest rating represents the weakest point of the overhead line system and therefore this lowest rating can be adopted as the RTR for the entire overhead line. The simulation results reported in sections 4.3.1 and 4.3.2 confirm that the thermal state estimation algorithm developed is able to estimate the conductor temperature, and therefore line rating, with a good degree of accuracy. Considering that the typical overhead line design operating temperature in UK ranges from 50 to 75 °C, the maximum average error measured (−2.2 °C) represents maximum average errors of −4.4 per cent and −2.9 per cent for the respective conductor operating temperatures. Furthermore, the extensive tests carried out on the algorithm allow sources of error to be identified. In light of this, the following suggestions for estimation error reduction are made. Regarding environmental conditions, the interpolation method used has proven efficient for air temperature estimation. However, it was less successful in estimating the wind speed and the wind direction in all operating conditions. A better estimation of the soil roughness parameters used in equation (9) and a more complex wind flow modelling algorithm with computational fluid dynamics are likely to increase the accuracy of environmental condition estimations. Commercial or open source software packages such as the ones used for wind farm design could easily be integrated in the algorithm, although this solution would be more computationally intensive. Since this state estimation algorithm was developed to inform an online control algorithm for the power output of DG, computational efficiency was one of the main priorities. Regarding solar radiation estimation, the model proposed does not consider the effect of cloud coverage or local environmental factors such as reflection from surfaces in proximity to the meteorological station. Regarding conductor temperature, a correct measurement of conductor parameters and, in particular, of conductor resistance and line direction would help us to increase the accuracy of the model. Work is ongoing at Durham University for improving the quality of the estimation produced by the thermal state estimation algorithm in light of these findings. Furthermore, in order to enhance the flexibility of the algorithm, research is carried out for producing rating forecasts at different time horizons [**25**].

5 CONCLUSION

This article has described an RTR estimation system developed at Durham University along with its validation using field data. The solution proposed consists of the use of a limited number of meteorological stations for measuring real-time meteorological information. These are used in a state estimation algorithm based on the Monte Carlo method and on physical models for calculating environmental conditions in every network component location and component rating. The estimation error for every environmental condition and for conductor temperature was measured in five different locations over a period of 71 days. An average error of −2.2, −1.9, −1.2, −1.9, and 1.4 °C was

measured for the estimation of conductor temperature in the five locations when comparing estimates to measured results, and the main source of error was ascribed to the physical models used. Suggestions on how to further reduce this error were given, along with the identification of further research areas.

ACKNOWLEDGEMENTS

The authors wish to acknowledge the Department for Innovation, Universities and Skills for funding, and the staff of AREVA T&D, Imass, PB Power, ScottishPower EnergyNetworks, and the MetOffice for their valuable input to this work.

REFERENCES

1 **Michiorri, A., Taylor, P. C., Jupe, S. C. E.,** and **Berry, C. J.** Investigation into the influence of environmental conditions on power system ratings. *Proc. IMechE, Part A: J. Power and Energy*, 2009, **223**(A7), 743–757. DOI: 10.1243/09576509JPE718.

2 **Neumann, A., Taylor, P., Jupe, S., Michiorri, A., Goode, A., Curry, D.,** and **Roberts, D.** Dynamic thermal rating and active control for improved distribution network utilisation. In Proceedings of the PowerGrid 08, Milan, Italy, 2008.

3 **Price, C.** and **Gibbon, R.** Statistical approach to thermal rating of overhead lines for power transmission and distribution. *IEE Proc.*, 1983, **130**(5), 245–256.

4 **McElvain, F. R.** and **Mulnix, S. S.** Statistically determined static thermal ratings of overhead high voltage transmission lines in the rocky mountains. *IEEE Trans. Power Syst.*, 1995, **10**, 1805–1812.

5 **Wan, H., McCalley, J. D.,** and **Vittal, V.** Increasing thermal rating by risk analysis. *IEEE Trans. Power Syst.*, 1999, **14**(3), 815–828.

6 **Helmer, M.** Optimized size of wind power plant transformer and parallel operation. In Proceedings of the Wind Power for the 21st Century, Kassel, Germany, September 2000.

7 **Belben, P. D.** and **Ziesler, C. D.** Aeolian uprating: how wind farms can solve their own transmission problems. In Proceedings of the World Wind Energy Conference and Exhibition, Berlin, July 2002.

8 **Yip, H. T., An, C., Aten, M.,** and **Ferris, R.** Dynamic line rating protection for wind farm connections. In Proceedings of the Ninth International Conference on *Developments power system protection*, Glasgow, UK, 2008.

9 **Soto, F., Latorre, J.,** and **Wagensberg, M.** Increasing the capacity of overhead lines in the 400 kV Spanish transmission network: real time thermal ratings. *Electra,* 1998, **22–211**, 1–6.

10 http://www.wasp.dk. Accessed January 2009.

11 **Nuijten, J. M. A.** and **Geschiere, A.** Future network planning and grid control. In Proceedings of the International Conference on *Future power systems*, Amsterdam, Netherlands, November 2005.

12 **Piccolo, A., Vaccaro, A.,** and **Villacci, D.** Thermal rating assessment of overhead lines by affine arithmetic. *Electr. Power Syst. Res.*, 2004, **71**, 275–283.

13 **Villacci, D.** and **Vaccaro, A.** Transient tolerance analysis of power cables thermal dynamic by interval mathematic. *Electr. Power Syst. Res.*, 2007, **77**, 308–314.

14 **Ippolito, L., Vaccaro, A.,** and **Villacci, D.** The use of affine arithmetic for thermal state estimation of substation distribution transformers. *COMPEL: Int. J. Comput. Math. Electr. Electron. Eng.*, 2004, **23**(1), 237–249.

15 **Bontempi, G., Vaccaro, A.,** and **Villacci, D.** Semiphisical modelling architecture for dynamic assessment of power components loading capability. *IEE Gener. Transm. Distrib.*, 2004, **151**(4), 533–542.

16 **Bernini, R., Minardo, A., Persiano, G. V., Vaccaro, A., Villacci, D.,** and **Zeni, L.** Dynamic loading of overhead lines by adaptive learning techniques and distributed temperature sensing. *IET Gener. Transm. Distrib.*, 2007, **1**.

17 **Lee, T. L.** and **Piekutowski, M.** Expert system application for the loading capability assessment of transmission lines. *IEEE Trans Power Syst.*, 1995, **10**(4), 1805–1812.

18 IEC. Overhead electrical conductors – calculation methods for stranded bare conductors. 1995. TR 1597.

19 CIGRE WG 22.12. The thermal behaviour of overhead conductors. Section 1 and 2: matematical model for evaluation of conductor temperature in the steady state and the application thereof. *Electra*. 1992, **144**, 108–125.

20 **Shepard D.** A two-dimensional interpolation function for irregularly-spaced data. In Proceedings of the 1968 23rd ACM National Conference, 1968, pp. 517–524.

21 **Pérez, I. A., García, M. A., Sánchez, M. L.,** and **de Torre, B.** Analysis and parameterisation of wind profiles in the low atmosphere. *Sol. Energy*, 2005, **78**(6), 809–821.

22 **Rubinstein, R. Y.** *Simulation and the Monte Carlo method*, 2007 (Wiley-Interscience, New York, USA).

23 http://www.itl.nist.gov/div898/handbook/NIST/SEMATECH *e-Handbook of Statistical Methods*, June 2009.

24 **Mathews, J. H.** *Numerical methods for computer science, engineering, and mathematics*, 1987 (Prentice-Hall, London, UK).

25 **Michiorri, A.** and **Taylor, P. C.** Forecasting real-time ratings for electricity distribution networks using weather forecast data. In Proceedings of the CIRED'09, Prague, 2009.

APPENDIX

Notation

a	beta distribution function minimum value
b	beta distribution function maximum value
D_c	conductor diameter (m)
h	reference height (m)
h_a	height of the anemometer (m)
h_c	height of the conductor (m)
i	index
I	current (A)

$k_{R,i}$	congruential random number generator, parameters
K_{dir}	direction coefficient
$K_{\mathrm{dir}-i}$	direction coefficient parameters
K_{shear}	ground roughness coefficient
$l_{i,k}$	distance between location i and k (m)
MS i	meteorological station
N	iteration number
Nu	Nusselt number
p	beta distribution function shape parameter
P	probability
q	beta distribution function shape parameter
q_{c}	convective heat exchange (W/m)
q_{r}	radiative heat exchange (W/m)
q_{s}	solar gain (W/m)
R	conductor resistance per unit length (Ω/m)
Re	Reynolds number
S_{r}	solar radiation (W/m^2)
t	time (s)
T_{a}	air temperature (°C)
T_{c}	conductor temperature (°C)
w	conductor temperature (°C)
w	generic variable
Wd	wind direction (°C)
Ws	wind speed (m/s)
Ws_{a}	measured wind speed at the anemometer (m/s)
Ws_{c}	calculated wind speed on the conductor (m/s)
x	generic variable
$\bar{x}$	beta distribution dimensionless average
x_{m}	beta distribution average
y	generic variable
z	generic variable
α_{abs}	conductor absorption coefficient
α_{em}	conductor emission coefficient
δ	wind-conductor relative angle (rad)
ϵ_N	dimensionless precision
$\rho\mathrm{th}_{\mathrm{a}}$	air thermal resistivity (m K/W)
$\bar{\sigma}$	beta distribution dimensionless standard deviation
σ_{m}	beta distribution standard deviation
σ_{SB}	Stefan–Boltzmann constant (W/m^{-2}/K^4)

Investigation into the influence of environmental conditions on power system ratings

A Michiorri[1*], **P C Taylor**[1], **S C E Jupe**[1], and **C J Berry**[2]
[1]School of Engineering, Durham University, Durham, UK
[2]ScottishPower EnergyNetworks, Birkenhead, UK

The manuscript was received on 24 October 2008 and was accepted after revision for publication on 21 April 2009.

DOI: 10.1243/09576509JPE718

Abstract: This article presents research that seeks to assist distribution network operators in the adoption of real-time thermal rating (RTR) systems. The exploitation of power system rating variations is challenging because of the complex nature of environmental conditions such as wind speed. The adoption of an RTR system may overcome this challenge and offers perceived benefits such as increased distributed generation (DG) accommodation and avoidance of component damage or premature ageing. Simulations, using lumped parameter component models, are used to investigate the influence of environmental conditions on overhead line, electric cable, and power transformer ratings. Key findings showed that the average rating of overhead lines, electric cables, and power transformers ranged from 1.70 to 2.53, 1.00 to 1.06, and 1.06 to 1.10 times the static rating, respectively. Since overhead lines were found to have the greatest potential for rating exploitation, the influence of environmental conditions on four overhead line types was investigated and it was shown that the value of an RTR system is location dependent. Furthermore, the additional annual energy yield from DG that could potentially be accommodated through deployment of an RTR system was found to be 54 per cent for the case considered.

Keywords: overhead lines, electric cables, power transformers, real-time ratings, distributed generation

1 INTRODUCTION

This article describes the offline simulation of power system thermal models populated with historical environmental conditions in order to derive real-time thermal ratings (RTRs). This information is used to quantify (in GWhs) the exploitable headroom that may be achieved by implementing an RTR system within distribution networks. In many cases the current carrying capacity of power system components is limited by a maximum allowable operating temperature. Actual component operating temperatures are determined by the ability of components to dissipate to the environment the heat produced by the Joule effect and by environmental conditions such as ambient temperature and wind speed, which are continuously varying. As a result, the current carrying capacity of components may be continually assessed and this is proportional to the RTR in MVA. For the purpose of this research, RTRs are defined as a time-variant rating that can be practically exploited without damaging components or reducing their life expectancy. Actual measurements of environmental conditions are used as the input to steady-state thermal models. In order to calculate and exploit the RTR, it is assumed that local environmental condition measurements are available and that there are no outages (planned or unplanned) present within the electrical power system. Short term transients, taking into account the thermal capacitance of power system components, are not included within the RTR assessment. It is felt that this would not materially affect the GWh/annum throughput of energy within the electrical power system. The mechanisms of heat exchange underpinning component ratings are well documented [**1**–**3**]. However, the estimation of component operating temperatures (and thus current carrying limits) is a non-trivial task. This is because of the complexity of monitoring and modelling environmental conditions. For this

*Corresponding author: School of Engineering, Durham University, South Road, Durham, DH1 3LE, UK.
email: andrea.michiorri@durham.ac.uk

reason component ratings based on fixed assumptions of environmental conditions are often used by distribution network operators (DNOs). The implementation of an RTR system has the potential to give DNOs greater visibility of network operating conditions thus reducing the risk of exceeding the component maximum operating temperature. This could be used both offline, to inform power system planning, and online, within future operational philosophies, in order to increase cautiously the utilization of power system components. However, system implementation requires a number of challenges to be overcome, including the measurement, estimation and communication of real-time component temperatures, and environmental conditions. At the distribution network level these are likely to be dispersed over complex terrains throughout wide geographical areas containing significant numbers of power system components. The research described in this article forms part of a UK Government part-funded project [**4**] that aims to develop and deploy an online power output controller for distributed generation (DG) based on component RTRs. In this project a DG power output controller compares RTRs with network power flows and produces set points that are fed back to the DG operator for implementation, as shown in Fig. 1. The research consortium includes ScottishPower EnergyNetworks, AREVA T&D, PB Power, and Imass and Durham University.

The article is structured in the following way: section 2 provides an overview of relevant work. In section 3, the models developed for network components and environmental conditions are described. Section 4 describes the component data, the environmental condition data, and the RTR simulation approach and, in section 5, simulation results are presented and discussed.

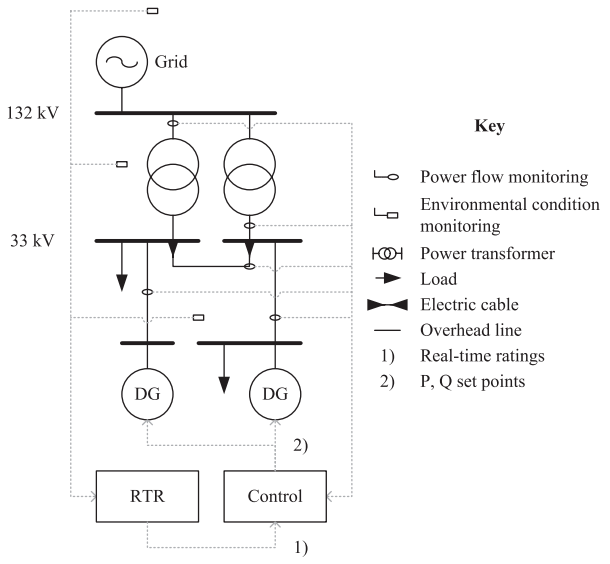

Fig. 1 DG power output controller informed by RTRs

2 RELEVANT WORK

Significant research has been carried out at the transmission level for RTR applications. Research tends to focus on overhead lines, which, because of their exposure to the environment, exhibit the greatest rating variability. A description of the cost and suitability of different uprating techniques for overhead lines is described in reference [**5**], taking into account different operating conditions. This work shows how RTRs can be a more appropriate solution than network reinforcement when connecting new customers to the network who are able to curtail their generation output or reduce their power demand requirement at short notice. Similarly, experience regarding thermal uprating in the UK is reported in reference [**6**] where it was suggested that RTRs could give overhead lines an average uprating of 5 per cent for 50 per cent of the year. An example of an RTR application for transmission overhead lines of Red Eléctrica de España is described in reference [**7**], where a minimal amount of weather stations are used to gather real-time data. The data are then processed using a meteorological model based on the Wind Atlas Analysis and Application Program (WAsP) [**8**], taking into account the effect of obstacles and ground roughness, and finally the rating is calculated. A similar system was developed in the USA by EPRI in the late 1990s, which considered overhead lines, power transformers, electric cables, and substation equipment. The system is described in reference [**9**] and preliminary results of field tests are given in reference [**10**]. A key finding was that up to 12 h of low wind speeds (<0.76 m/s) were observed during the field tests, which therefore suggests that overhead line RTRs may be lower than seasonal ratings for extended periods of time. Furthermore, a strong correlation was found to exist between independent air temperature measurements distributed along the lengths of the overhead lines. At the distribution level, an RTR project carried out by the Dutch companies NUON and KEMA is described in reference [**11**] that demonstrates the operating temperature monitoring of overhead lines, electric cables, and power transformers.

The advantages of an RTR system for the connection of DG, especially wind power, are reported in various sources, each of which considers only single power system components. It is demonstrated in reference [**12**] that the rating of transformers positioned at the base of wind turbines may presently be oversized by up to 20 per cent. Moreover, in reference [**13**] the power flowing in an overhead line close to a wind farm is compared to its RTR using WAsP. In this research, it was highlighted that high power flows resulting from wind generation at high wind speeds could be accommodated since the same wind speed has a positive effect on the line cooling. This observation makes the adoption of RTR systems

relevant in applications where strong correlations exist between the cooling effect of environmental conditions and electrical power flow transfers. Moreover, in references [**14**] to [**16**] the influence of component thermal model (CTM) input errors on the accuracy of RTR systems is studied. The application of different state estimation techniques, such as affine arithmetic, interval arithmetic, and Montecarlo simulations was studied for overhead lines, electric cables, and power transformers. Errors of up to ±20 per cent for an operating point of 75 °C, ±29 per cent for an operating point of 60 °C and ±15 per cent for an operating point of 65 °C were found when estimating the operating temperature of overhead lines, electric cables, and power transformers, respectively. This highlights the necessity to have reliable and accurate environmental condition monitoring. The thermal models, used to estimate RTRs for different types of power system components, are fundamental to this research as the accuracy of the models influences significantly the accuracy of RTRs obtained. Particular attention was given to industrial standards because of their wide application and validation both in industry and academia. For overhead lines, the model is described in references [**17**] and [**18**] that has been developed into industrial standards [**1**, **19**, **20**] by the IEC, CIGRE, and IEEE, respectively. Static seasonal ratings for different standard conductors and for calculated risks are provided by the Electricity Network Association (ENA) in reference [**21**]. Thermal model calculation methods for electric cable ratings are described in reference [**22**] and developed into an industrial standard by the IEC in reference [**2**]. The same models are used by the IEEE in reference [**23**] and the ENA in reference [**24**] to produce tables of calculated ratings for particular operating conditions. Power transformer thermal behaviour is described in reference [**25**] with further models described in the industrial standards [**3**, **26**, **27**] by the IEC, IEEE, and ENA, respectively.

The research presented in this article adds to the work described above by modelling the influence of environmental conditions on multiple power system component types simultaneously. This is of particular relevance in situations where the increased power flow resulting from the alleviation of the thermal constraint on one power system component may cause an entirely different component to constrain power flows. Furthermore, with the expected proliferation of DG the resulting power flows are likely to affect many components and it is important to take a holistic view of power system thermal ratings. Since this research project aims to develop and deploy an economically viable real-time system, it is important that algorithms are developed with fast computational speeds using a minimal amount of environmental condition monitoring. Thus an inverse distance interpolation technique is used for modelling environmental conditions across a wide geographical area, which offers faster computational speeds than applications such as WAsP. Beyond the research described above, this article also aims to quantify the annual energy throughput that may be gained through the deployment of an RTR system.

3 MODELLING APPROACH

3.1 Components

In order to assess, in a consistent manner, component RTRs because of the influence of environmental conditions, thermal models were developed based on IEC standards [**1**–**3**] for overhead lines, electric cables, and power transformers, respectively. Where necessary, refinements were made to the models using [**19**, **24**]. Steady-state models have been used in preference to dynamic models since this would provide a maximum allowable rating for long term power system operation. Moreover, the estimation of final steady-state component temperatures after a transient has occurred is influenced by initial conditions, which must also be estimated. It is felt that with the resolution of the available data (comprising hourly averaged environmental conditions) it is extremely difficult to obtain an acceptable precision for dynamic models, particularly for overhead lines with time constants of less than an hour.

3.1.1 Overhead lines

Overhead line ratings are constrained by a necessity to maintain statutory clearances between the conductor and other objects. The temperature rise causes conductor elongation which, in turn, causes an increase in sag. The line sag S depends on the tension H, the weight m applied to the conductor inclusive of the dynamic force of the wind and the length of the span. The sag can be calculated as a catenary or its parabolic approximation, as given in equation (1). To calculate the tension, it is necessary to consider the thermal-tensional equilibrium of the conductor, as shown in equation (2). For calculating the conductor operating temperature at a given current, or the maximum current for a given operating temperature, it is necessary to solve the energy balance between the heat dissipated in the conductor by the current, and the thermal exchange on its surface, as given in equation (3)

$$S = \frac{H}{\mathrm{mg}}\left[\cosh\left(\frac{\mathrm{mgL}}{2H}\right) - 1\right] \approx \frac{\mathrm{mgL}^2}{8H} \tag{1}$$

$$EA\beta\left(T_{\mathrm{c},2} - T_{\mathrm{c},1}\right) + \left(\frac{m_1^2 g^2 L^2 EA}{24H_1^2}\right) - H_1 = \left(\frac{m_2^2 g^2 L^2 EA}{24H_2^2}\right) - H_2 \tag{2}$$

$$q_{\mathrm{c}} + q_{\mathrm{r}} = q_{\mathrm{s}} + I^2 r \tag{3}$$

The formulae proposed in reference [**1**] were used for the calculation of the contribution of solar radiation q_s, radiative heat exchange q_r, and convective heat exchange q_c. These equations are shown in equations (4) to (6), respectively

$$q_s = \alpha D \,\mathrm{Sr} \tag{4}$$

$$q_r = \varepsilon \sigma_{S-B}(T_c^4 - T_a^4)\pi D \tag{5}$$

$$q_c = \pi Nu \lambda (T_c - T_a) \tag{6}$$

The influences of wind direction and natural convection on convective heat exchange are not considered in reference [**1**]. However, in this research these effects were considered to be important, particularly as a wind direction perpendicular to the conductor would maximize the turbulence around the conductor and hence the heat exchange on its surface whereas a wind direction parallel to the conductor would reduce the heat exchange with respect to perpendicular wind direction. Therefore, the modifications proposed in reference [**19**] and given in equations (7) and (10) were used. It is possible to calculate the Nusselt number *Nu* from the Reynolds number *Re* as shown in equation (8). The Reynolds number can be calculated using equation (9)

$$K_{dir} = K_{dir-1} + K_{dir-2} \sin^{K_{dir-3}}(\mathrm{Wd}) \tag{7}$$

$$Nu = K_{dir}(0.65\, Re^{0.2} + 0.23\, Re^{0.61}) \tag{8}$$

$$Re = 1.644 \times 10^9 \,\mathrm{Ws}\, D \left(\frac{T_c + T_a}{2}\right)^{-1.78} \tag{9}$$

For null wind speeds, the Nusselt number must be calculated as in equation (10) where *Gr* is the Grashof number, calculated as in equation (11), and *Pr* is the Prandtl number

$$Nu = K_{nat-1}(Gr\ Pr)^{K_{nat-2}} \tag{10}$$

$$Gr = \frac{D^3(T_c - T_a)g}{[(T_c + T_a)/2]\nu^2} \tag{11}$$

It should be noted that for wind speeds between 0–0.5 m/s the larger of the Nusselt numbers resulting from equations (8) and (10) should be used.

3.1.2 *Electric cables*

The current carrying capacity of electric cables is limited by the maximum operating temperature of the insulation. Sustained high currents may generate temperatures in exceedance of the maximum operating temperature, causing irreversible damage to the cable. In extreme cases this may result in complete insulation deterioration and cable destruction.

References [**2**], [**22**], and [**23**] were used to model the conductor temperature in steady-state conditions. This accounts for the heat balance between the power dissipated in the conductor by the Joule effect, and the heat dissipated in the environment through the thermal resistance R_T of the insulation and the soil as shown in equation (12). The electrical current rating may then be calculated, as shown in equation (13)

$$I^2 r = \frac{\Delta T}{R_T} \tag{12}$$

$$I = \sqrt{\frac{\Delta T}{r R_T}} \tag{13}$$

Refinements incorporating dielectric losses q_d, eddy currents and circulating currents in metallic sheaths ($\lambda_{1,2}$), resistance variation with temperature, skin and proximity effects, and the thermal resistance of each insulating layer $R_{T,i}$ lead to the more complex equation (14)

$$I = \sqrt{\frac{\Delta T - q_d[1/2\ R_{T,1} + n(R_{T,2} + R_{T,3} + R_{T,4})]}{r(T_c)[R_{T,1} + n(1+\lambda_1)R_{T,2} + n(1+\lambda_1+\lambda_2)(R_{T,3} + R_{T,4})]}} \tag{14}$$

Thermal resistances for cylindrical layers are calculated with equation (15) and soil thermal resistance is modelled with equation (16). Other calculation methods [**2**] have to be utilized when operating conditions differ from those stated above (for example when the cable is in a duct or in open air)

$$R_{T-1,2,3} = \frac{\rho_{s-T}}{2\pi} \ln\left(1 + 2\frac{D-d}{d}\right) \tag{15}$$

$$R_{T-4} = \frac{\rho_{s-T}}{2\pi} \ln \frac{2z_b}{D} + \sqrt{\left(\frac{2z_b}{D}\right)^2 + 1} \tag{16}$$

The model described above requires detailed knowledge of the electric cable installation. However, this information may not always be available and therefore it is difficult to make practical use of the model. In these circumstances an alternative model, described in reference [**24**] and summarized in equation (17), may be used. The rated current of electric cables I_0 is given in tables depending on the standardized cable cross-sectional area and laying conditions (trefoil, flat formation; in air, in ducts, or directly buried). The dependence of the cable ampacity on external temperature and soil thermal resistivity is made linear through the coefficients ξ_T and ξ_ρ, respectively.

$$I = I_0(A, V, \mathrm{laying})[\xi_T(T_s - T_{s\ \mathrm{rated}})][\xi_\rho(\rho_{s,T} - \rho_{s\ T\ \mathrm{rated}})] \tag{17}$$

Since this research concerns the influence of environmental conditions on component ratings, the effect of the voltage level V, which influences the dielectric loss q_d in equation (14) is not considered. The effect

of the heating given by adjacent components is also neglected as it is assumed that each cable has already been de-rated to take this effect into account.

3.1.3 Power transformers

The model described in reference [**3**] was used to calculate the winding hot spot temperature for power transformers. This is the most important parameter since hotspot temperature exceedance can damage the transformer in two ways. First, a temperature exceedance of 120–140 °C can induce the formation of bubbles in the coolant oil, which in turn is liable to cause an insulation breakdown because of the local reduction of dielectric insulation strength. Second, high temperatures increase the ageing rate of the winding insulation. For this reason the maximum operating temperature should not exceed the rated value. The thermal model consists of a heat balance between the power dissipated in the winding and iron core, and the heat transferred to the environment via the refrigerating circuit. Considering the thermal resistance between the winding and the oil ($R_{T,W}$), the thermal resistance between the heat exchanger and the air ($R_{T,HE}$) and the power dissipated into the core ($I^2 r_{windings}$), it is possible to calculate the hot spot temperature T_{HS} as in equation (18)

$$T_{HS} = T_a + I^2 r_{windings}(R_{T,W} + R_{T,HE}) \tag{18}$$

Equation (18) is discussed in reference [**25**] leading to the IEC standard model for rating oil-filled power transformers as shown in equation (19)

$$T_{HS} = T_a + (T_{TO} - T_a)\left(\frac{1 + RK^2}{1 + R}\right)^x + (T_{HS} - T_{TO})K^y \tag{19}$$

The maximum rating can be obtained by iteration, once the hot spot temperature has been set, and tabulated values for the parameters can be found in reference [**3**] for transformers with different types cooling system. Correction factors in reference [**3**] can be used to model other operating conditions such as transformers operating within enclosures. Transformer cooling systems are classified with an acronym summarizing (a) the coolant fluid: oil (O) or air (A); (b) the convection around the core: natural (N), forced (F) or direct (D); (c) the external refrigerating fluid: air (A) or water (W); and (d) the external convection method: natural (N) or forced (F). Typically distribution transformers have ONAN or ONAF cooling systems.

3.2 Environmental conditions

This section describes the approach adopted to estimate, correct, and interpolate environmental conditions to represent more accurately the actual environmental operating conditions for sections of the UK power system in different geographical areas.

3.2.1 Environmental condition interpolation

The inverse distance interpolation technique [**28**] allows environmental conditions to be determined over a wide geographical area using a reduced set of inputs. This is attractive for situations where a large amount of installed measurements may be financially unattractive to the DNO. The technique is also computationally efficient and allows the input locations to be readily adapted. The wind speed correction process is described in section 3.2.2. The soil parameter correction process is described in section 3.2.3. Wind direction, air temperature, and solar radiation values were included within interpolations but did not require the application of a correction factor. At each point in the geographical area k the value of the parameter Z representing the environmental condition can be estimated as a weighted average of the parameter values known at i points. The weighting factor is a function of the distance between the points as shown in equation (20)

$$Z_k = \frac{\sum_i (1/d_{i,k}^2) Z_i}{\sum_i 1/d_{i,k}^2} \tag{20}$$

3.2.2 Wind speed correction

Ground roughness influences wind speed profiles and may lead to differences between the wind speed recorded by anemometers and the actual wind speed passing across an overhead line, particularly if the anemometer and overhead line are installed at different heights. This may be corrected using the wind profile power law given in equation (21). The wind speed at two different heights is linked with the ground roughness through the exponent Kshear. Values of Kshear for different ground types may be found in reference [**29**]

$$\mathrm{Ws} = \mathrm{Ws}_a \left(\frac{z_{ref}}{z_a}\right)^{\mathrm{Kshear}_a} \left(\frac{z_c}{z_{ref}}\right)^{\mathrm{Kshear}_c} \tag{21}$$

Using equation (21), the anemometer wind speed Ws_a at the weather station height z_a is extrapolated to a reference height z_{ref} (in this case 100 m) to remove ground roughness dependence represented by the parameter Kshear_a. The values from different anemometer locations may then be interpolated, using equation (20) as described in section 3.2.1, to provide a wind speed estimate at the reference height for a particular geographical location. The ground roughness at this location is then taken into account through the coefficient Kshear_c along with the conductor height z_c in equation (21) to estimate the wind speed (Ws) across the overhead line.

3.2.3 Soil parameter estimation

Electric cable ratings are dependent on soil temperature and soil thermal resistivity, as well as cable construction, burial layout, and burial depth (which is typically 0.8–1 m). MetOffice [**30**] datasets contain information regarding soil temperatures at a depth of 0.3 m. However, no information was available from this source regarding soil thermal resistivity. Depth-dependent soil temperature distributions may be calculated using the Fourier law [**31**] as shown in equation (22)

$$\frac{\mathrm{d}T_{\mathrm{s}}}{\mathrm{d}t} = \frac{\mathrm{d}}{\mathrm{d}z}\left[\delta_{\mathrm{s-T}}(\theta)\frac{\mathrm{d}T_{\mathrm{s}}}{\mathrm{d}z}\right] \tag{22}$$

Boundary conditions were set up with a constant temperature of 10 °C at a depth of 2 m for the lower layer and MetOffice soil temperature readings for the upper layer. Soil thermal resistivity $\rho_{\mathrm{s-T}}$, may be calculated from equation (23) using the soil thermal diffusivity $\delta_{\mathrm{s-T}}$, the dry soil density $\rho_{\mathrm{s-density}}$, and the soil thermal capacity $C_{\mathrm{s-T}}$

$$\rho_{\mathrm{s-T}} = (\delta_{\mathrm{s-T}}\ \rho_{\mathrm{s-density}} C_{\mathrm{s-T}})^{-1} \tag{23}$$

Soil thermal diffusivity $\delta_{\mathrm{s-T}}$ and soil thermal capacity are influenced by soil composition N and water content θ and can be calculated using equations (24) and (25) [**32**]

$$\delta_{\mathrm{s-T}}(\theta) = -14.8 + 0.209\,N + 4.79\theta \tag{24}$$

$$C_{\mathrm{s-T}} = -0.224 - 0.00561\,N + 0.753\,\rho_{\mathrm{s-density}} + 5.81\theta \tag{25}$$

Ground water content may be determined using the closed form of Richard's equation [**33**] as described in equation (26) after the calculation of the unsaturated hydraulic diffusivity $\delta_{\mathrm{s}-\theta}(\theta)$ and the unsaturated hydraulic conductivity $k_{\mathrm{s}-\theta}(\theta)$ as described in reference [**34**]

$$\frac{\mathrm{d}\theta}{\mathrm{d}t} = \frac{\mathrm{d}}{\mathrm{d}z}\left[\delta_{\mathrm{s}-\theta}(\theta)\frac{\mathrm{d}\theta}{\mathrm{d}z} + k_{\mathrm{s}-\theta}(\theta)\right] \tag{26}$$

In order to solve equation (26), boundary and initial conditions must be specified. A constant water content equal to the saturation value was set at a depth of 2.5 m, corresponding to the water table. Furthermore, the ground-level water content was linked to MetOffice rainfall values l_{r} using the model described in equation (27), where Krain_1 and Krain_2 can be calculated using [**35**]

$$\frac{\mathrm{d}\theta}{\mathrm{d}t} = -\mathrm{Krain}_1\theta t + \mathrm{Krain}_2 lr(t) \tag{27}$$

3.2.4 Sensitivity analysis

It can be seen from the work presented above that there are many diverse parameters that affect the rating of power system components. These parameters may be categorized into component properties, geographical properties, and environmental conditions. A list of the parameters used in the offline simulations is given in Table 1. For the purposes of the offline simulations, component properties and geographical properties were assumed to be constants of the system. Therefore, the thermal models presented were underpinned by an extensive and rigorous sensitivity analysis that gave an indication of the influence of environmental conditions on power system component ratings. The sensitivity analysis was carried out such that one parameter was varied at a time while all other parameters were maintained at their credible mid range values. A summary of the results of this analysis is presented in Table 2 and shows the percentage variation in component rating for a given percentage variation of environmental conditions from credible mid-range parameter values. Moreover, in the sensitivity analysis, the soil thermal resistance is assumed to take into account the effect of rainfall. It can be seen that the rating of overhead lines is particularly sensitive to the environmental conditions of wind speed, wind direction, and ambient temperature, and that the rating of electric cables is particularly sensitive to the thermal resistance of the surrounding medium.

Furthermore, a series of credible worst case scenarios were selected to give an indication of the minimum component rating that would potentially result from the deployment of a real-time rating system. In this worst case analysis the following values were specified: Ta = 38.5 °C (the maximum temperature registered in England, August 2003) [**30**]; Ws = 0, Wd = 0, Sr = 0 W/m^2 (from studies carried out at CERL, the highest conductor temperature excursions are recorded at times of low wind speed where there is negligible solar radiation) [**36**]; Ts = 20 °C [**2**] and $\rho_{\mathrm{s-T}} = 3$ Km/W [**24**]. The resulting rating multipliers of the standard static component rating were 0.81, 0.86, and 0.78 for overhead lines, electric cables, and power transformers, respectively.

4 SIMULATION APPROACH

In Fig. 2, a general description of the simulation algorithm, with the different software applications, is provided. The algorithm uses three databases to store network component data, weather measurement data, and calculated rating data, respectively. It comprises two main applications: the environmental condition processor for simulating weather data, described in section 3.2 and the CTMs for calculating component ratings, as described in section 3.1. A third application

Table 1 Parameters affecting the rating of power system components

	Component properties			Geographical properties			Environmental conditions		
Component type	Name	Symbol	Unit	Name	Symbol	Unit	Name	Symbol	Unit
Overhead line	Conductor diameter	D	(m)	Ground roughness factor	Kshear	(dimensionless)	Wind speed	Ws	(m/s)
	Conductor resistance per unit length	r	(Ω/m)	Conductor height	z_c	(m)	Wind-conductor angle	Wd	(rad)
	Absorption coefficient	α	(dimensionless)	Weather station height	z_a	(m)	Air temperature	Ta	(°C)
	Emission coefficient	ε	(dimensionless)	Distance between weather station and component	$d_{i,k}$	(m)	Solar radiation	Sr	(W/m^2)
Electric cable	Rated ampacity	I_0	(A)	Sum of sand and clay percentage	N	(dimensionless)	Soil thermal resistivity	R_T	(m K/W)
				Normalized soil water loss	Krain_1	(day^{-1})	Soil temperature	Ts	(°C)
	Voltage	V	(V)	Normalized net rainfall coefficient	Krain_2	(day^{-1}/mm)			
				Distance between weather station and component	$d_{i,k}$	(m)	Rainfall	l_r	(mm)
Power transformers	Oil exponent	x	(dimensionless)	Distance between weather station and component	$d_{i,k}$	(m)	Air temperature	Ta	(°C)
	Winding exponent	y	(dimensionless)						
	Ratio of windings to core losses	R	(dimensionless)						

Table 2 Environmental condition sensitivity analysis (parameter variation versus rating variation)

Parameter (credible mid-range value)		Overhead lines (Lynx 50)				Electric cables (150 mm^2)		Transformers (ONAN 45)
		Ws (8 m/s)	Wd $\left(\frac{\pi}{4}\text{rad}\right)$	T_a (15 °C)	Sr (500 W/m^2)	R_T (1.2 WK/m)	T_s (10 °C)	T_a (15 °C)
Variation from mid-range value	−50%	−23.86%	−11.38%	+10.80%	+0.72%	+31.46%	+3.00%	+6.11%
	−25%	−10.73%	−4.97%	+5.52%	+0.36%	+12.36%	+1.50%	+3.09%
	−10%	−4.07%	−1.85%	+2.24%	+0.15%	+6.18%	+0.60%	+1.24%
	10%	+3.84%	+1.66%	−2.29%	−0.15%	−4.49%	−0.60%	−1.25%
	25%	+9.22%	+3.82%	−5.81%	−0.36%	−8.99%	−1.50%	−3.16%
	50%	+17.40%	+6.54%	−11.96%	−0.73%	−16.48%	−3.00%	−6.40%

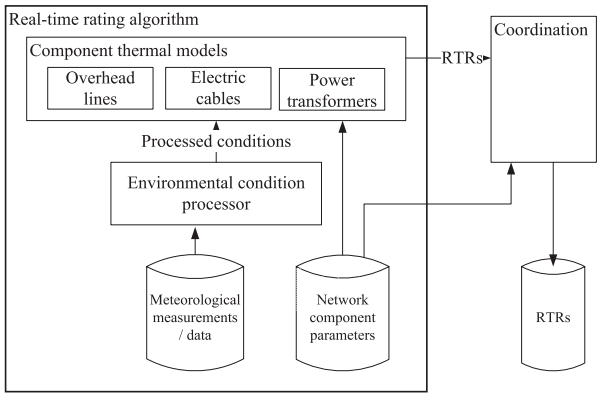

Fig. 2 Simulation scheme

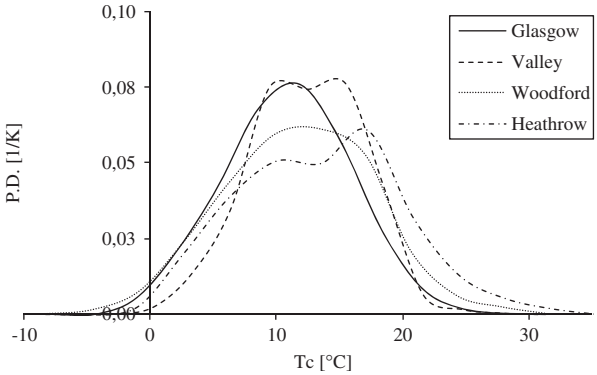

Fig. 4 Air temperature PD

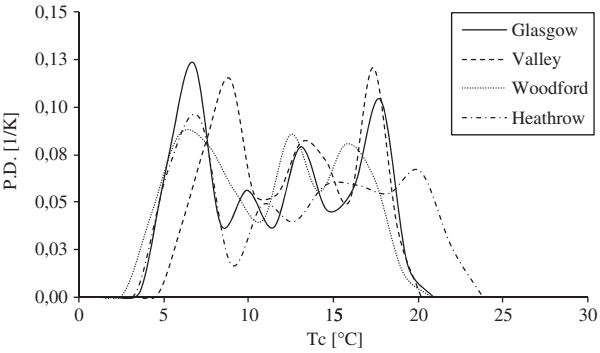

Fig. 5 Soil temperature PD

(coordination) was added to supervise the simulation dataflow. The offline simulation algorithm computes component real-time ratings with a temporal resolution of 1 h.

4.1 Weather

MetOffice datasets were used, referring to four British airports: Bishopton (Glasgow), Valley (Anglesey), Woodford (Manchester), and Heathrow (London). The data comprised hourly averages of wind speed, wind direction, air temperature, solar radiation, and soil temperature throughout the calendar year 2005. In Figs 3 to 5, the data from those sites are summarized and compared.

In Fig. 3, it is possible to observe the different site characteristics for the wind speed: Valley, on the west coast of Wales, is the windiest area with the highest maximum wind speed values and a probability distribution (PD) with the smallest peak. Heathrow, which is located in an urban environment, has wind speeds that are generally lower and more concentrated in the range between 2–7 m/s. As seen in Fig. 4, air temperature appears to be the least variable parameter. Different sites may be differentiated by average temperature values. In Fig. 5, the behaviour of the soil temperature is illustrated. Whereas the air temperature shows a variation with one peak across the year, soil temperature appears to vary with multiple peaks.

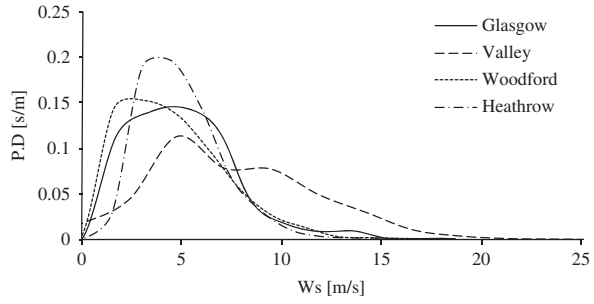

Fig. 3 Wind speed PD

Regarding wind direction, the presence of prevalent winds from the west and the north-west in the range 180–360° was noted for all areas. Some areas also exhibited site-specific prevalent wind directions, for example from the south-west in Woodford and from north-north-west in Bishopton. Regarding solar

radiation, no significant differences between the four sites were found.

4.2 Networks

In order to simulate in a rigorous manner the influence of environmental conditions on power system ratings, three network models were adapted from the United Kingdom Generic Distribution Systems (UKGDSs) [**37**], each of which contain the three component types considered in this article. Moreover, a portion of the ScottishPower EnergyNetworks distribution network was included in simulations as this will be instrumented in the near future for RTR validation purposes. Voltage levels in the four networks studied vary from 6.6 to 132 kV.

The ScottishPower EnergyNetworks Site network is shown in Fig. 6 and has a meshed topology, with a prevalence of Lynx 175 mm^2 overhead lines. The network also has eleven electric cable circuits of 150 mm^2 at the 33 kV level and 13 power transformers rated at 45 MVA, 60 MVA, 90 MVA, and 240 MVA. Topological representations of the UKGDSs can be found in Appendix 3. Technical characteristics for the overhead lines may be found in reference [**21**]. UKGDS_A has six overhead line circuits with Zebra and Lynx conductors rated at 50, 65, and 75 °C, 12 electric cables circuits with 150 and 240 mm^2 conductors, and 16 transformers with ratings from 14 to 500 MVA. UKGDS_B consists of six overhead lines with Zebra and Lynx conductors, eight electric cable circuits with 150 mm^2 conductors and 13 power transformers, with ratings from of 21 and 500 MVA. UKGDS_C is characterized by a prevalence of electric cable circuits and power transformers. It comprises two overhead lines with Zebra conductors, 12 electric cable circuits with 150 and 240 mm^2 conductors and 18 power transformers with ratings from 14 to 500 MVA. Electrical parameters for modelling the UKGDSs may be found in reference [**37**].

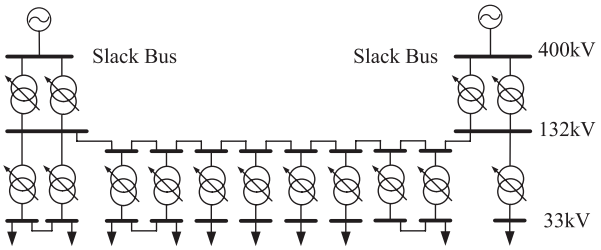

Fig. 6 Site trial

5 RESULTS AND ANALYSIS

In order to quantify the influence of environmental conditions on power system ratings, simulations were carried out on the networks described in section 4.2 subjected to a range of UK climatic conditions. For each scenario the minimum, maximum, and average rating values together with additional potential annual energy throughput (in GWh) were calculated and the results are tabulated in Appendix 3. These data may be summarized as follows: the average rating of overhead lines ranged from 1.70 to 2.53 times the static rating with minimum and maximum ratings of 0.81 and 4.23, respectively. The average rating of electric cables ranged from 1.00 to 1.06 times the static rating with minimum and maximum ratings of 0.88 and 1.23, respectively. The average rating of power transformers ranged from 1.06 to 1.10 times the static rating with minimum and maximum ratings of 0.92 and 1.22, respectively.

Simulations results were analysed in three different ways:

(a) comparing the rating cumulative probabilities of different component types against one another within the same network and environmental conditions;
(b) comparing the GWh headroom of four different overhead line types subjected to four different UK climates;
(c) assessing the increased energy throughput from DG that may be accommodated by using RTRs, as opposed to seasonal ratings, for a single overhead line.

5.1 Rating comparison of different component types

In Table 3, the simulation results for the site network exposed to the Valley climatic scenario are given. For each component type the average, minimum, and maximum RTRs are given, and the additional headroom theoretically obtainable with RTRs (as opposed to seasonal ratings) is quantified. The additional headroom was calculated by summing the difference

Table 3 Simulation results for SITE network components exposed to the Valley climatic scenario

Component	Static rating (MVA)	RTR average (MVA)	RTR minimum (MVA)	RTR maximum (MVA)	Additional RTR headroom (GWh/year)
Electric cable (150 mm^2)	21	21	19	23	1.83
Power transformer (ONAN 45)	45	48	44	52	30.7
Power transformer (OFAN 240)	240	257	235	276	149.1
Overhead line (Lynx 50)	89	253	107	419	1342

between the RTR and the seasonal ratings across the year in hourly intervals. For overhead lines, the seasonal ratings reported in reference [**21**] were used for this calculation. In Fig. 7(a), the rating cumulative probabilities for the four components described in Table 3 are shown. RTRs have been normalized using the static component rating. From inspection of Fig. 7(a) it is evident that overhead lines show the greatest potential for rating exploitation. As seen in Fig. 7(b), electric cable and power transformer ratings have a limited variability. This is because soil temperature, soil thermal resistivity, and air temperature are much less variable than wind speed and direction and it is these latter parameters that greatly influence the rating of overhead lines. This is in agreement with the analysis in section 4.1. By representing component ratings as cumulative probabilities, the potential comparison with power transfer duty (PTD) curves is facilitated. Moreover, DNOs are able to specify a probability with which they are comfortable to operate a particular component and an assessment of the corresponding rating may be made.

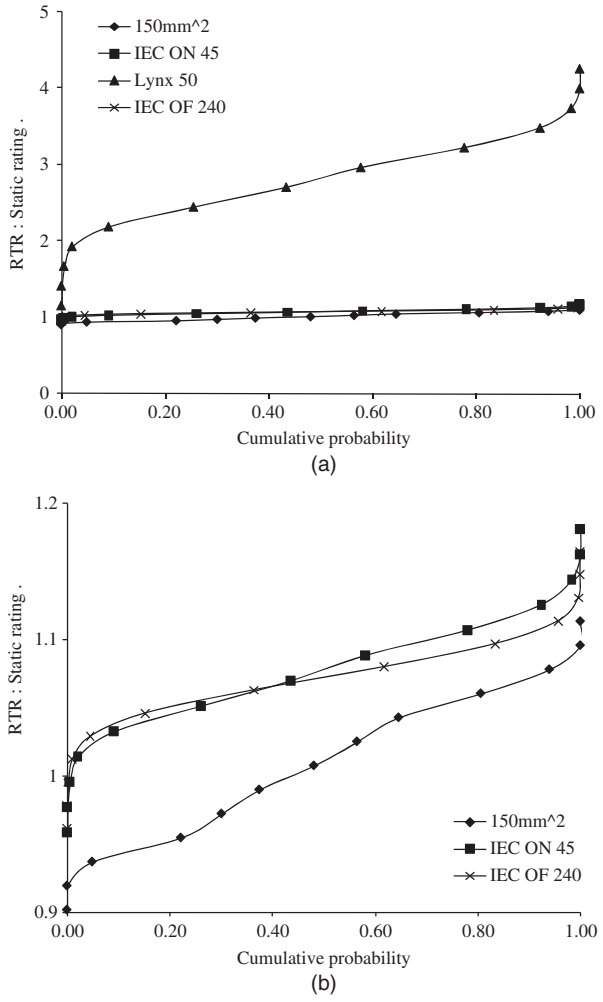

Fig. 7 (a) Rating cumulative probability for SITE network components exposed to the Valley climatic scenario and (b) magnified rating cumulative probability for SITE network components exposed to the Valley climatic scenario

5.2 Rating comparison of overhead line types

It was shown in Fig. 7 and Table 3 that overhead lines exhibit the greatest potential for RTR exploitation. Therefore, in Fig. 8 the average headroom for different overhead line types, exposed to different climatic scenarios, is compared. For each case, the average headroom is given along with the minimum and maximum headroom. Headroom variations exist since differences in component orientation and component location result in rating variations. Variation bars are representative of the possible headroom ranges simulated. The size of the variation band is determined by the number of components existing within each case study network. A large variation band represents a frequently occurring component. By inspecting the position of the lower variation band it is evident that the additional headroom is greater for conductors with a greater initial static rating, and this effect is accentuated by conductor rated temperature. This is because the conductor temperature rise above ambient temperature multiplies the heat exchange coefficient as seen in equation (6).

Regarding the influence of the climates, Valley exhibits the highest average wind speed values and Bishopton the lowest average temperatures as seen in Figs 3 and 4. Since overhead line ratings are more sensitive to wind speed than air temperature the climate of Valley leads to the greatest overhead line power transfer headroom. Clearly from this evidence the value of adopting an RTR system is dependent on geographical location. Therefore, any utility interested in deploying an RTR system should conduct a site specific study to assess the value of RTRs as the output varies according to climate, and therefore the economic value is

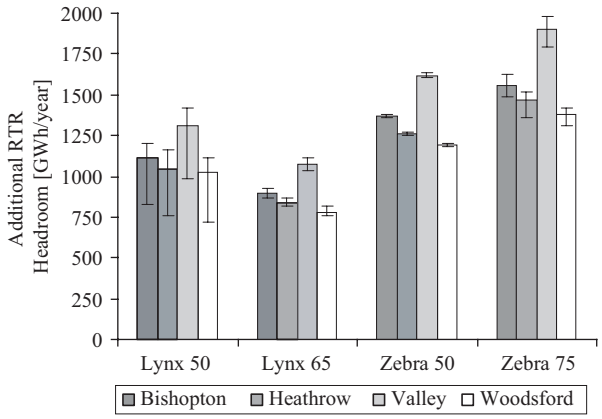

Fig. 8 Influence of different UK climates on overhead lines power transfer headroom

different. Furthermore, the quantification assessment presented in Fig. 8 allows a conservative approach to be adopted in developing RTR systems since an investor may choose to utilize the rating seen at the bottom of the variation band.

5.3 Power transfer accommodation assessment

This section presents a methodology for quantifying the practically exploitable headroom for the specific case of a 132 kV Lynx overhead line conductor with a maximum operating temperature of 50 °C subjected to the Valley climate in the site network. This location was selected since it is an area attractive to prospective wind farm development. The practically exploitable headroom was quantified as follows: meteorological wind data from the Valley site were used together with the GE 3.6 MW wind turbine power curve [**38**] to assess the power generated throughout the year and transferred through the overhead line conductor. Clearly the exposure of the overhead line conductor to environmental conditions varies as a function of line orientation and ground roughness. Therefore, when making an assessment of the RTR, the overhead line was divided into sections to represent the variation in these parameters. The section of overhead line with the lowest rating represents the weakest point of the overhead line system and therefore this lowest rating was adopted as the RTR for the entire overhead line. By comparing the power transfer across the year with the overhead line rating, for both seasonal and RTR regimes, the wind farm installed capacity was sized to correspond to a line cumulative overload probability of 1/1000 (8.76 h/annum). Results are summarized in Fig. 9, where the line RTR cumulative probability, along with the inverse cumulative probability for two different PTDs, seasonal and switchgear ratings are represented. The cumulative probability curve (the RTR distribution) may be interpreted by selecting an acceptable probability at which the component may be operated, e.g. 0.1 (10 per cent). This corresponds to a rating of 149 MVA. Therefore, there is the probability of 10 per cent that during the course of the year the rating is $\leqslant$149 MVA (conversely there is a 90 per cent probability that the rating is >149 MVA). Similarly the inverse cumulative probability (PTD curves 1 and 2) may be interpreted by selecting a PTD value, e.g. 76 MVA on PTD 2 curve. This corresponds to a probability of 10 per cent. Therefore there is a probability of 10 per cent that during the course of the year PTD 2 is $\geqslant$76 MVA (conversely there is a 90 per cent probability that the PTD is <76 MVA). For the seasonal rating regime an installed capacity of 89 MW (25 turbines) could be accommodated and an annual energy yield from the wind farm of 245 GWh could be attained. For the RTR regime, an installed capacity of 137 MW (38 turbines) could be accommodated and an annual energy yield from the wind farm of 377 GWh could be attained. This represents an increase in installed capacity and annual energy yield of 54 per cent, which is specific to the weather data used, the type of conductor, the risk at which the DNO is prepared to operate the asset and the type of turbine selected. An annual energy yield increase of 54 per cent would significantly enhance the revenue stream of a wind farm developer, demonstrating the value of an RTR approach. However, this is only 10 per cent of the theoretical average additional headroom for this type of overhead line conductor exposed to the Valley climate, as seen in Fig. 8. Installing a larger capacity of DG together with the adoption of an online power output

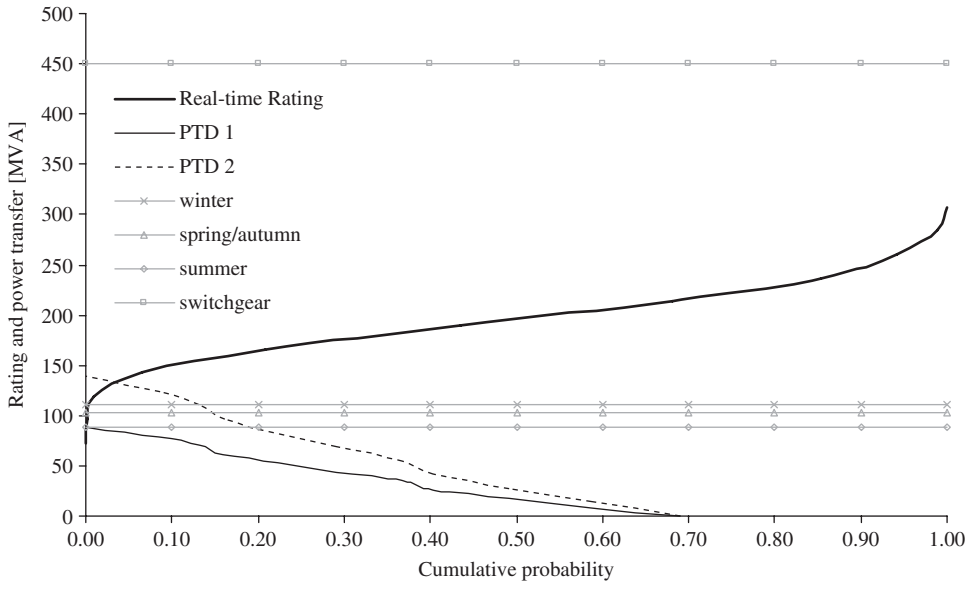

Fig. 9 Cumulative probability comparison for a Lynx conductor in the Valley scenario

controller [**39**] could allow a greater percentage of the theoretical average additional headroom to be realized while maintaining an acceptable level of risk to the DNO.

An estimation of the losses associated with the two PTD curves was carried out in the following way: from the average environmental conditions at the Valley site and from the average value of the power transfer, the average conductor temperature was calculated. From this, the average conductor resistance was calculated and, using the hourly values of the power transfer, it was possible to obtain the losses arising from Joule effect for the whole year. Loss values of 0.12 and 0.19 per cent of the entire annual energy throughput were obtained for PTD 1 and PTD 2, respectively.

6 CONCLUSIONS

This article described the offline simulation of power system thermal models populated with historical environmental conditions in order to derive RTRs. This information was used to quantify (in GWhs) the exploitable headroom that may be achieved by implementing an RTR system within distribution networks. Power system component models were developed based on IEC standards and environmental conditions were corrected and interpolated to represent, as closely as possible, actual network operating conditions. Component data and environmental condition data were used to populate the models in simulation to derive component RTRs. For a wide number of power system components and environmental conditions the minimum, maximum, and average ratings were quantified together with the additional power transfer headroom. This information is likely to be of use to DNOs in planning and operating future distribution networks that may be reaching a level of power transfer saturation. It was found that overhead lines exhibit the greatest potential RTR exploitation since they exhibit the greatest rating variability. Furthermore, it was found that power transformers and electric cables have a slight RTR exploitation potential relative to overhead lines. The value of adopting an RTR system is dependent on geographical location. Therefore any utility interested in deploying an RTR system should conduct a site specific study to assess the value of RTRs as the output varies according to climate, and therefore the economic value is different.

The increase in power transfer from DG that could be accommodated through an RTR system implementation was investigated. For a Lynx overhead line conductor with a maximum operating temperature of 50 °C it was found that a GWh energy throughput increase of 54 per cent could be accommodated by operating the line with an RTR regime as opposed to a seasonal rating regime. Work is continuing in this area to realize the potential of RTR system implementations.

ACKNOWLEDGEMENTS

The authors wish to acknowledge the Department for Innovation, Universities and Skills for funding, and the staff from AREVA T&D, Imass, PB Power, ScottishPower EnergyNetworks, and the MetOffice for their valuable input to this work.

REFERENCES

1 IEC TR 1597. Overhead electrical conductors – calculation methods for stranded bare conductors, 1995.
2 IEC 60287. Electric cables – calculation of the current rating, 1994.
3 IEC 60076-7. Power transformers – part 7: loading guide for oil-immersed power transformers, 2008.
4 **Neumann, A., Taylor, P., Jupe, S., Michiorri, A., Goode, A., Curry, D.,** and **Roberts, D.** Dynamic thermal rating and active control for improved distribution network utilisation. In PowerGrid 08, Milan, Italy, 2008.
5 **Stephen, R.** Description and evaluation of options relating to uprating of overhead transmission lines. *Electra*, 2004, **B2-201**, 1–7.
6 **Hoffmann, S. P.** and **Clark, A. M.** The approach to thermal uprating of transmission lines in the UK. *Electra*, 2004, **B2-317**, 1–8.
7 **Soto, F., Latorre, J.,** and **Wagensberg, M.** Increasing the capacity of overhead lines in the 400 kV Spanish transmission network: real time thermal ratings. *Electra*, 1998, **22–211**, 1–6.
8 Available at http://www.wasp.dk, accessed January 2008.
9 **Douglass, D. A.** and **Edris A. A.** Real-time monitoring and dynamic thermal rating of power transmission circuits. *IEEE Trans. Power Deliv.*, 1996, **11**(3), 1407–1418.
10 **Douglass D. A., Edris A. A.,** and **Pritchard G. A.** Field application of a dynamic thermal circuit rating method. *IEEE Trans. Power Deliv.*, 1997, **12**(2), 823–831.
11 **Nuijten, J. M. A.** and **Geschiere, A.** Future network planning and grid control. In Proceedings of the International Conference on *Future power systems*, Amsterdam, The Netherlands, 16–18 November, 2005.
12 **Helmer, M.** Optimized size of wind power plant transformer and parallel operation. In Wind Power for the 21st century, Kassel, Germany, 25–27 September 2000.
13 **Belben, P. D.** and **Ziesler, C. D.** Aeolian uprating: how wind farms can solve their own transmission problems. In Proceedings of the World Wind Energy Conference and Exhibition, Berlin, July 2002.
14 **Piccolo, A., Vaccaro, A.,** and **Villacci, D.** Thermal rating assessment of overhead lines by Affine arithmetic. *Electr. Power Syst. Res.*, 2004, **71**(3), 275–283.
15 **Villacci, D.** and **Vaccaro, A.** Transient tolerance analysis of power cables thermal dynamic by interval mathematic. *Electr. Power Syst. Res.*, 2007, **77**, 308–314.

16 **Ippolito, L., Vaccaro, A.,** and **Villacci, D.** The use of affine arithmetic for thermal state estimation of substation distribution transformers. *COMPEL, Int. J. Comput. Math. Electr. Electron. Eng.*, 2004, **23**(1), 237–249.
17 **House, H. E.** and **Tuttle, P. D.** Current carrying capacity of ACSR. *IEEE Trans. Power Appar. Syst.*, 1959, **78**(3), 1169–1177.
18 **Morgan, V. T.** The thermal rating of overhead-line conductors. 1. The steady-state thermal mode. *Electr. Power Syst. Res.*, 1982, **5**(2) 119–139.
19 WG 22.12. The thermal behaviour of overhead conductors – section 1. *Electra*, 1992, **144**(3), 107–125.
20 IEEE 738. Standard for calculating the current-temperature relationship of bare overhead conductors, 1993.
21 ENA ER P27. Current rating guide for high voltage overhead lines operating in the UK distribution system, 1986.
22 **Neher, J. H.** and **McGrath, M. H.** The calculation of the temperature rise and load capability of cable systems. *AIEE Trans.*, 1957, **76**(3), 752–772.
23 IEEE 835. IEEE Standard Power Cable Ampacity Tables, 1994.
24 ENA ER P17. Current rating for distribution cables, 2004.
25 **Susa, D., Lehtonen, M.,** and **Nordman, H.** Dynamic thermal modelling of power transformers. *IEEE Trans. Power Deliv.*, 2005, **20**(1), 197–204.
26 ANSI/IEEE, C57.92. Guide for loading mineral oil-immersed power transformers up to and including 100 MVA with 55 °C or 65 °C average winding rise, 1981.
27 ENA ER P15. Transformers loading guide, 1971.
28 **Shepard D.** A two-dimensional interpolation function for irregularly-spaced data. In Proceedings of the 23rd ACM National Conference, 1968, pp. 517–524.
29 IEC 60826. Loading and strength of overhead transmission lines, 1991.
30 Available at www.metoffice.gov.uk, accessed January 2008.
31 **Nairen, D., Qinyun, L.,** and **Zhaohong, F.** Heat transfer in ground heat exchangers with groundwater advection. *Int. J. Therm. Sci.*, 2004, **43**, 1203–1211.
32 **Abu–Hamdeh, N. H.** Thermal properties of soil as affected by density and water content. *Biosyst. Eng.*, 2003, **86**(1), 97–102.
33 **Celia, M., Boulotas, E.,** and **Zarba, R.** A general mass-conservative numerical solution for the unsaturated flow problem. *Water Resour. Res.*, 1990, **26**(7), 1483–1496.
34 **Van Genuchten, M.** A closed for equation for predicting the hydraulic conductivity of unsaturated soils. *Soil Sci. Soc. Am. J.*, 1980, **44**, 892–898.
35 **Rodríguez-Iturbe, I., Isham, V., Cox, D. R., Manfreda, S.,** and **Porporato, A.** Space-time modelling of soil moisture: stochastic rainfall forcing with heterogeneous vegetation. *Water Resour. Res.*, 2006, **42**, 1–11.
36 **Price, C.** and **Gibbon, R.** Statistical approach to thermal rating of overhead lines for power transmission and distribution. *IEE Proc.*, 1983, **130**(5), 245–256.
37 Available at http://www.sedg.ac.uk/ukgds.htm, accessed January 2008.
38 **Energy, G. E.** 3.6 MW Offshore Series Wind Turbine, 2005.
39 **Jupe, S. C. E., Taylor, P. C., Michiorri, A.,** and **Berry, C. J.** An evaluation of distributed generation constrained connection managers. In Proceedings of the MedPower 2008 – 6th Mediterranean Conference and Exhibition on *Power generation, transmission and distribution*, Thessaloniki, Greece, 2–5 November 2008.

APPENDIX 1

Notation

A	conductor cross-sectional area (m^2)
C_{s-T}	soil thermal capacitance (J/kg/K)
d	internal diameter (m)
d_{i-k}	distance from weather station to component (m)
D	external diameter (m)
E	Young's modulus of conductor (Pa)
g	gravitational acceleration (m/s^2)
Gr	Grashof number
H	tension (N)
i	index
I	current (A)
I_0	electric cable rated current (A)
k	number of weather stations
$k_{s-\theta}$	soil unsaturated hydraulic conductivity (m/s)
K	load ratio
K_{dir}	wind direction influence coefficient
$K_{dir-1,2,3}$	wind direction coefficient constants
$K_{nat-1,2}$	natural convection coefficients
$Krain_1$	normalized soil water loss (day^{-1})
$Krain_2$	normalized net rainfall coefficient (day^{-1}/mm)
$Kshear_{,a}$	ground roughness factor at the weather station
$Kshear_{,c}$	ground roughness factor at the conductor
l_r	rainfall (mm)
L	span (m)
m	mass per unit length (kg/m)
n	number of conductors in the cable
N	sum of sand and clay percentage
Nu	Nusselt number
P	real power set point dispatched to generator (MW)
Pr	Prandtl number
q_c	heat exchanged per unit length by convection (W/m)
q_d	dielectric loss per length unit (W/m)
q_r	heat exchanged per unit length by irradiation (W/m)
q_s	heat gained per unit length by solar radiation (W/m)
Q	reactive power set point dispatched to generator (MVAr)

r	conductor resistance per length unit (Ω/m)
r_{windings}	transformer windings resistance (Ω)
R	ratio between windings and core losses
R_{T}	thermal resistance (m K/W)
$R_{\text{T,HE}}$	transformer heat exchanger thermal resistance (m K/W)
$R_{\text{T,W}}$	windings to oil thermal resistance (m K/W)
Re	Reynolds number
S	sag (m)
Sr	solar radiation (W/m)
t	time (s)
T_{a}	air temperature (K)
T_{c}	conductor temperature (K)
T_{HS}	hot spot temperature (K)
T_{s}	soil temperature (K)
T_{TO}	top oil temperature (K)
V	voltage (V)
Wd	wind conductor angle (rad)
Ws	wind speed (m/s)
x	transformer oil exponent
y	transformer winding exponent
z_{b}	cable burial depth (m)
$z_{\text{c,ref,a}}$	conductor, reference, and weather station heights for wind correction (m)
Z_k	generic environmental condition parameter
α	absorption coefficient
β	conductor thermal expansion coefficient (K^{-1})
$\delta_{\text{s-T}}$	soil thermal diffusivity (m^2/s)
$\delta_{\text{s}-\theta}$	soil unsaturated hydraulic diffusivity (m^2/s)
ΔT	temperature difference (K)
ε	emission coefficient
θ	gravimetric water content
λ	air thermal conductivity (W/m/K)
$\lambda_{1,2}$	ratio between metal sheath losses and total losses
ν	kinematic viscosity (m^2/s)
ξ_{T}	electric cables rating temperature correction factor (K^{-1})
ξ_{ρ}	electric cables rating thermal resistivity correction factor (W/m/K)
$\rho_{\text{s-density}}$	dry soil density (kg/m^3)
$\rho_{\text{s-T}}$	soil thermal resistivity (m K/W)
$\sigma_{\text{S-B}}$	Stephen–Boltzmann constant ($\text{W/m}^2/\text{K}^4$)

APPENDIX 2

UKGDS networks

In Figs 10 to 12, a description of the UKGDS networks used is given.

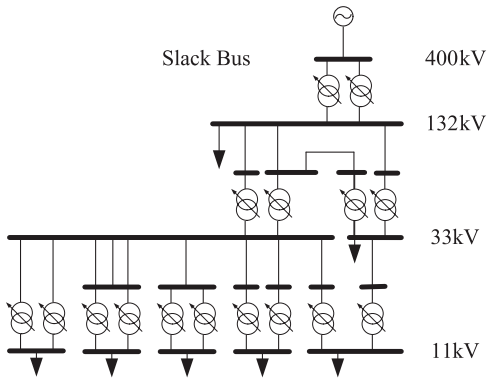

Fig. 10 UKGDS_A

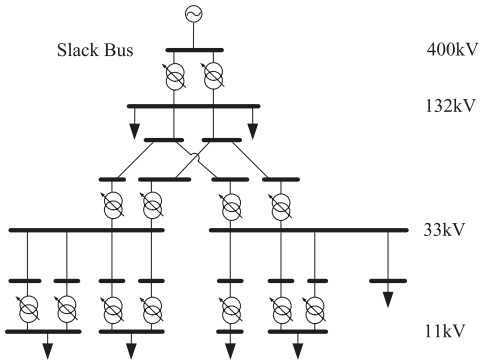

Fig. 11 UKGDS_B

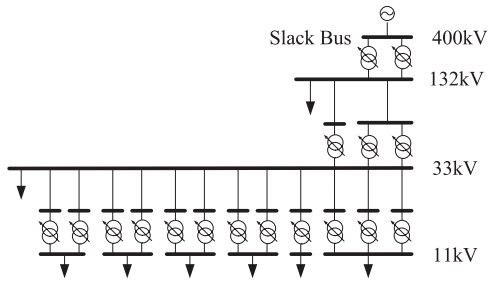

Fig. 12 UKGDS_C

APPENDIX 3

Simulation results

This section provides a summary of the simulation results. For each climate and each network, the average, minimum, and maximum calculated ratings are given in Table 4, along with the static rating and the average annual headroom for each component type. Overhead lines are described with their conductor codes and rated temperature, electric cables with the

Table 4 Simulation results, component ratings, and theoretical headroom

Component	Static rating (MVA)	RTR average (MVA)	RTR minimum (MVA)	RTR maximum (MVA)	RTR headroom (GWh/year)
Overhead line (Lynx 50)	89	213	84	419	988.48
Overhead line (Lynx 65)	108	220	94	390	898.94
Overhead line (Zebra 50)	154	328	125	595	1359.66
Overhead line (Zebra 75)	206	402	178	731	1576.20
Electric cable (150 mm^2)	21	21	18	25	2.94
Electric cable (240 mm^2)	30	32	27	37	13.33
Power transformer (ODAF 500)	500	532	469	580	282.41
Power transformer (OFAF 240)	240	258	223	284	154.75
Power transformer (ONAN 100)	100	108	92	120	70.80
Power transformer (ONAN 90)	90	97	83	108	63.72
Power transformer (ONAN 60)	60	65	55	72	42.48
Power transformer (ONAN 45)	45	49	41	54	31.87
Power transformer (ONAN 23)	23	25	21	28	16.28
Power transformer (ONAN 21)	21	23	19	25	14.87
Power transformer (ONAN 14)	14	15	13	17	10.80

conductor cross-sectional area, and power transformers with the cooling method and the rating. In Table 5, a list of the components within each network is given.

Table 5 Network components

Network	Component	Number of components
SITE	Overhead line (Lynx 50)	11
SITE	Electric cable (150 mm^2)	11
SITE	Power transformer (OFAF 240)	5
SITE	Power transformer (ONAN 45)	5
SITE	Power transformer (ONAN 60)	2
SITE	Power transformer (ONAN 90)	1
UKGDS_A	Overhead line (Lynx 50)	1
UKGDS_A	Overhead line (Lynx 65)	3
UKGDS_A	Overhead line (Zebra 75)	2
UKGDS_A	Electric cable (150 mm^2)	4
UKGDS_A	Electric cable (240 mm^2)	10
UKGDS_A	Power transformer (ODAF 500)	1
UKGDS_A	Power transformer (ONAN 23)	1
UKGDS_A	Power transformer (ONAN 60)	6
UKGDS_A	Power transformer (ONAN 90)	2
UKGDS_A	Power transformer (ONAN 14)	2
UKGDS_B	Overhead line (Lynx 65)	4
UKGDS_B	Overhead line (Zebra 75)	2
UKGDS_B	Electric cable (150 mm^2)	7
UKGDS_B	Electric cable (240 mm^2)	1
UKGDS_B	Power transformer (ODAF 500)	2
UKGDS_B	Power transformer (ONAN 100)	1
UKGDS_B	Power transformer (ONAN 21)	2
UKGDS_B	Power transformer (ONAN 23)	5
UKGDS_B	Power transformer (ONAN 45)	2
UKGDS_B	Power transformer (ONAN 90)	1
UKGDS_C	Overhead line (Zebra 50)	2
UKGDS_C	Electric cable (150 mm^2)	1
UKGDS_C	Electric cable (240 mm^2)	9
UKGDS_C	Power transformer (ODAF 500)	1
UKGDS_C	Power transformer (ONAN 60)	1
UKGDS_C	Power transformer (ONAN 14)	1
UKGDS_C	Power transformer (ONAN 23)	10
UKGDS_C	Power transformer (ONAN 60)	1
UKGDS_C	Power transformer (ONAN 14)	2
UKGDS_C	Power transformer (ONAN 23)	1

FORECASTING REAL-TIME RATINGS FOR ELECTRICITY DISTRIBUTION NETWORKS USING WEATHER FORECAST DATA

Andrea MICHIORRI
Durham University – UK
andrea.michiorri@dur.ac.uk

Philip C. TAYLOR
Durham University – UK
p.c.taylor@dur.ac.uk

ABSTRACT

Currently the operators of electrical distribution networks face a number of challenges, such as load growth, the proliferation of distributed generation and ageing infrastructure. This is drawing attention to techniques which will allow more efficient asset utilisation and facilitate network dynamic management. Power system component real-time ratings are a cost effective solution for increasing network power transfer capacity. Instantaneous ratings can be used for this purpose, but distribution network operator decision making capability regarding network power flow management would be enhanced by the adoption of rating forecasts. Therefore this paper presents an investigation into the technical challenges and potential benefits of power system component rating forecasts. Weather forecasts are used with power system component thermal models and a state estimation technique for calculating rating forecasts at different time horizons.

1 INTRODUCTION

The rating of power system components is influenced by external parameters such as wind speed or air temperature, but the possibility of exploiting any increase in rating is problematic due to the variability of these external parameters. The technique referred to as "real-time ratings" involves real-time measurement of component temperatures and external parameters, such as air temperature or wind speed, in order to estimate component real-time ratings. Durham University is participating in a collaborative project with AREVA T&D, Imass, PB Power and ScottishPower EnergyNetworks, which aims to develop, install and test a power output control system for distributed generation informed by dynamic thermal ratings. Within this research, dynamic thermal ratings are defined as a time-variant rating which can be practically exploited without damaging components or reducing their lifetime. Actual environmental parameter measurements are used as the input to steady state thermal models and it is assumed that there are no outages (planned or unplanned) present within the electrical power system. Previous research [1] has demonstrated the suitability of real-time ratings for distributed generation power output control. This paper describes research with a different approach: weather forecasts are used for producing rating forecasts for different time horizons. A number of perceived benefits are expected to be yielded by this approach: Firstly a reduction in the number of on-site weather stations would be possible since the necessary information could be gathered from meteorological offices. Secondly the availability of rating forecasts would enhance the decision making capability of distribution network operators regarding network power flow management. Decisions would be informed by both the instantaneous ratings as well as rating forecasts for different time horizons. Another innovation described in this paper is the utilization of an estimation technique, in order to assess the error associated with rating forecasts. The knowledge of the error associated with the use of state estimation techniques would potentially increase the distribution network operator's confidence in real-time rating systems. This paper is structured in the following way: Firstly a survey of related work is presented. Then the methodology used in the research is described and the data used for the simulations and the case study are presented and finally simulation results are given and conclusions are drawn.

2 RELATED WORK

This work aims to combine two different areas of research: power system component real-time ratings and forecast techniques. Research has been carried out on the two topics, but not on their combination. The concept behind real-time ratings is described in [1]. The description of an application of a real-time rating system for the transmission network in the region of Madrid is provided in [2]. In this case, a low number of weather stations are used to estimate wind speed and direction over a wide geographical area and these estimations are used for calculating the real-time rating of an overhead line. The Electric Power Research Institute (EPRI) developed a similar system in the late 1990s considering overhead lines as well as other power system components. In [3] and [4] the system and field test results are reported. It was found that for a complete network, rating increases of up to 15% of the static value were possible. Forecast techniques have been applied to predict energy demand and wind power production. In [5] different techniques for load demand forecasts such as ARIMA modelling, adapted exponential smoothing and weather forecasts were compared and it was found that the combination of weather forecasts and exponential smoothing provide a better approximation for load demand forecasts beyond one hour ahead. Another approach, described in [6], bases the energy demand forecast on weather ensemble forecasts- a method which provides a probability distribution of the possible weather parameter values. This method is considered for a time horizon of up to 10 days. Regarding wind power forecasts, in [7] the system used in the on-line management of the Spanish transmission system is described. It makes use of several models and of adaptive estimation for the parameters. The final prediction is then obtained as a weighted average of the results of the

different models. From the analysis of the research described above, it is possible to highlight the requirement for work in the area of components real-time rating forecasts. This paper aims to suggest a possible methodology for filling this gap.

3 METHODOLOGY

The research described in this paper adopts the following approach: Component thermal models available in literature are used for calculating component rating for particular weather conditions. A state estimation technique based on Montecarlo method is used for giving a more complete description of the possible states of the system, providing the minimum, maximum, average and standard deviation of the rating forecasts according to the possible forecasted weather conditions. Historical weather forecast data from the National Oceanic and Atmospheric Administration (NOAA) [8] is used as inputs to these models.

3.1 State estimation

In this section a description of the algorithm responsible for the state estimation is given. The aim of this algorithm is to provide a reliable estimation of circuit ratings described by an appropriate cumulative probability function. The circuit has been divided in several parts, for taking into account different soil roughness and line orientation. This makes it possible to calculate descriptors such as the minimum, maximum, average and standard deviation of the rating estimation. The algorithm developed is briefly illustrated in Figure 1, where it is possible to see the following steps:

1. Forecasted weather data is read from an external source (in this case the database "a"). This data, comprising the minimum, maximum, average and standard deviation of each parameter in the given period, is described in Section 3.3.
2. A set of values for weather parameters is calculated in the following way: From the data read in "1" the parameters of a cumulative probability function are calculated. In this case the Beta probability function is used. A random value for the probability is selected and from the cumulative probability function the corresponding parameter value is found. This is repeated for each weather parameter.
3. For each component of the circuit the rating is calculated using the models described in Section 3.2.1. The result is stored temporary in "b".
4. The circuit rating is calculated selecting the minimum rating of each component. The results are temporarily stored in "c".
5. The steps from 2 to 4 are repeated for a fixed number of times N.
6. The precision of the result is compared with a predefined value. If the result is not acceptable, a new value for N is calculated and the steps from 2 to 5 are repeated
7. Circuit ratings stored in "c" are analysed in order to calculate the minimum, maximum, average value and standard deviation for each time horizon.

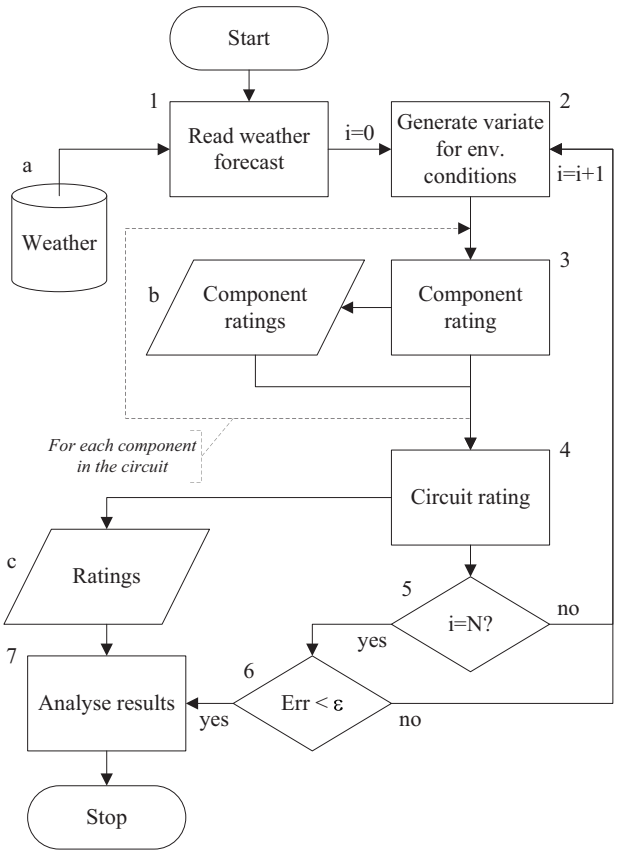

Figure 1: Montecarlo simulation basic flow chart

3.2 Models

3.2.1 Overhead line rating

The fundamental idea behind component ratings is that the operating temperature limit of the component must not be exceeded in order to avoid damaging the component. For overhead lines in particular, a temperature rise leads to a reduction in conductor tension and to an increase in the sag. Typical values for maximum conductor temperature are between 50 ºC and 90 ºC. Component temperature is not a constant value but depends upon the energy balance between the heat produced inside the component and the heat exchange on its surface. The energy dissipated depends on the load, however the heat exchange is mainly influenced by the temperature difference between cable and the environment and by other external factors such as wind speed or solar radiation. Considering the heat dissipated by the Joule effect (I^2R), the heat exchanged by convection (Q_c) and radiation (Q_r), and the solar radiation (Q_s), the energy balance for an overhead line conductor is described in Equation (1).

$$I^2R + Q_s = Q_c + Q_r \quad (1)$$

Different methods have been suggested for the calculation of each one of these parameters. In this research the methodology previously described in [1] was used.

3.2.2 Environmental condition interpolation

The inverse distance interpolation technique [9] allows environmental conditions to be determined over a wide geographical area using a reduced set of inputs. In this case meteorological inputs are the weather forecasts from the NOAA at a height of 10m from the ground. Wind speed is corrected with the method described in Section 3.2.3. Wind direction, air temperature and solar radiation values were included within interpolations but did not require the application of a correction factor. At each point in the geographical area (k) the value of the parameter (Z) representing the environmental condition can be estimated as a weighted average of the parameter values known at i points. The weighting factor is a function of the distance between the points as shown in Equation (2).

$$Z_k = \frac{\sum_i \frac{1}{d_{i,k}^2} Z_i}{\sum_i \frac{1}{d_{i,k}^2}} \quad (2)$$

3.2.3 Wind speed correction

Ground roughness influences wind speed profiles and may lead to differences between the wind speed estimated at a given height and location and the actual wind speed passing across an overhead line. This may be corrected using the wind profile power law given in Equation (3). The wind speed (w_s) at two different heights (z_1 and z_2) is linked with the ground roughness through the exponent K_{shear}. Values of K_{shear} for different ground types may be found in [10].

$$w_s\ z_1 = w_s\ z_2 \cdot \left(\frac{z_1}{z_2}\right)^{K_{shear}} \quad (3)$$

Using Equation (3) the forecasted wind speed is extrapolated to a reference height (in this case 100 meters) to remove ground roughness dependence. The values from different forecast locations may then be interpolated, using Equation (2), to provide a wind speed forecast estimate at the reference height for a particular geographical location. The ground roughness at this location is then taken into account and Equation (3) is used to estimate the wind speed across the overhead line.

3.3 Data

For the study described in this paper, weather forecasts from the NOAA [8] for the test area in Wales with a time step of 6 hours have been used. Data is described in Table **1**.

Table 1 weather forecast for 18/09/2008 on test area

	Time horizon [h]				
	0	**6**	**12**	**18**	**24**
Ws [m/s]	1.8	2.5	1.7	1.2	3.4
Wd [deg]	178	196	189	301	216
Ta [°C]	10.3	9.8	16.1	12.9	12

The Montecarlo simulation does not require simple parameter values, but a description of their probability, with the minimum, maximum, average and standard deviation. These values can be obtained with ensemble forecasts or time series analysis. In this study the precision of the forecast for different time horizons has been estimated from the precision of the forecast for each parameter in the period between 08-18/08/2008.

Table 2 Forecast error minimum, maximum average and standard deviation

		Time horizon [h]			
	[%]	**6**	**12**	**18**	**24**
Ws	**min**	-28.30	-17.78	-30.19	-38.55
	max	13.79	50.00	27.27	83.33
	st dev	14.24	21.60	18.17	38.96
Wd	**min**	-1.94	-3.33	-2.78	-8.33
	max	15.83	1.67	20.83	23.61
	st dev	5.00	1.44	6.70	8.11
Ta	**min**	-15.86	-9.93	-20.27	-16.22
	max	1.57	4.80	31.07	15.84
	st dev	6.07	5.78	12.06	8.51

The network studied is part of the Manweb distribution network situated in an area attractive to prospective wind farm development. It is composed of a 132kV Lynx overhead line conductor with a maximum operating temperature of 50°C connecting two towns 7 km apart. The line passes through the two towns in an area characterised mainly by the presence of grass and inhabited areas. This is important since the different in ground roughness influences the value of wind speed as calculated in Equation (3). In Figure 2 a representation of the network studied is provided.

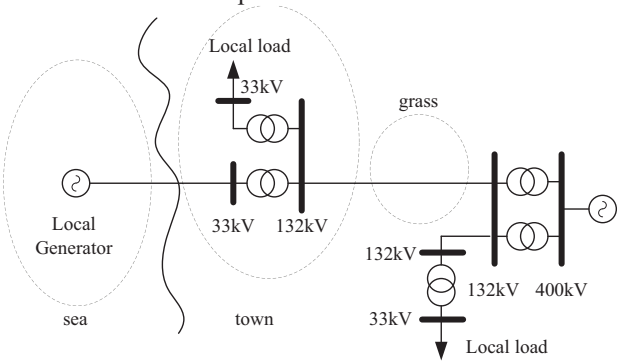

Figure 2: Network and site schematic representation

4 RESULTS AND DISCUSSIONS

The simulation results are shown in Table 3 and Figure 3, where the rating forecasts for the whole day are represented from the reference time of midnight. Two main considerations arise from the observation of these results: As expected, the error increases with the distance of the forecast from the reference time. At 6pm the possibility to have a real time rating below the value of the static seasonal rating is forecasted.

Table 3 Rating forecast in MVA for different time horizons

	Time horizon [h]				
[MVA]	**0**	**6**	**12**	**18**	**24**
min		108	109	75	85
max		142	134	141	152
aver	138	133	122	98	130
st dev		9	9	24	17

In this case the minimum forecasted rating in the late afternoon corresponds with the daily peak for the power transfer on the line. If the line utilization increased because of an increased connection of distributed generation, this would create a problem and the necessity to curtail part of the generation. On the other hand, the ability to forecast this situation and to quantify its probability, would allow appropriate decisions for generation control to be taken. Considering the different precision found for different time horizons, it is recommended to take into account this parameter, along with the distance from the forecast reference time, when developing control strategies for power flow management.

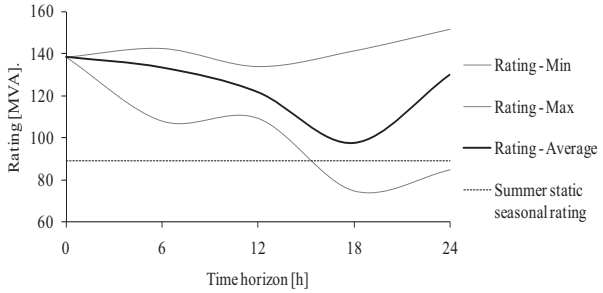

Figure 3: Rating forecast

5 CONCLUSION

In this paper a methodology for overhead line rating forecasts has been presented. This is based on the research regarding distribution network real-time rating estimations developed at Durham University. Weather forecasts were used with component thermal models and a state estimation technique based on the Montecarlo method in order to calculate a probability distribution for each circuit component's rating for different time horizons. The results have then been collated for calculating line rating probability distribution, and metrics such as minimum, maximum, average and standard deviation of the rating forecasts. The simulation highlights that the estimation precision tends to decrease with the distance from the reference time. It was also shown how a possible rating lower than the static seasonal rating was forecasted 18 hours ahead of the reference time. The work presented in this paper on rating forecasts is expected to enhance distribution network operator decision making capabilities regarding network power flow management. This is because decisions may be informed not only by instantaneous rating estimates, but also by the forecasted ratings for different time horizons. Work is continuing in this area to realise the potential of forecasted real-time ratings for electrical distribution networks.

6 ACKNOWLEDGMENTS

The authors wish to acknowledge the Department for Innovation, Universities and Skills for funding, and the staff from AREVA T&D, Imass, PB Power and ScottishPower Energy Networks for their valuable input to this work.

7 REFERENCES

[1] D. Roberts, P. C. Taylor, A. Michiorri., 2008, "Dynamic thermal rating for increasing network capacity and delaying network reinforcements", *CIRED Seminar 2008: SmartGrids for Distribution*, Frankfurt, 23 - 24 June 2008

[2] F. Soto, J. Latorre, M. Wagensberg, 1998, "Increasing the capacity of OHLs in the 400 kV Spanish transmission network: real time thermal ratings", *Electra* vol. 22-211

[3] D.A. Douglass, A.A. Edris, 1996, "Real-time monitoring and dynamic thermal rating of power transmission circuits", *IEEE Transactions on Power Delivery*, vol. 11 (3), 1407-1418

[4] D.A. Douglass, A.A. Edris, 1997, "Field application of a dynamic thermal circuit rating method", *IEEE Transactions on Power Delivery*, vol. 12 (2), 823-831

[5] J. W. Taylor, 2008, "An evaluation of methods for very short-term load forecasting using minute-by-minute British data", *International Journal of Forecasting* vol. 24, 645–658

[6] J. W. Taylor, R. Buizza, 2003, Using weather ensemble predictions in electricity demand forecasting", *International Journal of Forecasting*, vol. 19, 57–70

[7] I. Sanchez, 2006, "Short-term prediction of wind energy production", *International Journal of* Forecasting, vol. 22, 43– 56

[8] http://www.noaa.gov, accessed on 30/08/2008

[9] D. Shepard, 1968, "A two-dimensional interpolation function for irregularly-spaced data", Proceedings of the 1968 23rd ACM national conference, 517-524

[10] IEC 60826, 1991, "Loading and strength of overhead transmission lines"

An Evaluation of Distributed Generation Constrained Connection Managers

***Philip Taylor[1], Samuel Jupe[1], Andrea Michiorri[1], Christopher Berry[2]**
[1] School of Engineering, Durham University, UK, [2] ScottishPower EnergyNetworks, UK
[1] Science Laboratories, South Road, Durham, DH1 3LE, UK
[2] 3 Prenton Way, Birkenhead, Wirral, CH43 3ET, UK
***Tel. (+44) 191 334 2524, Fax. (+44) 191 334 2408, Email. p.c.taylor@durham.ac.uk**

ABSTRACT: This paper presents the technical considerations and economics of a number of solutions that would allow a greater installed capacity of distributed generation to be connected to, and managed within, the distribution network. The paper describes the various solutions and compares their relative energy yield and economics. It was found that a distributed generation constrained connection manager informed by dynamic thermal ratings is the most attractive solution for developers wishing to connect wind generation to this case study network when compared to alternative solutions.

Keywords: Distributed Generation, Dynamic Thermal Rating, Control, Constrained Connection, Economics.

I. INTRODUCTION

In order to meet the United Kingdom (UK) government's environmental targets for 2010, approximately 10GW of additional distributed generation (DG) will have to be connected to UK distribution networks [1]. As this growth in DG is realised, power flows within distribution networks are expected to become increasingly congested. This may act as a barrier, inhibiting the amount of DG that can connect to the network and may impact on the energy yield (and hence profitability) of existing schemes as network capacity becomes saturated. Thus methods to manage the connection of DG schemes, in light of power flow constraints, could be beneficial both in the UK and internationally. The current practices regarding DG connections may:

1) Constrain the size of schemes at the planning stage to the existing capacity of the network based on static component thermal ratings.
2) Entail relatively high network reinforcement costs to connect schemes in excess of the network's current capacity.
3) Involve basic 'tripping' schemes to manage the DG output at times of constraint.

For the case study considered, comprising DG with an intermittent power output, this paper demonstrates that the energy yield from the unconstrained reinforcement solution is only slightly more than that delivered by an alternative operational solution utilising dynamic circuit ratings. DG constrained connection managers (CCMs) are one approach that facilitates a greater energy yield from DG schemes based on the available network capacity. It is acknowledged that asset ratings are not a static phenomenon but vary as a result of the prevailing meteorological conditions throughout the year. Thus increased amounts of electricity can be passed through distribution networks if the thermal limits of the network components are calculated from present conditions rather than from a fixed seasonal figure.

For the purpose of this research, dynamic thermal ratings (DTRs) are defined as a time-variant rating which can be practically exploited without damaging components or reducing their lifetime. Actual environmental parameter measurements are used as the input to steady state thermal models. In order to calculate and exploit the DTR, it is assumed that local environmental parameters are available and that there are no outages (planned or unplanned) present within the electrical power system. Short term transients, taking into account the thermal capacitance of power system assets are not included within the DTR assessment. It is felt that this would not affect the MWh/annum throughput of energy within the electrical power system.

The 132kV section of the network presented in this paper is a subsection of a wider trial network forming the research basis for the 'Active Control of Distributed Generators based on Component Thermal Properties' [2]. The collaborative project (involving AREVA T&D, Durham University, Imass, PB Power and ScottishPower EnergyNetworks) aims to develop, install and test a CCM for DG informed by DTRs.

This paper makes a comparison between a network reinforcement solution, two DG tripping solutions and two CCM solutions. Each solution would allow a greater installed capacity of DG to be connected to a single point within the distribution network. The CCM solutions increase in sophistication both in the manner in which the DG power output is controlled (demand-following as opposed to tripping) and by utilising different component rating regimes. By incorporating a backup trip protection system into the more sophisticated solutions, the risk of CCM system failure is minimised and thus the security of the network is maintained. An energy yield, electrical loss and economic evaluation show that, in this case, a CCM informed by DTRs is the most attractive solution for facilitating DG developer revenue gains when compared to the alternative solutions.

II. BACKGROUND

Dynamic Thermal Ratings

Conductor temperature rise is influenced by the ability of the component to dissipate to the environment the heat produced by the Joule effect governed by external conditions such as ambient temperature and wind speed.

Due to the extreme variability and unpredictability of meteorological conditions, fixed seasonal conditions are used at present to determine the most appropriate component rating. A DTR approach to network management consists of estimating or measuring component temperatures and real current carrying capacities, in order to allow the utilisation of power system components to be safely increased but maintained within continuous design specifications.

Research carried out at Durham University aiming to develop a DTR system shows, for typical UK climates, that there is an average exploitable headroom for overhead lines, underground cables and power transformers in the region of 150%, 12% and 15%, respectively, beyond the static component rating,. This is in agreement with the findings described in [3].

The DTR system under development at Durham University comprises a number of different weather stations and temperature measurement devices, placed in different locations over a wide network area. These are connected to a centralised computer which is responsible for estimating the current carrying capacities of the network component based on the present meteorological conditions. This information may then be used as a decision support tool for the secure operation of the distribution network.

DG Constrained Connection Managers

Engineering Technical Recommendation (ETR) 124 [4] presents a number of different solutions that may be developed to actively manage the power flows associated with the connection of a single DG scheme. The most basic systems involve the disconnection of DG in the event that the power output from the DG scheme exceeds the capability of the network (assessed as static capacity of network assets plus the minimum load demand). This solution may be developed further by actively switching between seasonal fixed ratings and adjusting the number of disconnected generators accordingly. More sophisticated CCM solutions are developed from the principle of generation power output control, utilising technologies such as the pitch control of wind turbine blades to capture a desired amount of wind energy. In this approach the powers flowing in the critical feeders of the network are monitored, taking load demand into account, and the power exported from the DG scheme is controlled to ensure the capability of the network is not exceeded. This may be developed as a CCM utilising static asset ratings, with demand-following control of the DG output, or as a CCM utilising asset dynamic thermal ratings, with demand-following control of the DG output.

III. OVERHEAD LINE DYNAMIC RATING

This paper focuses on the application of a DTR system to overhead lines, but it has also been applied to cables and power transformers. The fundamental concept behind the component rating is that the temperature limits of the power component must not be exceeded in order to avoid damaging the component. For overhead lines in particular, a temperature rise leads to a reduction in conductor tension and to an increase in the sag. Typical values for maximum conductor temperature are between 50ºC and 90ºC.

Component temperature is not a constant value but depends upon the energy balance between the heat produced inside the component and the heat exchange on its surface. The heat dissipated depends on the electrical current flowing in the conductor as well as the conductor's resistance to the current flow. However, the heat exchange is mainly influenced by the temperature difference between the conductor and ambient environmental conditions, and by other external factors such as wind speed or solar radiation.

Considering the heat dissipated by the Joule effect (I^2R), the heat exchanged by convection (Q_c) and radiation (Q_r), and the solar radiation (Q_s), the energy balance for an overhead line conductor is described in Equation (1).

$$RI^2 + Q_s = Q_c + Q_r, \ \left[Wm^{-1}\right] \qquad (1)$$

The heat gained by solar radiation can be calculated as in Equation (2) considering solar radiation (W_s), conductor diameter (D) and an absorption coefficient (α)

$$Q_s = \alpha W_s D \qquad (2)$$

The radiative heat exchange depends on conductor temperature (T_c), ambient temperature (T_a), the Stefan-Boltzman constant (σ) and an emission coefficient (ε), as reported in Equation (3).

$$Q_r = \varepsilon\sigma\left(T_c^4 - T_a^4\right)\pi D \qquad (3)$$

Finally the convective heat exchange depends on air thermal conductivity (λ) and the Nusselt number (Nu)

$$Q_c = \pi Nu\lambda\left(T_c - T_a\right) \qquad (4)$$

The Nusselt number can be calculated using a wind direction correction factor (K_{dir}) and the Reynolds number (Re) as in Equation (5).

$$Nu = K_{dir} \cdot \left(0.65 \cdot \mathrm{Re}^{0.2} + 0.23 \cdot \mathrm{Re}^{0.61}\right) \qquad (5)$$

The wind direction correction factor and the Reynolds number can, in turn, be calculated using in Equations (6) and (7), using wind direction (W_d), wind speed (W_s) and empirical parameters (A, B, C)

$$K_{dir} = A + B\sin^C\left(W_d\right) \qquad (6)$$

$$\mathrm{Re} = 1.644 \cdot 10^9 \cdot W_s \cdot D\left(\frac{T_c + T_a}{2}\right)^{-1.78} \qquad (7)$$

More information about the overhead line thermal model may be found in [5] and [6]. The simulated daily dynamic

thermal rating of a Lynx conductor is given in Figure 1 for the calendar year 2005. The simulation used the model described in Equations (1) to (7) and historical meteorological data for the 'Valley' area of Wales, UK. As a comparison, the seasonal ratings for the conductor are also plotted in Figure 1.

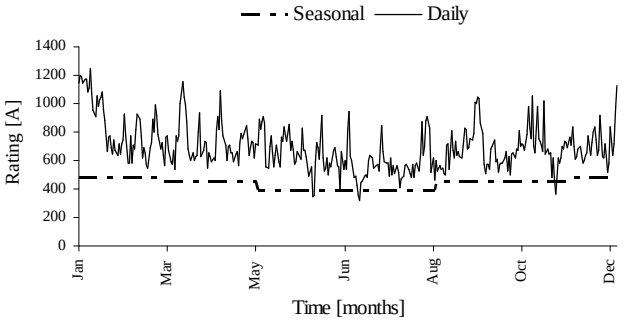

Figure 1- Rating variation of Lynx overhead line

IV. CASE STUDY NETWORK

The case study network shown in Figure 2 is derived from a section of ScottishPower's distribution network. Although it is not displayed in Figure 2, Engineering Recommendation P2/6 [7] 'security of supply' requirements are met for the connected load through an underlying meshed 33kV infrastructure. An installed wind capacity of 150MW was selected to create a constrained connection.

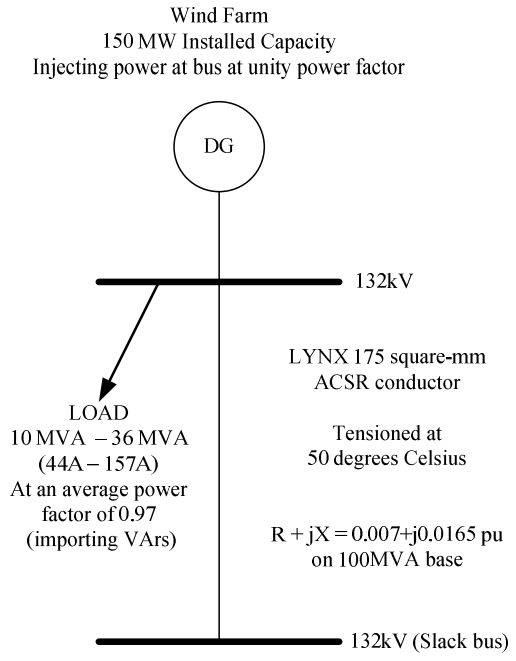

Figure 2 – The 132kV network

Analytical Considerations

The constrained connection configurations were simulated through an offline analysis of the typical half-hourly regional loading and wind farm output data for the calendar year 2005.

Table 1 displays the ratings used in the energy yield quantification analyses. The static and seasonal ratings were based on the SP Manweb Long Term Development Statement [8]. The average simulated daily minimum DTR is also given in Table 1. Offline analysis showed that a thermal constraint would be met in this section of the network before voltage or fault-level limitations.

Table 1 - Summary of Ratings Utilised

Conductor Type	Rating Condition	Rating (A)	Rating (MVA)
Lynx	Static	390	89
Lynx	Seasonal Summer Continuous	390	89
Lynx	Seasonal Spring / Autumn Continuous	450	103
Lynx	Seasonal Winter Continuous	485	111
Lynx	DTR (Average Daily Minimum)	695	159
Upas	Static	770	176

V. SOLUTION DESCRIPTIONS

Solution 1: DG tripping based on a static assessment of network availability
Solution 2: DG tripping based on component seasonal thermal ratings
Solution 3: DG output control through a CCM based on component static thermal ratings and load demand
Solution 4: DG output control through a CCM based on component dynamic thermal ratings and load demand
Solution 5: Network reinforcement to provide an unconstrained connection.

Each section below assesses the strengths and weaknesses of the particular solution, describes the algorithm used to manage the DG output and gives an approximate cost of the solution installation.

Tripping Solutions

The tripping solution schematic is shown in Figure 3 and implements the algorithm given in Equation (8).

If: Current > Rating (8)
Then: 'Trip' DG to Rating + Base Load

When this algorithm is implemented with the static rating of 390A, the DG output will be tripped to 434A at unity power factor (390A rating + 44A base load) if the current flow in the line exceeds 390A. This corresponds to the implementation of Solution 1.

Similarly, in a seasonal rating implementation [9], such as Solution 2, the DG output will be tripped to the seasonal rating plus the base load if line flow exceeds the seasonal rating. These solutions are conservative as they do not account for the dynamic nature of the load and thus they trip generators off rather than constraining them back. Furthermore, the seasonal rating approach bears the latent risk of an anomalous 'hot day' where the prevailing meteorological conditions mean that assets may be rated higher than it should be.

Estimated Basic Tripping Relay Cost:
Local tripping relay £10k

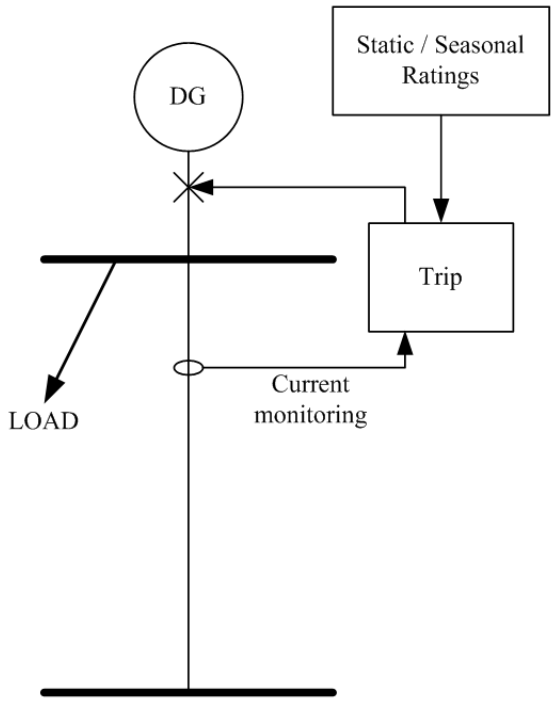

Figure 3 – The DG trip solution with static or seasonal thermal ratings

Constrained Connection Management Solutions

Figure 4 shows the schematic that allows the algorithm in Equation (9) to be implemented to control the DG output based on static or dynamic network availabilities and load demand.

If: Current > Rating (9)
Then: Control DG output to Rating + Load Demand

Control algorithm (9), implemented with a static rating of 390A, corresponds to Solution 3. The CCM solutions are more sophisticated than the DG trip options and have the potential to offer energy yield gains by taking into account the dynamic nature of the load demand. Additional power flow monitoring equipment is required to facilitate a demand-following DG output control regime.

In the case of the DTR-informed system (Solution 4), additional thermal and meteorological monitoring is also required. To ensure the safe and secure operation of the network assets, each CCM solution requires an auxiliary trip system, which calculates the same ratings as the control system, to act as a backup in the case of CCM system operation failure.

Estimated cost of demand-following DG output control based on static/seasonal ratings:
Monitoring and Regulation Equipment: £50k

Estimated Cost of demand-following DG output control based on DTRs:
Monitoring and Regulation Equipment: £100k

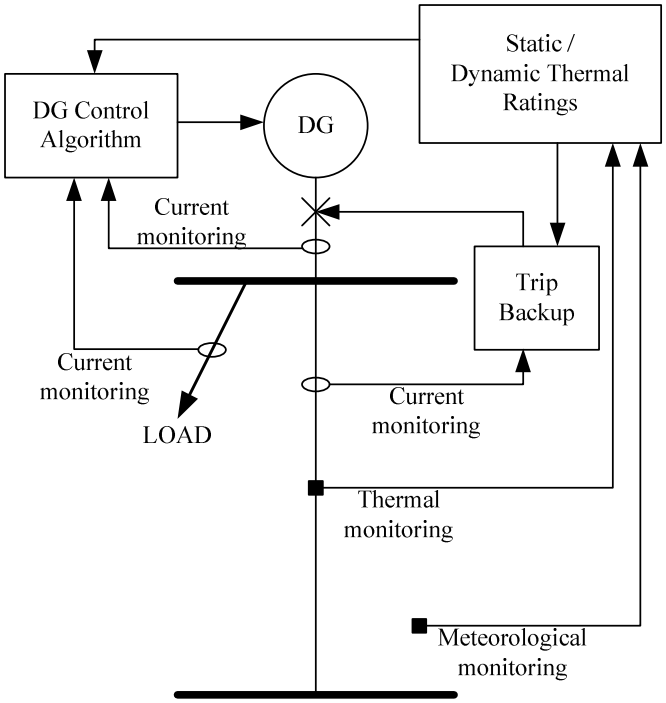

Figure 4 – The demand-following DG output control solution with static or dynamic thermal ratings

Network Reinforcement Solution

The network reinforcement option (Solution 5) would require a replacement 132kV overhead line to be constructed and the existing overhead line to be de-commissioned. It is assumed that the replacement line conductor is 'Upas' 300mm^2 AAAC. If this conductor is tensioned to maintain statutory ground clearances [10] at an operational temperature of 75^{o}C, the rating would be sufficient to provide an unconstrained annual energy yield from the DG scheme. However, it requires the largest capital investment [11] and could take several years to be installed due to the lengthy environmental assessments, planning permission, commissioning and building processes.

Estimated Reinforcement Cost:
Installation of up-rated 132kV line (7km) £2M

VI. QUANTIFICATION METHODOLOGY

Weather data from Valley (Wales, UK) was used to estimate weather parameter values along the length of the overhead line. These, in conjunction with the model described previously, were used to calculate a series of daily thermal ratings for the studied line. The method detailed in [5] was used for the overhead line modelling, with the correction for wind direction, as given in [6].

Control algorithms (8) and (9) were applied to the case study network (with the relevant rating operating regime) and the necessary constraints were implemented offline. The annual energy yield at the DG connection busbar was

calculated for each solution, by integrating the real power output of the DG scheme across the year in 30 minute intervals. The per unit electrical losses (I^2R) resulting from each solution implementation were calculated using the current flowing in the overhead line with per unit resistances of 0.0070 and 0.0041 for the 'Lynx' and 'Upas' conductors respectively. These were then summated across the year on a half-hourly basis to produce annual energy loss figures. For each solution the net annual revenue was calculated by multiplying the annual energy yield at the DG connection bus by £101.43/MWh (£52.15/MWh wholesale electricity price [12] + £49.28/MWh 'Renewables Obligation Certificate' sale price [13]) and making an adjustment for the cost of the losses incurred by transferring this energy to the slack busbar (calculated as the annual energy losses multiplied by the wholesale electricity price).

The basic tripping scheme based on summer static ratings (Solution 1) was taken as the datum solution with a capital cost of £10k and net annual revenue of £42.35M (based an energy yield at the DG connection busbar of 418.1GWh and 1.3 MWh lost through power transfer to the slack bus). The estimated marginal costs (due to additional network costs), predicted marginal revenues (due to additional energy yield) and marginal losses (resulting from electrical power transfer to the slack busbar and changes in electrical resistance of the line) were compared to this solution. This allowed a basic Net Present Value (NPV) comparison of the alternative solutions, based on their relative marginal costs and marginal revenues. A 10% discount rate and 20 year economic life was assumed [14]. The capital cost of the wind farm itself was neglected as this would be constant across each solution. Furthermore, because the wind farm is connected at via a single overhead line, any faults or scheduled maintenance on this line will cause it to shut down. Since such events have an equal constraint on the energy yield of each solution this effect was neglected. All the costs within the financial evaluations are estimates of equipment costs, based on the most appropriate data available at the time of consideration.

VII. RESULTS

The results from the quantification methodology are summarised in Table 2.

Solution 1: DG tripping based on a static assessment of network availability
Solution 2: DG tripping based on component seasonal thermal ratings
Solution 3: DG output regulation through a DGCCM based on component static thermal ratings and load demand
Solution 4: DG output regulation through a DGCCM based on component dynamic thermal ratings and load demand
Solution 5: Network reinforcement to provide an unconstrained connection

Table 2 – Quantification Methodology Results

Solution	Marginal Cost (£k)	Marginal Annual Energy Yield at DG Connection Bus (%)	Marginal Annual Energy Losses (%)	Marginal Net Annual Revenue (£M)	Marginal 20 Year NPV @ 10% dcf (£M)
1	0	0.00	0.00	0.00	0.00
2	0	4.93	18.41	2.08	17.71
3	40	5.24	18.99	2.21	18.76
4	90	10.75	43.39	4.53	38.46
5	1990	10.76	-16.31	4.58	36.97

VIII. DISCUSSION

For this case study, it appears that controlling DG output to follow load demand based on a single summer static rating (Solution 3) yields greater revenue for the developer than switching ratings on a seasonal basis and tripping DG as a result (Solution 2). DG tripping based on seasonal thermal ratings (Solution 2) requires a lower initial investment, however, the risk on the part of the DNO is greater if seasonal ratings are utilised. This is to due the possibility of an anomalous hot day occurring when ratings have been relaxed. This risk may be mitigated by investment in a dynamic thermal ratings system to provide accurate knowledge of the current thermal status of the network.

Economically, the most attractive solution to the developer is the CCM based on component dynamic thermal ratings and load demand (Solution 4). The annual revenue of the project is increased by £4.53M and shows the highest marginal NPV at £38.46M. For this case study, this solution appears to be more attractive than the alternative reinforcement option (Solution 5). This provides and unconstrained energy yield (and hence maximum annual revenue) but would require an extra capital investment of £1.99M to upgrade the overhead line.

Network reinforcement (Solution 5) would reduce network losses relative to the other solutions since the larger cross-sectional area of the conductor would reduce the electrical resistance to power flow. However, despite increasing electrical losses through implementing a CCM solution, the cost of capital for the DG developer is likely to make the active management solutions, with lower upfront costs, a more attractive investment.

IX. CONCLUSION

This paper has presented the technical solutions that would allow a greater installed capacity of distributed generation to be connected to, and managed within, the distribution network. This could be of value in situations where power flows have become congested as a result of distributed generation proliferation. For each solution the annual energy yield was quantified and used as a basis to compare solutions using an estimate of their relative Net Present Value to the distributed generation developer. It was demonstrated that a constrained connection manager informed by dynamic thermal ratings was the most cost effective solution for facilitating wind generation access to the case study network when compared to alternative

solutions. Work is continuing in this area to realise the potential of constrained connection manager solutions.

X. ACKNOWLEDGEMENTS

This work was funded by the Department for Innovation, Universities and Skills (DIUS), the United Kingdom Engineering and Physical Sciences Research Council (EPSRC) and the School of Engineering at Durham University, United Kingdom.

XI. REFERENCES

[1] Mott MacDonald, 2003, "Capacity mapping and market scenarios for 2010 and 2020"

[2] D. Curry, A Goode, S.C.E. Jupe, A. Michiorri, A. Neumann, D.A. Roberts, P.C. Taylor, 2008, "Dynamic thermal rating and active control for improved distribution network utilisation", *Proceedings PowerGrid Europe*, Italy.

[3] D.A. Douglass, A.A. Edris, 1996, "Real-time monitoring and dynamic thermal rating of power transmission circuits", IEEE Transactions on Power Delivery, vol. 11 (3), 1407-1418

[4] Energy Networks Association, 2003, *Engineering Technical Recommendation 124*, ENA, London, UK.

[5] IEC, 1995, "IEC/TR 61597 - Overhead electrical conductors – calculation methods for stranded bare conductors"

[6] WG 22.12, 1992, "The Thermal Behaviour of Overhead Conductors – Section 1". Electra, vol. 144-3

[7] Energy Networks Association, 2006, *Engineering Recommendation P2/6 – Security of Supply*, ENA, London, UK.

[8] Scottish Power Transmission and Distribution, 2005, *Distribution Long Term Development Statement for SP Manweb plc for the years 2005/06 to 2009/10*.

[9] D.A. Roberts, 2004, *Network Management Systems for Active Distribution Networks – A Feasibility Study*, Scottish Power Plc, UK.

[10] DTI, 2002, *The Electricity Safety, Quality and Continuity Regulations*, The Stationery Office, London, UK.

[11] Mott McDonald, 2003, *The Carbon Trust and DTI Renewables Network Impact Study, Annex 3*, London, UK.

[12] European Commission, 2005, *Quarterly Review of European Gas and Electricity Prices*, Luxembourg.

[13] Ofgem, 2008, *Renewables Obligation: Annual Report 2006-2007*, Ofgem, London, 7.

[14] BERR, 2004, *Wind Background – Cost of Wind Power Generation*, (http://www.offshoresea.org.uk).

XII. BIOGRAPHIES

Dr Philip Taylor, BEng, EngD, CEng, MIEE, MIEEE, FHEA

Phil Taylor is a Senior Lecturer in the Energy Group in the School of Engineering, Durham University. He received an Engineering Doctorate in the integration and control of renewable energy in electrical networks from the University of Manchester Institute of Science and Technology (UMIST) in 2001.

He has significant industrial experience as an electrical engineer including a period working in the transmission and distribution projects team at GEC Alsthom. His most recent position was Research and Development Director at Econnect, a consultancy firm specialising in the grid integration of renewable energy.

He acts as an independent assessor of research proposals for the DTI relating to their New and Renewable Energy Programme and is a member of the EPSRC Peer Review College.

He is a member of the CIGRE working group C6.11, "Development and Operation of Active Distribution Networks".

He is a member of the editorial board for the newly formed International Journal of Renewable Energy Technology (IJRET) www.inderscience.com/ijret

Samuel Jupe, M.Eng (Hons) Dunelm

Samuel Jupe is a doctoral researcher in the Energy Group at the School of Engineering, Durham University.

He is currently researching the active control of distributed generators based on component thermal properties. He received a Master of Engineering degree in General Engineering from Durham University in 2006. His interests include the management of distributed generation constrained connections and fuzzy control systems.

Andrea Michiorri

Andrea Michiorri graduated in Mechanical Engineering at the University of Rome "La Sapienza" in 2005. He is a doctoral researcher in the Energy Group at the School of Engineering, Durham University. His research involves the influence of environmental parameters on distribution network components and state estimation techniques. His scientific interests include energy conversion and transmission systems and computer applications in energy.

Christopher Berry, BSc (Hons), CEng, MBA, MIET

Christopher Berry has over 25 years experience in the UK electricity industry. He started his career as a Craft Apprentice with British Nuclear Fuels and progressed with them to achieve Chartered Engineer status with responsibility for the design of instrumentation, control and electrical aspects of a number of new major facilities for the Sellafield site. He then joined ScottishPower/Manweb where he has held a variety of power distribution system design and project management positions. Currently he is responsible for design standards for the SP Manweb plc distribution system at all voltage levels and leads a team of professional engineers responsible for the design and development of the 132kV and 33kV networks.

Chris is also an active member of the design work stream of the Distribution Working Group (DWG) – the United Kingdom Electricity Supply Industry focus group charged with identifying and co-ordinating R&D work to address the issues that affect the transition of power systems to a low-carbon future. He received his BSc (Hons) in Electrical and Electronic Engineering from the University of Manchester Institute of Science and Technology (UMIST) in 1985 and his MBA (Distinction) from the Edinburgh Business School in 2002. He is a corporate member of the Institution of Engineering and Technology (MIET).